Rhodoliths as environmental archives in the tropics

A THESIS BY **NICOLAS DARRENOUGUE**, SUBMITTED FOR THE DEGREE OF DOCTOR OF PHILOSOPHY OF THE AUSTRALIAN NATIONAL UNIVERSITY
RESEARCH SCHOOL OF EARTH SCIENCES

JULY 2013

Statement of authorship

I declare that this thesis has not been used towards the award of any other degree of any institution and to the best of my knowledge, this thesis is my own original work except where due reference is made in the text.

October 29th 2012

Nicolas Darrenougue

Acknowledgements

I had two main supervisors throughout this project, these being Patrick De Deckker and Steve Eggins.

Patrick has been my primary supervisor and was at the beginning of this project, which he introduced to me in early 2008. Ever since we first met, Patrick has been a pillar I could always rely on and one of the most inspiring human being I have ever met. Despite the brilliantly successful scientific carrier he had (and still fulfils) and the many recognitions he gathered over the years, he is one of the most humble person I know. Despite his incredibly busy schedule and his many responsibilities, he has always been there, for any matter, at any time. As a student, I am so grateful for his availability, his outstanding scientific knowledge, his ability to listen and his patience, his trust and his always-constructive comments and ideas. As a person, I admire his passion and his curiosity, his intellect and his professionalism, but most of all, his optimism and accessible, easygoing nature. I feel so privileged to have known him, both as supervisor and as a friend.

Steve has greatly contributed to define and (re)orientate this research project. He has played a key role, not only as the "guru" of many of the technical aspects involved, but also because of his always-spot-on comments and critiques on my research work and communication. I hope his sense of perfectionism and scientific rigour will be reflected in the following pages.

Without an expert on these wonderful creatures that are rhodoliths, this project could never have materialised. Claude Payri from the Institut de Recherche pour le Développement (IRD), Nouméa (New Caledonia) took on that part and has been incredibly resourceful throughout the project. She also organised and managed my multiple visits to the IRD in Nouméa, besides suggesting the great location of the Ricaudy Reef, which happened to provide an ideal study site for us. I am most grateful to her caring and excitement about this project as well as her trust and encouragements towards me to be able to carry it out.

I will be forever in debt to the late Guy Cabioch who was instrumental in visualising and organising the early stages of this research project. I will always remember his dedication and appetite for science as well as his kindness and humbleness.

I also have to express my deepest and sincerest gratitude to John Butcher (IRD) who took care of all the technicalities regarding the fieldtrips in New Caledonia, particularly for the collection and monitoring of the rhodoliths studied here. Without him, I would not have been able to participate in the underwater work, rhodolith sampling or the New Caledonian lagoon exploration under such great conditions. Those made out for many

memorable diving experiences. John has also collected *in situ* data when I could not be out in the field but in my very-much-indoor Canberran office. His experience in the field, associated with his friendly, easygoing attitude has been an invaluable asset for this project.

Numerous researchers and technicians within the Research School of Earth Sciences (RSES) have been involved to a small or larger extent to this project. Among them, Chantal Alibert and Les Kinsley have been essential on every aspects related to laser ablation and solution ICPMS analyses, from setting up the instrument to the interpretation of the results, through to the reflexions on how to improve the measurements performances and to their help on the data treatment. I am infinitely grateful for their patience and interest in this work.

Ian Williams supervised the oxygen isotope analyses carried out using the SHRIMP II. His experience of working with the machine and trust in this project made it possible to pioneer the use of high-resolution SIMS for coralline red algae geochemistry. I much appreciated his involvement as well as his encouragements, advices and comments regarding the research directions this project took.

Stewart Fallon provided invaluable help and support regarding the radiocarbon dating of the rhodoliths (together with Bec Norman for sample preparation). His interest and comments on early versions of several of the chapters herein were greatly appreciated.

Critical technical help during my stay at RSES was provided by Tony Phimphisane and John Vickers on the making and polishing of rhodolith thick and thin sections. EPMA analyses were supervised by Robert Rapp while Linda McMorrow helped with the ICP-AES analyses and Joe Cali was involved in the conventional oxygen isotope analyses. Charlotte Allen intervened in the early LA-ICPMS analyses while Dave Heslop and Brian Harrold provided support with the use of statistics. Brian has also been the ideal go-to person for any informatics-related issue and his kindness and professionalism have repeatedly been crucial to escape from inextricable computer situations.

I also need to address sincere thanks to the "Nouméa people" who, through critical sharing of ideas and/or data, have contributed to advances in this project. Jean-Michel Fernandez, Christophe Menkès, Farid Juillot and Emmanuel Fritsch from the IRD, Stéphan Chevalier from the Direction du Développement Rural (DDR) and Pierre Maurizot from the Direction de l'Industrie, des Mines et de l'Energie de Nouvelle Calédonie (DIMENC), who also provided access to the site of the former Olympia nickel mine, near Nouméa.

Back at RSES, inspiring discussions have been shared with Brad Opdyke, Michael Elwood, Dave Ellis, Bear McPhail, Anne Felton and Keith Crook, to name a few. I also would like to particularly thank Judith Shelley and Maureen Davies for their critical comments and corrections on early versions of many of the writings presented here. I am also very grateful to Maree Coldrick and Joy McDermid for their help on any, and every, administrative matter.

Mo Davies, Matt Valetich and especially Nigel Craddy have been the great colleagues and friends I could turn to in need of escaping the often-tumultuous, always-brain-demanding world of scientific research, for the time of a short talk, a daily coffee break or... else. I will greatly miss those moments.

This research project would not have been possible without financial support, especially the one provided by an Australian National University Postgraduate Scholarship and various allowances from RSES. A 2011 AFAS (Australian French Association for Science and technology) award grant also supported additional fieldtrips to New Caledonia that have been essential for the success of this project.

Finally, I will have to write in French to appropriately thank my family for their support:

Un immense merci à toute ma famille pour leur soutien tout au long de cette expérience. Mes parents bien sûr, pour leurs encouragements et leur soutien dans tout ce que j'ai entrepris jusqu'alors. Cela vaut également pour mes grands-parents et mon frère Andoni.

Puis, bien évidemment, Mél, sans qui je ne serais pas ce que je suis aujourd'hui. Les mots ne suffisent pas pour te remercier pour ton soutien constant pendant cette aventure, ainsi que pour tout ce que tu m'apportes au quotidien.

Thank you all so much!

Nicolas.

Abstract

Rhodoliths are free-living forms of calcareous, coralline red algae that are found worldwide, from the tropics to the poles, in relatively shallow (0->250m) waters. They can live hundreds of years and continuously form a high-Mg calcite skeleton that presents periodical growth bands. Recent coralline red algae studies show that the variations of specific trace elements along these growth bands can reflect secular changes in various environmental parameters. This study aims at assessing and further extending the ability of rhodolith-forms of coralline red algae to reconstruct environmental changes. Modern rhodoliths of the species *Sporolithon durum* from the Ricaudy Reef in New Caledonia were chosen for this project. The use of laser ablation inductively coupled plasma mass spectrometry (LA-ICPMS) permitted to investigate the distribution pattern of Mg across single rhodolith branches. The combination of LA-ICPMS analyses with alizarin red S staining and radiocarbon dating enabled us to determine the seasonal character of the major Mg/Ca cycles recorded along rhodoliths branches, as well as characterise the seasonal pattern of 14 other trace elements over the year 2010-2011. A statistical approach was employed to separate these trace elements into three groups of similar behaviour that respond essentially to either environmental, biologic or anthropogenic influences. A 46-year record of Mg/Ca, Sr/Ca and Li/Ca variations obtained from multiple rhodolith branches display a high level of correlation with the local, instrumental seawater temperature dataset over the last five decades, at both monthly and interannual resolutions. Mg/Ca variations also record larger scale climate pattern such as El Nino – Southern Oscillation (ENSO) variations, and compare well with the commonly used Sr/Ca-temperature proxy of corals. In addition, interannual-to-decadal variations in specific trace metals concentrations (Mn, Fe and Ni) reflect the intensity of former mining activities that occurred in the studied area from the 1960s to the late 1970s, making *S. durum* rhodoliths a potentially useful tool for the determination of anthropogenic pollution. Variations of the $\delta^{18}O$ composition in the skeleton of *S. durum* were also investigated using sensitive high-resolution ion microprobe (SHRIMP). After correction for the instrumental mass fractionation (IMF), the $\delta^{18}O$ average value is found to be consistent with conventional mass spectrometer measurements but shows a negative offset compared to equilibrium that is, however, consistent with previously-reported vital effects for coralline red algae. The range of $\delta^{18}O$ values recorded by the SHRIMP was too large to be explained solely by changes in environmental parameters. Consequently, we proposed that high-resolution SHRIMP measurements of $\delta^{18}O$ may alternatively be used to obtain critical insights into metabolic and/or calcification processes in coralline red algae.

Table of contents

List of figures

CHAPTER II - Coralline red algae / rhodoliths: literature review

CHAPTER III - An investigation of Mg/Ca distribution in *Sporolithon durum* coralline red algae

CHAPTER IV - Growth and chronology of the rhodolith-forming, coralline red algal species *Sporolithon durum* from the tropics

CHAPTER V - Seasonal patterns in trace elemental composition of coralline red algae from a tropical lagoon: environmental, biological and anthropogenic influences

CHAPTER VI - Sea-surface temperature reconstruction from trace elements variations of tropical coralline red algae

CHAPTER VII - A record of mining and industrial activities in New Caledonia based on trace elements in rhodolith-forming coralline red algae

CHAPTER VIII - Oxygen isotopic composition of tropical coralline red algae using a sensitive, high-resolution ion microprobe (SHRIMP II)

List of tables

CHAPTER I

Introduction

I-1 Climate Change and human impact reconstructions

Since the end of the 19th century, the Earth's surface temperature has been increasing globally. This temperature increase, associated with a rise of sea level and a retreat of most glaciers and ice covers throughout the world, has been qualified by the scientific community with the term "Climate Change" (IPCC, 2007). Whether Climate Change is a natural phenomenon or is the result of anthropogenic activities is still not fully understood and is a matter of intense debate among several scientists (e.g. Leroux, 2005; Plimer, 2009), although findings "incriminating" humans, through the addition of greenhouse gases into the atmosphere, are largely supported. Putting aside this debate, the biggest question yet to be answered regarding Climate Change is how and how much will the climate change in the future? The underlying question being how would this affect human populations?

In order to address these questions, two critical aspects need to be thoroughly understood:

(1) The current state of the Earth's climate, its behaviour and variability;

(2) How did climate behave in the past and how did it evolve until today.

Advanced methods of monitoring (e.g. satellites, data loggers) as well as recent historical records (e.g. thermometers, weather pages in periodicals, vintage periods reports) permit to observe that the Earth's Climate system is very complex and numerous parameters need to be taken into account in order to draw a comprehensive picture of its modern behaviour. Solar radiation appears to be the initial, crucial parameter governing climate variability as the primary source of heat at the surface of our Planet. However, the Sun's influence is often equalled or even surpassed by Earth-related forces playing a role of feedback in the climate system (Shindell et al., 1999; Rind, 2002).

The atmospheric Greenhouse Effect is one of the most important feedback forces influencing the climate (Mitchell, 1989), so is the reflection of the Sun's heat into the

atmosphere by the Earth's surface (called albedo), and in particular by ice covered areas (e.g. Rind et al., 1995). This is one of the reasons why ice retreat and the addition of greenhouse gases into the atmosphere by human activities are taken so seriously by the scientific community (IPCC, 2007). Other critical feedback forces reacting to the initial input of solar radiation and controlling the Earth's climate variability, are the coupling ocean and atmospheric circulations. Indeed, most of the solar energy reaches the tropical zones. This energy is, then, redistributed to the high latitudes via oceanic and atmospheric teleconnections (Lau and Lim, 1984). These teleconnections feature essential entities and climate phenomena affecting dramatically, wide areas of the Planet. The El Niño Southern Oscillation (ENSO) phenomenon and the African and Australasian monsoons are the best-known of these climatic phenomena affecting the Tropics and the North Atlantic Oscillation (NAO) as well as the Southern Annular Mode (SAM) widely control the climate of the mid- to high- latitudes. The connections and interactions between all these climatic forces are extremely complex and mathematical models to try to reconstruct the current state of the Earth's climate are not able to reproduce this complexity with great fidelity (e.g. Roeckner et al., 1992; Anagnostopoulos et al., 2010). Therefore, Future scenarios predicting the behaviour and effects of Climate Change are subject to a lot of uncertainties (IPCC, 2007).

In order to reduce the uncertainties and, thus, improve the predictions of Future Climate Change, scientists need to understand how the climate looked like in the past and how it has evolved to its current state.

When it comes to gather information about past climates (i.e. beyond the instrumental and historical records), palaeoclimatology can rely on a different array of tools that, naturally, recorded past environmental conditions on various timescales.

Oceanic sediment and ice sheets are the essential archives of past climate at timescales spanning from millennia to millions of years. For example, the analysis of the isotopic composition of the oxygen ($\delta^{18}O$) present in foraminifera (calcareous microfossils) along a sediment core demonstrated that the temperature of the Earth is oscillating at regular intervals since the beginning of the Quaternary period (2.6 Ma) and that these oscillations are linked to regular variations in the Earth's orbit around the Sun, which controls the amount of solar energy received by the Planet (Emiliani, 1955). These astronomical cycles, called Milankovitch cycles, are well determined and can be predicted for the Future (e.g. Berger, 1978; Berger and Loutre, 2002). Analysing gas bubbles contained in ice core layers, Petit et al. (1999) determined the variations of temperature and ice cover over the last ~400 kyrs at Vostok, Antarctica. These authors showed that these variations are cyclic and correspond to solar radiation variations linked to the Milankovitch cycles. It also

appears that, for this period of time lasting several hundred thousand years, the Earth's temperature and the concentration of greenhouse gases (CO_2, CH_4) into the atmosphere are closely related (Petit et al., 1999). Similarly, see also the study by Wolff et al. (2010) on an ice core from the EPICA Dome C site, also in Antarctica, revealing 800 kyrs of environmental changes.

From millennial to decadal timescales, other proxies, offering a better resolution, are preferably used. For example, corals are the most commonly used archives of tropical, shallow-water oceanic changes and can give information about past variations of the ENSO phenomenon (e.g. Tudhope et al., 2001) and speleothems from tropical areas can record the past behaviour of the monsoon (e.g. Wang et al., 2001; 2008). Past land climates are generally recorded in tree rings (e.g. Briffa et al., 1990) and extra-tropical climate changes at a high-resolution can, at times, be determined through the analysis of bivalve mollusc shells (e.g. Putten et al., 2000; Goodwin et al., 2003).

All these tools can provide climate modellers with invaluable insights into past climatic conditions and greatly help with the future climate predictions. However, none of these archives is perfect and they all have uncertainties associated with their use. Two pathways are therefore available for future research: (1) either attempt to improve the performance of existing climate proxies in order to reduce their uncertainties, or (2) focus on the discovery and development of new proxies that can contribute to filling the gaps left void by other archives. These two pathways should be conducted in parallel with the aim of linking all the climate components together so the most reliable predictions for Future Climate Change can be achieved.

In addition to the future climate concerns, humans' direct influence on the biotic communities is one of the major preoccupations of environmental scientists. Particularly, anthropogenic pollution of marine environments by way of discharge of excessive carbon, phosphorus or toxins from industrial or agricultural activities into the rivers, ultimately entering the ocean, largely affects the sustainability of the marine biota. In order to prevent dramatic changes and protect the biodiversity, these anthropogenic impacts have to be characterised and monitored. One option is to use organisms as "biomonitors" to determine their sensitivity and response to changes in the environment (Holt and Miller, 2011). However, most of these organisms are limited by their short lifespan in the time scale of reconstruction of environmental impacts (e.g. Smith and Rainbow, 2006; Hédouin et al., 2008). Scleractinian corals, for example, represent one of the few marine organisms that are able to provide longer-term (decades to centuries) records of anthropogenic disturbances (e.g. Fallon et al., 2002; McCulloch et al., 2003; David, 2003; Alibert et al., 2003). Expanding the variety of organisms capable of providing environmental records

over relatively long periods of time and from various types of environments would be greatly beneficial to better understand and manage the impacts of human activities on the marine biota.

I-2 Objectives and overview of the study

The objective of this research project is to propose a contribution to fill the existing gaps in the current array of tools used for climate and environmental reconstructions. Here, coralline red algae are investigated, under their rhodolith (or free-living) form, as potential archives of the environment in a tropical system, mainly focusing on the geochemistry of the high-Mg calcite skeleton, which these benthic organisms form during growth. Research on coralline red algal geochemistry as a recorder of environmental change was only pioneered in the early 2000s and there is a critical need for further developments and improvements.

This study essentially aims at:

(1) using a different coralline red algal species from the tropics to assess the validity of previously published results and relationships between coralline red algae from the high-latitudes and various climatic parameters, and more particularly, the Mg composition – seawater temperature relationship;

(2) extending the range of currently available geochemical proxies to assess the potential of coralline red algae as recorders of anthropogenic disturbance in near-shore, shallow water environments;

(3) experimenting novel analytical techniques for coralline red algal geochemistry and evaluate their ability to provide insightful information on the environment in which they grow.

This thesis is organised around 6 results chapters, starting with a literature review and ending up with a conclusion chapter. The results chapters are presented in a manuscript format for ease of publication, therefore leading to a degree of repetition that is minimised as much as possible.

Chapter II presents a summary of the current state of knowledge on coralline red algae and rhodoliths. It takes the form of a literature review in which these organisms are characterized at various levels. The distribution of coralline red algae and rhodoliths around the world is discussed and complemented by the identification of environmental factors influencing this distribution. The temporal evolution of

coralline red algae through geological times is also presented along with evolutionary patterns regarding past changes of seawater chemistry and Future Climate Change. This chapter also includes an overview of the biological characteristics of coralline red algae and rhodoliths, and particularly their role in the global carbonate production, the various morphological aspects they can take as well as their typical calcification and growth patterns. A section on geochemical studies undertaken on coralline red algae compiles age and growth rates determination, as well as the use of geochemistry to reconstruct environmental parameters. Lastly, previous attempts at palaeoenvironmental interpretations are discussed.

Chapter III endeavours to investigate the distribution of Mg into the calcite skeleton of rhodolith forms of the coralline red algal species *Sporolithon durum* from the Ricaudy Reef in New Caledonia. Using various instrumental settings of a laser ablation, inductively coupled plasma mass spectrometer (LA-ICPMS), 11 parallel profiles display high-resolution variations of Mg/Ca concentrations across a rhodolith branch. Accuracy and precision of the LA-ICPMS Mg/Ca measurements are assessed by independent analysis of the Mg/Ca concentration in the same rhodolith using solution ICPMS, inductively coupled plasma atomic emission spectrometry (ICP-AES) and electron probe micro analyses (EPMA). In addition to the high-Mg calcite skeleton deposited by the growing alga, other components of the rhodolith potentially bearing Mg, such as the organic part or the presence of dolomite, are investigated.

Chapter IV reports experiments conducted on the growth and chronology of *S. durum* rhodoliths from the Ricaudy Reef. Annual extension rates and growth patterns for the organisms' last living year (2010-2011) are characterised through the use of Alizarin Red S (ARS) stain and the determination of Mg/Ca seasonal cycles on 43 rhodolith branches. A combination of radiocarbon dating and annual Mg-cycles and visual growth band counting is presented as a reliable chronological approach to determine the age of long-lived rhodoliths. Influential factors on the variability of the growth pattern and extension rates are discussed based on the comparison of our data with instrumental records of local environmental parameters.

Chapter V investigates the seasonal pattern of 15 trace elements along the 43 *S. durum* rhodolith branches for which the 2010-2011 extension rates and growth pattern have been determined (Chapter IV). The use of statistical methods such as pairwise correlation and hierarchical clustering enables to sort the studied trace elements in different groups of similar behaviour. Discussions involve the variability of the trace

elemental profiles recorded using LA-ICPMS as well as the environmental, biological or anthropogenic influences on the observed seasonal patterns.

Chapter VI presents a >45 year-long record of sea-surface temperature (SST) for the Ricaudy Reef area based on the variations of Mg/Ca, Sr/Ca and Li/Ca in *S. durum* rhodoliths. LA-ICPMS measurements along 5 different branches recorded high-resolution trace elemental signals that are analysed for their reproducibility and compared to local instrumental SST data at monthly to interannual timescales over the last 50 years. Interannual Mg/Ca variations are compared with an index of ENSO changes over the same period to assess the ability of *S. durum* rhodoliths to also record regional-scale climate patterns. The reliability of Mg/Ca in rhodoliths as a tool for SST reconstruction is also tested through a comparison with a previously generated record of Sr/Ca variations in a *Porites* sp. coral from the same reef.

Chapter VII focuses on the use of specific trace elements in *S. durum* rhodoliths to attempt a reconstruction of anthropogenic perturbation in the southwest lagoon of New Caledonia and more particularly around the Ricaudy Reef. An approximately 50 years record of high-resolution Mn/Ca, Fe/Ca, Ni/Ca and Co/Ca variations measured by LA-ICPMS along 5 rhodolith branches is presented. Calibration of the trace elements concentrations is achieved by the use of independent measurements from LA-ICPMS, solution ICPMS and ICP-AES. The variability of the trace elemental records is discussed and long-term patterns are compared to the evolution of local mining activities in the catchment of the studied area, as well as changes in rainfall since the 1960s.

Chapter VIII reports pioneer results on the use of SHRIMP to record oxygen isotopic composition in coralline red algae. Experiments on and quantification of the instrumental mass fractionation (IMF) for high-Mg carbonate materials were carried out and high-resolution $\delta^{18}O$ variations in *S. durum* rhodolith from the Ricaudy Reef are presented. Discussion involves the potential role of various environmental and biological factors upon the incorporation of oxygen isotopes into the rhodolith skeleton. The ability of SHRIMP-derived $\delta^{18}O$ variations in the studied sample to archive SST and salinity (SSS) is envisaged and future, encouraging paths of using the SHRIMP in coralline red algal research are also mentioned.

Chapter IX summarises the conclusions of previous chapters in order to assess the potential of *S. durum* rhodoliths from the Ricaudy Reef, New Caledonia, as recorders of environmental changes. In this endeavour, confirmations of previous studies on coralline red algal geochemistry as well as new elements provided by this project are recalled and limits and future directions for coralline red algal research are identified.

References

Anagnostopoulos, G.G., Koutsoyiannis, D., Christofides, A., Efstratiadis, A., Mamassis, N., 2010. A comparison of local and aggregated climate model outputs with observed data. *Hydrological Sciences Journal* **55**(7), 1094-1110.

Alibert, C., Kinsley, L., Fallon, S. J., McCulloch, M. T., Berkelmans, R., and McAllister, F. (2003). Source of trace element variability in Great Barrier Reef corals affected by the Burdekin flood plumes. *Geochimica et Cosmochimica Acta* **67**(2), 231-246.

Berger, A. L. (1978). Long-term variations of daily insolation and Quaternary climatic changes. *Journal of the Atmospheric Sciences* **35**(12), 2362-2367.

Berger, A., and Loutre, M. F. (2002). An exceptionally long interglacial ahead? *Science* **297**, 1287-1288.

Briffa, K. R., Bartholin, T. S., Eckstein, D., Jones, P. D., Karlen, W., Schweingruber, F. H., and Zetterberg, P. (1990). A 1,400-year tree-ring record of summer temperatures in Fennoscandia. *Nature* **346**, 434-439.

David, C. P. (2003). Heavy metal concentrations in growth bands of corals: a record of mine tailings input through time (Marinduque Island, Philippines). *Marine pollution bulletin* **46**(2), 187-196.

Emiliani, C. (1955). Pleistocene temperatures. *The Journal of Geology* **63**, 538-578.

Fallon, S. J., White, J. C., and McCulloch, M. T. (2002). Porites corals as recorders of mining and environmental impacts: Misima Island, Papua New Guinea. *Geochimica et Cosmochimica Acta* **66**(1), 45-62.

Goodwin, D. H., Schone, B. R., and Dettman, D. L. (2003). Resolution and fidelity of oxygen isotopes as paleotemperature proxies in bivalve mollusk shells: models and observations. *Palaios* **18**, 110-125.

Hédouin, L., Bustamante, P., Fichez, R., and Warnau, M. (2008). The tropical brown alga *Lobophora variegata* as a bioindicator of mining contamination in the New Caledonia lagoon: A field transplantation study. *Marine environmental research* **66**(4), 438-444.

Holt, E. A., and Miller, S. W. (2011). Bioindicators: Using organisms to measure environmental impacts. *Nature Education Knowledge* **3**(10), 8.

IPCC (2007). Fourth Assessment Report. Core Writing Team (R. K. a. R. Pachauri, A., Ed.), pp. 104, IPCC, Geneva, Switzerland.

Lau, K. M., and Lim, H. (1984). On the dynamics of equatorial forcing of climate teleconnections. *Journal of the Atmospheric Sciences* **41**, 161-176.

Leroux, M. (2003). "Global Warming: Myth or Reality? The Erring Ways of Climatology." Springer Praxis Books / Environmental Sciences.

McCulloch, M., Fallon, S., Wyndham, T., Hendy, E., Lough, J., and Barnes, D. (2003). Coral record of increased sediment flux to the inner Great Barrier Reef since European settlement. *Nature* **421**, 727-730.

Mitchell, J. (1989). The'greenhouse' effect and climate change. *Reviews of Geophysics* **27**, 115-139.

Petit, J. R., Jouzel, J., Raynaud, D., Barkov, N. I., Barnola, J. M., Basile, I., Bender, M., Chappellaz, J., Davis, M., and Delaygue, G. (1999). Climate and atmospheric history of the past 420,000 years from the Vostok ice core, Antarctica. *Nature* **399**, 429-436.

Plimer, I. (2009). "Heaven and Earth?" Connor Court Publishing Pty Ltd.

Putten, E. V., Dehairs, F., Keppens, E., and Baeyens, W. (2000). High resolution distribution of trace elements in the calcite shell layer of modern *Mytilus edulis*: Environmental and biological controls. *Geochimica et Cosmochimica Acta* **64**, 997-1011.

Rind, D., Healy, R., Parkinson, C., and Martinson, D. (1995). The Role of Sea Ice in $2xCO_2$ Climate Model Sensitivity. Part I: The Total Influence of Sea Ice Thickness and Extent. *Journal of Climate* **8**, 449-463.

Rind, D. (2002). The sun's role in climate variations. *Science* **296**, 673-677.

Roeckner, E., Arpe, K., Bengtsson, L., Brinkop, S., Duemenil, L., Esch, M., Kirk, E., Lunkeit, F., Ponater, M., and Rockel, B. (1992). Simulation of the present-day climate with the ECHAM model: Impact of model physics and resolution. *Project Report* **93**.

Shindell, D., Rind, D., Balachandran, N., Lean, J., and Lonergan, P. (1999). Solar cycle variability, ozone, and climate. *Science* **284,** 305-308.

Smith, B. D., and Rainbow, P. S. (2006). Comparative biomonitors of coastal trace metal contamination in tropical South America (N. Brazil). *Marine Environmental Research* **61**(4), 439-455.

Tudhope, A. W., Chilcott, C. P., McCulloch, M. T., Cook, E. R., Chappell, J., Ellam, R. M., Lea, D. W., Lough, J. M., and Shimmield, G. B. (2001). Variability in the El Nino-Southern Oscillation through a glacial-interglacial cycle. *Science* **291,** 1511.

Wang, Y. J., Cheng, H., Edwards, R. L., An, Z. S., Wu, J. Y., Shen, C. C., and Dorale, J. A. (2001). A high-resolution absolute-dated late Pleistocene monsoon record from Hulu Cave, China. *Science* **294,** 2345.

Wang, Y., Cheng, H., Edwards, R. L., Kong, X., Shao, X., Chen, S., Wu, J., Jiang, X., Wang, X., and An, Z. (2008). Millennial-and orbital-scale changes in the East Asian monsoon over the past 224,000 years. *Nature* **451,** 1090-1093.

Wolff, E.W., Barbante, C., Becagli, S., Bigler, M., Boutron, C.F., Castellano, E., De Angelis, M., Federer, U., Fischer, H., Fundel, F., Changes in environment over the last 800,000 years from chemical analysis of the EPICA Dome C ice core. *Quaternary Science Reviews* **29** (1), 285-295.

CHAPTER II

Coralline red algae / rhodoliths: literature review

II-1 Introduction - Definitions

Rhodoliths are free-living forms of encrusting coralline red algae (Foster, 2001). They form when algal cells first settle on a non-cohesive substrate. The latter will, then, become the nucleus of an unattached, concentrically-growing, calcareous structure that is called a rhodolith (Bosence, 1983b; Goldberg, 2006). In this regard, rhodoliths are classified as a type of coated grain (oncoid - Bosence, 1983b; Harris et al., 1996) in which the nucleus can have many different sizes and/or shapes, and can also be quite different in nature: a nucleus can be either a fragment of coral, a mollusk shell, a cobble/pebble, or, often, a fragment of a dead rhodolith (e.g. Harris et al., 1996; Basso et al., 2009). More generally, the nature of the nucleus depends upon the supply of fragmented material from a nearby hard substrate (Adey and MacIntyre, 1973). Rhodoliths are generally found in aggregates, forming so-called rhodolith beds (Foster, 2001) that may entirely cover the seafloor (Figure II-1).

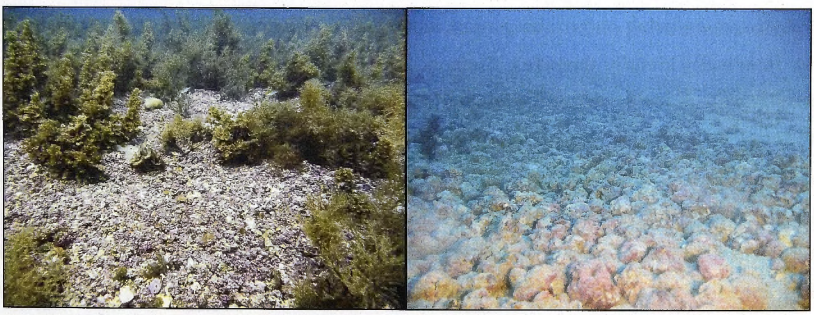

Figure II-1: Rhodolith beds (left) near the Ricaudy Reef, New Caledonia, 4-5 m deep; (right) off Point Addis National Park, Victoria, Australia, approx. 40 m deep (Photo from Parks Victoria).

Coralline algae have been of particular interest for scientists since the end of the 18th century, mainly as they play a major role in the building of reefs in the tropics, but also, because they are dredged and used as a soil fertilizer, particularly in North-Western Europe where they are called maërl (Adey and MacIntyre, 1973; Foster, 2001). However, the difficulty in identifying and differentiating generic and specific variations within the group has prevented many scientists from conducting detailed studies involving crustose corallines. When these researchers did, misnomers and misunderstandings regarding taxonomy were frequent until the comprehensive "re-evaluation" of coralline algae by Adey and McIntyre (1973), which helped clarify the basics of taxonomy of crustose coralline algae. However, despite this significant advance, uncertainties between species could still be an issue as confirmed by the recent study of (da Nobrega Farias et al., 2009). This latter study presents a coralline algal species, with descriptive criteria that correspond to a well-known species in Brazil: *Lithothamnion heteromorphum*. However, these authors also found that their species could also fit into the description of *Lithothamnion superpositum*, a species known to occur in South Africa and Australia, but not in Brazil. Thus, the authors assume that the two species are the same and that *L. superpositum* extends further west in the Atlantic Ocean than previously thought. Additionally, the resolution of the classification and phylogeny of the coralline red algae is still on-going and greatly benefits from recent advances in molecular analyses. One result, for example, is the formerly-recognised family Sporolithaceae from the order Corallinales, which was elevated in the classification and is now recognized as the order Sporolithales (Le Gall et al., 2010). Similarly, phylogenetic relationships are consistently clarified and the systematics of the coralline red algae still evolves (e.g. Bittner et al., 2011).

Another aspect of confusion leading to an uneasy way for multidisciplinary scientists to communicate during the early days of coralline algae research was the denomination of what is now named as "rhodoliths". Some authors called them "*Lithothamnion* balls" (*Lithothamnion* being one of the genera of the Melobesioideae subfamily) without being able to actually identify them (e.g. Stetson, 1953). Others referred to these algal balls as "oncolites" (e.g. McMaster and Conover, 1966). "Rhodolites" and "rhodoids" were also proposed by Bosellini and Ginsburg (1971) and Peryt (1983), respectively, but were rejected as well, since the study of Bosence (1983a). Indeed, the term "rhodolite" is already used to name a variety of garnet (Binda, 1973) and "rhodoid" is etymologically incorrect (rhodoid means "red-like" - Bosence, 1983a). It is only since the arguments of Adey and McIntyre (1973) and Bosence (1983a) that the term "rhodolith" (rhodophycean or "red rock") is now well accepted within the scientific community to define the free-living forms of crustose coralline red algae.

II-2 Coralline red algae and rhodoliths - A world approach

II-2.a A global distribution

Coralline red algae and rhodoliths are widely distributed across the world's oceans, from the tropics to the poles (Figure II-2). Extensive rhodolith beds for instance, are reported in the Western Pacific off the coasts of Japan, Korea (Riosmena-Rodriguez, 2009), the east coast of Australia (Lund et al., 2000; Littler et al., 1991; Chisholm, 2000; Harris et al., 2006), Indonesia (Verheij, 1993), New Zealand (Nalin et al., 2008; Basso et al., 2009; Nelson, 2009), New Caledonia (this study) or French Polynesia in the central South Pacific (Payri, 1997). They can also be found in the Eastern Pacific from Alaska to Chile, in Hawaii (e.g. Konar et al., 2006, Riosmena-Rodriguez, 2009) and most particularly in the Gulf of California, Mexico (e.g. Foster et al., 1997; Steller et al., 2003; 2009). Rhodoliths also occur in the Indian Ocean, off the coasts of Western Australia (Kendrick and Brearley, 1997; Goldberg and Heine, 2008), as well as Zanzibar (Semesi et al., 2009) and southern Mozambique (Foster, 2001; Perry, 2005). In the North Atlantic, high concentrations of rhodoliths are present on the west coasts of Ireland (Bosence, 1976; 1983b) and Scotland (e.g. Kamenos et al., 2008; Kamenos and Law, 2010; Kamenos, 2010), Brittany in France (Grall and Hall-Spencer, 2003; Martin et al., 2007a;b), Spain (Adey and McKibbin, 1970), up to Canada (Gagnon et al., 2012) and Greenland (Kamenos et al., 2012a) but also in the Mediterranean (Bosence, 1983b; Basso, 1998; Foster, 2001), Florida (Bosence, 1983b) and the Carribean (e.g. Ballantine et al., 2000). Of all these locations, the east coast of Brazil in the South Atlantic is where rhodoliths are the most abundant. Indeed, rhodolith beds extend from 2°N to 27°S, with the Abrolhos Shelf bearing the largest rhodolith bed in the world, covering ~20,900 km^2 (Amado-Filho et al., 2012), an area comparable to the one covered by coral reefs of the Great Barrier Reef in Australia (23,865 km^2; Vecsei, 2004). The southernmost occurrence of coralline red algae was reported by Schwarz et al. (2005) in the Ross Sea, Antarctica.

From a depth perspective, coralline red algae span the whole range of the photic zone, from intertidal flats and shallow (<10 m) waters (Adey and MacIntyre, 1973; Payri, 1997; Chisholm, 2000; Payri and Cabioch, 2004; Ries, 2006; Basso et al., 2009) to intermediate (20-60 m) depths (Adey and MacIntyre, 1973; Harris et al., 1996; Lund et al., 2000; Schwarz et al., 2005; Goldberg, 2006; Steller et al., 2009) and down to zones of limited light availability (>100 m) (Adey and MacIntyre, 1973; Harris et al., 1996, Lund et al., 2000; Cabioch et al., 2008), with the deepest living rhodoliths reported at a 290-m depth along the slope of the San Salvador Sea Mount, Bahamas (Littler et al., 1991).

Coralline red algae and rhodoliths thrive on a variety of substrates ranging from muddy to rocky environments (Foster, 2001; Nelson, 2009). Indeed, encrusting coralline red algae are essentially found on hard bottoms, with the algae sometimes entirely covering rocky substrates (e.g. Adey and MacIntyre, 1973; Schwarz et al., 2005; Halfar et al., 2008) whereas rhodoliths are commonly observed on biogenic, calcareous sediments (Foster, 2001; this study) or soft, muddy to sandy environments (Goldberg, 2006; Harvey and Bird, 2008; Basso et al., 2009).

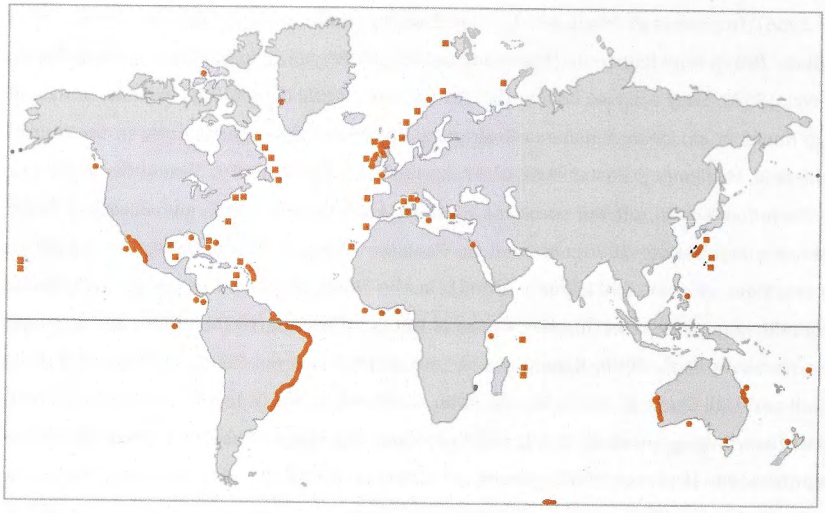

Figure II-2: Map showing the location of the reported presence of rhodoliths (adapted from Foster, 2001). Notice the high concentrations off Brazil, Western Australia, the Brtish Isles and the Gulf of California. Note: this map is non exhaustive.

II-2.b Influencing factors

The global distribution of coralline red algae in the world's oceans suggests that neither seawater temperature nor light intensity are limiting factor for their development. However, that is, only if coralline red algae are considered as a group. Indeed, these two factors become critical and condition the occurrence of these benthic organisms when the distribution of particular families or genera is considered. In this respect, attempts at a classification of coralline red algae according to their predominant milieu of occurrence are present in the literature. For instance, the genera *Lithothamnion*, *Mesophyllum* or *Clathromorphum* are commonly associated with high-latitudes, relatively shallow-water environments (e.g. Adey and MacIntyre, 1973; Halfar et al., 2000; Aguirre et al., 2000;

Kamenos et al., 2008; Hetzinger et al., 2009; Basso et al., 2009; Kamenos, 2010), whereas the dominant genera in tropical settings are usually *Hydrolithon, Neogoniolithon* and *Lithophyllum* for the shallow waters (Adey and MacIntyre, 1973; Aguirre et al., 2000; Basso et al., 2009) and *Sporolithon* is commonly found in tropical deep waters (Adey and MacIntyre, 1973; Aguirre et al., 2000; Henriques et al., 2009). It has to be noted however that this type of classification is limited as the same genus can occur in very different environments. *Lithothamnion*, for example, is not exclusive to high-latitudes. Representatives of the genus were also reported in the shallow, temperate waters of the Gulf of California, Mexico (Halfar et al., 2000; Frantz et al., 2000; Steller et al., 2009) or in a tropical reef sequence (Payri and Cabioch, 2004) where they may correspond to deep-water environments (Adey and MacIntyre, 1973; Aguirre et al., 2000). In such cases, the identification of the organisms to the species level may be critical, but even then, some species such as *Sporolithon durum* can also be found in a variety of environments. Henriques et al. (2009) reported the presence of *S. durum* in the deep (~50 m) waters of Bahia and Espiritu Santo states in Brazil, while Basso et al. (2009) studied the same species in a near-surface environment in the North Island of New Zealand and Goldberg and Heine (2008) reported *S. durum* rhodoliths from the shallow waters of Rottnest Island, Western Australia. *S. durum* has also been observed to be the most abundant coralline red algal species in a shallow, tropical reef environment in New Caledonia (this study).

At a local scale, however, it seems that temperature and light are controlling factor on the occurence of coralline red algae (Adey and MacIntyre, 1973). In addition, water motion is a critical parameter influencing the distribution of rhodoliths. Generally a rhodolith bed can only form when there is sufficient current to provide from sediment deposition that causes burial (Adey and MacIntyre, 1973; Harris et al., 1996; Foster, 2001) and no so much as to break the calcareous structure of the rhodoliths (Adey and MacIntyre, 1973; Bosence, 1983b). Consequently, rhodoliths beds are commonly found in moderate water motion settings that correspond to semi-protected environments where the current can be based either on wave action or tidal energy (e.g. Steller et al., 2009). In some cases, the morphology of the rhodolith bed or the rhodoliths can be characteristic of particular energy conditions (Bosence, 1983a;b; Steller et al., 2009) but care should be taken as to interpret water motion conditions based only on the morphology of the rhodoliths (see section below).

In conclusion, although coralline red algae and rhodoliths can virtually be found "anywhere" in the photic zone, they definitely do not occur "everywhere". Their global distribution is highly discontinuous (Figure II-2) and the adequate environmental settings

required for the development of these organisms are complex and far from being fully understood, as, so far, they have mainly been interpreted based on limited field surveys and short term environmental observations.

II-3 Geological History

The geological fingerprint of coralline red algae dates back to the beginning of the Palaeozoic eon. It is even thought that they were already present in the primitive oceans of the Precambrian, over 600 million years (Ma) ago (Steneck and Martone, 2007). This qualifies these calcareous algae as one of the oldest organisms still living on Earth.

II-3.a Origins and extinction patterns

During the period before the Mesozoic (~250 Ma), coralline algae are placed into a slightly different classification than the modern one. The group of encrusting algae Solenoporaceae and the genus *Archaeolithophyllum* were the main representatives of the phylum Rhodophyta from the Cambrian to the end of the Permian (540-250 Ma - Ries, 2006). They were, for example, thought to thrive in relatively high latitudes (35-45°) during the Late Ordovician/Devonian – Middle Paleozoic (Copper, 1994; Fig.5). *Archaeolithophyllum* have been observed to be one of the major skeletal contributors of the carbonate facies, under crustose or rhodolith form, from the Pennsylvanian to the Late Permian (320-250 Ma – Wray, 1964; 1977; Figure 1 in Stanley and Hardie, 1998). Both of these members of the crustose coralline algae are now extinct: *Archaeolithophyllum* did not survive the major Permo-Triasic biotic crisis and the Solenoporaceae disappeared after the Neogene period (Ries, 2006). Hence, they are considered to be ancestral forms of the coralline red algae that thrive in modern oceans. Indeed, some of the major characteristics such as morphology (size, shape, internal tissue and reproductory organs), mineralogy and environmental distribution are very similar to the ones of the modern family Corallinaceae that comprises, in particular, the genus *Lithophyllum* (Wray, 1964; 1977).

Modern representatives of crustose coralline algae originated in the early Cretaceous (~140 Ma) and evolved and diversified since then to become one of the most important calcifiers that are now present in the world's oceans. The global number of coralline species, reflecting their diversity, increased exponentially from the early Cretaceous to the early Miocene (~20 Ma) to reach a peak with 245 different species. At the time of Miocene global changes, mainly characterized by the onset of the East Antarctic ice sheet, inducing

changes in ocean circulation and a related enhancement of nutrient in the worldwide waters (Zachos et al., 2001), coralline algae were so important that they replaced coral communities by being the major carbonate producers in the oceans (Halfar and Mutti, 2005). Later on, coralline algal diversity slightly decreased down to 43 species in the late Pliocene (~2.5 Ma) and finally approximately doubled in number (~90 species) during the Pleistocene (Aguirre et al., 2000).

Three orders of coralline red algae are now recognised to be part of the phylum Rhodophyta: the most common Corallinales, incuding the families Hapalidiaceae (Melobesioideae) and Corallinaceae, the Sporolithales and the Rhodogorgonales (Bittner et al., 2011).

The orders Corallinales and Sporolithales varied in opposite patterns throughout geological times (Figure I-3). These two orders had similar species diversity during the Early Cretaceous (~140-120 Ma) and appear to have been restricted to the tropics, mainly in the Tethys region. As temperature increased during the Cretaceous, the Sporolithales expanded to reach their maximum of diversity and become the most species-rich corallines around the Turonian (~90 Ma). At the same time, the number of species from the order Corallinales decreased to their lowest diversity. After the Cretaceous/Tertiary crisis, which led to the extinction of 58-67% of the coralline species, and during the Paleocene and Eocene (early Cenozoic, 65-35 Ma), a global cooling of the oceans permitted cool, deep-waters species from the Hapalidiaceae family (Corallinales) to drastically expand geographically and in diversity. During the Oligocene-early Miocene period (~35-20 Ma), the onset of the Southern Hemisphere glaciations helped global latitudinal climatic differentiation, resulting in an increase partitioning of shallow water habitats, thus, allowing shallow- warm-waters species from the Corallinaceae family (Corallinales) to rapidly expand. An increase in scleractinian coral diversity is also observed at the same period (e.g. Coates and Jackson, 1985). The Corallinales reached a maximum of more than 40 species in the early Miocene (~20 Ma), whereas the Sporolithales slightly decreased. Since then, both orders seem to maintain a relatively stable pattern, although showing a slight decrease in species diversity (Aguirre et al., 2000). Note that the classification used in Aguirre et al. (2000) is different from the currently-accepted one. As we used the current classification, orders and families described here may not correspond to the ones published in Aguirre et al. (2000) (Figure II-3).

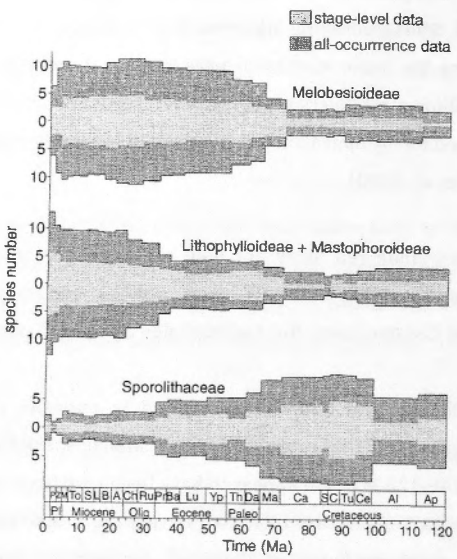

Figure II-3: Evolution of species richness of three sub families of coralline algae since the Cretaceous (Figure 6 in Aguirre et al., 2000). Note that the taxonomy used in this study is now obsolete. For instance, the Sporolithaceae family displayed here has been elevated to a new order: Sporolithales (Le Gall et al., 2010; Bittner et al., 2011)

According to Aguirre et al. (2000), these opposite variations in the diversity of the two main orders of coralline red algae through time might be explained by the different optimal-growth environments that are observed today in their distribution patterns. It is also noteworthy that these variations correlate quite well with seawater-temperatures-related variations of $\delta^{18}O$ in benthic foraminifera (Savin, 1977). The order Sporolithales shows a direct correlation with temperature whereas Corallinales shows a negative correlation (Aguirre et al., 2000).

It is important to state that the geological history of the evolution and diversity of coralline red algae has not been linear through time but has suffered from several crisis or massive extinction events as well as periods of species originations, all of these, cumulated, resulting in an important species turnover. The main extinction events for corallines occurred in the late Cretaceous with the Cretaceous/Tertiary biological crisis (~65 Ma). At that time, 67% of the coralline species disappeared. The late Eocene period (~35 Ma) was also marked by significant species extinction as 27.5% of corallines were affected. These two crises are the only ones that are correlated to well-known mass extinctions for other groups. The range of loss for corallines is also somewhat similar to

the one for the other groups (Aguirre et al., 2000). The other extinction events that each eliminated more than 20% of coralline species are not as significant as for other groups. However, the late Paleocene-early Eocene extinction event (55 Ma) also affected benthic foraminifera, scleractinian corals and terrestrial organisms (e.g. Benton, 1995; Sepkoski Jr, 1990). In the same respect, the coralline crisis that occurred during the early Pliocene (5 Ma) has been recognised in other marine animals (see Raup and Sepkoski Jr, 1986), but was not as significant as it was for coralline red algae.

The fact that the overall coralline diversity continued to increase despite these extinction periods from the early Cretaceous until the early Miocene is related to major origination periods that almost immediately followed the major crises (Aguirre et al., 2000). The best example is the early Cenozoic (65 Ma) coralline species origination that reached almost 70% and then compensated and even surpassed the loss of species during the prior major crisis. This 'compensation' has been interpreted as new species filling habitats that the extinct species left void (see Stanley, 1979).

II-3.b Coralline red algae and secular changes in seawater Mg/Ca ratio

It is also interesting to note that not only coralline species distribution and abundances change over geological times, but also did their chemical composition and especially the proportion of Mg incorporated in their skeleton.

Over the Phanerozoic eon, according to the variations of the $MgCO_3$ proportion in the global seawater, Earth oceans have oscillated, on a 100,000 to 200,000 years basis, between what Sandberg (1983) introduced as "calcite seas" and "aragonite seas". These oscillations, which were proved to be closely related to the rate of expansion of the mid-ocean ridges through time (Hardie, 1996) , are responsible for the modifications in mineralogy of abiotic carbonates as well as biogenic $CaCO_3$ produced by reef-builder organisms (e.g. Hardie, 1996; Ries, 2009). Indeed, most of the latter organisms generate a calcareous skeleton in which the Mg content varies accordingly to the Mg content of the ambient seawater. That is, during a "calcite sea" period when the $MgCO_3$ content of the global ocean is low (<4% $MgCO_3$), biotic and abiotic carbonate production will essentially be under a low-Mg calcite form, whereas during an "aragonite sea" phase when $MgCO_3$ of seawater is over 4%, aragonite and high-Mg calcite will be produced. The alternations between one and the other most favourable form of calcium carbonate deposited is thought to be the major cause of alternating between dominant reef-building species over the geological record (Stanley and Hardie, 1998; 1999). Stanley and Hardie (1998; 1999) showed, for example, that coralline algae, which currently produce a high-magnesium

calcite skeleton, were one of the major reef builders in the Permian-Triasic "aragonite seas II" (~370-200 Ma) as they are in nowadays' "aragonite seas III" (Foster, 2001). However, as stated in the above paragraphs, coralline algae were present and evolved during all the Phanerozoic eon and were significant carbonate producers all through this time, even in "calcite seas". The difference is that, in a low-$MgCO_3$ sea, coralline algae (as well as the majority of reef-builder organisms) produced a low-Mg calcite skeleton, adapting their mineralogy to the $MgCO_3$ content of the ambient seawater (Stanley et al., 2002; Ries, 2006; 2009). Ries (2006), after conducting controlled conditions experiments, showed that crustose coralline algae could have adapted extremely well through geological times, switching between a high-Mg calcite skeleton in the early Cenozoic and the modern oceans (molar Mg/Ca=5.2) and a low-Mg calcite skeleton in waters where the molar Mg/Ca ratio was significantly lower as in the Palaeozoic or the Cretaceous.

II-3.c The fate of coralline red algae in a changing climate

With the increasing awareness of the significance of coralline red algae and rhodolith beds around the world in the global carbon cycle and as major carbonate producers (see below), a major question arises on how, and to what extent, they will be affected by future changes in ocean acidification and temperature. Indeed, various climate scenarios predict an increase in global ocean temperatures of 2 to 3°C by the end of the 21st century, in association with a decrease of pH (due to an elevated pCO_2) of ~ 0.5 pH units, compared to pre-industrial revolution (mid 18th century) levels (IPCC, 2007). This increase in ocean acidification (OA) may have dramatic effects on most carbonate producers around the world due to the reduction of the $CaCO_3$ saturation state, thus leading to conditions less favourable to calcification and more prone to dissolution (e.g. Raven et al., 2005). The less stable form of $CaCO_3$ mineral is high-Mg calcite (compared to aragonite and calcite), which is therefore the form being the most susceptible to dissolution (e.g. Morse et al., 2006; Andersson et al., 2008; Basso, 2012). As coralline red algae produce a skeleton that is almost exclusively composed of high-Mg calcite, they are predicted to be one of the most vulnerable organisms to OA (Amado-Filho et al., 2012).

The effects of OA and warming have become one of the main foci of the latest coralline red algal studies: i.e. from the response of the individual organism, to the modification of the species biological cycle and the role of rhodolith beds or encrusting coralline algae-dominated substrates in the global carbon cycle (Basso, 2012). For instance, under elevated temperature scenarios associated with a pH value similar to the one predicted for the end of the century (~7.8; Feely et al., 2009), Anthony et al. (2008) recorded increased

bleaching, productivity loss and a 50% calcification reduction for the species *Hydrolithon onkodes* typically found in the Indo-Pacific region. Similarly, in controlled-conditions, tropical reef mesocosms, Jokiel et al. (2008) observed a decrease of 86% of the algal cover on hard substrate and a 2.5 times-decrease in rhodolith calcification. Using a comparable experimental scenario for temperate water environments, the death percentage of *Lithophyllum cabiochae* collected in the Mediterranean increased 2 to 3 fold and the rates of dissolution of the dead thalli increased 3 to 4 times (Martin and Gattuso, 2009). Coralline red algal growth rates and recruitment have also been shown to be adversely affected by a reduction of pH (e.g. Kuffner et al., 2008). The internal structure of rhodoliths may also be modified by low pH, as the presence of cracks was observed in *L. glaciale* between the cell walls (Raggazzola et al., 2012; Burdett et al., 2012), rendering the internal structure of the rhodoliths more fragile and more suitable for mechanical breakage such as caused by wave energy or boring activities. Another potential effect of elevated pCO_2 in the oceans (and thus, low pH) is a modification of the relative proportion of different metabolic processes occurring in coralline red algae. Indeed, it has been observed for some species that when pH decreases, calcification is generally reduced but photosynthesis increases concomitantly, and *vice versa* (Semesi et al., 2009; Martin et al., 2012).

Mixed responses to OA have also been also reported. Ries et al. (2009), for example, did not see any significant changes in the net calcification of *Neogoniolithon* sp. when doubling the seawater CO_2 concentration. Different species from temperate waters also displayed different responses to the same stressors depending on the natural living environment (e.g. Martin et al., 2012). The species living in the intertidal zone and commonly subject to a high amplitude of pH variations on a daily basis was more resistant to a pH increase than other species naturally living under more stable pH conditions (Martin et al., 2012). In another study, it was observed that live *L. glaciale* rhodoliths were able to buffer most of the experimental pH reduction and, consequently, maintain their high-Mg calcite structure (Kamenos et al., 2012b). Dead rhodoliths, however, were more affected by the pH stressor, which materialised by an important loss of Mg from the skeleton. These authors therefore concluded that, while alive, coralline red algae seem to have the ability to buffer against future pCO_2 enrichment (Kamenos et al., 2012b).

Although the majority of the studies on the effects of OA and rising temperatures on the growth and calcification of coralline red algae worldwide suggests severe degradation, further research is critical. The mixed responses to stressors observed in some cases suggest that a role of the living component of the alga may indeed counteract the effects predicted by theoretical geochemistry, leading to a potential species specific ability to withstand elevated levels of pCO_2 and temperature modeled for the near future.

II-4 Biological features

II-4.a Role in carbonate production

Coralline red algae are major carbonate producers in the oceans. That characteristic is related to the tremendous area covered by these algae on the seafloor. Foster (2001) even made them one of the "Big Four" benthic communities, the most important being the marine macrophytes and the two others, kelp beds and forest along with seagrass meadows.

From the early Palaeozoic, coralline red algae have been one of the major reef-builders in the global ocean (see "Geological History" section) and they are, now, sharing this exclusive characteristic only with scleractinian corals (e.g. Stanley and Hardie, 1998; 1999).

In the tropics, coralline algae crusts and/or rhodoliths are frequently found at the bottom of barrier reef carbonate sequences where they play a significant role in the early building of the reef and its stabilization throughout its growth and expansion. In New Caledonia, for instance, a thick 12.3-m rhodolith sequence was described directly above the bedrock and underlying the coral reef, relating the deposition of the rhodoliths to the early stages of the barrier reef development (Payri and Cabioch, 2004). The same observation has been made for the Australian Great Barrier Reef (GBR) and the Isla Cerralvo in Baja California, Mexico, where, respectively, Alexander et al. (2001) and Tierney and Johnson (2011) found rhodoliths and crustose coralline algae at the base of the coral reef sequence, implying a critical role of the corallines-generated carbonate substrate in the settlement of the modern reefal structure.

In modern tropical reefs ecosystems, rhodoliths and/or crustose coralline algae are almost always associated with coral colonies, in varying proportions according to the local environmental parameters, but they are always significant contributors to the primary and carbonate production of the reefs. From crustose corallines embedded in the reef of Lizard Island, Northern GBR, Australia, Chisholm (2000) measured the calcification rate of four representative species commonly described for the Indo-Pacific reefs. The experiment was conducted over a period from the end of March to Mid-July (late autumn-early winter) 1986 on the windward slope of the reef, from 0 to 18 meters deep. The estimated averaged net carbonate budget was an increase of 1.5 to 10.3 kg $CaCO_3$. $m^{-2}.y^{-1}$ for the slope of Lizard Island, implying an upward expansion of the reef of about 7 $mm.y^{-1}$, considering only the contribution from coralline algae. The actual observations on the average expansion of worldwide reefs indicate a much slower rate of expansion (e.g.

Davies, 1983). This suggests the inevitable presence of eroding factors counteracting the theoretical accretion induced by coralline algae. However, the study by Chisholm (2000) still infers the predominant role of coralline algae in the edification and sustainability of reefs environments. Still in the tropics, Amado-Filho et al. (2012) recently reported rates of $CaCO_3$ production for the largest rhodolith bed in the world, on the Abrolhos Shelf off eastern Brazil. This production is estimated to be of 1.07 kg $CaCO_3$ m^{-2} y^{-1}, with a total production of 0.025 Gt yr^{-1}, which corresponds to approximately 5% of the world's total carbonate banks production, making the tropical South West Atlantic rhodolith beds "gigantic $CaCO_3$ bio-factories" (Amado-Filho et al., 2012).

Aside from their major contribution to the accretion of tropical reefs, another critical input from coralline red algae into the global carbonate production comes from areas where scleractinian corals are absent: outside the tropics. Indeed, crustose corallines and/or rhodoliths cover huge parts of the seafloor in temperate and cold waters where they are the essential reef-builders and one of the most efficient carbonate-sediment producers. Martin et al. (2006; 2009) carried out a quantitative experiment comparable to the one of Chisholm (2000) in the temperate waters of the Bay of Brest (Brittany, France). They reported a primary production for the rhodolith bed of 10 to 600 g $C.m^{-2}.y^{-1}$ and a calcification rate ranging from 0.3 to 3 kg $CaCO_3.m^{-2}.y^{-1}$ according to depth and algal cover of the substrate. The net accretion of the bed (taking into account calcification and dissolution) was estimated to be 500 g $CaCO_3.m^{-2}.y^{-1}$. So, even if this rhodolith bed is a heterogeneous system in which respiration is more important than gross production, it is one of the most important carbonate producer and plays a major role in carbon and carbonate cycles of the temperate shallow waters in the western part of France. Similarly, in the cold waters of northern Norway, coralline red algae and rhodoliths-derived coralline algae fragments were described to account for 45 to 56% in weight of the total carbonate secreting organisms (Freiwald and Henrich, 1994). Overall, the fact that coralline algae can cover such large proportions of substrate in areas where they thrive argues for the significant potential of these algae in the production of carbonate for temperate and cold waters. From an acoustic mapping survey of a part of the carbonate shelf of the Gulf of California, Mexico, Hetzinger et al. (2006) reported that the rhodoliths cover about 40% of the seafloor and are the main carbonate producers of the surveyed area (~45 km^2). That confirms the previous observations of Foster et al. (1997) where rhodoliths were even reported to completely cover the seafloor in some places of the Gulf. Around Australia, rhodolith beds are widely distributed around the Recherche archipelago and contribute to 13.7% of the 1054 km^2 of substrate mapped in Goldberg's study (2006).

They are also the main component of the seafloor from ~50 to 110 m deep around Fraser Island and cover 40 to 50% of the substrate (Lund et al., 2000).

Their ability to adapt to a wide range of environments also enables coralline algae to thrive in quite extreme conditions, making them the main calcifiers where other carbonate producer cannot adapt as easily. This is the case, for example, in some relatively deep waters where Littler et al. (1991) observed 17.4% of rhodolith cover on the descending slope of the San Salvador Sea Mount, at a water depth of more than 91 m down to 290 m. On the platform of the seamount, rhodoliths represent a 95.8% of covering and contribute to an estimated 391 tons of organic carbon per year to deep sea productivity (Littler et al., 1991). Another example would be for polar regions where corallines are the most important organisms that produce carbonate, particularly on hard substrates (Adey and MacIntyre, 1973). Living crustose coralline algae have even been reported to grow under a 2.5 m-thick sea-ice layer in Antarctica. There, they cover from 4 to 60% of the substrate, and on hard bottoms (i.e. rocks), 47 to 97% is covered (Schwarz et al., 2005).

Hence, we can assess the major contribution of coralline algae to the global oceanic carbonate production and their invaluable role as main reef-builders in the wide areas they cover in the tropical zones, as well as from the mid-latitude, temperate waters to the cold waters of the polar regions.

II-4.b Morphology

Similar morphological patterns exist between modern genera of encrusting coralline algae across the oceans, largely due to a common and parallel evolution of all the taxa from the Cenozoic period (Adey and MacIntyre, 1973). Moreover, it appears that the morphology of coralline algae is not necessarily controlled by the taxonomy but, often, it is thought that the environment, the biology and/or the ecology of individuals play an essential role on which form the algae will develop into (e.g. Bosence, 1983b; Foster, 2001).

Typically, coralline algae are distinguished between three extreme morphologies, which relate to the properties of the crust, whether it is thin, thick or branched (Steneck, 1986; Figure II-4). A crust is generally considered as thin when the thallus does not exceed 0.5 mm. Over that commonly accepted value, a coralline alga will be described as growing a thick crust. On another aspect, crustose corallines are differentiated according to their "degree of adherence" to a substrate (Steneck, 1986), ranging from totally encrusted on a substrate, through partially fixed and presenting a leafy characteristic, to being completely

free-living nodules that are called rhodoliths. Obviously, intermediate shapes and characteristics between these extremes are very common as morphologies are strongly influenced by environmental and ecological parameters. However, despite the fact that some genera could potentially adopt each of these growth forms depending on the conditions they live in, some others seem to avoid one or the other, preferring certain specific morphologies. For example, the genus *Mesophyllum* has never been reported as forming rhodoliths and is exclusively growing as crusts over hard substrates. On the same principle, *Pseudolithophyllum* will only be observed as crusts and, moreover, *Leptophytum* and *Titanoderma* usually avoid growing thick or branched crusts. The genus *Clathromorphum* displays, most of the time, a thick and unbranched thallus whereas *Lithothamnion* is almost always a branched coralline (Steneck, 1986).

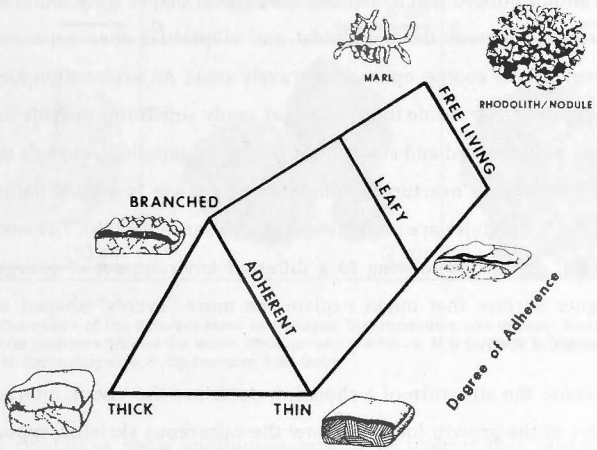

Figure II-4: Various morphological aspects of coralline red algae. The schemes represent the end points of morphological types but all the different combinations between these end points can be observed in the environment (Figure 3 in Steneck, 1986)

For the crustose coralline algae forming rhodoliths, another morphological classification can be applied to describe the different growth forms (Figure II-5). Bosence (1983a) presented a descriptive classification of rhodoliths with three levels of morphological criteria. This classification can be applied to every encountered specimen, living or fossil, and is commonly employed in the literature (e.g. Basso et al., 2009). It is based on four main features that can be determined in every rhodolith:

(1) *The specificity*: if a rhodolith consists of a single species throughout its growth and formation, it will be characterized as "monospecific". If a succession of species

appears in a single rhodolith, marked by transitions in the growth pattern, then the rhodolith will be qualified as "multispecific".

(2) *The size*: the size of a rhodolith should ideally be measured through its long (L), intermediate (I) and short (S) axes. Then, it should be reported, either as the "arithmetic mean diameter" length, as proposed by Bosellini and Ginsburg (1971); or as the volume of an ellipsoid ($\sqrt{LIS/4\pi}$) as used by Bosence (1976). Sizes of rhodolith nodules range from a few centimetres to about 15 cm in diameter (Littler et al., 1991).

(3) *The shape*: according to the relative length of their 3 axes, rhodoliths can be classified in three distinct types of shapes: spheroidal, ellipsoidal or discoidal. Bosence (1983b) observed that the shape of rhodoliths might be related to the kind of substrate they grow onto. Indeed, among a rhodolith bed in Mannin Bay, Ireland, this author noticed that a majority of discoidal shapes were found living on sandy substrate, whereas the spheroidal and ellipsoidal ones appeared to be more present on the coarse, open-algal gravels areas. An explanation for this apparent discrepancy may reside in the fact that sandy substrates provide an even surface where only upward and sideways growths are possible. And as a discoidal shape favours frequent overturning, the upward growth is greatly limited; hence, the sides of the nodules are more developed (Bosence, 1983b). The coarse open-algal gravels, as well as relating to a different environment of energy, represent a rougher surface that might explain the more "evenly" shaped ellipsoidal and spheroidal forms.

(4) *The structure*: the structure of a rhodolith describes the visual, internal or external, aspect of the growth form and how the calcareous skeleton appears during the expansion of the nodule. In this respect, the morphology of a rhodolith can be classified as either laminar, columnar or branching. Laminar rhodoliths are nodules made from a succession of thin crusts, growing over one another. This type of morphology is typical when several phases of growth are observed within the same individual. It indicates periods of cessation of growth and later re-colonisation by coralline algal crusts overgrowing the previous ones. The result of this growth-pattern is generally the presence of thin concentric crusts separated by distinct discontinuities. This is the most common morphology for "multispecific" rhodoliths. Rhodoliths described as foliaceous, presenting a leafy pattern, constitute an alternative to this concentrically-growing behaviour, however, they are also considered as laminar forms (Bosence, 1983a).

A rhodolith is qualified as columnar when its crust presents little protuberances on the surface that resemble short "hummocks" arising from the crust. These columns are generally as high as they are wide (usually in the order of one centimetre) so they cannot be pictured as proper branches. The internal structure of a column generally represents continuous growth layers that, occasionally, display the reproductive structures (=conceptacles) of the algae.

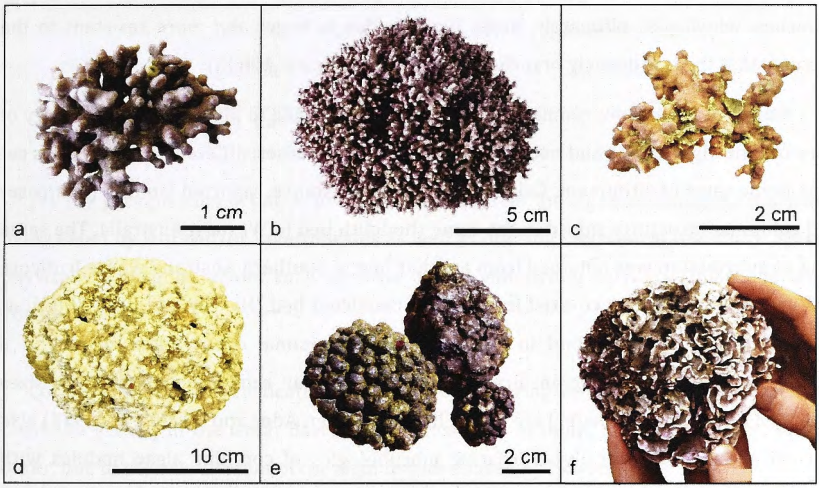

Figure II-5: An illustration of the different sizes and shapes that rhodoliths can display. Rhodoliths are from various locations around the world. Photography credits: a. M.D Castets; b. Kamenos et al., 2008; c-d. N. Darrenougue; e. P. De Deckker; f. M. Guiry.

Branching rhodoliths show continuous growth of their thallus into long and thin multiple patterns, from a common center of growth, generally represented by the nucleus. Hence, in most cases, the presence of branches in a rhodolith is synonymous with a monospecific individual. Single branches usually present a succession of growth increments that can be determined as annual to sub-annual bands (e.g. Foster, 2001). A further distinction can be made within the branched rhodoliths according to the density of their branch pattern. Four degrees are established to describe the level of branch density that a nodule possesses: I represents a single branch; II, few branches; III, frequent branches, and the fourth degree (IV) is used for rhodoliths with very dense and inter-grown branches. A single rhodolith species can adopt each of the four degree of branching depending on its growing environment (e.g. Bosence, 1976). Indeed, water motion is the primary factor that appears to control the density of the branches: heavily branched

rhodoliths are the most common in the highest energy environments, whereas open-branched nodules are characteristics of moderate- to low-energy sites. This observation is rather contradictory as, physically, the rhodoliths with the more branches offer more resistance to the fluid and, hence, are subject to more instability and overturning than their counterparts with less branches. Bosence (1983b) explains this by the fact that a frequent overturning leads to the growth of lateral branches that allow individual branches to link together, thus, strengthening the thallus. It appears, then, that the strong energy resulting from the high water motion helps the rhodoliths to possess inter-grown branches, which will, ultimately, make their thallus stronger and more resistant to the currents that the less densely branched structures (Bosence, 1983b).

It may appear that environmental parameters have a role to play in the morphology of the coralline algae crusts and nodules. However, in some cases, different morphologies co-exist in the same environment. Goldberg (2006), for instance, reported laminar (fruticose) and columnar structures mixed in the same rhodolith bed in Western Australia. The same kind of information was obtained from another bed in Southern Australia where fruticose and branched rhodoliths co-exist in the same restricted bed (Harvey and Bird, 2008); as well as for the Ricaudy Reef in New Caledonia (personal observation) where, in a moderate water-motion region, branching and columnar rhodoliths of different sizes (from ~3 to 10 cm in diameter) are found, living together. Adey and MacIntyre (1973) also warned about systematically associating morphologies of coralline algae nodules with energy conditions, beyond the assumption that massive rhodoliths are likely to have lived in a high-energy situation. As for sizes, it has been demonstrated that the shape of small rhodoliths are more often dictated by the shape of the nucleus they grow around, rather than by external conditions (Basso et al., 2009).

Concerning the specificity of a single species to grow under a specific form, even if it has been reported that, on a large spatial scale, one species could adopt many different morphologies, it seems, however, that at the local scale (i.e. one rhodolith bed), a single species is often found under a unique growth form and/or size-range that permits to link, *a priori*, a typical morphology to a typical species.

II-4.c Calcification and growth patterns

Marine calcareous algae usually precipitate the aragonite form of $CaCO_3$. Calcite is commonly a freshwater algae characteristic. Coralline red algae (Rhodophyta) and

coccolithophorids (Prymnesiophyta=Haptophyta – Coccolithophoraceae) are the only two exceptions that precipitate calcite in marine environments (Bilan and Usov, 2001).

The precipitation of calcium carbonate by calcareous algae is thought to have different functions. (1) During photosynthesis, a considerable amount of HCO_3^- is taken from the environment and produces OH^- ions in excess within the alga (a). The calcification process helps neutralise the excess of these OH^- ions by precipitating $CaCO_3$ and producing hydrogen positive ion (b), which will combine with OH^- anions to form water (c).

(a) $HCO_3^- \leftrightarrow CO_2 + OH^-$ (photosynthesis)

(b) $Ca^{2+} + HCO_3^- \leftrightarrow CaCO_3 + H^+$ (calcification)

(c) $Ca^{2+} + 2HCO_3^- \leftrightarrow CO_2 + CaCO_3 + H_2O$

(2) The precipitation of $CaCO_3$ provides protection for the algae, enabling them to avoid being eaten by fish and/or invertebrates as well as offering mechanical resistance against physically-damaging factors such as wave action and strong currents (Bilan and Usov, 2001).

Coralline red algae calcification usually occurs during daylight as demonstrated by Chisholm (2000) in the Great Barrier Reef, Australia. At night, a dissolution pattern can occur, due to the acidification of the algal tissues caused by respiration.

On a seasonal timescale, the carbonate production is generally higher during the spring/summer months with poorly calcified but large cells being generated whereas, during winter, small but more heavily calcified cells are observed (Moberly, 1968). This contrast in size and density of the cells between summer and winter periods is responsible for the presence of well-defined growth increments forming a characteristic seasonal banding along the alga main axis of growth (e.g. Foster, 2001; Halfar et al., 2008; Kamenos et al., 2008). It also has been observed that, in addition to the seasonal banding presented by the coralline red algae, higher frequency banding may occur (Halfar et al., 2000; Foster, 2001); the first order of banding being usually a single row of cells. Between this first order banding and the seasonal banding, there could be two or three orders, including monthly- or weekly-formed bands (Adey, 1965; Moberly, 1968).

In a lot of crustose coralline algae species, the annual growth bands (pairs of large and less calcified summer cells and small and dense winter cells) can also be determined by the presence of uncalcified cavities aligned along the growth axis and called conceptacles. The conceptacles host the sporangial and gametangial, reproductive structures of the alga. For the group *Clathromorphum*, in which they are easily identifiable (e.g. Lebednik, 1977;

Hetzinger et al., 2009 with *C. nereostratum* and Halfar et al., 2008 with *C. compactum*), they are thought to form during the fall/winter months by a decalcification of the previous summer-grown cells (Adey, 1965). As the alga continues to grow throughout the next spring/summer season, these 'holes' in the calcite skeleton are overgrown by newly deposited calcite layers leaving, each year, evidence of a hiatus during the alga growth, defined as staining lines (Hetzinger et al., 2009). These hiatuses, however, do not appear all along the growth bands: Lebednik (1977) estimated them to occupy approximately 65% of the annual increment. They can, therefore, be avoided during analysis, if a comprehensive growth record is needed (e.g. Hetzinger et al, 2009, 2011). In some coralline algae species though, the conceptacles are not easily visible or absent as they can be buried, or their roof can be abraded and the cavity filled. In those cases, the determination of the annual cycles has to rely on the observation of the growth bands of different densities (e.g. *Lithothamnion glaciale* - Kamenos et al., 2008, *Sporolithon durum* – this study).

Concerning the processes of calcification at a cellular level, in marine calcareous algae, they typically occur in the organic matrix (usually the upper layer of cells which corresponds to the living tissue). According to the algal groups, three different types of calcification can be distinguished:

- Extra and intercellular calcification;
- Calcification of cell walls;
- Intracellular calcification.

The green algae *Halimeda* and the coccolithophorids are the most studied representatives of two opposite types of calcium carbonate precipitation: the calcification process of the genus *Halimeda* takes place between the cells, making it a particular case of extracellular calcification. This type of $CaCO_3$ precipitation implies very little or no influence of organic molecules in the calcification process. However, some polyanions of a polysaccharide nature, present in several species of *Halimeda*, had been found to be able to bind Ca^{2+} ions due to the presence of anionic groups in their molecules (Borowitzka and Larkum, 1976). This suggests that these polysaccharides might play a role in the calcification process. On the other hand, it also had been found that these organic molecules tend to form before the actual formation of $CaCO_3$ crystals (Nakahara and Bevelander, 1978). These findings argue towards a passive process of crystallisation in the *Halimeda* green algae which is more likely to be driven by the increase of pH during photosynthesis (De Beer and Larkum, 2001).

The calcification of coccoliths (calcareous scales forming a 'crust' at the surface of the coccolithophorids' surface) is much more complex as it takes place within the algal cells. The coccoliths are formed inside the cells in special vesicles where polysaccharide molecules play a major role in the fixation of Ca^{2+} cations, as well as in their transportation towards organic preforms of coccoliths where the mineralisation process begins (Bilan and Usov, 2001). Afterwards, mature coccoliths are brought outside the vesicles and make their way inside the cell to reach the outside and form the calcitic 'coccosphere'. During this complex process, organic influence on the final crystallisation form of the coccoliths cannot be ignored, as the polysaccharides are even thought to regulate the shape of the calcitic crystal (Henriksen et al., 2004). Therefore, there is no doubt about a significant 'vital effect' during the calcification of these unicellular algae.

The coralline red algae, as a group (Rhodophyta), are situated in between the *Halimeda* and the coccolithophorids when considering the calcification process. Indeed, the calcium carbonate is not formed outside, nor within the living cell, but within the cell walls (Chisholm, 2003). There, photosynthesis creates an organic environment in which the calcite crystals are deposited. It was observed that a unique type of polysaccharide is present inside the cell walls and that, at the beginning of the mineralisation process, calcium carbonate crystals are situated along these fibril-forming polysaccharides, tangentially to the cell membrane (Bilan and Usov, 2001). The authors therefore suggest that there is a likely relationship between these polysaccharide fibrils and the deposition of calcite within the cell walls.

Furthermore, the peculiar polysaccharides that coralline red algae possess are exclusive to their group and radically different from the ones of the other groups of red algae that are non calcareous. It is then proposed that this special feature is directly related to the calcification process in coralline algae (Bilan and Usov, 2001). Another study has also enlightened the fact that these polymers could be responsible for favouring the formation of magnesium calcite over aragonite, as they seem to inhibit growth of newly-formed aragonite nuclei (Wada et al., 1993). They could, then, be able to transform into more stable calcite crystals. This might explain the singularity of the coralline red algae in forming magnesium calcite in the oceans whereas all the other calcareous algal groups (except coccolithophorids) form aragonite. This specificity of coralline red algae to secrete calcite in an environment where aragonite is the most stable form of calcium carbonate has also been observed by (Ries, 2009) in an experimental study: coralline algae were grown in several experimental seawaters where the molar Mg/Ca ratios (mMg/Ca) varied. For a ratio of 7.0, abiotic precipitation tends to form aragonite (Hardie, 1996). For this mMg/Ca ratio, Ries (2006; 2009) found that coralline red algae would still form a high-Mg

calcite, suggesting that the alga plays an active role in the mineralisation of calcium carbonate into calcitic polymorphs.

Bilan and Usov (2001) have also found other unusual polymers within the cell walls of the majority of coralline algae that could participate in the formation of calcite: alginic acids. It is noteworthy that these polymers are known to be specific components of the cell walls of brown seaweeds and are unknown to be synthetised by any other plants but only some specific bacteria. The significant characteristic of these alginic acids is that they potentially have a high affinity to bivalent cations (including Ca^{2+}). This fact could engender alginates possibly be implicated in the calcification process of coralline algae. However, among all the genera of brown algae (for which alginic acids are a specification), only one, *Padina*, secretes calcium carbonate under an aragonitic form and the type of calcification is extracellular (Bilan and Usov, 2001). So, the role of alginates in the precipitation of calcite in coralline algae might have to be reconsidered.

In summary, the Ca^{2+} binding potential of the polysaccharides may need to be taken into account to explain the biomineralisation of coralline red algae. This characteristic could, for example, justify the slight differences recorded in the fractionation of bivalent cations between abiotic calcite and coralline algae (e.g. Ries, 2006). However, it is thought that the 'vital effect' on the calcification of these organisms remains relatively small, therefore making the calcareous skeleton of coralline red algae, a reflection of its surrounding environment (see the "Geochemistry" section – e.g. Halfar et al., 2000; Ries, 2006; 2009; Kamenos et al., 2008; 2009; Hetzinger et al., 2009).

II-4.d Succession of species in the same organism

Rhodoliths are frequently monospecific and continuously growing (i.e. the same species forms the entire nodule, without obvious cessation of growth through time – e.g. Halfar et al., 2000; Goldberg and Heine, 2008; Harvey and Bird, 2008). However, they also can present discontinuities in their growth pattern, arguing for a stop in the activity of the alga for a certain period of time (e.g. Littler et al., 1991; Lund et al., 2000; Basso et al. 2009; Figueiredo et al., 2012). This cessation of production from the coralline algae can have different causes. The most common in the case of rhodoliths is burial of the nodule by sediment for quite sometime, generally more than a few months (Figueiredo et al., 2009). As rhodoliths need an environment with reasonable water motion to develop, that characteristic can also, at times, play against them as the current can roll the ball-like organisms to an unsuitable area where they will sink into the soft sediment, or simply be

covered by the sediment (often sand) transported in the water flow (Littler et al., 1991; Goldberg, 2006). Another reason for stopping the algae's activity can be a drop in seawater temperature, going under the optimal temperature range for a specific species to continue growing. Coralline red algae living in high latitudes are the most favourable subjects for this type of growth cessation (e.g. Halfar et al., 2007). In polar regions as well, light can play a major role in stopping the productivity of calcareous algae. Either because of an over exposition or a lack of light, coralline algae can stop developing at some stage of their growth (see Schwarz et al., 2005).

After a cessation of growth long enough to lead to the death of the algae (in the case of burial into the sediment, this period can go from a few years to several thousands of years (Littler et al. 1991), a climatic (or other) event can make the rhodoliths or the crusts re-appear to the surface or back to acceptable conditions so they can be re-colonised by other coralline algae. The re-colonisation can come from the same species of coralline or from a new species. Frequently, interruptions of growth in a rhodolith are quite easily distinguishable and are characterised by thin layers of a darker colour (Littler et al., 1991; Lund et al., 2000; Basso et al., 2009), thin sandy layers or empty spaces (personnal observation), but sometimes, especially in the case of the same species re-colonising, these successions of growth phases are more ambiguous (see Goldberg, 2006). Regarding the succession of species or genera in a single rhodolith, two hypotheses are envisaged. The first one tends to state that different species are most favourable in settling over different sizes of substrate. Adey and MacIntyre (1973) suggested that a change in the dominant species of coralline red algae reflects the difference in the potential of these species to colonise a more stable or unstable substrate. For instance, these authors observed that very thin and rapidly growing crustose species of the genus *Fosliella* are the most frequent dominant species on bare pebbles or at the start of a rhodolith sequence, when the substrate is very unstable. Then, by the time the nodule gets bigger and more stable, other species, mostly branching, from different genera such as *Lithothamnion* or *Neogoniolithon*, will take over and be the dominant rhodolith-formers. This theory is supported by the study of Steneck (1986), who suggested that the global pattern of succession in corallines over time is a replacement of the thinner, unbranched crusts by thicker and/or branched specimens.

On the other hand, a question about secular environmental changes being responsible for the changes in coralline species remains. As different species/genera have different abilities to thrive in variable environments, this could play a significant role in the succession of species along the same rhodolith. This argument has been raised, for example by Basso et al. (2009) where 40% of the rhodoliths from New Zealand these authors observed, presented clear transitions between several distinct periods of growth.

The large majority of the specimens, though, does not show a change in species as the nodule grew, meaning that an increase in size does not necessarily involve the onset of a succession of species if the environmental conditions remain the same.

In any case, more work is needed on the variation of coralline algae species along the same rhodolith to be able to determine whether it is a result of environmental changes, change in the size of the nodule or a combination of both of these factors. Concerning the latter, it is interesting to note that Basso et al. (2009) did find some of their specimens that had preserved their original, internal, thin crust from the genus *Lithophyllum*, and then, showed a transition to a branching species of *Sporolithon*.

II-5 Geochemistry

Ever since scientists became interested in a better understanding of the mode of growth and calcification or the elemental composition of the coralline red algae, geochemical studies became an essential tool to push the investigations further. However, in comparison with the number of papers published on the ecology, taxonomy or colony description, very few projects involving chemistry appeared in the literature. Nevertheless, with advances in the technologies, the recent years have seen a bloom of successful geochemical interests in coralline algae. Geochemical studies particularly involve radiocarbon dating, which considerably helped with age estimations of individuals. Invaluable information on the growth rates of these organisms has also been obtained from this technique. Very recently, age determination of coralline algae using uranium-series methods has also been tested. Other studies focused on exploring how the geochemistry of the coralline skeleton could provide us with new insights into their surrounding environment and, in particular, seawater temperature or ocean circulation. These studies generally involve the measurement of the isotopic composition of oxygen ($\delta^{18}O$) or the proportion of trace elements incorporated into the carbonate skeleton of the algae during their growth. Most of these projects greatly benefited from recent advances in the techniques that were successfully carried out.

II-5.a Age determination and growth rate

Several studies used radiocarbon dating in order to determine the age of rhodoliths or coralline red algae crusts and deduce the growth rate of individuals. All of these studies chose the Accelerator Mass Spectrometry (AMS) as the preferred technique to obtain their data. Littler et al. (1991), among others, found that modern rhodoliths from the San

Salvador seamount, Bahamas, had ages much older than expected (112-880 years old). These authors also reported quite a big gap between the outermost layers of the nodules and the central layers ranging from 625 to 1295 years old. This confirmed the hypothesis, already made by visual observations, that hiatuses exist in the growth pattern of the organisms in the area. Indeed, the large age differences between different sections of the rhodoliths suggest a cessation of growth during a burial period and a re-colonisation when the nodules re-appeared at the surface (Littler et al., 1991). The same conclusions were reached by Goldberg (2006), also based on ^{14}C dates carried out on rhodoliths from Esperance Bay, Western Australia. The outer layers gave a modern age whereas the inner ones could be as old as AD 1050. These differences between the two ranges of age could not be explained by a continuous growth at the average 0.4 $mm.y^{-1}$ growth rate proposed by Foster (2001). Hence, these rhodoliths have been interpreted as one (or multiple) period(s) of burial and re-exposure of the rhodoliths through time (Goldberg, 2006).

With the help of radiocarbon dating, Frantz et al. (2000; 2005), on the other hand, proved that rhodoliths and coralline red algae crusts can be growing continuously and, therefore, that ^{14}C dates can represent a great tool in the determination of growth rates. From a modern specimen of *Lithothamnion crassiusculum* from the southern Gulf of California, Mexico, Frantz et al. (2000) analysed 52 samples along a ~5 cm-long transect, the samples being taken at 1 mm interval. The results showed pre-bomb and post-bomb $\Delta^{14}C$ levels and an abrupt change in the values in between, which enabled them to calibrate their dates and calculate an average growth rate of 0.6 ±0.1 $mm.y^{-1}$ for the rhodolith (Frantz et al., 2000). The same technique was used to determine the growth rate and age of a modern *Clathromorphum nereostratum* crust from the Aleutian Islands (Frantz et al., 2005). The $\Delta^{14}C$ values were correlated to the 'Atom bomb peak' in the atmosphere, then an age of 61-75 years old and a growth rate of 0.30 $mm.y^{-1}$ could have been deduced (Frantz et al., 2005).

Another dating method involving the uranium (U) and thorium (Th) series was tested on coralline red algae. Halfar et al. (2007) used a Multi Collector Inductively Coupled Plasma Mass Spectrometer (MC-ICP-MS) to obtain two U/Th dates for one of their coralline algal species *C. nereostratum*. The two dates of 99 ±21 and 34 ±16 years old matched exactly their growth band counting (Halfar et al., 2007), confirming (1) that the individual grew continuously over its lifespan and (2) that the U/Th dating seems to be a reliable tool to estimate the age of a coralline red algae. In the same study, a specimen of *C. nereostratum* was also successfully U/Th-dated at 850 ±28 years cal BP (Halfar et al., 2007).

The only other study dealing with coralline U/Th dating used Thermal Ionisation Mass Spectrometry (TIMS) and seems to be in contradiction with the optimistic findings of Halfar et al. (2007). Linge et al. (2008) were interested in dating much older coralline red algae as well as recent ones to better constrain the initial U/Th conditions to evaluate the fossil results. Their findings suggest rejecting every date obtained by the U-Th methods as both recent and fossil samples present signs of open-system conditions (Linge et al., 2008). The activity ratio of modern samples was too variable to lead to reliable dates and, for the fossil samples, the concentrations of uranium and thorium as well as the activity ratio increased along with the stratigraphy, suggesting a post-mortem uranium and thorium enrichment. Hence, when comparing U/Th ages with the stratigraphy (independently dated), some samples showed older ages, suggesting an enrichment of uranium through open-system condition phases; but most of the analysed samples revealed younger ages than expected, implying a significant uptake of thorium in the system that is not fully understood (Linge et al., 2008). In any case, these authors imply that the use of U/Th dating for fossil coralline algae does not seem to be reliable.

However, concerning the variability of the uranium activity in recent samples, there is a need to measure the activity ratio of seawater to assess if there is a real disequilibrium between the sample and the surrounding seawater, which has not been done in the study. If there is disequilibrium, then the measurement for the recent samples made by Linge et al. (2008) could be, in fact, considered as reliable. Also, considering the fact that TIMS technique was used for this study and the measurements of U and Th were usually very close to the detection limit (Linge et al., 2008), it is likely that this technique might not have the required sensitivity to measure such small quantities of material, leading to a potential very important contamination factor in the outcomes of the analysis. The use of a MC-ICP-MS, which could lead to precision of measurements 5 times higher than the TIMS (Fietzke et al., 2005), could compensate for this potential source of error and might allow for accurate dating using the U- Th-series method as illustrated in Halfar et al. (2007).

II-5.b Coralline red algal skeleton geochemistry as an archive of the environment

II-5.b.1 Magnesium variations as a proxy for seawater temperature

Chave (1954) was the first to publish information on the relation between the proportion of magnesium (Mg) present in calcareous algae and their environment. In his investigations, using X-Ray and wet chemistry techniques to gain insights into the

biochemistry of Mg in marine organisms, he noticed that, as for most other organisms (e.g. corals, foraminifera, ostracods), calcareous algae show a positive correlation between their magnesium carbonate ($MgCO_3$) content and the surrounding seawater temperature. This relationship between Mg and temperature was, however, stated as "less perfect" than in the other groups studied (Chave, 1954). A proposed explanation was the wider variety in taxonomy presented by calcareous algae compared to the other groups. Indeed, Chave (1954) conducted his experiments on very different types of algae, from the articulated genus *Amphiroa*, to the crustose *Lithothamnion*. He, therefore, based his observations on a wide range of families and genera and concluded that the study of one particular family or genus is most likely to give a much better correlation between the $MgCO_3$ content and the water temperature (Chave, 1954).

One had to wait more than ten years for the publication of another study involving the Mg geochemistry of coralline algae (Chave and Wheeler, 1965). This time, the authors focused on a single organism of the cold-water species *Clathromorphum compactum*. X-Ray diffraction analyses along the growth axis show significant changes (>40%) in the Mg composition of the skeleton during the growth of the alga. These variations were related to annual cycles and assumed to be a consequence of the temperature variations at the site of study (Chave and Wheeler 1965). The annual cycles displayed by the changes in $MgCO_3$ were also used to estimate the average growth rate of the individual to ~500 $\mu m.y^{-1}$. Pointing to a similar direction, Moberly (1968), used electron microprobe analyses to show that the Mg content of coralline algal skeleton may not only reflect temperature, but also growth changes of the algae.

Despite these encouraging findings on the geochemistry of coralline algae as a potential proxy for environmental reconstructions, no significant study in this area was published until advances in analytical technologies permitted great improvements in sampling resolution and rapidity of analysis, some 25 years later. Halfar et al. (2000) used an electron microprobe to obtain a rapid, high-resolution record of the Mg variations along two rhodolith transects, respectively from a subtropical and a subarctic location. The $MgCO_3$ signals show, in both cases, well-defined cyclic patterns that the authors attributed to the annual variations of temperature at the sites of study. The signals also presented second order cycles that were interpreted as being sub-annual (Halfar et al., 2000). The good correlation they found between the annual extreme peaks of $MgCO_3$ (mol%) and the extreme temperatures enabled them to publish the first $MgCO_3$-temperature calibration equations. The relationship between temperature (T) and, respectively, subtropical and subarctic rhodoliths $MgCO_3$ content was expressed as follow:

$T = 1.15\ MgCO_3\ (mol\%) + 8.15$ (subtropical)

$MgCO_3$ values range from 13.2 to 22.5 mol%;

$T = 0.98\ MgCO_3\ (mol\%) - 7.90$ (subarctic)

$MgCO_3$ values range from 7.7 to 18.5 mol%.

These correlations lead to a variation factor of ~1 mol% $MgCO_3.°C^{-1}$ for both subtropical and subarctic samples. However, temperature reconstructions showed lower amplitude of variations as well as small offsets, relative to the measured temperature. This tends to suggest that other factors (such as a "vital effect") may play a role in Mg incorporation in coralline red algae (Halfar et al., 2000).

The latter study by Halfar et al. (2000) and its promising results marked the "new beginning" of the geochemistry of coralline algae envisaged as an environmental tracer and, particularly, of the use of the Mg content in the skeleton of the algae as a proxy for temperature reconstructions. Halfar's team continued on the investigations on these potential high-resolution archives of extra-tropical climate and came up with another study on a Northern Pacific, subarctic, encrusting coralline algae in which the robustness of the Mg/Ca proxy was assessed by significantly correlated variations of the Mg/Ca signals measured in two organisms of the same species at sites several hundreds of kilometres apart (Hetzinger et al., 2009). In this project, the electron microprobe was used to measure the Mg/Ca ratio along a few-centimetres-long section of the crustose coralline red alga at a resolution of ~15 samples per year. Both signals showed pronounced annual cycles in the Mg/Ca ratio that were related to the regional Sea Surface Temperature (SST) variations of the late spring – late fall period. For *C. nereostratum* from the Amchitka Islands, this relationship was expressed as:

$$SST = 0.266\ MgCO_3\ (mol\%) + 8.788 \qquad (r=0.50;\ n=792)$$

For this region, and that species, it thus seems that the variation factor between the $MgCO_3$ (mol%) and the SST is about 4 times smaller than the one reported by Halfar et al. (2000). However, when compared to a more local SST for a period of 7 years, the variation factor approaches the 1 mol% $MgCO_3.°C^{-1}$ previously observed (Halfar et al., 2000). The range of changes displayed by the Mg/Ca ratio (molar) is 0.096 and fluctuates from 0.084 to 0.180, which correspond to a 7.76 mol% $MgCO_3$ variation, from 6.02 to 13.78 mol% $MgCO_3$, in agreement with previous records of subarctic coralline algae (Chave and Wheeler, 1965, Halfar et al., 2000).

At the same time, in Scotland, another team of researchers grew an interest in the potential outcomes that the climate reconstructions derived from coralline algae could allow. Kamenos et al. (2008) subsequently published the results of a monitoring experiment carried out on a *L. glaciale* and a *P. calcareum* species from Scotland. This comprehensive study aimed at calibrating $MgCO_3$ (along with $SrCO_3$) variations against SST and *in situ* temperatures (IST) using both electron and ion microprobe techniques. Kamenos et al. (2008)'s results show excellent correlations between the Mg/Ca (and $MgCO_3$) geochemical proxy and both IST and SST, further confirming the major temperature control over the Mg variations in the coralline algae skeleton. $MgCO_3$ (mol%) ranges from 12.9 to 24.6 in *L. glaciale* and from 14.7 to 23.8 for *P. calcareum*. This range of values, while still in agreement with previously published ranges, presents higher amplitudes than the ones determined by Halfar et al. (2000) and Hetzinger et al. (2009) that were attributed to a higher resolution of sampling, resulting in a better recording of the extreme values (Kamenos et al. 2008). On the same principle, the linear factor relating SST (and IST) to the $MgCO_3$ content is higher than the ~1 $MgCO_3$ (mol%) $.°C^{-1}$ reported before. Kamenos et al. (2008) found a factor of 1.27 (for IST) and 1.76 (for SST) $MgCO_3$ (mol%) $.°C^{-1}$ for *L. glaciale* and 1.19 $MgCO_3$ (mol%) $.°C^{-1}$ for *P. calcareum*, only compared with SST. The authors also suggested the higher sampling resolution as the explanation for these discrepancies regarding the previously published factors of variation.

Pushing further the assessment that the Mg incorporation in the coralline skeleton is primarily a function of temperature, Kamenos et al. (2009) investigated the location of the Mg atoms within the calcareous structure of their two previously studied rhodoliths of the species *L. glaciale* and *P. calcareum* (see Kamenos et al., 2008). The use of Synchrotron Mg-X-ray Absorbance Near Edge Structure (XANES) allowed them to state that Mg atoms are, indeed, incorporated directly into the calcite lattice, all year round and in the whole thallus areas. Moreover, no contamination by organic sources nor diagenetic process or post-mortem enrichment has been detected, either for modern or sub-fossil samples (Kamenos et al., 2009). This further confirms that Mg variation within the skeleton of coralline red algae is a robust palaeo-temperature proxy.

Most recently, Gamboa et al. (2010) and Hetzinger et al. (2011) used laser ablation ICPMS to obtain high-resolution Mg/Ca variation profiles along transects of coralline red algal crusts both from a previously studied specimen *C. nereostratum* from the Amchitka Islands in the North Pacific and from *C. compactum* from Newfoundland in the North Atlantic. Results of their studies essentially confirmed the ability of the Mg/Ca proxy to reliably record seawater temperatures variations in the high latitudes of the Northern Hemisphere.

Most of the studies on the variations of the Mg content in coralline algae therefore suggest a quasi-exclusive relationship with the surrounding temperatures. However, Ries (2006) conducted a long-scale experiment on the determination of the contribution from the Mg/Ca ratio of the seawater (Mg/Ca_{sw}) to the Mg/Ca ratio in the algae. The results show a strong correlation between the two parameters, implying that the Mg/Ca_{sw} must be taken into account in the calculation of Mg-derived temperatures. The author proposed the following relationship:

$$Mg/Ca = 0.0134\, e^{0.0457\, T} \cdot Mg/Ca_{sw}^{1.01}$$

It is interesting to note the exponential relationship proposed here, instead of the most commonly used linear link between Mg/Ca and temperature. Also noteworthy is the fact that Ries (2006) observed that the correlation does not change with the absolute Mg or Ca concentration in the seawater but only with the Mg/Ca ratio. It appears that the Mg fractionation in the algae is quasi-similar to the one for abiotic-precipitated calcite, suggesting that the algal vital effect must be reduced to a minimum during the Mg incorporation process (Ries, 2006).

The dependence of the Mg/Ca ratio in coralline algae upon the Mg/Ca_{sw} has, therefore, been determined. However, considering the residence time of both Mg and Ca in the ocean (respectively 13 My and 1 My; e.g. Chester and Jickells 2009), the timescale of potential Mg/Ca variations in the oceans well exceeds the one usually dealt with for palaeoclimatic reconstructions from corallines (several decades to centuries). Therefore, it is easily conceivable to assume that the Mg/Ca_{sw} is constant throughout any period of high-resolution study. Then, a quasi-exclusive temperature-derived explanation could be advanced for the observed oscillations of the Mg/Ca signal in the coralline red algae skeleton at any given time.

II-5.b.2 *Other temperature indicators: $\delta^{18}O$, Sr/Ca, U/Ca and Ba/Ca*

Interestingly, despite the measurement of the oxygen isotopic composition ($\delta^{18}O$) being a very commonly used proxy for palaeo-temperature reconstructions from various biogenic carbonates over the years (e.g. Waelbroeck et al., 2005 for foraminifera; Corrège, 2006 for corals), its use on coralline red algae was not assessed until the study by Halfar et al. (2000). Besides their interest for the Mg incorporation into the algal skeleton, these authors also measured the $\delta^{18}O$ in *L. crassiusculum* (subtropics) and *L. glaciale* (subarctic), using mass spectrometry, to assess the $\delta^{18}O$ relationship with the surrounding environmental parameters. The $\delta^{18}O$ signals recorded in both rhodolith species show

distinctive cyclic patterns that the authors attributed to the annual variations of SST in both, the subtropical and subarctic regions. Hence, a generic equation of calibration was proposed, linking the $\delta^{18}O$ measured in coralline red algae, to the temperature, by:

$$T = 16.5 - 4.3\,(\delta^{18}O_s - \delta^{18}O_{sw}) + 0.14\,(\delta^{18}O_s - \delta^{18}O_{sw})^2 + 0.06B$$

Where: $\delta^{18}O_s$: $\delta^{18}O$ of the sample
$\delta^{18}O_{sw}$: $\delta^{18}O$ of seawater
B: correction factor for the algal Mg content of +0.06‰.mol% $MgCO_3^{-1}$ (from Tarutani et al., 1969)

The SST reconstructions presented from this relationship suggest that the $\delta^{18}O$ could be a reliable proxy for temperature variations (Halfar et al., 2000). However, in both cases, an offset from the absolute SST value recorded was observed. This offset was +6°C for *L. crassiusculum* and ~+12°C for *L. glaciale*. The offset on the calculated temperature values was attributed to either a variation in the $\delta^{18}O_{sw}$ or other effects that have not been taken into consideration, in particular, a potential vital effect (Halfar et al., 2000). The authors suggested that this offset might be constant within a species or genus, and if so, the $\delta^{18}O$ variations of coralline red algae could potentially be a reliable indicator of temperature change overtime.

Further investigation on the $\delta^{18}O$ composition of coralline red algae were reported in Halfar et al. (2007) and most particularly Halfar et al. (2008), in which the first monitoring experiment was conducted on a *C. compactum* crust section, with the aim of calibrating the $\delta^{18}O$ variations against instrumental temperature. It resulted a reliable reconstruction of local SST (r=0.85) over a yearlong period, further confirming the potential of the $\delta^{18}O$ signal in coralline algae as a temperature proxy (Halfar et al., 2008).

The first results on $SrCO_3$ composition of a coralline algal skeleton were presented in Kamenos et al. (2008) as a potential indicator of temperature variations. Although the relationships between $SrCO_3$ (mol%) and IST and SST are weaker than for the $MgCO_3$, they still are highly significant (respectively, r=0.66 and r=0.83; p<0.0001). However, due to the better temperature reconstruction provided by the $MgCO_3$ variations, Kamenos et al. (2008) recommend the use of the latter for future studies. The same conclusion has been reached by Hetzinger et al. (2011) in their study of coralline crusts where Sr/ca variations are significantly correlated with seawater temperature changes but are weaker than for Mg/Ca. These authors also found an unconvincing, however still statistically significant, anti-correlation between SST and U/Ca and Ba/Ca variations for the species *C. compactum*

from the North Atlantic (r=-0.37; p<0.01 for both signals), whereas the other analysed species *C. nereostratum* showed no significant correlation between seawater temperature and U/Ca or Ba/Ca signals (Hetzinger et al., 2011).

II-5.b.3 Most recent developments

With the objective of expanding the array of environmental parameters that it is possible to record using coralline red algae, the most recent geochemistry studies involve variations of the Ba/Ca composition used as a proxy for freshwater runoff to reconstruct salinity changes in the North Pacific (Chan et al., 2011) or $\delta^{13}C$ as a water masses tracker to get insight into upwelling variability in the North Pacific and the Bering Sea (Williams et al., 2011).

II-6 Palaeoenvironmental interpretations

Coralline algae usually present a relatively long-lived carbonate skeleton (up to ~850 years old; Littler et al., 1991; Halfar et al., 2007) that preserves very well into sediment. Frequently, rhodoliths or coralline red algae crusts have been observed as fossils in geological sequences. These faculties of great conservation through time, as well as the singular characteristics they possess, lead the scientific community to try to use these organisms as palaeoenvironmental indicators.

Taxonomic assemblages and morphology have been used to interpret palaeoenvironments (Lund et al., 2000; Payri and Cabioch, 2004), however, considering the discussions above, in most cases it seems highly ambitious to use these criteria to obtain precise and reliable information about past living conditions. This cautionary approach has previously been suggested by Adey and McIntyre (1973) and Foster (2001) in their respective reviews.

On long-term time frames, the presence of rhodoliths or coralline crusts facies may, however, be an indicator of changes in the nutrient richness of shallow waters environments. Indeed, there exists a nutrient-quantity gradient in the optimal living range of corals, coralline algae and molluscs/bryozoans, corals being the most abundant community in oligotrophic environments and molluscs/bryozoans preferring eutrophic settings (Mutti and Hallock, 2003). Halfar and Mutti (2005) used these observations to suggest an increase of nutrients, resulting from an increase of trophic resources and primary production in the oceans, during the Middle Miocene (10-17 Ma). This latter period was characterised by a replacement of the coral reefs in the tropical/subtropical zones, by coralline algae communities, representative of mesotrophic environments

(Halfar and Mutti, 2005). The potential of coralline algae as a palaeoenvironmental proxy was also suggested by Ries (2006; 2009) who envisaged the possibility of reconstructing past Mg/Ca ratios of seawater (Mg/Ca_{sw}) using the Mg/Ca ratio of corallines. The latter being essentially influenced by temperature and the Mg/Ca of seawater, on larger timescales. If, for example, the temperature effect can be corrected, then, coralline red algae could become archives of past changes in the Mg/Ca_{sw} throughout the Phanerozoic (Ries, 2006; 2009).

At smaller (centuries to potentially millennia) timescales, coralline red algae recently showed a promising capability to be palaeoenvironmental indicators through the periodic growth increments that they form and the geochemical composition of their calcareous skeleton.

Annual growth increments were used by Halfar et al. (2010) to reconstruct a 115-year old record of climate variability of the North Atlantic region from multiple specimens of *C. compactum* collected in multiple sites in the area. In this study, changes in widths of coralline red algal growth increments were related to a well known warming of the northwestern Atlantic SST in the 1990s as well as they highlighted a possible warmer period than previously thought in the area during the 1920-1930s (Halfar et al., 2010). The same technique was also employed to reconstruct a 225-year climate record in the Bering Sea region, with the coralline red algal growth-increment widths used as a proxy of light intensity (Halfar et al., 2011). The variability in light intensity was interpreted as changes in marine cloud cover and abundance of phytoplankton in the water column, two phenomena closely related to the strength of the dominant climate pattern in the region, the Aleutian Low (Halfar et al., 2011). Despite these successful reconstructions, growth-increment widths cannot always be correlated with environmental parameters as shown by the absence of correlation observed by Burdett et al. (2011) between their 96-years record of growth-increment widths measured along branches of *L. glaciale* rhodoliths from Scotland and the regional instrumental SST and marine cloud cover patterns. However, these authors were able to use changes in the calcification pattern of the rhodoliths to get insights into multi-decadal climate variations in the region (Burdett et al., 2011). More recently, annual growth bands of coralline red algae were used to reconstruct runoff from a section of the Greenland Ice Sheet, covering the 1939-2002 period (Kamenos et al., 2012a). This study links local summer marine temperatures to the intensity of the discharges. It manages in particular to reconstruct a trend of increasing runoff since the mid-1980 that is backed up by instrumental data (Kamenos et al., 2012a).

The depletion in radiocarbon values along a rhodolith transect has been used for palaeoenvironmental reconstructions as it showed to be linked to changes in past oceanic conditions related to the ENSO phenomenon in the Gulf of California (Frantz et al., 2000).

During the strong El Niño phases of 1957, 1982 and 1992, older water masses from the Deep Pacific came into the Gulf of California, replacing the usual source of water composed with surface to sub-surface water masses. These differences in apparent reservoir age have been recorded in a *L. crassiusculum* rhodolith skeleton, assessing the use of the $\Delta^{14}C$ values, not only as an age indicator, but also as a potential proxy for past oceanic circulations (Frantz et al., 2000).

Using the relationship between the magnesium content of the calcareous structure and SST, Kamenos et al. (2008) suggested that for the North Atlantic SST variations during the early Holocene could have been two times less pronounced than today. These results, for example, could contribute in refining climatic reconstructions for this high-latitude area for the Holocene.

A high-resolution (i.e. sub-annual) $\delta^{18}O$ record, ranging from -2 to 2 ‰ was obtained from a 117-years old *C. nereostratum* from the northern Pacific (Aleutian Islands) and showed a significant correlation with the regional SST over a 43 years period ($r=-0.46$; $p<0.0015$; Halfar et al., 2007). As this relationship appears not to be exclusive, the authors invoked a role of the $\delta^{18}O_{sw}$ variations as the second main parameter influencing the alga $\delta^{18}O$ signal. Hence, when they observe a correlation between the $\delta^{18}O$ of the coralline red algae and the Pacific Decadal Oscillation (PDO) or the NINO4 index, they conclude a "warming and/or freshening" of the water during positive PDO or NINO4 index; and "cooler and/or more saline" waters when these indexes are negative (Halfar et al., 2007). In the northern Atlantic, $\delta^{18}O$ data from a coralline crust collected in the Gulf of Maine indicate similar patterns as a 30 year-long record of the North Atlantic Oscillation (NAO) signal (Halfar et al., 2008). The signal particularly displays a strong effect of Labrador Current inputs of colder waters in the area when the NAO is strongly positive (Halfar et al., 2008). Following this study, inter-annual variations of the Mg/Ca composition of *C. compactum* from the North Atlantic provided a 116-year reconstruction of SST changes that were linked to NAO variability and its effect on the water circulation in the region (Gamboa et al., 2010). Similarly, several-decades-long records of SST variations at monthly to sub-monthly resolution were obtained in the North Atlantic and North Pacific from coralline red algal Mg/Ca composition (Hetzinger et al., 2009; 2011) and the longest SST time series generated so far was obtained from *L. glaciale* rhodoliths from Scotland and spans the last ~650 years, dating back to 1353 AD, therefore covering the Little Ice Age (Kamenos, 2010). Implications of the rising of SST since the end of the Little Ice Age, and most particularly since the beginning of the 20th century are discussed in the latter study, in relation with the NAO, the Atlantic Multidecadal Oscillation (AMO), the Atlantic

Meridional Overturning Circulation (AMOC) as well as a perspective on the regional marine zooplankton evolution pattern (Kamenos, 2010).

More recently, upwelling activity and the climate pattern of the multidecadal pattern of the Aleutian Low (North Pacific) were reconstructed from carbon isotopic composition ($\delta^{13}C$) variations in *C. nereostratum* and suggest, for instance, a possible intensification of this regional climatic phenomenon form the 1960s to the 1990s (Williams et al., 2011). Changes in ocean circulation and particularly the Alaska Coastal Current were also observed through salinity changes recorded by Ba/Ca variations in the same coralline red algae species. A 60-year-long record was generated that indicated a recent intensified freshening of the Alaska Coastal Current that may be linked to an increase of ice melting and precipitation in the northeastern Pacific since the beginning of the 21st century (Chan et al., 2011).

In summary, the last decade has seen the emergence and expansion of the use of coralline red algae as a potential tool for palaeoenvironmental reconstruction, for various parameters, especially in the high latitudes. These encouraging, successful pioneer studies need, however, to be complemented with the use of different species, in different locations, particularly in the tropics in order to assess the potential of coralline red algae as a group, as a reliable proxy at the global scale. This way, coralline red algal climate data could be incorporated into general climatic models and help improve Future Climate predictions. This thesis is a contribution to this endeavour.

References

Adey, W., H., and MacIntyre, I., G. 1973. Crustose coralline algae: a re-evaluation in the geological sciences. *Geological Society of America Bulletin* **84**, 883-904.

Adey, W. H. 1965. The genus Clathromorphum (Corallinaceae) in the Gulf of Maine. *Hydrobiologia* **26**(3), 539-573.

Adey, W. H., and McKibbin, D. 1970. Studies on the maerl species *Phymatolithon calcareum* (Pallas) nov. comb. and *Lithothamnium coralloides* Crouan in the Ria de Vigo. *Botanica Marina* **13**(2), 100-106.

Aguirre, J., Riding, R., and Braga, J., C. 2000. Diversity of coralline red algae: origination and extinction patterns from the Early Cretaceous to the Pleistocene. *Paleobiology* **26**(4), 651-667.

Alexander, I., Andres, M. S., Braithwaite, C. J. R., Braga, J. C., Cooper, M. J., Davies, P. J., Elderfield, H., Gilmour, M. A., Kay, R. L. F., and Kroon, D. 2001. New constraints on the origin of the Australian Great Barrier Reef: results from an international project of deep coring. *Geology* **29**, 483-486.

Amado-Filho, G. M., Moura, R. L., Bastos, A. C., Salgado, L. T., Sumida, P. Y., Guth, A. Z., Francini-Filho, R. B., Pereira-Filho, G. H., Abrantes, D. P., and Brasileiro, P. S. 2012. Rhodolith beds are major $CaCO_3$ bio-factories in the tropical south west atlantic. *PloS one* **7**(4), e35171.

Andersson, A. J., Mackenzie, F. T., and Bates, N. R. 2008. Life on the margin: implications of ocean acidification on Mg-calcite, high latitude and cold-water marine calcifiers. *Marine Ecology Progress Series* **373**, 265-273.

Anthony, K. R. N., Kline, D. I., Diaz-Pulido, G., Dove, S., and Hoegh-Guldberg, O. 2008. Ocean acidification causes bleaching and productivity loss in coral reef builders. *Proceedings of the National Academy of Sciences* **105**(45), 17442-17446.

Ballantine, D. L., Bowden-Kerby, A., and Aponte, N. E. 2000. Cruoriella rhodoliths from shallow-water back reef environments in La Parguera, Puerto Rico (Caribbean Sea). *Coral Reefs* **19**(1), 75-81.

Basso, D. 1998. Deep rhodolith distribution in the Pontian Islands, Italy: a model for the paleoecology of a temperate sea. *Palaeogeography, Palaeoclimatology, Palaeoecology* **137**(1), 173-187.

Basso, D., Nalin, R., and Nelson, C., S. 2009. Shallow-water *Sporolithon* rhodoliths from North Island (New Zealand). *Palaios* **24**, 92-103.

Basso, D. 2012. Carbonate production by calcareous red algae and global change. *Geodiversitas* **34**(1), 13-33.

Benton, M. J. 1995. Diversification and extinction in the history of life. *Science* **268**, 52-58.

Bilan, M. I., and Usov, A. I. 2001. Polysaccharides of calcareous algae and their effect on the calcification process. *Russian Journal of Bioorganic Chemistry* **27**(1), 2-16.

Binda, P. L. 1973. Form and internal structure of Recent algal nodules (rhodolites) from Bermuda: a discussion. *The Journal of Geology* **81**(2), 238-238.

Bittner, L., Payri, C. E., Maneveldt, G. W., Couloux, A., Cruaud, C., De Reviers, B., and Le Gall, L. 2011. Evolutionary history of the Corallinales (Corallinophycidae, Rhodophyta) inferred from nuclear, plastidial and mitochondrial genomes. *Molecular phylogenetics and evolution* **61**(3), 697-713.

Borowitzka, M. A., and Larkum, A. W. D. 1976. Calcification in the green alga *Halimeda*: II. The exchange of Ca2+ and the occurence of age gradients in calcification and photosynthesis. *Journal of Experimental Botany* **27**(5), 864-878.

Bosellini, A., and Ginsburg, R. N. 1971. Form and Internal Structure of Recent Algal Nodules (Rhodolites) from Bermuda. *The Journal of Geology* **79**(6), 669-682.

Bosence, D., W. J. 1983a. Description and Classification of Rhodoliths (Rhodoids, Rhodolites). *In* "Coated Grains." (T. M. Peryt, Ed.), pp. 217-224. Springer-Verlag, Berlin.

Bosence, D., W., J. 1983b. The Occurence and Ecology of Recent Rhodoliths - A Review. *In*

"Coated Grains." (T. M. Peryt, Ed.), pp. 225-242. Springer-Verlag Berlin.

Bosence, D. W. J. 1976. Ecological studies on two unattached coralline algae from western Ireland. *Palaeontology* **19**(2), 365-395.

Burdett, H., Kamenos, N. A., and Law, A. 2011. Using coralline algae to understand historic marine cloud cover. *Palaeogeography, Palaeoclimatology, Palaeoecology* **302**(1-2), 65-70.

Burdett, H., Aloisio, E., Calosi, P., Findlay, H., Widdicombe, S., Hatton, A., and Kamenos, N. A. (2012). Biochemical and morphological effect of low pH on *Lithothamnion glaciale*. *In* "IV International Rhodolith Workshop." Granada, Spain.

Cabioch, G., Montaggioni, L., Frank, N., Seard, C., Sallé, E., Payri, C., E., Pelletier, B., and Paterne, M. 2008. Successive reef depositional events along the Marquesas foreslopes (French Polynesia) since 26 ka. *Marine Geology* **254**, 18-34.

Chan, P., Halfar, J., Williams, B., Hetzinger, S., Steneck, R., Zack, T., and Jacob, D. E. 2011. Freshening of the Alaska Coastal Current recorded by coralline algal Ba/Ca ratios. *Journal of Geophysical Research* **116**(G1), G01032.

Chave, K., E., and Wheeler, B., D., Jr. 1965. Mineralogic changes during growth in the red alga, *Clathromorphum compactum*. *Science* **147**, 621.

Chave, K. E. 1954. Aspects of the biogeochemistry of magnesium 1. Calcareous marine organisms. *The Journal of Geology* **62**(3), 266-283.

Chester, R., and Jickells, T. 2009. Marine geochemistry (3rd Edition). Wiley-Blackwell, 448pp.

Chisholm, J., R.M. 2000. Calcification by crustose coralline algae on the northern Great Barrier Reef, Australia. *Limnology and Oceanography* **45**(7), 1476-1484.

Chisholm, J., R.M. 2003. Primary productivity of reef-building crustose coralline algae. *Limnology and Oceanography* **48**(4), 1376-1387.

Coates, A. G., and Jackson, J. B. C. (1985). Morphological themes in the evolution of clonal and aclonal marine invertebrates. *In* "Population biology and evolution of clonal organisms." (L. W. B. J. B. C. Jackson, and R. E. Cook, Ed.). Yale University Press, New Haven, Conn.

Copper, P. 1994. Ancient reef ecosystem expansion and collapse. *Coral Reefs* **13**(1), 3-11.

Corrège, T. 2006. Sea surface temperature and salinity reconstruction from coral geochemical tracers. *Palaeogeography, Palaeoclimatology, Palaeoecology* **232**(2), 408-428.

da Nobrega Farias, J., Riosmena-Rodriguez, R., Bouzon, Z., Oliveira, E., C., and Horta, P., A. (2009). *Lithothamnion superpositum* (Corallinales; Rhodophyta) - First description for Western Atlantic or a rediscovery of an old known species? *In* "III International Rhodolith Workshop." Buzios, Brazil.

Davies, P. J. 1983. Reef growth. *In* "Perspectives on coral reefs." (D. J. Barnes, Ed.), pp. 69–95. Brian Clouston, A.C.T., Australia,.

De Beer, D., and Larkum, A. W. D. 2001. Photosynthesis and calcification in the calcifying algae *Halimeda discoidea* studied with microsensors. *Plant, Cell & Environment* **24**(11), 1209-1217.

Feely, R. A., Doney, S. C., and Cooley, S. R. 2009. Ocean acidification: present conditions and future changes in a high-CO_2 world. *Oceanography* **22**(4), 36-47.

Fietzke, J., Liebetrau, V., Eisenhauer, A., and Dullo, C. 2005. Determination of uranium isotope ratios by multi-static MIC-ICP-MS: method and implementation for precise U- and Th-series isotope measurements. *Journal of Analytical Atomic Spectrometry* **20**(5), 395-401.

Figueiredo, M. A. O., Coutinho, R., Villas-Boas, A. B., Tamega, F. T. S., and Mariath, R. 2012. Deep-water rhodolith productivity and growth in the southwestern Atlantic. *Journal of Applied Phycology* **24**(3), 487-493.

Figueiredo, M. A. O., Villas-Boas, A. B., Tamega, F. T. S., Mariath, R., and Khader, S. (2009). Burial effects on the primary production of coralline algae of a shallow rhodolith bed in Buzios, Brazil. *In* "III International Rhodolith Workshop." Buzios, Brazil.

Foster, M., S. 2001. Rhodoliths: Between rocks and soft places. *Journal of Phycology* **37**,

659-667.

Foster, M. S., Riosmena-Rodriguez, R., Steller, D. L., and Woelkerling, W. M. J. 1997. Living rhodolith beds in the Gulf of California and their implications for paleoenvironmental interpretation. *Geological Society of America Special Paper* **318**, 127-139.

Frantz, B., R., Kashgarian, M., Coale, K., H., and Foster, M., S. 2000. Growth rate and potential climate record from a rhodolith using ^{14}C accelerator mass spectrometry. *Limnology and Oceanography* **45**(8), 1773-1777.

Frantz, B. R., Foster, M. S., and Riosmena-Rodrìguez, R. 2005. *Clathromorphum nereostratum* (Corallinales, Rhodophyta): The oldest alga? *Journal of Phycology* **41**(4), 770-773.

Freiwald, A., and Henrich, R. 1994. Reefal coralline algal build-ups within the Arctic Circle: morphology and sedimentary dynamics under extreme environmental seasonality. *Sedimentology* **41**(5), 963-984.

Gagnon, P., Matheson, K., and Stapleton, M. 2012. Variation in rhodolith morphology and biogenic potential of newly discovered rhodolith beds in Newfoundland and Labrador (Canada). *Botanica Marina* **55**(1), 85.

Gamboa, G., Halfar, J., Hetzinger, S., Adey, W., Zack, T., Kunz, B., and Jacob, D. E. 2010. Mg/Ca ratios in coralline algae record northwest Atlantic temperature variations and North Atlantic Oscillation relationships. *Journal of Geophysical Research* **115**(C12), C12044.

Goldberg, N. 2006. Age estimates and description of rhodoliths from Esperance Bay, Western Australia. *Journal of the Marine Biological Association of the United Kingdom* **86**, 1291-1296.

Goldberg, N., and Heine, J., N. 2008. Age estimates of *Sporolithon durum* (Corallinales, Rhodophyta) from Rottnest Island, Western Australia, based on radiocarbon-dating methods. *Journal of the Royal Society of Western Australia* **91**, 27-30.

Grall, J., and Hall-Spencer, J. M. 2003. Problems facing maerl conservation in Brittany. *Aquatic Conservation: Marine and Freshwater Ecosystems* **13**(S1), S55-S64.

Halfar, J., Hetzinger, S., Adey, W., Zack, T., Gamboa, G., Kunz, B., Williams, B., and Jacob, D. E. 2010. Coralline algal growth-increment widths archive North Atlantic climate variability. *Palaeogeography, Palaeoclimatology, Palaeoecology*,

Halfar, J., and Mutti, M. 2005. Global dominance of coralline red-algal facies: A response to Miocene oceanographic events. *Geology* **33**(6), 481-484.

Halfar, J., Steneck, R., S., Joachimski, M., Kronz, A., and Wanamaker Jr., A., D. 2008. Coralline red algae as high-resolution climate recorders. *Geology* **36**(6), 463-466.

Halfar, J., Steneck, R., S., Schöne, B., R., Moore, G., W., K., Joachimski, M., Kronz, A., Fietzke, J., and Estes, J. 2007. Coralline alga reveals first marine record of subarctic North Pacific climate change. *Geophysical Research Letters* **34**, L07702.

Halfar, J., Williams, B., Hetzinger, S., Steneck, R. S., Lebednik, P., Winsborough, C., Omar, A., Chan, P., and Wanamaker, A. D. 2011. 225 years of Bering Sea climate and ecosystem dynamics revealed by coralline algal growth-increment widths. *Geology* **39**(6), 579.

Halfar, J., Zack, T., Kronz, A., and Zachos, J., C. 2000. Growth and high-resolution paleoenvironmental signals of rhodoliths (coralline red algae): A new biogenic archive. *Journal of Geophysical Research* **105**(C9), 22,107-22,116.

Hardie, L., A. 1996. Secular variation in seawater chemistry: An explanation for the coupled secular variation in the mineralogies of marine limestones and potash evaporites over the past 600 m.y. *Geology* **24**(3), 279-283.

Harris, P., J., Tsuji, Y., Marshall, J., F., Davies, P., J., Honda, N., and Matsuda, H. 1996. Sand and rhodolith-gravel entrainment on the mid- to outer-shelf under a western boundary current: Fraser Island continental shelf, eastern Australia. *Marine Geology* **129**, 313-330.

Harvey, A., S., and Bird, F., L. 2008. Community structure of a rhodolith bed from cold-temperate waters (southern Australia). *Australian Journal of Botany* **56**, 437-450.

Henriksen, K., Stipp, S. L. S., Young, J. R., and Marsh, M. E. 2004. Biological control on calcite crystallization: AFM investigation of coccolith polysaccharide function. *American*

Mineralogist **89**(11-12), 1709.

Henriques, M. d. O., M., C., Nunes, D. S. P., Coutinho, L. M., Riosmena-Rodriguez, R., and Figuereido, M., A., O. (2009). Deep water *Sporolithon* (Sporolithalceae, Corallinales, Rhodophyta) from Bahia and Espiritu Santo states, Brazil. *In* "III International Rhodolith Workshop." Buzios, Brazil.

Hetzinger, S., Halfar, J., Kronz, A., Steneck, R., Adey, W., H., Lebednik, P., A., and Schöne, B., R. 2009. High-resolution Mg/Ca ratios in a coralline red alga as a proxy for Bering Sea temperature variations from 1902 to 1967. *Palaios* **24**, 406-412.

Hetzinger, S., Halfar, J., Riegl, B., and Godinez-Orta, L. 2006. Sedimentology and acoustic mapping of modern rhodolith facies on a non-tropical carbonate shelf (Gulf of California, Mexico). *Journal of Sedimentary Research* **76**(4), 670-682.

Hetzinger, S., Halfar, J., Zack, T., Gamboa, G., Jacob, D. E., Kunz, B. E., Kronz, A., Adey, W., Lebednik, P. A., and Steneck, R. S. 2011. High-resolution analysis of trace elements in crustose coralline algae from the North Atlantic and North Pacific by laser ablation ICP-MS. *Palaeogeography, Palaeoclimatology, Palaeoecology* **302**(1-2), 81-94.

IPCC (Intergovernmental Panel on Climate Change) 2007. Climate change 2007: Synthesis report. Summary for policy makers. http://www.ipcc.ch/pdf/assessment-report/ar4/syr/ar4_syr_spm.pdf

Jokiel, P. L., Rodgers, K. S., Kuffner, I. B., Andersson, A. J., Cox, E. F., and Mackenzie, F. T. 2008. Ocean acidification and calcifying reef organisms: a mesocosm investigation. *Coral Reefs* **27**(3), 473-483.

Kamenos, N., A., Cusack, M., Huthwelker, T., Lagarde, P., and Scheibling, R., E. 2009. Mg-lattice associations in red coralline algae. *Geochimica et Cosmochimica Acta* **73**, 1901-1907.

Kamenos, N., A., Cusack, M., and Moore, P., G. 2008. Coralline algae are global palaeothermometers with bi-weekly resolution. *Geochimica et Cosmochimica Acta* **72**, 771-779.

Kamenos, N. A. 2010. North Atlantic summers have warmed more than winters since 1353, and the response of marine zooplankton. *Proceedings of the National Academy of Sciences* **107**(52), 22442-22447.

Kamenos, N. A., Hoey, T. B., Nienow, P., Fallick, A. E., and Claverie, T. (2012a). Reconstructing Greenland ice sheet runoff using coralline algae. *Geology* **40**(12), 1095-1998.

Kamenos, N. A., Dunn, J. D., Calosi, P., Findlay, H., Widdicombe, S., Aloisio, E., and Burdett, H. (2012b). Buffering of skeletal calcium carbonate changes by red coralline algae in response to ocean acidification. *In* "IV International Rhodolith Workshop." Granada, Spain.

Kamenos, N. A., and Law, A. 2010. Temperature controls on coralline algal skeletal growth. *Journal of Phycology* **46**(2), 331-335.

Kendrick, G. A., and Brearley, A. 1997. Influence of *Sargassum* spp. attached to rhodoliths on sampling effort and demographic analyses of *Sargassum* spp. (Sargassaceae, Phaeophyta) attached to a reef. *Botanica Marina* **40**(1-6), 517-522.

Konar, B., Riosmena-Rodriguez, R., and Iken, K. 2006. Rhodolith bed: a newly discovered habitat in the North Pacific Ocean. *Botanica Marina* **49**, 355-359.

Kuffner, I. B., Andersson, A. J., Jokiel, P. L., Rodgers, K. S., and Mackenzie, F. T. 2008. Decreased abundance of crustose coralline algae due to ocean acidification. *Nature Geoscience* **1**(2), 114-117.

Le Gall, L., Payri, C., Bittner, L., and Saunders, G. W. 2010. Multigene phylogenetic analyses support recognition of the Sporolithales ord. nov. *Molecular phylogenetics and evolution* **54**(1), 302-305.

Lebednik, P. A. 1977. Postfertilization development in *Clathromorphum, Melobesia* and *Mesophyllum* with comments on the evolution of the Corallinaceae and the Cryptonemiales (Rhodophyta). *Phycologia* **16**, 379-406.

Linge, H., Lauritzen, S.-E., Mangerud, J., Kamenos, N., A., and Gherardi, J.-M. 2008. Assessing the use of U-Th methods to determine the age of cold-water calcareous algae.

Quaternary Geochronology **3**, 76-88.

Littler, M., M., Littler, D., S., and Hanisak, D., M. 1991. Deep-water rhodolith distribution, productivity, and growth history at sites of formation and subsequent degradation. *Journal of Experimental Marine Biology and Ecology* **150**, 163-182.

Lund, M., Davies, P., J., and Braga, J., C. 2000. Coralline algal nodules off Fraser Island, Eastern Australia. *Facies* **42**, 25-34.

Martin, S., Castets, M. D., and Clavier, J. 2006. Primary production, respiration and calcification of the temperate free-living coralline alga Lithothamnion corallioides. *Aquatic Botany* **85**(2), 121-128.

Martin, S., Clavier, J., Chauvaud, L., and Thouzeau, G. 2007a. Community metabolism in temperate maerl beds. I. Carbon and carbonate fluxes. *Marine Ecology Progress Series* **335**, 19-29.

Martin, S., Clavier, J., Chauvaud, L., and Thouzeau, G. 2007b. Community metabolism in temperate maerl beds. II. Nutrient fluxes. *Marine Ecology Progress Series* **335**, 31-41.

Martin, S., Clavier, J., Thouzeau, G., Chauvaud, L., Hall-Spencer, J., and Gattuso, J.-P. (2009). The role pf coralline algae in carbon and carbonate cycles and their response to ocean acidification and global warming. *In* "III International Rhodolith Workshop." Buzios, Brazil.

Martin, S., and Gattuso, J. P. 2009. Response of Mediterranean coralline algae to ocean acidification and elevated temperature. *Global Change Biology* **15**(8), 2089-2100.

Martin, S., Noisette, F., Egilsdottir, H., and Gattuso, J. P. (2012). Physiological responses of temperate coralline algae to ocean acidification. *In* "IV International Rhodolith Workshop." Granada, Spain.

McMaster, R. L., and Conover, J. T. 1966. Recent algal stromatolites from the Canary Islands. *The Journal of Geology* **74**(5), 647-652.

Moberly, R. 1968. Composition of Mg-calcite of algae and pelecypods by electron microprobe analysis. *Sedimentology* **11**(1), 61-82.

Morse, J. W., Andersson, A. J., and Mackenzie, F. T. 2006. Initial responses of carbonate-rich shelf sediments to rising atmospheric pCO2 and "ocean acidification": role of high Mg-calcites. *Geochimica et Cosmochimica Acta* **70**(23), 5814-5830.

Mutti, M., and Hallock, P. 2003. Carbonate systems along nutrient and temperature gradients: some sedimentological and geochemical constraints. *International Journal of Earth Sciences* **92**, 465-475.

Nakahara, H., and Bevelander, G. 1978. The formation of calcium carbonate crystals in *Halimeda incrassata* with special reference to the role of the organic matrix. *Japanese Journal of Phycology* **26**, 9-12.

Nalin, R., Nelson, C. S., Basso, D., and Massari, F. 2008. Rhodolith-bearing limestones as transgressive marker beds: fossil and modern examples from North Island, New Zealand. *Sedimentology* **55**(2), 249-274.

Nelson, W. A. 2009. Calcified macroalgae,Âicritical to coastal ecosystems and vulnerable to change: a review. *Marine and Freshwater Research* **60**(8), 787-801.

Payri, C., E., and Cabioch, G. 2004. The systematics and significance of coralline red algae in the rhodolith sequence of the Amédée 4 drill core (Southwest New Caledonia). *Palaeogeography, Palaeoclimatology, Palaeoecology* **204**, 187-208.

Payri, C. E. 1997. *Hydrolithon reinboldii* rhodolith distribution, growth and carbon production of a French Polynesian reef. *Proceedings of the 8th International Coral Reef Symposium Panama*, 755-760.

Perry, C. T. 2005. Morphology and occurrence of rhodoliths in siliciclastic, intertidal environments from a high latitude reef setting, southern Mozambique. *Coral Reefs* **24**(2), 201-207.

Peryt, T. M. (1983). Coated grains from the Zechstein Limestone (Upper Permian) of Western Poland. *In* "Coated grains." (T. M. Peryt, Ed.), pp. 587-598. Springer-Verlag, Berlin.

Ragazzola, F., Foster, L. C., Form, A., Anderson, P. S. L., Hansteen, T. H., and Fietzke, J. 2012. Ocean acidification weakens the structural integrity of coralline algae. *Global Change*

Biology **18**(9), 2804-2812.

Raup, D. M., and Sepkoski Jr, J. J. 1986. Periodic extinction of families and genera. *Science* **231**, 833-836.

Raven, J., Caldeira, K., Elderfield, H., Hoegh-Guldberg, O., Liss, P., Riebesell, U., Shepherd, J., Turley, C., and Watson, A. 2005. Ocean acidification due to increasing atmospheric carbon dioxide. *Reports of the Royal Society of London* **12**(5), 68pp.

Ries, J., B. 2006. Mg fractionation in crustose coralline algae: Geochemical, biological, and sedimentological implications of secular variation in the Mg/Ca ratio of seawater. *Geochimica et Cosmochimica Acta* **70**, 891-900.

Ries, J., B. 2009. Review: The effects of secular variation in seawater Mg/Ca on marine biocalcification. *Biogeosciences Discussions* **6**, 7359-7367.

Ries, J. B., Cohen, A. L., and McCorkle, D. C. 2009. Marine calcifiers exhibit mixed responses to CO_2-induced ocean acidification. *Geology* **37**(12), 1131-1134.

Riosmena-Rodriguez, R. (2009). An overview of the rhodolith beds around the world: a forgotten habitat. *In* "III International Rhodolith Workshop." Buzios, Brazil.

Sandberg, P. A. 1983. An oscillating trend in Phanerozoic non-skeletal carbonate mineralogy. *Nature* **305**, 19-22.

Savin, S. M. 1977. The history of the Earth's surface temperature during the past 100 million years. *Annual Review of Earth and Planetary Sciences* **5**(1), 319-355.

Schwarz, A.-M., Hawes, I., Andrew, N., Mercer, S., Cummings, V., and Thrush, S. 2005. Primary production potential of non-geniculate coralline algae at Cape Evan, Ross Sea, Antarctica. *Marine Ecology Progress Series* **294**, 131-140.

Semesi, I. S., Kangwe, J., and Björk, M. 2009. Alterations in seawater pH and CO2 affect calcification and photosynthesis in the tropical coralline alga, *Hydrolithon* sp.(Rhodophyta). *Estuarine, Coastal and Shelf Science* **84**(3), 337-341.

Sepkoski Jr, J. J. 1990. The taxonomic structure of periodic extinction. *Geological Society of America Special Paper* **247**, 33-44.

Stanley, S. M. 1979. Macroevolution: Pattern and Process. 332 pp. *WB Freeman and Co,*

Stanley, S. M., and Hardie, L. A. 1998. Secular oscillations in the carbonate mineralogy of reef-building and sediment-producing organisms driven by tectonically forced shifts in seawater chemistry. *Palaeogeography, Palaeoclimatology, Palaeoecology* **144**, 3-19.

Stanley, S. M., and Hardie, L. A. 1999. Hypercalcification: paleontology links plate tectonics and geochemistry to sedimentology. *GSA Today* **9**(2), 1-7.

Stanley, S. M., Ries, J. B., and Hardie, L. A. 2002. Low-magnesium calcite produced by coralline algae in seawater of Late Cretaceous composition. *Proceedings of the National Academy of Sciences* **99**(24), 15323-15326.

Steller, D., L., Riosmena-Rodriguez, R., and Foster, M., S. (2009). Living Rhodolith Bed Ecosystems in the Gulf of California. *In* "Atlas of Coastal Ecosystems in the Gulf of California: Past and Present." (M. E. J. y. J. Ledesma-Vázquez, Ed.). University of Arizona Press.

Steller, D. L., Riosmena-Rodriguez, R., Foster, M. S., and Roberts, C. A. 2003. Rhodolith bed diversity in the Gulf of California: the importance of rhodolith structure and consequences of disturbance. *Aquatic Conservation: Marine and Freshwater Ecosystems* **13**(S1), S5-S20.

Steneck, R., S., and Martone, P., T. (2007). Algae, Calcified. *In* "Encyclopedia of Tidepools." (M. W. D. a. S. D. Gaines, Ed.), pp. 21-24. Berkeley: University of California Press.

Steneck, R. S. 1986. The ecology of coralline algal crusts: convergent patterns and adaptative strategies. *Annual Review of Ecology and Systematics* **17**(1), 273-303.

Stetson, H. C. 1953. The sediments of the western Gulf of Mexico. I. The continental terrace of the western Gulf of Mexico: its surface sediments, origin, and development. *Papers in Physical Oceanography and meteorology, Massachussetts Institute of Technology and Woods Hole Oceanographic Institution* **12**, 5-44.

Tarutani, T., Clayton, R. N., and Mayeda, T. K. 1969. The effect of polymorphism and magnesium substitution on oxygen isotope fractionation between calcium carbonate and water. *Geochimica et Cosmochimica Acta* **33**(8), 987-996.

Tierney, P. W., and Johnson, M. E. 2011. Stabilization role of crustose coralline algae during Late Pleistocene reef development on Isla Cerralvo, Baja California Sur (Mexico). *Journal of Coastal Research* **28**(1), 244-254.

Vecsei, A. 2004. A new estimate of global reefal carbonate production including the fore-reefs. *Global and Planetary Change* **43**(1), 1-18.

Verheij, E. 1993. The genus *Sporolithon* (Sporolithaceae fam. nov., Corallinales, Rhodophyta) from the Spermonde Archipelago, Indonesia. *Phycologia* **32**(3), 184-196.

Wada, N., Okazaki, M., and Tachikawa, S. 1993. Effects of calcium-binding polysaccharides from calcareous algae on calcium carbonate polymorphs under conditions of double diffusion. *Journal of Crystal Growth* **132**(1-2), 115-121.

Waelbroeck, C., Mulitza, S., Spero, H., Dokken, T., Kiefer, T., and Cortijo, E. 2005. A global compilation of late Holocene planktonic foraminiferal $\delta^{18}O$: relationship between surface water temperature and d18O. *Quaternary Science Reviews* **24**(7), 853-868.

Williams, B., Halfar, J., Steneck, R. S., Wortmann, U. G., Hetzinger, S., Adey, W., Lebednik, P., and Joachimski, M. 2011. Twentieth century ^{13}C variability in surface water dissolved inorganic carbon recorded by coralline algae in the northern North Pacific Ocean and the Bering Sea. *Biogeosciences* **8**(1), 165-174.

Wray, J. L. 1964. *Archaeolithophyllum*, an abundant calcareous alga in limestones of the Lansing Group (Pennsylvanian), southeastern Kansas. *Kansas Geological Survey, Bulletin* **170**, 13-32.

Wray, J. L. (1977). Late Paleozoic calcareous red algae. *In* "Fossil algae, recent results and developments. Springer, Berlin." (E. Flügel, Ed.), pp. 167-176.

Zachos, J., Pagani, M., Sloan, L., Thomas, E., and Billups, K. 2001. Trends, rhythms, and aberrations in global climate 65 Ma to present. *Science* **292**, 686-693.

CHAPTER III

An investigation of Mg/Ca distribution in *Sporolithon durum* coralline red algae

Keywords: rhodoliths, laser ablation, electron microprobe, organic matter, seasonal cycle, growth pattern, New Caledonia

Abstract

Mg/Ca concentration and high-resolution variations in tropical specimens of *Sporolithon durum* rhodoliths (=unattached forms of coralline red algae) were measured using laser ablation inductively coupled plasma mass spectrometry (LA-ICPMS). Different instrumental configurations were tested to record 11 profiles along the same rhodolith branch. The consistency of the Mg/Ca content recorded in all LA-ICPMS profiles and the concordant average Mg/Ca concentrations obtained between LA-ICPMS and inductively coupled plasma atomic emission spectrometry (ICP-AES) as well as solution ICPMS measurements indicate that LA-ICPMS is a precise and accurate technique for determining the Mg/Ca concentration in *S. durum* rhodoliths. Lower Mg/Ca values measured by electron probe micro-analysis (EPMA) and after H_2O_2 treatment of *S. durum* reveal that Mg does not exclusively occur inside the calcite lattice that constitutes the coralline algal skeleton. The presence of a significant fraction of the total Mg associated with organic matter inside the cell structure of the alga is suspected. H_2O_2 treatment, however, does not significantly affect Mg/Ca variations along a rhodolith branch. The LA-ICPMS Mg/Ca profiles present similar variations, suggesting good reproducibility of the LA-ICPMS technique and a homogenous distribution of Mg/Ca across a rhodolith branch. Two types of Mg/Ca variations were recognised in all the profiles and could be partly decoupled providing adjustments in the laser spot size. A ~500 µm-period, major cyclicity likely reflects seasonal variations in local sea-surface temperature (SST), whereas ~30-100 µm-period minor variations are linked to the high-resolution pattern of algal growth.

III-1 Introduction

Encrusting coralline red algae are distributed throughout the photic zone from the tropics to the poles (Adey and McIntyre, 1973; Bosence, 1983a; Steneck, 1986). Coralline red algae can occur either attached to hard substrates or as free-living forms, known as rhodoliths (Steneck, 1986; Foster, 2001). Rhodoliths are usually found on sandy bottoms, which they often entirely cover, constituting a rhodolith bed (Foster, 2001). Rhodoliths form when algal cells first settle on a non-cohesive substrate that can be of various origins (Harris et al., 1996; Basso et al., 2009), from which, a concentrically-growing calcareous structure will evolve (Bosence, 1983b; Goldberg, 2006). Rhodoliths, and coralline red algae in general, are slow growing (0.01 to ~1 $mm.y^{-1}$ – Foster, 2001) with potential lifespans of centuries (Frantz et al., 2005; Halfar et al., 2007) during which they may form thick crusts (often >10 cm – Bosence, 1983b). These characteristics have raised a particular interest in their use for palaeoenvironmental reconstructions, which often relies on the geochemical composition of their high-magnesium calcite skeleton (Nelson, 2009).

Early geochemical studies on coralline red algae focused on the measurement of their Mg content and the first suggestion that the bulk Mg composition of their skeleton co-varies with seawater temperature is found in Chave (1954). Electron probe micro-analyses (EPMA) have since shown that the most significant variations of the Mg content in coralline red algae mainly correspond to the annual cycle of seawater temperature (e.g. Halfar et al., 2000; Kamenos et al., 2008; Hetzinger et al., 2009). Sub-seasonal Mg variations have also been determined in a rhodolith form of the *Lithothamnion glaciale* species (Halfar et al., 2000).

Laser ablation inductively coupled plasma mass spectrometry (LA-ICPMS) allows a simultaneous, rapid analysis of a large array of trace elements at high resolution and with high sensitivity (e.g. Eggins et al., 1998). This technique is regularly used for environmental reconstructions in various marine, calcareous organisms (e.g. corals: Sinclair et al., 1998; Fallon et al., 1999; foraminifera: Eggins et al., 2003; Hathorne et al., 2003; bivalve molluscs: Schöne et al., 2011). Only recently has LA-ICPMS been used for high-resolution studies of coralline red algae (Gamboa et al., 2010; Hetzinger et al., 2011a; Chan et al., 2011). This series of studies focused on the genus *Clathromorphum* from the high latitudes of the Northern Hemisphere and was based on a single combination of instrumental settings for the LA-ICPMS analyses.

In this study, we propose to expand the utility of the LA-ICPMS technique for coralline red algal studies by using various instrumental combinations to measure the Mg/Ca

content and variations in rhodolith-forms of the *Sporolithon durum* coralline red algae species from the lagoon of New Caledonia. This, in combination with both EPMA analysis and the characterisations of the organic component by the mapping of the sulphur content and a H_2O_2 bleaching experiment, will give new insights into the distribution of Mg in *S. durum* rhodoliths.

III-2 Material and methods

III-2.a Rhodolith collection and sample preparation

The *S. durum* rhodoliths studied here were collected using SCUBA from ~4 m deep, in October 2009 (BSA specimen) and February 2011 (MSA specimen), from the edge of the Ricaudy Reef (22°18'57" S; 166°27'26" E) near the city of Nouméa, New Caledonia (Figure III-1A). The nodules are 8.1 cm and 8.5 cm in diameter (BSA and MSA specimens, respectively) and present a degree IV branching structure according to the classification of Bosence (1983b). Collected specimens were dried before being set in araldite resin blocks. Sections parallel to the long axis of the ellipsoidal nodules were cut using a diamond rock saw. Polished sections were photographed at high-resolution using a Digital Sight DS-Fi1 digital camera attached to a Nikon AZ100 optical microscope at the Research School of Earth Sciences (RSES) of the Australian National University (ANU). Prior to LA-ICPMS analysis or sampling for solution ICPMS and ICP-AES, sections were sonicated and oven-dried (40°C) overnight.

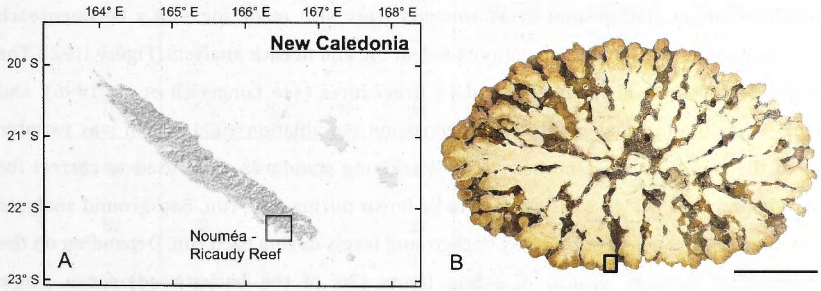

Figure III-1 **A: Location map of New Caledonia showing the region of Nouméa and the Ricaudy Reef in the southwest of the main island. B: Cross section of the BSA rhodolith specimen showing the area of LA-ICPMS analyses (black square). Scale bar: 2 cm.**

III-2.b LA-ICPMS analyses

An area of ~3 mm² near the top of a branch along the short axis of the BSA specimen (Figure III-1B) was chosen for LA-ICPMS analyses at the RSES, ANU, using a Varian 820 ICPMS, coupled to an ANU Helex ArF excimer laser ablation system. Variations in ^{24}Mg, ^{25}Mg and ^{43}Ca were measured along 11 different, ~2 mm-long profiles parallel to the axis of branch main growth. General settings for the laser ablation unit and the ICPMS instrument are given in Table III-1A, and the various configurations used for each profile are shown in Table III-1B. In summary, the energy level and pulse rate of the laser, along with the ablation spot diameter were the main varying settings between the 4 profiles labelled "Tr" and primarily influenced the volume of ablated material reaching the ICPMS detector for each measurement. The profiles labelled "N" were set with the same settings as the Tr profiles but with different laser scan speeds. The individual isotope dwell times and counting modes on the ICPMS were also modified in order to optimise the count rates obtained for each isotope measured by the ICPMS detector (Table III-1B).

A dolomitic type of Carrara marble (e.g. Herz and Dean, 1986) was used as a matrix-matched, external standard for rhodolith Mg/Ca calibration. The composition of the Carrara marble standard was independently determined using inductively coupled plasma atomic emission spectrometry (ICP-AES), solution ICPMS and EPMA methods (see section III-2.c), all of which gave consistent results (Table III-2). The glass SRM NIST610 (National Institute of Standards and Technology) was also used as a secondary standard. All LA-ICPMS analyses followed the same analytical procedure (Figure III-2). Prior to analysis, the sample surface was cleaned of possible contamination by a pre-ablation run. Standard reference materials were measured for ~60 s, before and after the measurement of the rhodolith sample. Background measurements were also made for ~60 s between each measurement as well as at the beginning and at the end of each analysis (Figure III-2). The data reduction method followed standard procedures (see Longerich et al., 1996), and used ^{43}Ca as the internal calibration to constrain the ablation yield, which was variable due to the sample surface porosity. The bracketing standards were used to correct for instrumental drift, which was assumed to be linear during each run. Background analyses were used to interpolate subtracted background levels during each run. Depending on the experimental settings, typical detection limits (3σ of the background) for a single measurement in the Tr profiles were: ^{24}Mg: 15-125 ppm; ^{25}Mg: 30-350 ppm; ^{43}Ca: 250-1200 ppm, and for the N profiles, were: ^{24}Mg: 15-80 ppm; ^{25}Mg: 10-70 ppm; ^{43}Ca: 100-650 ppm.

Results are presented as Mg/Ca molar ratio against distance from the top of the rhodolith branch. To compare the profiles and to compensate for irregularities of the sampling area, the main features observed in each profile were linked using the data analysis software AnalySeries (Paillard et al., 1996).

A

Laser unit	
Energy	5 - 10 J.cm^{-2}
Spot Dimensions	13 - 47 µm diameter
Scan Speed	3 - 10 µm.s^{-1}
Pulse Rate	5 - 10 Hz
Wavelength	193 mn

ICPMS	
Data Acquisition Method	Time Resolved, pulse counting, 1 point per peak
Gas flows	Cool: 15l/min, Aux: 1 l/min Carrier: 0.9-1.20 l/min Ar; 0.5 l/min He
Plasma Power	1350 W
Measured isotopes	^{24}Mg, ^{25}Mg, ^{43}Ca
Integration Mode	Medium Attenuation - No Attenuation
Individual dwell time	Tr tracks: 30ms; N tracks: 60-600 ms
Total integration time	0.51 - 0.75 s
Intensity range	5,000 - 1,000,000 cps

B

LA-ICPMS tracks	Laser settings				ICPMS settings		
	Energy Level (J.cm^{-2})	Pulse rate (Hz)	Speed (µm.s^{-1})	Spot diameter (µm)	Dwell time (ms) / Mode Average recorded intensity (cps)		
					^{24}Mg	^{25}Mg	^{43}Ca
Tr1	10	5	10	47	30 / MA 500,000	30 / MA 50,000	30 / MA 10,000
Tr2	10	5	10	22	30 / MA 100,000	30 / MA 10,000	30 / NO 200,000
Tr3	10	5	10	13	30 / MA 50,000	30 / MA 5,000	30 / NO 100,000
Tr4	5	10	10	42	30 / MA 200,000	30 / MA 20,000	30 / NO 400,000
N1 series	10	10	7	47	70 / MA 800,000	600 / MA 100,000	60 / NO 1,000,000
N2	10	10	5	22	300 / MA 200,000	60 / NO 1,000,000	150 / NO 400,000
N3 series	10	10	3	13	600 / MA 100,000	120 / NO 500,000	300 / NO 200,000
N4	5	10	5	42	300 / MA 200,000	60 / NO 1,000,000	150 / NO 400,000

Table III-1 **A. General settings used in this study for the LA-ICPMS machine. B. Specific laser and ICPMS configuration set for each profile.**

Mg/Ca (mol.mol^{-1})	Mean	Stderr	n
ICP-AES	0.993	0.006	5
Solution ICPMS	0.997	0.008	5
EPMA	0.994	0.010	2

Table III-2 **Mean and standard error of the mean for the Mg/Ca concentration in the sample of Carrara marble used as an external standard for the LA-ICPMS analyses measured by three independent techniques. The number of samples (n) used to calculate each average is also indicated.**

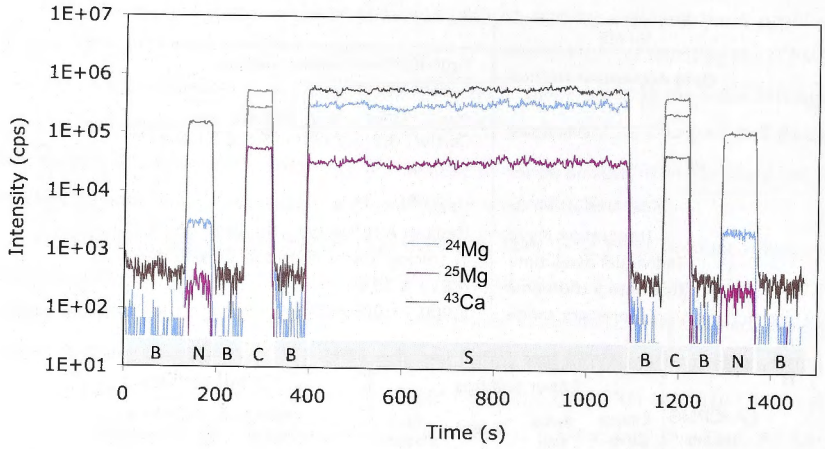

Figure III-2 **Typical trace element profile obtained from an individual LA-ICPMS run. The sample analysis (S) is bracketed between measurements of both standards (N: NIST 610 SRM and C: Carrara marble), with successive measurements separated with ~60 s of background (B) acquisition.**

III-2.c ICP-AES, Solution ICPMS and EPMA

We analysed a single rhodolith sample by both ICP-AES and solution ICPMS methods. Bulk carbonate powder was obtained by drilling a sequence of holes of ~2 mm in diameter and ~1 mm depth, one branch from the BSA specimen. Approximately 1 mg of powder from each hole was dissolved in a 10 ml, 2% HNO_3 solution for analyses.

A Varian Vista Pro Axial ICPAES from the RSES, ANU was used to analyse the rhodolith samples, following a method similar to the one of de Villiers et al. (2002). We used a sample-standard bracketing technique, which consisted in an in-house matrix-matched standard solution of known Mg and Ca composition being measured repeatedly between each sample and which was used both calibrate Mg and Ca responses and to correct from instrumental variations throughout the run. Detection limits for Mg and Ca were

respectively 0.01 and 0.10 $mg.l^{-1}$, more than 20x lower than the sample concentration. Standard deviations on the measured elemental concentrations of the rhodolith sample studied here were 0.44 and 0.45% for Mg and Ca, respectively.

A Varian 820 ICPMS (RSES, ANU) was used for solution ICPMS analysis. Four standard solutions of known Mg and Ca concentrations were prepared from AccuTrace solutions (National Institute of Standards and Technology) and used to establish calibration curves and assess instrumental reproducibility. A pure 2% HNO_3 (i.e. "blank") solution was repeatedly measured and used to correct for instrumental-drift as well as to determine detection limits for Mg and Ca, which were 0.14 and 1.7 ppb, respectively (3σ of the blanks; n=8).

EPMA was conducted on a carbon-coated thin section of the BSA rhodolith, using a Cameca SX100 electron probe at the RSES, ANU. Energy-dispersive spectrometry (EDS) was used to obtain quantitative, simultaneous analyses of Mg and Ca from various areas of the rhodolith skeleton. Measurements were carried out using a 10 µm-diameter spot, with 15 keV acceleration voltage and 20nA beam current. 60.3% Mg in MgO periclase modified standard was used for Mg calibration and 34.5% Ca in $CaSiO_3$ modified standard was used for Ca calibration. Standard reduction was set for Mg-Ka on TAP crystal and Ca-Ka on LPET crystal. Detection limits for Mg and Ca were respectively <300 and <200 $\mu g.g^{-1}$ and analytical errors (weight %) were <2.5% and <0.6%, respectively. Areas (200-300x300-600 µm grid) where quantitative information was collected were mapped for their relative Mg and Ca concentrations using a 3-µm spot size and 3-µm steps. Relative abundances of S from the same areas were also mapped. Back-scattered electron (BSE) images of these areas were also taken using the in-built scanning electron microscope (SEM) device.

Results of the quantitative analyses of Mg and Ca for the BSA rhodolith using ICP-AES, solution ICPMS and EPMA techniques are presented in Table III-3 as Mg/Ca ($mol.mol^{-1}$) ratios, along with error estimates.

LA-ICPMS tracks	Mg/Ca ($mol.mol^{-1}$)		
	Average	Stdev	Range
Tr1	0.307	0.039	0.206-0.460
Tr2	0.308	0.049	0.193-0.508
Tr3	0.314	0.058	0.159-0.544
Tr4	0.290	0.038	0.204-0.415
N1a	0.305	0.035	0.234-0.423
N1b	0.302	0.031	0.238-0.428
N2	0.294	0.036	0.215-0.440
N3a	0.312	0.043	0.226-0.443
N3b	0.293	0.039	0.215-0.413
N3c	0.301	0.041	0.218-0.434
N4	0.288	0.034	0.216-0.411
All	0.301	0.040	0.159-0.544

Table III-3 **Results of the LA-ICPMS analyses showing the average Mg/Ca content, the standard deviation and range of Mg/Ca values for each of the 11 profiles as well as for the entire analytical dataset.**

III-2.d Rhodolith staining and H_2O_2 treatment

To assess the possible presence of different carbonate minerals in the rhodoliths, we followed the procedure proposed by Dickson (1965) that used the different solubilities of calcite and dolomite in hydrochloric acid (HCl). After etching in a 5% HCl solution for ~10 s, a thin section containing a few branches of the BSA rhodolith was immersed in a dilute solution of alizarin red S ($2g.l^{-1}$) in 5% HCl for approximately 45 s. After rinsing with distilled water, calcite appears as a pink-red colour whereas dolomite remains uncoloured. The calcite also appears more etched than the dolomite.

To remove the organic phase from the rhodolith skeleton, a resin slab of the MSA specimen was immersed in a hot (60°C) H_2O_2 (30%) solution buffered with 0.1 *N* NaOH in equal volumes (e.g. Stoll et al., 2001). After approximately 1 hour, when bubbling ceased, the slab was rinsed with distilled water, sonicated and oven-dried at 40°C overnight. Mg/Ca profiles along the same MSA rhodolith branch were measured by LA-ICPMS under the same conditions (method in section III-2.b), on different sessions, before and after H_2O_2 treatment.

III-3 Results

III-3.a Mg/Ca calibration

Averaged measured Mg/Ca values are consistent between each LA-ICPMS track, even when different laser ablation and ICPMS settings are used (Table III-3). The overall average Mg/Ca value obtained from the LA-ICPMS technique is 0.301 ±0.003 $mol.mol^{-1}$ (Table III-4; uncertainties are presented as standard errors of the mean). This value is identical, within error of the Mg/Ca values obtained from the bulk sample of the outermost part of another branch of the same rhodolith, analysed by ICP-AES and solution ICPMS (respectively, 0.305 ±0.002 and 0.298 ±0.006 $mol.mol^{-1}$). However, the Mg/Ca average value resulting from EPMA is about 30% lower for a similar region of the same rhodolith (0.215 ±0.003 $mol.mol^{-1}$; range: 0.192-0.238 $mol.mol^{-1}$; n=3). The average Mg/Ca obtained from the same LA-ICPMS measurements, this time calibrated using the SRM NIST 610 instead of the Carrara marble, also displays a slightly lower value (0.286 ±0.006 $mol.mol^{-1}$) than the one obtained by LA-ICPMS (Carrara), ICP-AES and solution ICPMS (Table III-4, Figure III-3).

Mg/Ca (mol.mol^{-1})	Average	Stderr	n
LA-ICPMS NIST610	0.286	0.006	11
LA-ICPMS Carrara	0.301	0.003	11
ICP-AES	0.305	0.002	1
Solution ICPMS	0.298	0.006	1
EPMA	0.215	0.003	3

Table III-4 **Mean value and standard error of the mean or of a single measurement for the Mg/Ca content in the outermost area of the BSA rhodolith measured by different techniques. The number of samples (n) used to calculate each average is also indicated. LA-ICPMS NIST610 is using the NIST 610 SRM as external standard for calibration of the LA-ICPMS records, whereas LA-ICPMS Carrara is using the Carrara marble for calibration of the same LA-ICPMS records.**

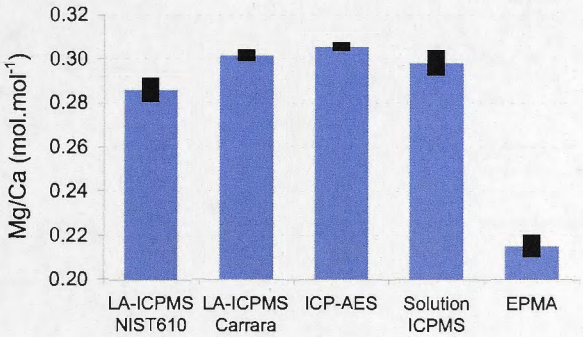

Figure III-3 **Average concentration of Mg/Ca in the outer region of the BSA *S. dürum* rhodolith measured using different techniques (blue bars). Black bars represent 2 σ_M (standard error of the mean).**

III-3.b Mg/Ca distribution

The EPMA mapping of Mg/Ca variations along a rhodolith branch reveals a layered/banded pattern of the Mg/Ca distribution that appears to follow the semi-horizontal cell alignment within the branch (Figure III-4A-D). This translates, in the vertical growth direction, to cyclic variations in the Mg/Ca pattern that are observed on all maps and are generally associated with the alternation of small cells with thick walls (low Mg/Ca) and longer cells with thinner walls (high Mg/Ca) observed in the BSE images (Figure III-4A-D). On light microscope images, this pattern appears as a 30-70 µm-thick banding. Most of the cell openings (black holes in the BSE images) are relatively well defined as dark regions in the Mg/Ca maps that correspond to the lowest Mg/Ca values. The interior of the cells are often associated with the highest S/Ca values, particularly in the outermost region of the rhodolith branch (Figure III-4A). A peculiar, vertically-orientated feature can be seen in Figure III-4C that is fully calcified and breaks the

horizontal cell alignment. This few-hundred-µm scale feature has the highest Mg/Ca values recorded in the map of that region, and also presents elevated S/Ca concentrations.

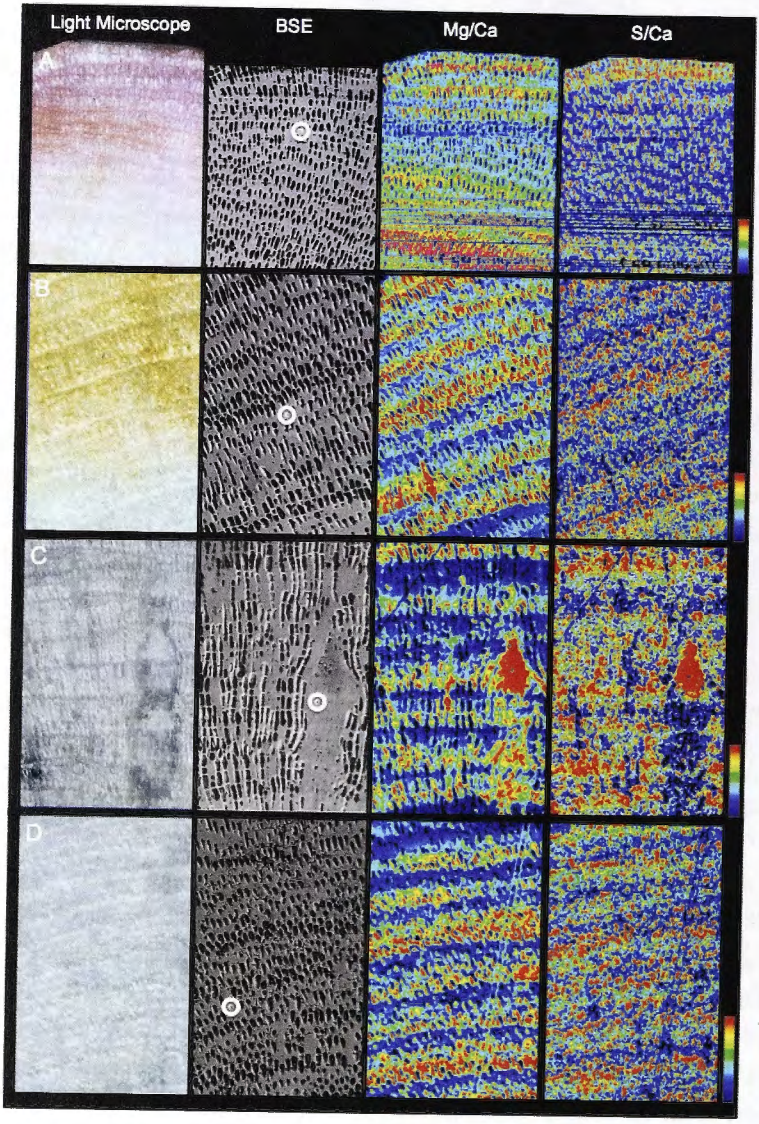

Figure III-4 Light microscope images of different regions of the BSA rhodolith specimen (from edge toward centre of the nodule – A to D) with corresponding BSE images and Mg/Ca and S/Ca distribution maps obtained from EPMA. Intensity scales for each region are 100 µm and figure relative elemental concentrations (higher concentrations in red; lower concentrations in blue). Note that the colouration does not necessarily represent the same scale for different regions neither for Mg/Ca and S/Ca. The white circles on the BSE images figure the location of the quantitative EPMA analyses (spot diameter: 10µm).

The staining of the rhodolith thin section reveals most of the skeleton is made of calcite, with a few areas of dolomite, mostly concentrated near the bottom and sides of some branches (Figure III-5A). "Patches" of dolomite also seem to be scattered along the skeleton, aligned roughly along the growth direction. These patches are of the order of a hundred µm-long (Figure III-5B-C) and can be related to the higher-Mg feature observed in the EPMA.

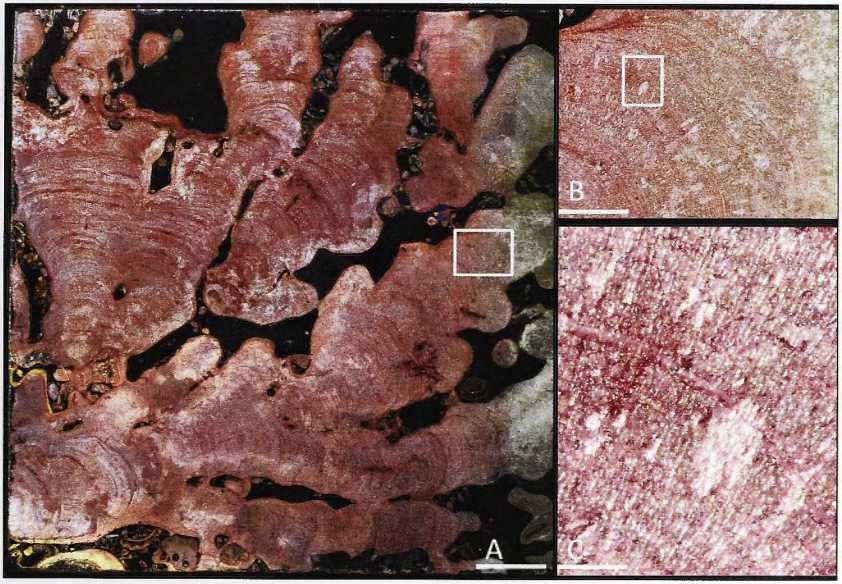

Figure III-5 Thin section of several branches from the BSA rhodolith after HCl etching and alizarin red S staining (A). Close-ups of the white rectangles in A and B are shown in B and C, respectively. Pink-reddish areas are calcite whereas the white/translucid patches represent dolomitic material. Scale bars A: 2 mm; B: 500 µm; C: 100 µm. The darkened areas are epoxy resin.

The treatment of a branch of *S. durum* rhodolith with H_2O_2 significantly lowers the Mg/Ca concentrations recorded by LA-ICPMS (Figure III-6) by ~0.06 mol.mol^{-1} on average, or about 20%. However, it appears that this effect is constant throughout the profile and does not significantly affect the Mg/Ca variations along the studied rhodolith branch (Figure III-6 – F-Test; $p<0.0001$).

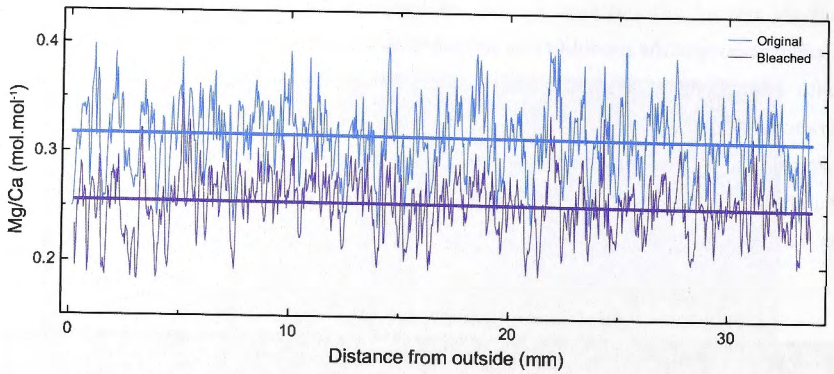

Figure III-6 **Comparison between Mg/Ca variations, along the same branch of the MSA rhodolith, recorded by LA-ICPMS before (blue) and after (purple) H_2O_2 treatment. Note the decrease of ~20% in the Mg/Ca concentration after treatment, whereas the Mg/Ca variations are unaffected.**

III-3.c Mg/Ca variations measured by LA-ICPMS

The Mg/Ca profiles have a relatively similar standard deviation ranging from 0.031 (N1b) to 0.058 (Tr3) and ranges in Mg/Ca values vary from 0.159 to 0.544 (Tr3 – Table III-3). The Tr2 and Tr3 profiles are notably more variable, especially when considering their high Mg/Ca values, and show poor, albeit significant, correlations between their respective ^{24}Mg/Ca and ^{25}Mg/Ca records (r=0.45 for Tr2 and r=0.35 for Tr3 - Figure III-7). This poor correlation between these signals reflects a high degree of uncertainty on each measurement, which is associated with counting statistics. Tr1 and Tr4, on the other hand, are very similar and show less counting statistics error (^{24}Mg/Ca-^{25}Mg/Ca: r=0.77 and r=0.78, respectively). The N profiles systematically display cleaner (i.e. with less error associated with counting statistics) Mg/Ca records than their Tr counterparts. This characteristic, that is particularly evident for N2 and N3a-b-c, enables clearer observations of the Mg/Ca variation pattern (Figure III-7).

Correlations between the 11-measured Mg/Ca profiles are highly significant ($0.48<r<0.87$ or $0.66<r<0.87$ if Tr2 and Tr3 are avoided due to high counting statistics uncertainty; $p<0.0001$ - Table III-5), indicating that they all share similar Mg/Ca variations. Two different levels of cyclic variations are observable and the different instrumental settings used for each profile may result in these patterns being more or less distinguishable. A low-frequency, major pattern with a ~500 µm wavelength is clearly displayed in Tr1 and Tr4 as well as N1a-b and N4, all of which were set with the biggest spot sizes. This pattern is more difficult to determine in Tr3 and N3a-b-c, for which the smallest spot size was used (Table III-1B, Figure III-7). The latter profiles, however, show

a higher-frequency, minor cyclicity with a ~50-100 µm period that is more dominant in the Mg/Ca variations, whereas it is hardly distinguishable in the biggest-spot-sizes profiles. For an intermediate spot size, Tr2, and especially N2, also present an intermediate profile where the two frequencies of Mg/Ca variations are observed but neither is as clearly displayed as in the other profiles.

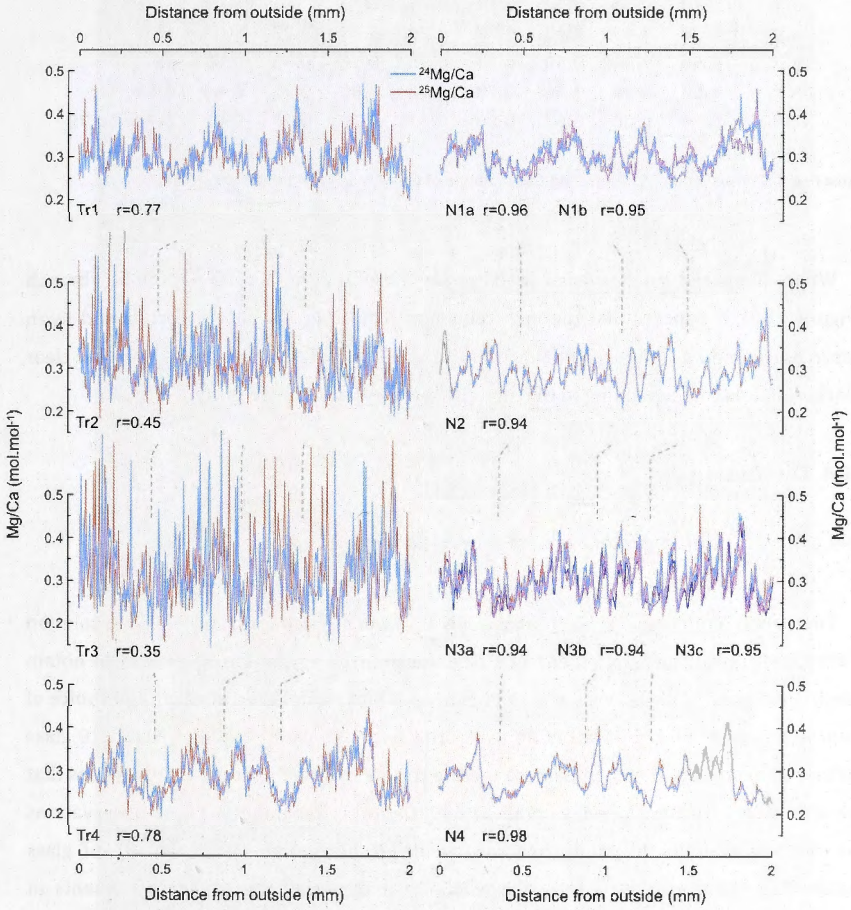

Figure III-7 Individual ^{24}Mg/Ca and ^{25}Mg/Ca LA-ICPMS profiles analysed along the outermost region of the same BSA rhodolith branch, using different instrumental settings. Note that the N1a and N1b profiles are displayed on the same plot and so are N3a, b and c. Correlation coefficients between the ^{24}Mg/Ca and ^{25}Mg/Ca records are also figured for each profile. Observable common features in the Mg/Ca variations are linked by the vertical dashed-lines.

r	Tr1	Tr2	Tr3	Tr4	N1a	N1b	N2	N3a	N3b	N3c
Tr1										
Tr2	0.60									
Tr3	0.54	0.56								
Tr4	0.76	0.66	0.64							
N1a	0.80	0.64	0.60	0.81						
N1b	0.72	0.57	0.62	0.78	0.80					
N2	0.70	0.63	0.50	0.74	0.75	0.75				
N3a	0.70	0.48	0.48	0.70	0.70	0.76	0.77			
N3b	0.66	0.54	0.50	0.74	0.75	0.76	0.78	0.87		
N3c	0.68	0.54	0.56	0.72	0.73	0.80	0.72	0.85	0.83	
N4	0.76	0.68	0.62	0.86	0.83	0.79	0.77	0.72	0.75	0.78

Table III-5 Correlation matrix for the Mg/Ca variations of the 11 individual LA-ICPMS profiles.

When compared to the visual features on the photograph of the rhodolith branch (Figure III-8), it appears that the low-frequency, major Mg/Ca pattern correspond to an observable banding composed of alternating pair of clear and darker bands, with the clear (darker) bands corresponding to the high (lower) Mg/Ca values (Figure III-8).

III-4 Discussion

III-4.a Mg/Ca content and its distribution in *S. durum*

The agreement between the average Mg/Ca values obtained from ICP-AES, solution ICPMS and LA-ICPMS, strengthens our confidence in using the latter method to obtain precise and accurate Mg/Ca measurements in *S. durum* rhodoliths. However, the choice of external standards for calibration appears critical as the use of the SRM NIST 610 glass instead of the matrix-matched Carrara marble results in lower average Mg/Ca values that are also different from the ones obtained with the other techniques. These observations are concordant with the study by Craig et al. (2000) showing that the use of glass standards consistently leads to a negative bias in the calibration of trace elements in carbonate matrices. For this study, we mainly attribute that difference to the Mg/Ca value in the SRM NIST 610 being an order of magnitude lower than the one in *S. durum* rhodoliths (~0.01 and 0.30, respectively), making it particularly unsuitable for calibration.

The lower Mg/Ca content recorded by the EPMA might be explained by the sampling strategy. Indeed, the electron beam of the electron probe needs to be projected on a flat surface to prevent from adverse effects on the recorded signal caused by sample porosity.

Figure III-8 Intensity map of the area studied in the LA-ICPMS analysis composed of the 11 Mg/Ca profiles plotted on top of the light microscope image showing their respective laser tracks. The length and width of the Mg/Ca profiles match the ones of the physical tracks (~2 mm-long and 13-47 µm-wide). Mg/Ca intensity range from 0.20 (dark blue colour) to 0.45 (red colour). 4 years of algal growth are represented here.

In that respect, the thin cell walls were avoided and the 10-µm spot was directed to thicker walls, which are generally associated with lower Mg/Ca values (Figure III-4). Consequently, the average Mg/Ca obtained by EPMA could be biased toward the lower end of the Mg/Ca range.

Significantly lower Mg/Ca values are also obtained after H_2O_2 treatment of *S. durum*. This could be attributed to portions of Mg present as adsorbed ions or incorporated into interstitial or defected site, hence favouring their dissolution during the bleaching process (Love and Woronow, 1991), or to the preferential dissolution of high-Mg calcite during the H_2O_2 treatment (Martin and Lea, 2002). However, Stoll et al. (2001), reported an Mg/Ca diminution of up to ~5% in non-biogenic carbonate after H_2O_2 treatment. Here, the difference observed in *S. durum* is ~20%.

The most probable explanation for the lower Mg/Ca values obtained both with EPMA and after H_2O_2 treatment in *S. durum* is the presence of Mg directly or indirectly associated with organic matter inside the cell structure. Recently, the presence of dolomite and magnesite that could be biologically-related was identified in the cell structure of tropical coralline red algae *Hydrolithon onkodes* (Nash et al., 2011). We determine the possible presence of dolomite in *S. durum* (Figure III-5) associated with potential traces of organic matter recorded by high S/Ca values (Figure III-4C). However, the dolomitic features observed in this study are much bigger than the size of a cell and can be easily avoided when carrying out EPMA or LA-ICPMS analyses. Yet, although the BSE images and the Mg/Ca maps suggest that the cells of *S. durum* are empty and show the lowest Mg/Ca values, the presence of organic matter is indicated by the highest S/Ca values generally appearing inside the cells (Figure III-4A-D). We speculate that some Mg-bearing material is associated with this organic matter inside the cell structure. This portion of the total Mg content would, consequently, be removed, along with the organic matter, during the H_2O_2 treatment. It would also not appear in the quantitative EPMA that only recorded the Mg/Ca concentration in the cell walls. In contrast, the LA-ICPMS, ICP-AES and solution ICPMS techniques do not differentiate the material of the cell walls from the one within the cell and would, therefore, record this Mg "excess". Milliman et al. (1971) identified an "excess" of Mg present in various species of coralline red algae when compared to the Mg concentration determined only from their calcite peaks in X-Ray diffraction (XRD) analyses. This difference was particularly significant for tropical species of coralline red algae. Our results further support the fact that Mg in tropical coralline red algae may not be exclusively incorporated into the calcite lattice that constitutes the skeleton (in contradiction with what Kamenos et al. (2009) proposed for a cold-water species), but that other forms of Mg may also contribute to the total Mg concentration.

III-4.b Mg/Ca variations

Results of the LA-ICPMS analysis imply that optimising the amount of material reaching the ICPMS detector for each measurement is critical in order to drastically reduce the error associated with counting statistics on the recorded signal. As changing any of the laser or ICPMS settings alone has no significant effect on the noise of the recorded signal (e.g. Tr1 vs. Tr4 and all N profiles), we suggest that any configuration can be used to reliably measure Mg/Ca variations in *S. durum*, as long as the ICPMS detector's counts-per-second are optimised for each analysed isotope.

The highly significant correlations between the 11 LA-ICPMS Mg/Ca profiles indicate good reproducibility of the technique as well as a homogenous distribution of the Mg/Ca variations across the rhodolith branch.

A comparison of the average Mg/Ca profiles with the local SST (Figure III-9) strongly suggests that the common major, ~500 µm-wavelength Mg/Ca variations in *S. durum* are related to the seasonal pattern of SST, with high (low) Mg/Ca values occurring during periods of high (low) SST in the austral summer (winter). This implies that the major visual banding associated with the low-frequency Mg/Ca variations (Figure III-8) also occurs annually. The relationship between SST and Mg variations was established in various studies, for other species of coralline red algae (e.g. Halfar et al., 2000; Kamenos et al., 2008; Hetzinger et al., 2009; 2011a;b; Gamboa et al., 2010) and the major banding pattern has also been recognised to be annual (Kamenos and Law, 2010) and sometimes used to establish chronologies in rhodoliths (Burdett et al., 2010). Our observations further suggest a co-variation between these parameters; however, further studies need to be conducted to confidently assess the Mg-SST relationship as well as the annual character of the major, visual banding in *S. durum*. This will be undertaken in the following chapters of this thesis, particularly Chapters IV and VI. If this is confirmed, the minor, ~30-100 µm-wavelength Mg/Ca cycles recorded in the LA-ICPMS measurements would then occur at a sub-seasonal scale. Sub-annual patterns in Mg/Ca have been recognised on other rhodolith species and were inconclusively suggested to reflect lunar cycles (e.g. Moberly, 1968; Halfar et al., 2000). Similarly, this study does not provide enough information to reliably characterise the periodicity of the minor Mg/Ca cycles. However, as shown by the EPMA maps, we were able to assess that these Mg/Ca high-frequency variations are intimately linked to the *S. durum* growth pattern.

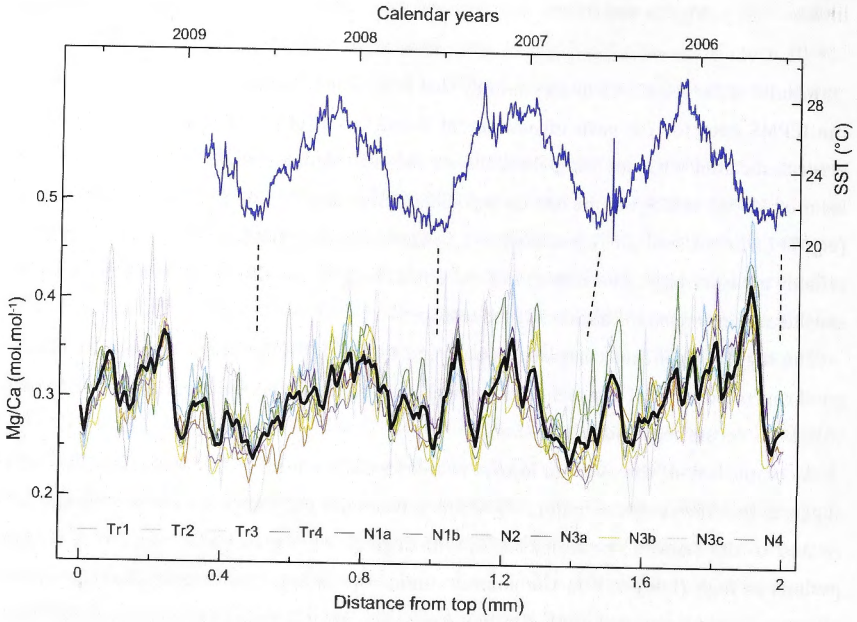

Figure III-9 **Comparison plot between the local, daily SST record for the 2005-2009 period (top blue curve) and the 11 individual (bottom thin coloured lines) as well as the average (bottom thick black line) 2 mm-long Mg/Ca profiles recorded using LA-ICPMS along the outermost region of a *S. durum* rhodolith branch. The rhodolith is from the Ricaudy Reef, some 2 km from the instrumental SST station. The individual profiles have been resampled to appear on the same scale (see text for details). Low SST and low Mg/Ca values are matched by the vertical dashed-lines.**

The use of different laser spot sizes for the LA-ICPMS analyses enables to focus on either one of these observed cyclic variations. Using a small spot size (10-20 µm) provides a clear determination of the minor Mg/Ca cycles, and hence, highlights the growth pattern influence on the Mg/Ca variations in *S. durum* rhodoliths, whereas bigger spot sizes (~40-50 µm) permit to smooth the high-frequency variability, highlighting the major Mg/Ca cycles that seems more prone to be influenced by the seasonal variations of environmental parameters, and particularly SST.

III-5 Conclusion

Mg/Ca content and variations in *S. durum* rhodoliths can be precisely and accurately measured by LA-ICPMS, provided a matrix-matched external standard is used for calibration and the amount of sample material reaching the ICPMS detector is optimised.

Under these conditions, instrumental configuration changes do not appear to significantly affect the quality of the recorded signal.

Lower Mg/Ca concentrations recorded by EPMA and after H_2O_2 treatment suggest that Mg is not exclusively incorporated into the calcite lattice forming the *S. durum* skeleton and that a significant fraction of the total Mg is likely to be associated with actual or remnants of organic matter present inside the cell structure. The H_2O_2 treatment, however, does not significantly affect the Mg/Ca variations along a rhodolith branch.

Dolomitic structures of the order of ~100 µm-long, scattered across the rhodolith skeleton of *S. durum* have been identified and could bias the Mg/Ca records. They are easily distinguishable and can be avoided when setting the laser path for LA-ICPMS analysis.

Mg/Ca variations are reproducible across the same rhodolith branch, suggesting a homogenous lateral distribution across the axis of main growth.

Two types of Mg/Ca variations, related to the rhodolith visual banding, have been observed and the use of different laser spot sizes enables identification of either one. Bigger spot sizes better record major, low-frequency Mg/Ca cycles that likely reflect local environmental seasonality, whereas smaller spot sizes more clearly record minor, high-frequency Mg/Ca cycles that seem to be intimately linked to the internal growth pattern of the coralline red alga.

References

Adey, W., H., and MacIntyre, I., G. (1973). Crustose Coralline Algae: A Re-evaluation in the Geological Sciences. *Geological Society of America Bulletin* **84,** 883-904.

Basso, D., Nalin, R., and Nelson, C., S. (2009). Shallow-water *Sporolithon* rhodoliths from North Island (New Zealand). *Palaios* **24,** 92-103.

Bosence, D., W. J. (1983a). Description and Classification of Rhodoliths (Rhodoids, Rhodolites). *In* "Coated Grains." (T. M. Peryt, Ed.), pp. 217-224. Springer-Verlag, Berlin.

Bosence, D., W., J. (1983b). The Occurence and Ecology of Recent Rhodoliths - A Review. *In* "Coated Grains." (T. M. Peryt, Ed.), pp. 225-242. Springer-Verlag Berlin.

Burdett, H., Kamenos, N. A., and Law, A. (2010). Using coralline algae to understand historic marine cloud cover. *Palaeogeography, Palaeoclimatology, Palaeoecology* **302,** 65-70.

Chan, P., Halfar, J., Williams, B., Hetzinger, S., Steneck, R., Zack, T., and Jacob, D. E. (2011). Freshening of the Alaska Coastal Current recorded by coralline algal Ba/Ca ratios. *Journal of Geophysical Research* **116,** G01032.

Chave, K. E. (1954). Aspects of the biogeochemistry of magnesium 1. Calcareous marine organisms. *The Journal of Geology* **62,** 266-283.

Craig, C. A., Jarvis, K. E., and Clarke, L. J. (2000). An assessment of calibration strategies for the quantitative and semi-quantitative analysis of calcium carbonate matrices by laser ablation-inductively coupled plasma-mass spectrometry (LA-ICP-MS). *Journal of Analytical Aomic Spectrometry* **15,** 1001-1008.

de Villiers, S., Greaves, M., and Elderfield, H. (2002). An intensity ratio calibration method for the accurate determination of Mg/Ca and Sr/Ca of marine carbonates by ICP-AES. *Geochemistry, Geophysics, Geosystems* **3,** 1001.

Dickson, J. A. D. (1965). A modified staining technique for carbonates in thin section. *Nature* **205,** 587.

Eggins, S., De Deckker, P., and Marshall, J. (2003). Mg/Ca variation in planktonic foraminifera tests: implications for reconstructing palaeo-seawater temperature and habitat migration. *Earth and Planetary Science Letters* **212,** 291-306.

Fallon, S. J., McCulloch, M. T., van Woesik, R., and Sinclair, D. J. (1999). Corals at their latitudinal limits: laser ablation trace element systematics in *Porites* from Shirigai Bay, Japan. *Earth and Planetary Science Letters* **172,** 221-238.

Foster, M., S. (2001). Rhodoliths: Between rocks and soft places. *Journal of Phycology* **37,** 659-667.

Frantz, B. R., Foster, M. S., and Riosmena-Rodrìguez, R. (2005). *Clathromorphum nereostratum* (Corallinales, Rhodophyta): The oldest alga? *Journal of Phycology* **41,** 770-773.

Gamboa, G., Halfar, J., Hetzinger, S., Adey, W., Zack, T., Kunz, B., and Jacob, D. E. (2010). Mg/Ca ratios in coralline algae record northwest Atlantic temperature variations and North Atlantic Oscillation relationships. *Journal of Geophysical Research* **115,** C12044.

Goldberg, N. (2006). Age estimates and description of rhodoliths from Esperance Bay, Western Australia. *Journal of the Marine Biological Association of the United Kingdom* **86,** 1291-1296.

Halfar, J., Steneck, R., S., Schöne, B., R., Moore, G., W., K., Joachimski, M., Kronz, A., Fietzke, J., and Estes, J. (2007). Coralline alga reveals first marine record of subarctic North Pacific climate change. *Geophysical Research Letters* **34,** L07702.

Halfar, J., Zack, T., Kronz, A., and Zachos, J., C. (2000). Growth and high-resolution paleoenvironmental signals of rhodoliths (coralline red algae): A new biogenic archive. *Journal of Geophysical Research* **105,** 22,107-22,116.

Harris, P., J., Tsuji, Y., Marshall, J., F., Davies, P., J., Honda, N., and Matsuda, H. (1996). Sand and rhodolith-gravel entrainment on the mid- to outer-shelf under a western

boundary current: Fraser Island continental shelf, eastern Australia. *Marine Geology* **129,** 313-330.

Hathorne, E. C., Alard, O., James, R. H., and Rogers, N. W. (2003). Determination of intratest variability of trace elements in foraminifera by laser ablation inductively coupled plasma-mass spectrometry. *Geochemistry, Geophysics, Geosystems* **4,** 8408.

Hetzinger, S., Halfar, J., Kronz, A., Steneck, R., Adey, W., H., Lebednik, P., A., and Schöne, B., R. (2009). High-resolution Mg/Ca ratios in a coralline red alga as a proxy for Bering Sea temperature variations from 1902 to 1967. *Palaios* **24,** 406-412.

Hetzinger, S., Halfar, J., Zack, T., Gamboa, G., Jacob, D. E., Kunz, B. E., Kronz, A., Adey, W., Lebednik, P. A., and Steneck, R. S. (2011a). High-resolution analysis of trace elements in crustose coralline algae from the North Atlantic and North Pacific by laser ablation ICP-MS. *Palaeogeography, Palaeoclimatology, Palaeoecology* **302**(1-2), 81-94.

Hetzinger, S., Halfar, J., Mecking, J. V., Keenlyside, N. S., Kronz, A., Steneck, R. S., Adey, W. H., and Lebednik, P. A. (2011b). Marine proxy evidence linking decadal North Pacific and Atlantic climate. *Climate Dynamics*, 1-9.

Kamenos, N., A., Cusack, M., Huthwelker, T., Lagarde, P., and Scheibling, R., E. (2009). Mg-lattice associations in red coralline algae. *Geochimica et Cosmochimica Acta* **73,** 1901-1907.

Kamenos, N., A., Cusack, M., and Moore, P., G. (2008). Coralline algae are global palaeothermometers with bi-weekly resolution. *Geochimica et Cosmochimica Acta* **72,** 771-779.

Kamenos, N. A., and Law, A. (2010). Temperature controls on coralline algal skeletal growth. *Journal of Phycology* **46,** 331-335.

Longerich, H. P., Jackson, S. E., and Günther, D. (1996). Laser ablation inductively coupled plasma mass spectrometric transient signal data acquisition and analyte concentration calculation. *Journal of Analytical Atomic Spectrometry* **11,** 899-904.

Love, K. M., and Woronow, A. (1991). Chemical changes induced in aragonite using treatments for the destruction of organic material. *Chemical geology* **93,** 291-301.

Martin, P. A., and Lea, D. W. (2002). A simple evaluation of cleaning procedures on fossil benthic foraminiferal Mg/Ca. *Geochemistry, Geophysics, Geosystems* **3,** 8401.

Milliman, J. D., Gastner, M., and Müller, J. (1971). Utilization of magnesium in coralline algae. *Geological Society of America Bulletin* **82,** 573-580.

Moberly Jr, R. (1968). Composition of Magnesian Calcites of Algae and Pelecypods by Electron Microprobe analysis. *Sedimentology* **11,** 61-82.

Nash, M. C., Troitzsch, U., Opdyke, B. N., Trafford, J. M., Russell, B. D., and Kline, D. I. (2011). First discovery of dolomite and magnesite in living coralline algae and its geobiological implications. *Biogeosciences* **8,** 3331-3340.

Nelson, W. A. (2009). Calcified macroalgae - critical to coastal ecosystems and vulnerable to change: a review. *Marine and Freshwater Research* **60,** 787-801.

Paillard, D., Labeyrie, L., and Yiou, P. (1996). Macintosh program performs time-series analysis. *Eos Transactions AGU* **77,** 379.

Schöne, B. R., Zhang, Z., Radermacher, P., Thébault, J., Jacob, D. E., Nunn, E. V., and Maurer, A. F. (2011). Sr/Ca and Mg/Ca ratios of ontogenetically old, long-lived bivalve shells (*Arctica islandica*) and their function as paleotemperature proxies. *Palaeogeography, Palaeoclimatology, Palaeoecology* **302,** 52-64.

Sinclair, D. J., Kinsley, L. P. J., and McCulloch, M. T. (1998). High resolution analysis of trace elements in corals by laser ablation ICP-MS. *Geochimica et Cosmochimica Acta* **62,** 1889-1901.

Steneck, R. S. (1986). The ecology of coralline algal crusts: convergent patterns and adaptative strategies. *Annual Review of Ecology and Systematics* **17,** 273-303.

Stoll, H. M., Encinar, J. R., Garcia Alonso, J. I., Rosenthal, Y., Probert, I., and Klaas, C. (2001). A first look at paleotemperature prospects from Mg in coccolith carbonate: Cleaning techniques and culture measurements. *Geochemistry, Geophysics, Geosystems* **200,** 2GC000144.

CHAPTER IV

Growth and chronology of the rhodolith-forming, coralline red algal species *Sporolithon durum* from the tropics

Keywords: CCA, extension rate, radiocarbon, seasonal pattern

Manuscript published as: Darrenougue N. (70%), De Deckker (12%), P., Payri C. (5%), Eggins S. (8%), Fallon S (5%). 2013. Growth and chronology of the rhodolith-forming, coralline red alga *Sporolithon durum*. *Marine Ecology Progress Series* **474**, p105-119.

Numbers after each author's name refer to the percentage of their respective contribution to this paper.

Abstract

We report extension rates and growth patterns of the coralline red algal species *Sporolithon durum* (rhodolith form) from New Caledonia. Alizarin red S staining was used to mark 43 rhodolith branches and helped determine extension rates over the rhodoliths last living year. A combination of radiocarbon dating, major Mg/Ca-cycles and growth band determinations provided a chronological approach to characterise extension rates for five branches over the last five decades. A seasonal asymmetry in the extension rates is observed, with higher extension during the austral summer-fall-winter period, indicating that variations in ambient seawater temperature are not of major influence in the seasonal growth pattern of *S. durum*. At the sub-seasonal level, minor growth bands were observed with a maximum frequency of a fortnight but were too variable to be considered as a reliable chronological tool. The concordance of the results from both the monitoring experiment over the 2010-2011 year and the chronological approach applied to the 1968-2008 period suggests that an average extension rate of 0.6 ± 0.2 mm y^{-1} is typical of the *S. durum* community at the site. However, annual extension rates vary considerably between branches and individuals. Long-term trends still appear, such as a decrease during the early 1970s attributed to the impact of mining activity. A slight but consistent decrease is observed in the annual extension rates throughout the record and may reflect an ontogenic effect potentially enhanced by reduced light penetration due to increasing suspended particulate matter in the water column.

IV-1 Introduction

Rhodoliths are unattached nodules essentially composed of calcareous coralline red algae. As they grow, deposits of calcium carbonate form a calcareous skeletal structure that can be preserved after the death of the algae and may accumulate, along with the skeletons of other organisms of the same community, over thousands of years (Freiwald, 1991; Basso, 2012). Fossil coralline red algae occur in the geological record since the Cretaceous (Aguirre, 2000). The modern distribution of these organisms spans all latitudes, from the tropics to the poles, and ranges from the intertidal zone down to the limit of the photic zone (Foster, 2001). The major contribution of coralline red algae to reef building, in tropical as well as extra-tropical regions, has been recognised in numerous studies (e.g. Borowitzka, 1983; Littler and Littler, 1988; Foster, 2001; Schäfer et al., 2011; Basso, 2012). In the tropics, coralline red algae are often associated with coral reefs where their calcareous skeletons provide the cement that is crucial for consolidating the reef structure (e.g. Steneck, 1997; Payri, 1997; 2001).

Early studies focused mainly on the ecology and the taxonomy of coralline red algae (see Adey and MacIntyre, 1973; Bosence, 1983b for reviews). In recent years, interest has arisen in using these organisms as environmental archives because of their global distribution and their slow growth rates (between 0.01 and 2.7 mm y^{-1}; Foster, 2001; Böhm et al., 1978) associated with the thick crusts they form (up to several cm). The geochemical composition of the coralline algal skeleton has been shown to record various environmental parameters (in particular, Mg/Ca variations can record changes in seawater temperature at sub-annual resolution over decades to centuries; Halfar et al., 2000; Kamenos et al., 2008, Hetzinger et al., 2009; 2011; Kamenos, 2010; but see also Frantz, 2000; Halfar et al., 2007, Williams et al., 2011, Chan et al., 2011). Calcification changes have also been used for environmental reconstruction (Halfar et al., 2011a-b; Burdett et al., 2010), as various species of coralline red algae display calcification rates varying with environmental conditions, in particular light and seawater temperature (e.g. Foster, 2001; Kamenos and Law, 2010).

In seasonally contrasted regions, annual cycles in calcification can be observed as couplets of light and dark bands characterised by short, heavily calcified cells usually produced during the winter months and longer, less calcified cells produced in summer (e.g. Basso, 1994, 1995; Halfar et al., 2008; Kamenos and Law, 2010), a property useful in establishing chronologies for palaeo-environmental reconstructions (e.g. Burdett et al., 2010). This occurs along with changes in Mg content of the coralline red algal calcite

skeleton, covarying with seawater temperature, which result in well-defined Mg/Ca annual cycles (Hetzinger et al., 2009; 2011; Chan et al., 2011). In addition to the major, annual banding, several coralline red algae species display higher-frequency minor bands. The cause of these sub-annual bands remains uncertain, although they have generally been interpreted either as marking growth cessation (Cabioch, 1966) or as representing approximate monthly or lunar cycles (Agegian, 1981; Freiwald and Henrich, 1994; Blake and Maggs, 2003). The growth rate and pattern of coralline red algae vary, both from species to species (Blake and Maggs, 2003) and with various environmental conditions (Adey and McIntyre, 1973; Foster, 2001). Therefore, it is crucial to evaluate these parameters for any particular species prior to attempting palaeo-environmental reconstructions. Furthermore, a better understanding of the growth rate and pattern of coralline red algae is a key to assess how these organisms will be affected by global climate changes in the Future.

Sporolithon durum (Foslie) Townsend & Woelkerling is a widely distributed coralline red algal species belonging to the recently recognised order Sporolithales (Le Gall et al., 2010; Bittner et al., 2011). *S. durum* occurs either as attached or as free-living forms, from the tropics to temperate oceanic environments (e.g. Townsend et al., 1995; Womersley, 1996; Goldberg and Heine, 2008; Basso et al., 2009). Previous reports on modern, individual rhodoliths with a potential lifespan of several decades (e.g. Goldberg and Heine, 2008) indicate this species may be a suitable candidate for environmental reconstructions with sub-annual resolution. However, accurate growth rates and pattern information on *S. durum* have not previously been determined.

Accordingly, this study aims to characterise the extension rates and growth patterns of *S. durum*, through *in situ* monitoring of rhodoliths in a tropical environment and by establishing multi-approach chronologies for nodules collected from the same rhodolith bed. It is the first time this type of study is conducted for the coralline red algal order Sporolithales.

IV-2 Material and methods

IV-2.a Study site and sample collection

The rhodoliths studied here were collected near Nouméa, by SCUBA diving on the outer edge of the Ricaudy Reef (22°18'57"S; 166°27'26"E) in the SW lagoon of New Caledonia, at depths ranging from 4 to 5 m (Figure IV-1). The climate of New Caledonia is characterised by a tropical regime with pronounced seasonal variation from a hot and wet summer (Jan-

Mar) to a cool and humid winter (Jul-Aug), with drier weather occurring during the intermediate months (Apr-May and Sep-Dec). On an inter-annual timescale, the climate system is mainly influenced by the El Niño Southern Oscillation (ENSO) phenomenon, with typically cooler and drier periods during El Niño events and warmer and wetter periods during La Niña events (Nicet and Delcroix, 2000). Seawater temperatures closely follow the atmospheric temperatures at seasonal and inter-annual scales.

The studied rhodoliths are monospecific and formed by the coralline red alga *S. durum* that was identified using histological analyses as the most abundant species at the site, and which forms beds that can entirely cover the substratum. The sampled rhodoliths are spheroidal in shape with thick and dense branches ("degree IV" branching structure according to the classification of Bosence (1983a)). The nodules range in size from ~4 to > 8 cm (long axis), and are representative of the *S. durum* rhodoliths observed at the site.

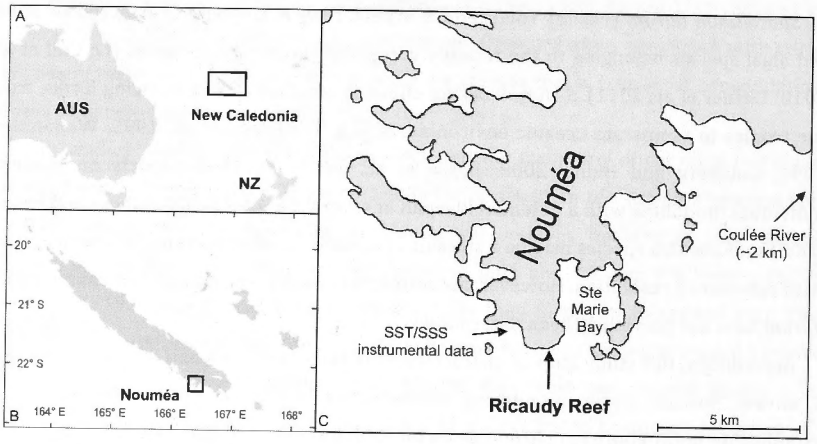

Figure IV-1 **Location maps showing New Caledonia in the tropical Western Pacific (A), Nouméa, the capital city (B) and the Ricaudy Reef, at the south end of the Sainte Marie Bay, near Nouméa (C). The site of instrumental sea surface temperature (SST) and salinity (SSS) measurements is also shown in C, as well as the direction and distance to the Coulée River mouth.**

Over 60 rhodoliths were collected in February 2011 and were used for the growth-monitoring experiment. For the chronology and extension rate determination of entire nodules, three rhodoliths were selected from separate dives in October 2009 (labelled specimen BSA) and February 2011 (labelled specimens MSA and SSA) as being the largest and visually healthiest (i.e. bright pink in colour and physically undamaged) specimens encountered during the dives.

IV-2.b Monitoring experiment

IV-2.b.1 Staining, experimental conditions and sample preparation

The specimens collected for the monitoring experiment were placed for 48h in tanks, each containing ~10 litres of seawater from the Ricaudy Reef, in which 75 mg of Alizarin Red S powder was dissolved (adapted method from Payri (1997)). After staining, the rhodoliths were placed back into their natural environment, inside a ~1x1 m enclosure built within the rhodolith bed (4-5 m-deep), for the duration of the experiment (FigureIV-2A). A TinyTag TG-4100 Aquatic 2 temperature logger was attached to the enclosure to monitor hourly *in situ* temperature (IST) in the immediate vicinity of the organisms. *In situ* temperature recording using this device started in November 2009. All the stained rhodoliths were retrieved in August 2011, after 196 days (28 weeks) in the enclosure. Based on the size range of the stained rhodoliths, seven representative nodules were selected, oven dried (40°C) and set into resin to preserve the fragile branching structure during the sectioning process. Thick sections (2-5 mm) were cut along the long axis of the nodules using a diamond rock-saw. High-resolution photographs of the polished sections were obtained using a Digital Sight DS-Fi1 digital camera attached to a Nikon AZ100 optical microscope (Figure IV-2B-C).

IV-2.b.2 Growth determination

Based on the definitive presence of the ARS stain layer (see Figure IV-2C), 43 branch tips from the seven selected rhodoliths were analysed for their extension rate and growth pattern (Table IV-S1). High-resolution digital images were processed using the ImageJ version 1.45 digital analysis software (available as freeware at http://rsbweb.nih.gov/ij) to measure growth with a precision of 1 µm. Measurements were systematically taken along the axis of branch main growth, perpendicular to cell alignment, so the maximum extension rate could be obtained. The distance from the pink Alizarin-stained layer to the surface layer of each branch tip was attributed to the growth during the 28-week monitored period (Feb-Aug11).

Annual growth rates were determined using the outermost Mg/Ca cycle recorded along each branch that was measured by laser ablation inductively coupled plasma mass spectrometry (LA-ICPMS – see e.g. Eggins et al., 1998) with a 30 µm resolution corresponding to a sub-monthly sampling. Based on the observed covariance between Mg/Ca variations and seawater temperature in coralline algae (e.g. Halfar et al., 2000; Kamenos et al., 2008; Hetzinger et al., 2009), we were able to link the lowest Mg/Ca values

to the months with the lowest temperature of the last 13 months (July 2010 and August 2011). The distance corresponding to this 13-month period for each branch was then linearly transformed to obtain 12 months, annual growth rates.

The minor banding was determined visually from digitised high-resolution images by the alternation of clear and darker layers of cells (Figure IV-2C). The number of minor bands from the stained layer to the surface of the branch was reported for the Feb-Aug11 period, and the number from the penultimate lowest value of the Mg/Ca cycle to the stained layer was attributed to the Jul10-Feb11 period. The average length of the minor bands was calculated from the distance measured for each period and the corresponding observed number of minor bands.

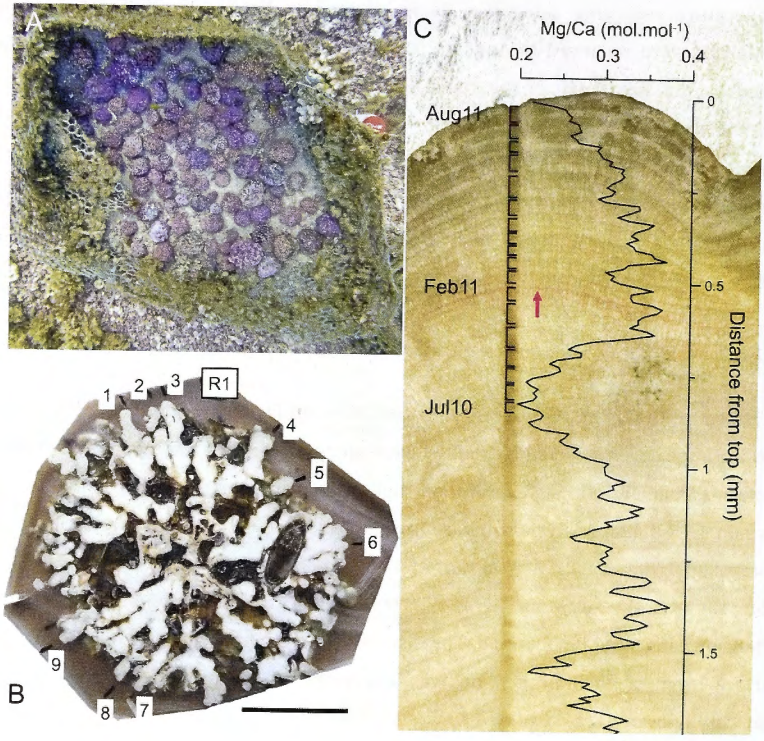

Figure IV-2 Monitoring experiment and growth rate determination. A: Rhodolith enclosure (~1 x 1 m) at the Ricaudy Reef. Photograph taken 2 days after staining (February 2011). B: Epoxy block sectioned across the long axis of a monitored rhodolith (mostly white in colour), showing the branch-tips analysed (black ticks with numbers). Scale bar: 2 cm. C: Close up of the R1-4 branch tip, showing the Mg/Ca variations recorded by LA-ICPMS. The arrow points to the Alizarin red S stain layer (pink layer), which corresponds to February 2011. The top of the branch is August 2011 and the following lowest Mg/Ca peak was attributed to July 2010. Minor bands are indicated by the black half-boxes.

IV-2.b.3 Back-scattered electron (BSE) images

To characterise the growth pattern of *S. durum* at the cellular level, we used the Cameca SX100 electron microprobe at the Research School of Earth Sciences (RSES) of the Australian National University (ANU) to obtain back-scattered electron (BSE) images. The BSE images were captured from a 1-µm polished, carbon coated thin section of a rhodolith branch.

IV-2.c Chronology and extension rate of entire nodules

The sample preparation for the BSA, MSA and SSA rhodoliths is identical to the one mentioned for the analysis of the monitored specimens (section IV-2.b.1). As no obvious mark of cessation of growth (i.e. green algal levels or sign of breakage) was observed in any of the rhodolith thick section, we considered the organisms to have grown continuously throughout their living period.

IV-2.c.1 Radiocarbon dating

10 mg samples of the rhodolith's carbonate skeleton were obtained by drilling along two branches situated on the long (BSA_L – Figure IV-3A) and short (BSA_S) axes of the BSA nodule. Every hole was 1-2 mm in diameter and was drilled with a 2-3 mm step from top to bottom along the branches. Radiocarbon measurements were carried out at the ANU, using the single stage accelerator mass spectrometer (SSAMS) facility (Fallon et al., 2010). The CO_2 was liberated from the carbonate samples by addition of phosphoric acid to vacuum-sealed blood vials, the CO_2 was then reduced to graphite using a Fe-catalyst in the presence of hydrogen (Vogel et al., 1987). IAEA C-1 marble (^{14}C free) was used for background subtraction. Results are presented in pMC (percent Modern Carbon). The data analysis software AnalySeries (Paillard et al., 1996) was used to fit the pMC values to the calibrated pMC curve obtained by Fallon et al. (2003) for a coralline sponge from Vanuatu, following the atomic bomb curve from the 1950s. Similarities in the oceanography of the Vanuatu and New Caledonia regions, both located at the northwestern edge of the South Pacific gyre, likely produced similar trends in the variations of the oceanic ^{14}C enrichment in the area after the atomic bomb tests, thus making the Fallon et al. (2003) calibration suitable to our study. This fitting method, which does not require any reservoir effect correction, is commonly used to establish age models for modern (i.e. post 1950) samples, when the sampling resolution is sufficient (e.g. Frantz et al., 2000 for a rhodolith).

Due to the relatively large amount of carbonate material needed to perform the radiocarbon analysis, in conjunction with the generally slow growth rate of coralline red algae, the sampling technique is likely to be responsible for an uncertainty close to one to two years on every date. The analytical errors on the pMC values averaged 0.3%. This, in combination with the small pMC variations recorded after the bomb spike for the Vanuatu sponge (Fallon et al., 2003), leads to an additional date uncertainty of a couple of years based on the curve-fitting process. Overall, we estimate the age uncertainty of each radiocarbon date to be higher than 1 year but to not exceed 5 years.

IV-2.c.2 Band counting and Mg/Ca cycles

The radiocarbon chronology for the BSA rhodolith was compared to an independent chronological approach mainly based on the determination of the seasonal Mg/Ca cycles along each branch (Figure IV-3A-B), as previously used for various species of coralline red algae (e.g. Hetzinger et al., 2009, 2011; Gamboa et al., 2010). With the aid of the AnalySeries software (Paillard et al., 1996), we used the low points in Mg/Ca cycles as anchor points that were matched to the coolest months of successive years in the SST record. The distance between two anchor points determines reported annual extension rates.

Using a 30-µm diameter spot for the LA-ICPMS analysis of rhodoliths, we achieved a sub-monthly resolution. However, despite efforts to cut a sampling surface exactly parallel to the main axis of growth, the three-dimensional complexity of the branches' structure at high resolution may lead to bands that appear compressed or stretched. This, in addition to other potential factors influencing seasonal and sub-seasonal Mg/Ca distribution and variability in the analysed *S. durum* rhodoliths (full details will be reported in a separate communication; Darrenougue et al., *in prep*), sometimes prevent from distinguish clear minima in the Mg/Ca variations. In such cases, the identification of major, annual bands on the high-resolution photographs confirmed the boundaries of the seasonal cycles. It has to be noted that the major, annual banding was not always clear (e.g. Figure 3B), however, using both the major banding and the major Mg/Ca cycles enabled us to compensate for the uncertainty bound to either method. As a result, we estimate the age uncertainty of this model to be no more than a year.

IV-2.d Environmental dataset

Météo France and the Institut de Recherche pour le Développement (IRD) provided monthly records of local sea surface temperature (SST), global solar radiation, rainfall and

wind strength for the 1960-2011 period. The Direction des Mines et de l'Energie de Nouvelle Calédonie (DIMENC) provided the annual mining production data the for duration of the mining activity in the Coulée region.

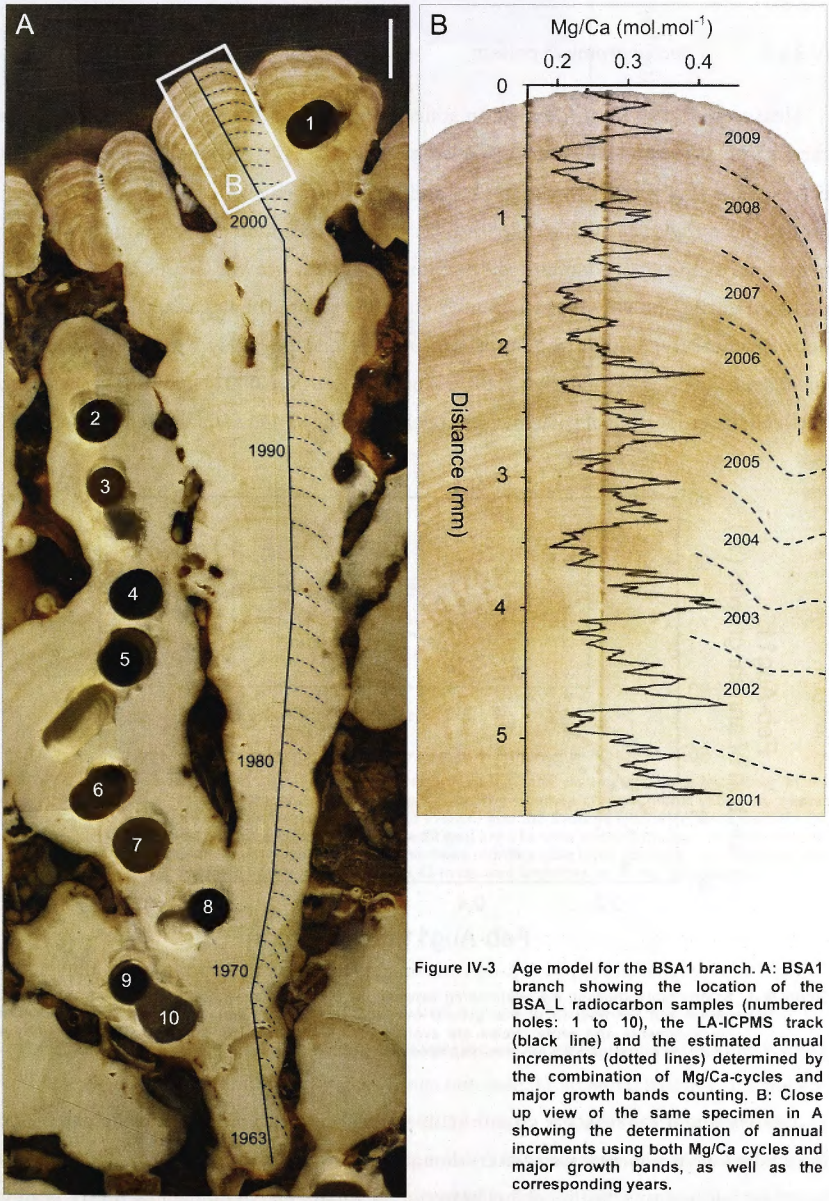

Figure IV-3 Age model for the BSA1 branch. A: BSA1 branch showing the location of the BSA_L radiocarbon samples (numbered holes: 1 to 10), the LA-ICPMS track (black line) and the estimated annual increments (dotted lines) determined by the combination of Mg/Ca-cycles and major growth bands counting. B: Close up view of the same specimen in A showing the determination of annual increments using both Mg/Ca cycles and major growth bands, as well as the corresponding years.

IV-3 Results

IV-3.a Monitored rhodoliths

IV-3.a.1 Seasonal growth pattern

Measured growth from the Alizarin stain to the surface of each of the 43 branch tips ranges from 0.146 and 0.894 mm and averages 0.452 ± 0.176 (1σ) mm (Table IV-S1). This corresponds to a growth range of 33% and 80%, respectively, of the total Jul10-Feb11 growth period, with an average of 65 ± 12%. With the exception of a few branches (mainly belonging to the R2 rhodolith), the greatest rhodolith growth in the last 13 months occurred during the Feb-Aug11 period (Figure IV-4). Both the linear and logarithmic fits between measurements of the latter two periods display highly significant correlation coefficients (r^2 = 0.72 and r^2 = 0.82, respectively; $p < 0.0001$) indicating covariance between the proportion of growth occurring in Feb-Aug11 and annual extension rates.

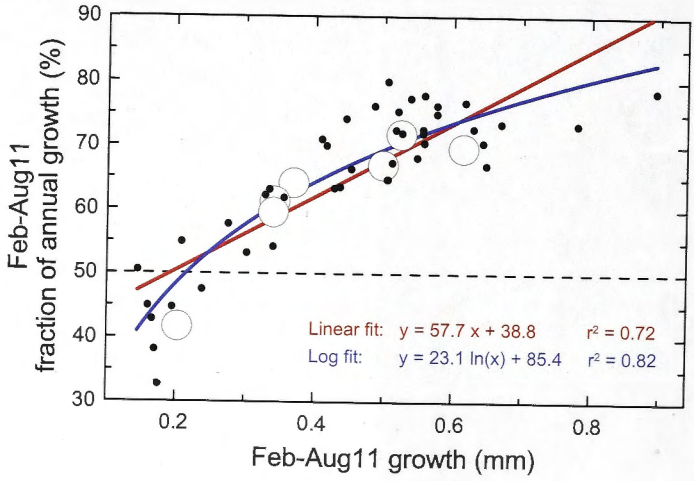

Figure IV-4 **Scatter plots showing the relationship between the distances measured for the Feb-Aug11 growth period and the fraction of that growth over the Jul10-Aug11 period. Black dots are individual measurements and white circles are averages for each rhodolith. Linear (red) and logarithmic (blue) fits and equations are also displayed along with the respective correlation coefficients.**

The asymmetrical seasonal growth pattern recorded for *S. durum* and the patterns of the studied environmental parameters do not correspond, as the latter globally display no significant differences (within error) between the Jul10-Feb11 and the Feb-Aug11 periods (Figure IV-5).

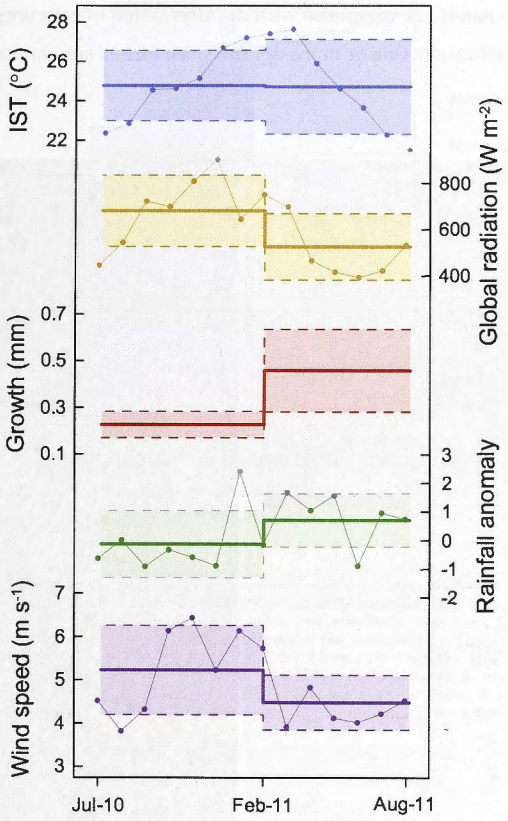

Figure IV-5 **Comparison between the average of various environmental parameters recorded either at the study site (in situ temperature: IST) or for the nearby Nouméa station (global radiation, rainfall anomaly and wind speed - data from Météo France) and the average extension rates (red) for the periods Jul10-Feb11 and Feb-Aug11. Shaded areas are ±1σ over each of the two latter periods for each environmental parameter based on the mean monthly data (also displayed as thin lines) and the variable extension rates recorded in the 43 measured branches for these two periods.**

The number of minor, sub-annual bands for the Feb-Aug11 period ranges from 3 (R2-2, R2-4, R4-1 and R5-2) to 14 (R1-2 and R1-5), half of which fall within 6 and 12 (Table IV-S1). The average length of the minor bands occurring between February and August 2011 is 0.049 ± 0.009 mm and individual values range between 0.030 and 0.070 mm, for the R5-1 and R1-7 branches, respectively. For the Jul10-Feb11 period, less minor bands are generally observed than for the Feb-Aug11 period. 3 to 9 bands typically occur in each branch. These minor bands also appear to be slightly shorter, with an average length of 0.039 ± 0.007 mm and a range of 0.023 (R7-5) to 0.054 mm (R1-1 – Table IV-S1).

The close up optical image, as well as its corresponding SEM image show that the minor, sub-annual bands are composed with the alternation of cells with different lengths and degrees of calcification. One or more cell rows can form a sub-annual band (Figure IV-6).

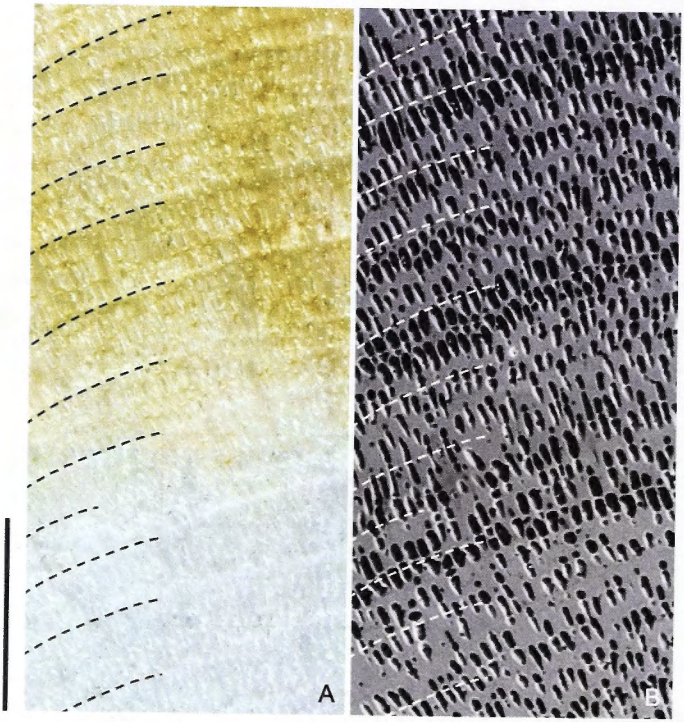

Figure IV-6 Optical image (A) and corresponding back scattered electron (BSE) image (B) of a portion of rhodolith branch where the minor banding is clearly visible (dashed lines) and consists of the alternation of small, heavily calcified cell layers and longer, less calcified ones. Also note the general trend from small, heavily calcified cells at the bottom of the BSE image towards longer, less calcified cells at the top of the image, which constitutes the major banding pattern. Scale bar: 200 µm. The growth direction of the specimen is from the bottom to the top of the images.

IV-3.a.2 Annual extension rates

The measured extension rates for the 2010-2011 year are reported in Table IV-S1, with the distribution and summary statistics presented in Figure IV-7 (n = 43). Extension rates range from 0.267 to 1.053 mm y^{-1} and average 0.622 ± 0.170 mm y^{-1}, with 50% of the values occurring between 0.493 and 0.720 mm y^{-1}.

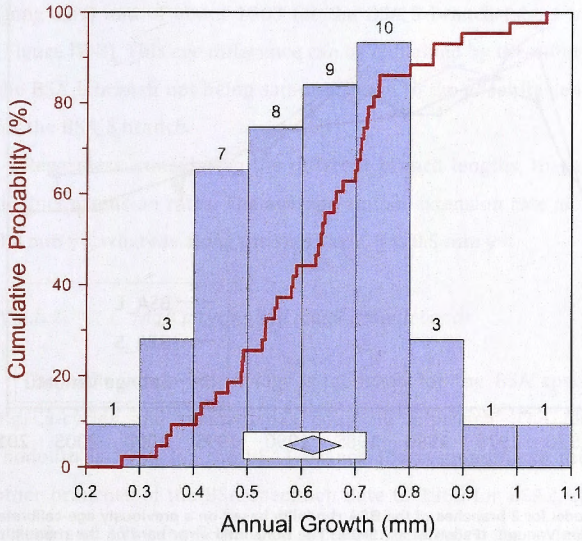

Moments	
Mean	0.622
Std Dev	0.170
Std Err Mean	0.026
Upper 95% Mean	0.674
Lower 95% Mean	0.569
Max	1.053
75% Quartile	0.720
Median	0.635
25% Quartile	0.493
Min	0.267
N	43

Figure IV-7 **Cumulative probability and distribution plots of annual extension rates recorded for the monitored rhodoliths. The blue histograms show the number of branch tips with annual extension sorted in bins of 0.1 mm, from 0.2-0.3 to 1.0-1.1 mm. The step plot (red line) display the cumulative distribution function of the extension rates versus the cumulative probability measured from the 43 tips. The white box at the bottom of the bar chart illustrates the statistical moments of the series right table): the edges of the box are the 25% and 75% quartiles, the line inside the box is the median value and the blue diamond represents the average, with the vertical diagonal being the average value and the edges of the horizontal diagonal being the lower and upper 95% mean values.**

IV-3.b Entire rhodolith specimens

IV-3.b.1 Radiocarbon dating

Radiocarbon results for the BSA_L and BSA_S branches are presented in Figure IV-8 and Table IV-1. pMC values for the BSA_L branch show a steady decrease from 114.9 ± 0.3 in the sample nearest to the start of growth, to 109.1 ± 0.4 at the top of the branch. pMC values for the BSA_S branch increase sharply from 103.8 ± 0.3 to 113.9 ± 0.3 close to the centre of the rhodolith, then, as for BSA_L, steadily decrease to a value of 107.7 ± 0.3 near the top of the branch. The sharp increase and then slow decrease in the BSA_S branch pMC values matches the evolution of the atomic bomb spike in the South Pacific region, from the late 1950s to the early 1970s, also recorded in corals (e.g. Toggweiler et al., 1991; Guilderson et al., 2000) and sponges (Fallon et al., 2003). The BSA_L pMC values do not record this sharp increase and therefore, the oldest radiocarbon date is considered to be younger than 1970.

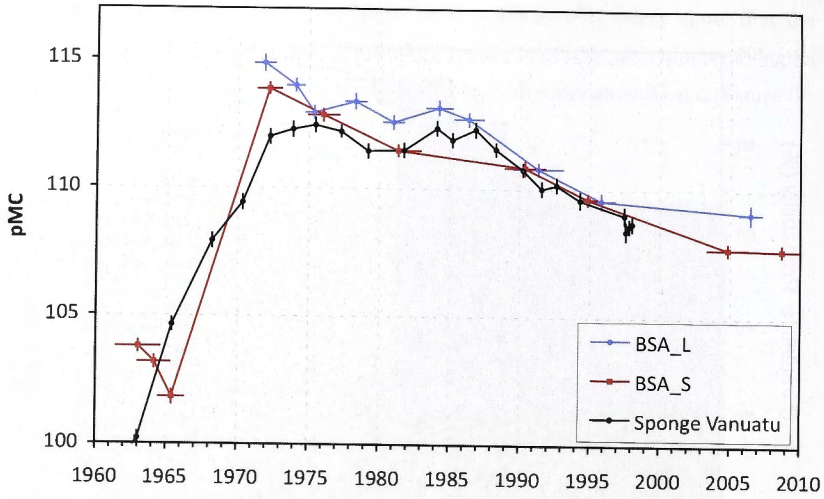

Figure IV-8 **Radiocarbon age model for 2 branches of the BSA rhodolith based on a previously age-calibrated coralline sponge from Vanuatu (Fallon et al., 2003). The horizontal error bars on the rhodolith's radiocarbon data correspond to the size of the sampled material (1-2 mm along the branch, corresponding to 1-4 years interval – see text for more info). pMC: percent modern carbon.**

Sample	#	Distance from top (mm)	Percent Modern Carbon (pMC)	Calibrated Date
BSA_L				
	1	2.9 ±0.7	109.07 ±0.41	2007
	2	11.7 ±0.9	109.56 ±0.33	1996
	3	14.7 ±1.5	110.78 ±0.28	1991
	4	19.6 ±0.9	112.70 ±0.30	1986
	5	21.2 ±0.8	113.15 ±0.32	1984
	6	23.2 ±0.7	112.58 ±0.31	1981
	7	25.5 ±0.6	113.37 ±0.33	1978
	8	28.0 ±0.6	112.94 ±0.28	1975
	9	28.9 ±0.6	114.00 ±0.28	1974
	10	30.7 ±0.6	114.86 ±0.34	1972
BSA_S				
	1	2.4 ±0.8	107.67 ±0.26	2009
	2	4.6 ±0.9	107.70 ±0.27	2005
	3	7.1 ±0.4	109.62 ±0.25	1995
	4	9.9 ±0.9	110.82 ±0.31	1990
	5	13.7 ±1.0	111.47 ±0.26	1981
	6	16.0 ±0.7	112.83 ±0.27	1976
	7	18.3 ±0.6	113.87 ±0.26	1972
	8	21.0 ±0.6	101.84 ±0.31	1965
	9	23.1 ±0.7	103.19 ±0.27	1964
	10	25.6 ±1.0	103.81 ±0.26	1963

Table IV-1 **Radiocarbon results for BSA_L (long axis) and BSA_S (short axis). Calibrated dates were determined using the AnalySeries computer program (Paillard et al., 1996. Typical uncertainty on calibrated dates is < 5 years (see text for details).**

The radiocarbon chronology gives an oldest date of about 1972 for the BSA_L branch (long axis) and of about 1963 for the BSA_S branch (short axis) of the same specimen (Figure IV-8). This age difference can be explained by the difference in sampling locations, the BSA_L branch not being sampled down to the absolute centre of the rhodolith, unlike for the BSA_S branch.

Regardless, considering the different branch lengths, these two series of dates imply distinct extension rates. The average annual extension rate along the long axis (BSA_L) is 0.8 mm y^{-1}, whereas along the short axis, it is 0.5 mm y^{-1}.

IV-3.b.2 Mg/Ca cycles and major growth bands

The radiocarbon chronology established for the BSA specimen is supported by the Mg/Ca-cycles and major-bands counting approach. The oldest record for the BSA rhodolith is 1963 for the BSA1 branch (corresponding to the BSA_L branch). The two other branches of the BSA specimen date to 1965 for BSA2, corresponding to the BSA_S branch and 1964 for BSA3. The agreement between these dates indicates an age of ~46 years for the BSA rhodolith. Mg/Ca-cycles and major-bands counting gives an age of 48 years for the MSA1 branch and an age of 49 years for the SSA1 branch, with an oldest date of 1962.

The annual extension rates for the BSA, MSA and SSA rhodoliths, measured along 5 branches for the 1963-2010 period ranges from 0.19 to 1.24 mm y^{-1} with an average of 0.64 ± 0.23 mm y^{-1} (n = 227; Table IV-S2). For each branch annual extension rates averaged over their respective living period, are 0.78 ± 0.25 mm y^{-1} (BSA1), 0.50 ± 0.19 mm y^{-1} (BSA2), 0.66 ± 0.25 mm y^{-1} (BSA3), 0.66 ± 0.20 mm y^{-1} (MSA) and 0.61 ± 0.19 mm y^{-1} (SSA1) (Table IV-2).

Annual extension rate (mm yr^{-1})	BSA1 (n = 45)	BSA2 (n = 43)	BSA3 (n = 44)	MSA1 (n = 47)	SSA1 (n = 48)
Average	0.75	0.49	0.66	0.66	0.62
Stdev	0.29	0.19	0.25	0.20	0.21

Table IV-2 **Average and standard deviation of annual extension rates measured for 5 different rhodolith branches over the 1963-2011 period using the combination of major growth banding and Mg/Ca cycles. n: number of years for each branch. See Appendix 2 for full dataset.**

Annual extension rates vary widely among the 5 measured branches (Figure IV-9; Table IV-3), with only the BSA1-SSA1 pair showing a significant, albeit weak, correlation at

the 95% confidence interval (r = 0.34; p = 0.02). Despite this, a slightly decreasing trend appears in the average extension rates over the last five decades and the early 1970s also display shorter annual extension rates for most of the branches (Figure IV-9).

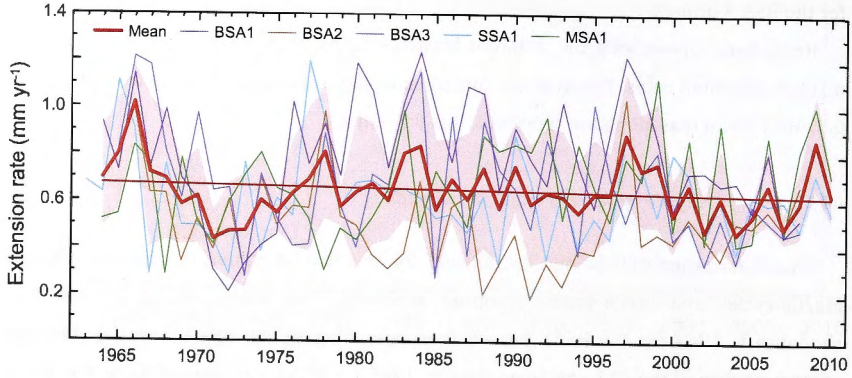

Figure IV-9 Annual extension rates along five rhodolith branches (thin lines) for the 1963-2010 period. Mean extension rates curve for the 1964-2008 period (thick red line), standard deviation (±1σ - shaded area) and the slightly decreasing trend line for the record (thin red line) are also displayed. For branch codes, refer to text.

r	BSA1	BSA2	BSA3	MSA1
BSA2	0.23			
BSA3	0.21	0.24		
MSA1	0.02	-0.20	0.14	
SSA1	0.34*	0.25	0.00	-0.12

Table IV-3 Correlation matrix for extension rates variations for the 1964-2008 period, between each rhodolith branch analysed. None of the correlations are significant at the 95% level (p > 0.05), except for * (p = 0.02).

No significant correlation at the 95% confidence interval (p > 0.05 for all the correlations) was observed between the annual data of *S. durum* annual extension rates and any of the environmental parameters recorded in Nouméa for the 1964-2008 (Figure IV-10). However, shorter extension rates in the early 1970s are contemporaneous with the peak of mining activity in the Coulée region.

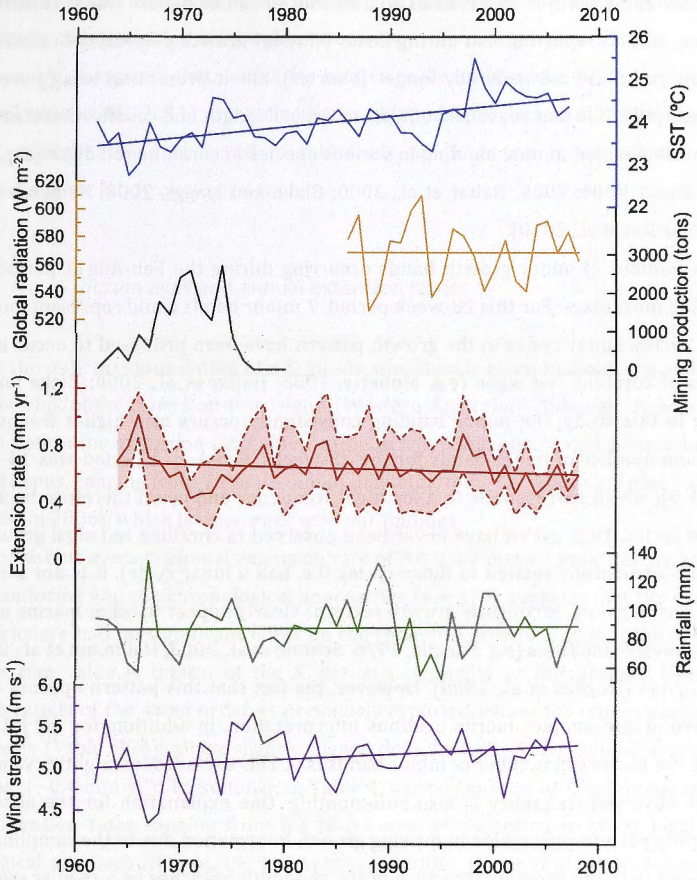

Figure IV-10 Comparison between the annual variations of the average rhodolith extension rates recorded for the 1964-2008 period at the Ricaudy Reef and various local environmental parameters measured for the Nouméa meteorological station (data from Météo France). Trend lines of each parameter for the studied period are displayed. Global solar radiation data is only available since 1986 at the site. Annual mining production in the Coulée River region during the 1960-1981 period also appear. SST: sea-surface temperature.

IV-4 Discussion

IV-4.a Seasonal growth pattern in *S. durum*

The monitoring experiment revealed a general asymmetric seasonal growth pattern in *S. durum* with higher overall growth measured between the Feb-Aug 2011 period, associated with longer minor bands widths. Consequently, for the Jul10-Feb11 period,

slower overall growth is observed as well as shorter minor bands. This is consistent with previous studies reporting that during faster (slower) growth periods, the cells formed by coralline red algae are generally longer (shorter), albeit presenting less (more) heavily calcified walls. It is that seasonal contrast in the cell length and calcification that form the recognisable major, annual banding in various species of coralline red algae (e.g. Moberly, 1968; Basso, 2004; 2005; Halfar et al., 2000; Blake and Maggs, 2003; Kamenos and Law, 2010; Burdett et al., 2010).

The number of minor growth bands occurring during the Feb-Aug11 period is more than 7, in most cases. For this 28-week period, 7 minor bands could represent monthly (or lunar) cycles. Lunar cycles in the growth pattern have been proposed to occur in various species of coralline red algae (e.g. Moberly, 1968; Halfar et al., 2000; Blake and Maggs, 2003). In this study, the minor banding consistently occurs at a higher frequency. The maximum number of minor bands for the 28-weeks, Feb-Aug11 period was 14 (for R1-2 and R1-5), which corresponds to a fortnight frequency and could therefore be attributed to tidal cycles. Tidal cycles have never been observed in coralline red algal growth but as they are intrinsically related to lunar cycles (i.e. half a lunar cycle), it is not a surprising result. Furthermore, fortnightly growth patterns clearly appear in other marine organisms such as bivalve molluscs (e.g. Panella, 1976; Schöne et al., 2003; Hallmann et al., 2011) and brachiopods (Hughes et al., 1988). However, the fact that this pattern appears clearly in only two of our samples merits cautious interpretation. In addition, for the Jul10-Feb11 period, the maximum number of minor bands is 9. This excludes fortnightly cycles, yet the highest observed frequency is also sub-monthly. One explanation for the absence of a fortnightly pattern may reside in missing growth information due to the sampling process associated with the complex structure of the rhodolith branches or a regular overturning of the rhodoliths (see discussion below). However, if the observations accurately reflect the rhodolith growth pattern, they may reveal a temporally undetermined shift in the banding periodicity, from monthly to fortnightly. It is plausible that during times of slow growth, the minor banding is only observable every lunar cycle, whereas when growth conditions are more favourable, a tidally-influenced pattern may prevail. To our knowledge, such shift in the periodicity of growth increments has thus far never been reported for any marine organism and, then again, the inconsistency of our observations calls for a future monitoring study of *S. durum* at a sub-monthly frequency to more rigorously assess this hypothesis.

The growth pattern that produces the annual, major banding in *S. durum* is repeated at the sub-seasonal level to also form the minor banding (Figure IV-6). One to a few layers of each type of cells (i.e. short, heavily calcified and long, less calcified) appears to be part of the minor banding. Hence, single rows of cells might be formed as frequently as sub-

weekly. However, the variability of this pattern precludes the determination of consistent periodicity for the deposition of a single row of cells.

In summary, it appears that, unlike for bivalve molluscs (Panella, 1976; Schöne et al., 2003; Hallmann et al., 2011) and/or some brachiopods (Hughes et al., 1988), the sub-seasonal, minor banding observed in this study for *S. durum* is too variable to be considered as a useful chronological tool.

IV-4.b *S. durum* ages and annual extension rates

So far, the only previous dating of a *S. durum* specimen is given by Goldberg and Heine (2008) for rhodoliths from Rottnest Island (Western Australia). Although these authors could not determine extension rates, their radiocarbon results estimated a maximum age for 3 specimens, ranging from 73 to 83 mm in diameter, to be 56 years old (post 1950, for a collection in 2006), which is consistent with our findings.

The consistent average annual extension rate of 0.6 ± 0.2 mm y^{-1} indicated by both the *in situ* monitoring and the chronological approaches (n = 270) suggests that the presence of the enclosure had no significant effect on the rhodolith growth, and that the observed extension rate value is typical of the *S. durum* community at the Ricaudy Reef. This extension rate is of the same order as previously reported values for other coralline red algal species (Table IV-4), albeit slightly higher than Foster's (2001) global average for rhodoliths (~0.4 mm y^{-1}). To summarise Table 4, various species of *Lithothamnion* show annual extension rates ranging from 0.2 to 0.6 mm y^{-1} according to study location or chronological approach (Rivera, 1999; Frantz et al., 2000; Halfar et al., 2000; Kamenos et al., 2008, Schäfer et al., 2011). In colder areas, regardless of the studied species, annual extension rates are generally lower (Chave and Wheeler, 1965; Halfar et al., 2000; 2007; 2008; 2011a-b; Kamenos et al., 2008). We mainly attribute this to the temperature difference between these regions and the tropical waters of New Caledonia. However, environmental factors cannot always explain the differences (or similarities) in the extension rates of various species of coralline red algae, rather, it appears that an internal, species-specific effect sometimes prevail. For instance, the same extension rates are reported for *Phymatholithon calcareum* from a temperate (Spain; Adey and McKibbin, 1970) and a cold-water environment (N. Ireland; Blake and Maggs, 2003). Conversely, *Hydrolithon onkodes* (Payri, 1997) and *S. durum* (this study) present very different extension rates in a shallow tropical environment (Table IV-4).

Species	Location	Growth/Extension (mm yr^{-1})	Chronological method	Authors
Lithothamnion crassiusculum	Gulf of California (Mexico)	0.6 ± 0.1	Radiocarbon dating	Frantz et al. (2000)
		0.63	ARS	Rivera (1999)
		0.25 - 0.45	Mg/Ca, $\delta^{18}O$	Halfar et al. (2000)
Lithothamnion glaciale	Newfoundland (Canada)	0.25 - 0.45	Mg/Ca, $\delta^{18}O$	Halfar et al. (2000)
	Loch Sween (Scotland)	0.15 - 0.17	ARS, Mg/Ca, major banding	Kamenos et al. (2008)
Lithothamnion sp.	Gulf of Panama (Panama)	0.16	Mg/Ca, major banding	Shäfer et al. (2011)
	Gulf of Chiriquí (Panama)	0.17	Mg/Ca, major banding	Shäfer et al. (2011)
Clathromorphum nereostratum	Aleutian Islands (United States)	0.30 ± 0.03	Radiocarbon dating	Frantz et al. (2005)
		0.35 (0.19 - 0.65)	Major banding, U/Th	Halfar et al. (2007)
Clathromorphum compactum	Gulf of Maine (United States)	~0.5	Mg/Ca	Chave and Wheeler (1965)
		0.42 ± 0.08	ARS	Halfar et al. (2008)
	Newfoundland, Quebec (Canada)	0.30 ± 0.08	Mg/Ca	Halfar et al. (2010)
Phymatholithon calcareum	Isle of Arran (Scotland)	0.13 - 0.19	ARS, Mg/Ca, major banding	Kamenos et al. (2008)
	Strangford Lough (N Ireland)	0.92	ARS	Blake and Maggs (2003)
	Ria de Vigo (Spain)	~0.9	Monthly, *in situ* growth measurements	Adey and McKibbin (1970)
Hydrolithon reinboldii	Tahiti (French Polynesia)	0.37	ARS	Payri (1997)
Sporolithon durum	Nouméa (New Caledonia)	0.6 ± 0.2	ARS, radiocarbon dating, Mg/Ca, major banding	*This study*
Various rhodolith-forming species	Worldwide (depth <20 m)	~0.4	Literature review	Foster (2001)

Table IV-4 **Annual growth/extension rates reported in the literature for various modern species of coralline red algae across the world. For each study, the technique used to determine the growth is also indicated. ARS: Alizarin red stain monitoring; Mg/Ca: measurements of annual, cyclic variations in Mg composition; δ18O: measurements of annual, cyclic variations in oxygen isotopic composition; Major banding: counting of annual, major bands patterns.**

IV-4.c Controls on the *S. durum* extension rate variations

Results from the monitoring experiment and from the chronological approach report extension rates for *S. durum* that can considerably vary for any given year, at different levels. The ellipsoidal shape of the *S. durum* rhodoliths may facilitate the overturning of the specimens about the long axis of growth. This would result in the parts at the opposite ends of the long axis of the nodule being more prone to remain under optimal living conditions throughout the growth period, whereas the remaining algal surface would periodically face the substratum. Although coralline red algae have been shown to have the ability to survive and continue to grow in a shaded environment for relatively long periods (e.g. Scoffin et al., 1985; Freiwald and Henrich, 1994; Bulleri, 2006, Underwood, 2006; Basso, 2009), Dethier and Steneck (2001) showed that the shaded growth rates are generally lower than the ones exposed to direct light. In our case, lateral accretion of the nodules would be favoured most of the time, resulting in extension rates being greater parallel to the long axis of the rhodoliths relative to the short axis (see BSA_L/BSA1 versus BSA_S/BSA2). Therefore, irregular overturning of the nodules could play a significant role in explaining the extension rates variability observed within the same rhodolith specimen. Episodic burial into the sediment might also slacken the rhodolith growth for variable periods of times, without necessarily stopping it (e.g. Freiwald and Henrich, 1994). This could account for some of the inter-rhodolith variability. Genetic variability resulting in individualised responses to the environment might also contribute to the inter-rhodolith variability

The complex branch structure and three-dimensional growth pattern of the rhodoliths may also provide a potential explanation for the reported extension rate variability along a single *S. durum* branch. It has been recognised that the sectioning process of a rhodolith branch could lead to the measurement of slightly shorter or longer extension rates than the actual linear extension rate of the organism along its axis of main growth (e.g. Halfar et al, 2000, 2010; Burdett et al., 2010; section IV-2.c.2). Using attached forms of coralline red algae could reduce this type of variability (Halfar et al., 2000; 2011a). Unfortunately, no attached form of *S. durum* is encountered at the Ricaudy site (N. D. and C. P. personal observations).

In spite of the significant variability in extension rates reported for *S. durum* in this study, overall, common trends in the growth pattern still stand out.

At the seasonal level, it was unexpected that highest rhodolith growth consistently takes place between the months of February and August, which corresponds to the austral

summer-fall-winter. Indeed, other coralline red algal studies generally present higher growth rates during the spring-summer period (e.g. Moberly, 1968; Halfar et al., 2008). Spring and summer in New Caledonia are also the most favourable seasons for phytoplanktonic algal blooms (Rodier and LeBorgne, 2008) and benthic primary production (Clavier and Garrigue, 1999). Ambient seawater temperature does not explain the contrasted seasonal growth pattern of *S. durum* as the IST at the monitoring site between the Jul10-Feb11and the Feb-Aug11 periods remains virtually constant (Figure IV-5). Seasonal contrast in global solar radiation at the site is also to be ruled out in the explanation of the growth pattern observed here (Figure IV-5). A potential factor on slower growth in spring is the record of higher wind velocity (Figure IV-5) that may contribute to an increased resuspension of particles in the water column (e.g. Ouillon et al., 2010), leading to a reduced light penetration through the water column. Internal biological factors are also likely to play a large role in the control of the seasonal growth pattern of *S. durum*, however, their determination was beyond the scope of this study.

The absence of correlation between the annual variations of the average extension rate recorded for the rhodoliths and the local environmental parameters for the 1964-2008 period (Figure IV-10) was to be expected due to the high variability of extension rates displayed by the analysed branches. However, in the longer-term trends, it appears that the slight decrease in rhodolith extension rate during the early 1970s might be related to a period of intense mining production in the Coulée River region starting in the early 1960s and ending in 1981 (Fernandez et al., 2006). This period of highest mining production (up to 3000 tons of extracted material per year – Figure IV-10) was also coeval, to some extent, with increased rainfall over Nouméa. Debenay and Fernandez (2009) determined a drastic change in the depositional regime in western Sainte Marie Bay (Figure IV-1) concordant with the intense mining activities in the Coulée River basin, likely caused by higher sedimentation rates. We suggest that an increased sediment load from the Coulée River into the lagoon might also explain the observed reduction of rhodolith growth during the mining activities due to higher turbidity of the lagoon waters leading to an effective reduction of the light penetration through the water column. However, *S. durum* show higher, more stable extension rates only a few years after the perturbation, when the sediment load transported by the Coulée River is likely to have remained high (Fernandez et al., 2006), suggesting the ability of *S. durum* to overcome periods of reduced irradiance (as previously suggested for other coralline red algal species, e.g. Wilson et al., 2004).

The slight decrease in average *S. durum* extension rates over the last five decades might be result from a stress caused by the slight temperature rise (Figure IV-10), however, this is in contradiction with several studies showing that higher temperatures, as well as increased light intensity as observed here with the solar radiation (Figure IV-10), have a

positive effect, if any, on coralline red algal calcification and growth (Kamenos and Law, 2010; Dethier and Steneck, 2001). The observed decrease in extension rates may also reflect an ontogenic effect in *S.durum*. An ontogenic effect in coralline red algae was thought to be absent. Coralline red algae are thought not to suffer from any ontogenic effect (e.g. Halfar et al., 2007; 2011a; Wanamaker et al., 2011; Williams et al., 2011), however, from our observations, such an effect that results in extension rates being slower as the organism ages cannot be ruled out for *S. durum*. In addition, the increasing trend of wind-strength recorded over Nouméa might have contributed to stronger wind-driven currents in the lagoon, thus favouring more sediment resuspension. The gradually increasing amount of particles in the water column may have reduced light availability for the rhodoliths, leading to a slight decrease in extension rates over the studied period. This is consistent with the propositions for the seasonal growth pattern observed in *S. durum*. This effect could have also been amplified by increased terrigenous inputs into the lagoon resulting from slightly increasing rainfall recorded over the studied period (Figure IV-10).

IV-5 Conclusion

We determined major (seasonal) and minor (sub-seasonal) growth patterns in *S. durum* rhodoliths from southwest New Caledonia through a staining experiment. The major, seasonal banding corresponds to the alternation of higher extension rates during the austral summer-fall-winter period, and lower extension rates during the winter-spring-summer months. This seasonal contrast is associated with a respectively longer and shorter, sub-seasonal, minor banding. Minor bands, composed of two-to-several individual cell layers, were clearly observed and appear to have a maximum periodicity of a fortnight. However, as this fortnightly periodicity could not be characterised in the majority of the analysed branches, especially during periods of slower growth, we consider the minor bands in *S. durum* rhodoliths to be too variable to represent a reliable chronological tool.

Typical extension rates for the *S. durum* community average 0.6 ± 0.2 mm y^{-1}, which is in good agreement with reports for other coralline red algal species in the literature. Extension rates of *S. durum* rhodoliths present a considerable variability for any given year. However, common, longer-term trends in the inter-annual variations could be distinguished and related to environmental factors. Intense mining activities that occurred in the Coulée River basin until 1981 and peaked in the early 1970s appear to have had an adverse effect on rhodolith growth that lasted several years before recovery to higher,

more stable extension rates. Although the slight decrease in rhodolith extension rate observed over the last five decades potentially reflects an ontogenic effect, it may also have been enhanced by a gradual reduction of light penetration in the lagoon waters caused by an increase in current-driven sediment resuspension and/or terrigenous inputs. No influence of the seawater temperature on the pattern or rate of extension in the *S. durum* rhodoliths, was observed, at any of the studied scales.

References

Adey WH, MacIntyre IG (1973) Crustose coralline algae: a re-evaluation in the geological sciences. Geological Society of America Bulletin 84:883-904

Adey WH (1970) The effects of light and temperature on growth rates in boreal subartic crustose corallines. Journal of Phycology 6:269-276

Adey WH, McKibbin DL (1970) Studies on the maerl species *Phymatolithon calcareum* (Pallas) nov. comb. and Lithothamnium coralloides Crouan in the Ria de Vigo. Botanica Marina 13:100-106

Agegian CR (1981) Growth of the branched coralline alga, *Porolithon gardineri* (Foslie) in the Hawaiian Archipelago. Proceedings of the Fourth International Coral Reef Symposium, Manila, 2:419-423

Aguirre J, Riding R, Braga JC (2000) Diversity of coralline red algae: origination and extinction patterns from the Early Cretaceous to the Pleistocene. Paleobiology 26:651-667

Basso D (1994) Study of living calcareous algae by a paleontological approach: the non-geniculate Corallinaceae (Rhodophyta) of the soft bottoms of the Tyrrhenian Sea (western Mediterranean), The genera *Phymatolithon* Foslie and *Mesophyllum* Lemoine. Riv. It. Paleont. Strat. 100:575-596

Basso D (1995) Study of living calcareous algae by a paleontological approach: the genus *Lithothamnion* Heidrich nom. cons. from the soft bottoms of the Tyrrhenian Sea (Mediterranean). Riv. It. Paleont. Strat. 101:349-366

Basso D (2012) Carbonate production by calcareous red algae and global change. In: Basso D, Granier B (eds) Calcareous algae and global change: from identification to quantification. Geodiversitas 34:13-33

Basso D, Nalin R, Nelson CS (2009) Shallow-water *Sporolithon* rhodoliths from North Island (New Zealand). Palaios 24:92-103

Blake C, Maggs CA (2003) Comparative growth rates and internal banding periodicity of maerl species (Corallinales, Rhodophyta) from northern Europe. Phycologia 42:606-612

Böhm L, Schramm W, Rabsch U (1978) Ecological and physiological aspects of some coralline algae from the western Baltic. Calcium uptake and skeleton formation in *Phymatolithon calcareum*. Kieler Meeresforschung 4:282-288

Borowitzka MA (1983) Calcium carbonate deposition by reef algae: morphological and physiological aspects. In: Barnes, DJ (eds) Perspectives on Coral Reefs. AIMS Contribution 200:16-27

Bosence DWJ (1983a) Description and classification of rhodoliths (Rhodoids, Rhodolites). In: Peryt TM (eds) Coated Grains. Springer-Verlag, Berlin, p 217-224

Bosence DWJ (1983b) The occurence and ecology of recent rhodoliths - A review. In: Peryt TM (eds) Coated Grains. Springer-Verlag Berlin, p 225-242

Bulleri F (2006) Duration of overgrowth affects survival of encrusting coralline algae. Marine Ecology Progress Series 321:79-85

Burdett H, Kamenos NA, Law A (2010) Using coralline algae to understand historic marine cloud cover. Palaeogeography, Palaeoclimatology, Palaeoecology 302:65-70

Cabioch J (1966) Contribution à l'étude morphologique, anatomique et systématique de deux Mélobésiées: *Lithothamnium calcareum* (Pallas) Areschoug et *Lithothamnium corallioides* Crouan. Botanica Marina 9:33-53

Chan P, Halfar J, Williams B, Hetzinger S, Steneck R, Zack T, Jacob DE (2011) Freshening of the Alaska Coastal Current recorded by coralline algal Ba/Ca ratios. Journal of Geophysical Research 116:G01032

Chave KE, Wheeler BD Jr. (1965) Mineralogic changes during growth in the red alga, *Clathromorphum compactum*. Science 147:621

Clavier J, Garrigue C (1999) Annual sediment primary production and respiration in a large coral reef lagoon (SW New Caledonia). Marine Ecology Progress Series 191:79-

Debenay JP, Fernandez JM (2009) Benthic foraminifera records of complex anthropogenic environmental changes combined with geochemical data in a tropical bay of New Caledonia (SW Pacific). Marine Pollution Bulletin 59:311-322

Dethier MN, Steneck RS (2001) Growth and persistence of diverse intertidal crusts: survival of the slow in a fast-paced world. Marine Ecology Progress Series 223:89-100

Eggins SM, Kinsley LPJ, Shelley JMG (1998) Deposition and element fractionation processes during atmospheric pressure laser sampling for analysis by ICP-MS. Applied Surface Science 127:278-286

Fallon SJ, Fifield LK, Chappell JM (2010) The next chapter in radiocarbon dating at the Australian National University: Status report on the single stage AMS. Nuclear Instruments and Methods in Physics Research Section B: Beam Interactions with Materials and Atoms 268:898-901

Fallon SJ, Guilderson TP, Caldeira K (2003) Carbon isotope constraints on vertical mixing and air-sea CO_2 exchange. Geophysical Research Letters 30:2289

Fernandez JM, Ouillon S, Chevillon C, Douillet P, Fichez R, Gendre RL (2006) A combined modeling and geochemical study of the fate of terrigenous inputs from mixed natural and mining sources in a coral reef lagoon (New Caledonia). Marine Pollution Bulletin 52:320-331

Foster MS (2001) Rhodoliths: Between rocks and soft places. Journal of Phycology 37:659-667

Frantz BR, Kashgarian M, Coale KH, Foster MS (2000) Growth rate and potential climate record from a rhodolith using ^{14}C accelerator mass spectrometry. Limnology and Oceanography 45:1773-1777

Freiwald A, Henrich R (1994) Reefal coralline algal build-ups within the Arctic Circle: morphology and sedimentary dynamics under extreme environmental seasonality. Sedimentology 41:963-984

Freiwald A, Henrich R, Schäfer P, Willkomm H (1991) The significance of high-boreal to subarctic maerl deposits in northern Norway to reconstruct Holocene climatic changes and sea level oscillations. Facies 25:315-340

Gamboa G, Halfar J, Hetzinger S, Adey W, Zack T, Kunz B, Jacob DE (2010) Mg/Ca ratios in coralline algae record northwest Atlantic temperature variations and North Atlantic Oscillation relationships. Journal of Geophysical Research 115:C12044

Goldberg N, Heine JN (2008) Age estimates of *Sporolithon durum* (Corallinales, Rhodophyta) from Rottnest Island, Western Australia, based on radiocarbon-dating methods. Journal of the Royal Society of Western Australia 91:27-30

Guilderson TP, Schrag DP, Goddard E, Kashgarian M, Wellington GM, Linsley BK (2000) Southwest subtropical Pacific surface water radiocarbon in a high-resolution coral record. Radiocarbon 42:249-256

Halfar J, Zack T, Kronz A, Zachos JC (2000) Growth and high-resolution paleoenvironmental signals of rhodoliths (coralline red algae): A new biogenic archive. Journal of Geophysical Research 105:22,107-22,116

Halfar J, Steneck RS, Schöne BR, Moore GWK, Joachimski M, Kronz A, Fietzke J, Estes J (2007) Coralline alga reveals first marine record of subarctic North Pacific climate change. Geophysical Research Letters 34:L07702

Halfar J, Steneck RS, Joachimski M, Kronz A, Wanamaker Jr. AD (2008) Coralline red algae as high-resolution climate recorders. Geology 36:463-466

Halfar J, Hetzinger S, Adey W, Zack T, Gamboa G, Kunz B, Williams B, Jacob DE (2011a) Coralline algal growth-increment widths archive North Atlantic climate variability. Palaeogeography, Palaeoclimatology, Palaeoecology 302:71-80

Halfar J, Williams B, Hetzinger S, Steneck RS, Lebednik P, Winsborough C, Omar A, Chan P, Wanamaker AD (2011b) 225 years of Bering Sea climate and ecosystem dynamics revealed by coralline algal growth-increment widths. Geology 39:579-582

Hallmann N, Schöne BR, Irvine GV, Burchell M, Cokelet ED, Hilton MR (2011) An improved understanding of the Alaska Coastal Current: The application of a bivalve growth-

temperature model to reconstruct freshwater-influenced paleoenvironments. Palaios 26:346

Harvey AS, Woelkerling WJ, Millar AJK (2002) The Sporolithaceae (Corallinales, Rhodophyta) in south-eastern Australia: taxonomy and 18S rRNA phylogeny. Phycologia 41:207-227

Hetzinger S, Halfar J, Kronz A, Steneck R, Adey WH, Lebednik PA, Schöne BR (2009) High-resolution Mg/Ca ratios in a coralline red alga as a proxy for Bering Sea temperature variations from 1902 to 1967. Palaios 24:406-412

Hetzinger S, Halfar J, Zack T, Gamboa G, Jacob DE, Kunz BE, Kronz A, Adey W, Lebednik PA, Steneck RS (2011) High-resolution analysis of trace elements in crustose coralline algae from the North Atlantic and North Pacific by laser ablation ICP-MS. Palaeogeography, Palaeoclimatology, Palaeoecology 302:81-94

Hughes WW, Rosenberg GD, Tkachuck RD (1988) Growth increments in the shell of the living brachiopod *Terebratalia transversa*. Marine Biology 98:511-518

Kamenos NA, Cusack M, Moore P, G. (2008) Coralline algae are global palaeothermometers with bi-weekly resolution. Geochimica et Cosmochimica Acta 72:771-779

Kamenos NA, Law A (2010) Temperature controls on coralline algal skeletal growth. Journal of Phycology 46:331-335

Littler MM, Littler DS (1988) Structure and role of algae in tropical reef communities. In Lembi CA, Waaland JR (eds) Algae and human affairs. Cambridge University Press, Cambridge, p 30-56

Moberly Jr R (1968) Composition of magnesian calcites of algae and pelecypods by electron microprobe analysis. Sedimentology 11:61-82

Nicet JB, Delcroix T (2000) ENSO-related precipitation changes in New Caledonia, Southwestern tropical Pacific: 1969-98. Monthly Weather Review 128:3001-3006

Paillard D, Labeyrie L, Yiou P (1996) Macintosh program performs time-series analysis. Eos Transactions AGU 77:379

Pannella G (1976) Tidal growth patterns in recent and fossil mollusc bivalve shells: a tool for the reconstruction of paleotides. Naturwissenschaften 63:539-543

Payri C (1997) *Hydrolithon reinboldii* rhodolith distribution, growth and carbon production of a French Polynesian reef. Proceedings of the 8th International Coral Reef Symposium Panama, p 755-760

Payri C, Maritorena S, Bizeau C, Rodière M (2001) Photoacclimation in the tropical coralline alga *Hydrolithon onkodes* (Rhodophyta, Corallinaceae) from a French Polynesian reef. Journal of Phycology 37:223-234

Rivera MG (1999) Edad y crecimiento de *Lithothamnium crassiusculum* (Foslie) Mason (Corallinales, Rhodophyta) en el suroesete del Golfo de California Mexico. Tesis, Universidad Autonoma de Baja California. 63pp.

Rodier M, Le Borgne R (2008) Population dynamics and environmental conditions affecting *Trichodesmium* spp. (filamentous cyanobacteria) blooms in the south-west lagoon of New Caledonia. Journal of Experimental Marine Biology and Ecology 358:20-32

Santos GM, Southon JR, Druffel-Rodriguez KC, Griffin S, Mazon M (2004) Magnesium perchlorate as an alternative water trap in AMS graphite sample preparation: a report on sample preparation at KCCAMS at the University of California, Irvine. Radiocarbon 46:165-174

Schäfer P, Fortunato H, Bader B, Liebetrau V, Bauch T, Reijmer JJG (2011) Growth rates and carbonate production by coralline red algae in upwelling and non-upwelling settings along the Pacific coast of Panama. Palaios 26:420-432

Schöne B, Tanabe K, Dettman DL, Sato S (2003) Environmental controls on shell growth rates and $\delta^{18}O$ of the shallow-marine bivalve mollusk *Phacosoma japonicum* in Japan. Marine Biology 142:473-485

Scoffin TP, Stoddart DR, Tudhope AW, Woodroffe C (1985) Rhodoliths and coralliths of Muri Lagoon, Rarotonga, Cook Islands. Coral Reefs 4:71-80

Steneck RS (1997) Crustose corallines, other algal functional groups, herbivores and

sediments: complex interactions along reef productivity gradients. Proceedings of the 8th International Coral Reef Symposium Panama, p 695-700

Toggweiler JR, Dixon K, Broecker WS (1991) The Peru upwelling and the ventilation of the South Pacific thermocline. Journal of Geophysical Research 96:20467-20420,20497

Townsend RA, Woelkerling WJ, Harvey AS, Borowitzka M (1995) An account of the red algal genus *Sporolithon* (Sporolithaceae, Corallinales) in southern Australia. Australian Systematic Botany 8:85-121

Underwood AJ (2006) Why overgrowth of intertidal encrusting algae does not always cause competitive exclusion. Journal of Experimental Marine Biology and Ecology 330:448-454

Vogel JS, Nelson DE, Southon JR (1987) C-14 background levels in an accelerator mass-spectrometry system. Radiocarbon 29:323-333

Wanamaker Jr AD, Hetzinger S, Halfar J (2011) Reconstructing mid-to high-latitude marine climate and ocean variability using bivalves, coralline algae, and marine sediment cores from the Northern Hemisphere. Palaeogeography, Palaeoclimatology, Palaeoecology 302:1-9

Williams B, Halfar J, Steneck RS, Wortmann UG, Hetzinger S, Adey W, Lebednik P, Joachimski M (2011) Twentieth century ^{13}C variability in surface water dissolved inorganic carbon recorded by coralline algae in the northern North Pacific Ocean and the Bering Sea. Biogeosciences 8:165-174

Wilson S, Blake C, Berges JA, Maggs CA (2004) Environmental tolerances of free-living coralline algae (maerl): implications for European marine conservation. Biological Conservation 120:279-289

Womersley HBS (1996) The marine benthic flora of southern Australia, Part III B: Gracilariales, Rhodymeniales, Corallinales and Bonnemaisoniales. Australian Biological Resources Study, Canberra, pp392

Supplementary material

Table IV-S1: Extension rates and growth pattern of the 43 analysed tips for the Jul10-Aug11 record.

Sample	Feb-Aug11 Growth (mm)	Mg cycle length (mm)	Annual Growth (mm)	Feb-Aug11 fraction of growth (%)	Feb-Aug11		Jul10-Feb11	
					Counted minor bands	Average band width (mm)	Counted minor bands	Average band width (mm)
R1-1	0.648	0.969	0.894	66.9	12	0.054	6	0.054
R1-2	0.894	1.140	1.053	78.4	14	0.064	6	0.041
R1-3	0.506	0.782	0.722	64.7	11	0.046	8	0.035
R1-4	0.505	0.780	0.720	64.7	11	0.046	7	0.039
R1-5	0.780	1.066	0.984	73.2	14	0.056	6	0.048
R1-6	0.629	0.866	0.799	72.6	11	0.057	6	0.040
R1-7	0.558	0.718	0.663	77.8	8	0.070	5	0.032
R1-8	0.341	0.629	0.581	54.2	6	0.057	8	0.036
R1-9	0.669	0.912	0.842	73.4	10	0.067	6	0.041
R2-1	0.303	0.571	0.527	53.2	5	0.061	9	0.030
R2-2	0.167	0.389	0.359	42.8	4	0.042	5	0.044
R2-3	0.171	0.449	0.415	38.1	3	0.057	8	0.035
R2-4	0.175	0.534	0.493	32.7	3	0.058	7	0.051
R3-1	0.643	0.913	0.843	70.4	11	0.058	7	0.039
R3-2	0.548	0.805	0.743	68.1	12	0.046	6	0.043
R3-3	0.520	0.691	0.638	75.3	12	0.043	5	0.034
R3-4	0.576	0.769	0.710	74.9	13	0.044	5	0.039
R3-5	0.526	0.732	0.676	71.9	11	0.048	4	0.051
R3-6	0.437	0.688	0.635	63.5	9	0.049	7	0.036
R3-7	0.505	0.632	0.583	79.9	13	0.039	3	0.042
R3-8	0.410	0.578	0.533	70.9	12	0.034	5	0.034
R3-9	0.558	0.793	0.732	70.4	12	0.047	7	0.034
R4-1	0.161	0.359	0.331	44.9	3	0.054	5	0.040
R4-2	0.486	0.639	0.590	76.1	10	0.049	3	0.051
R4-3	0.429	0.678	0.625	63.3	8	0.054	5	0.050
R4-4	0.445	0.600	0.554	74.1	9	0.049	4	0.039
R4-5	0.329	0.529	0.488	62.2	9	0.037	5	0.040
R5-1	0.209	0.380	0.351	54.9	7	0.030	6	0.029
R5-2	0.146	0.289	0.267	50.5	3	0.049	4	0.036
R5-3	0.453	0.683	0.631	66.3	11	0.041	7	0.033
R5-4	0.576	0.757	0.699	76.2	12	0.048	5	0.036
R5-5	0.356	0.577	0.533	61.8	9	0.040	6	0.037
R5-6	0.276	0.478	0.442	57.7	5	0.055	5	0.040
R6-1	0.196	0.439	0.405	44.7	4	0.049	7	0.035
R6-2	0.239	0.502	0.464	47.5	6	0.040	8	0.033
R6-3	0.417	0.596	0.550	69.9	12	0.035	7	0.026
R6-4	0.335	0.531	0.490	63.1	6	0.056	4	0.049
R6-5	0.517	0.714	0.659	72.4	11	0.047	5	0.039
R7-1	0.512	0.761	0.702	67.3	12	0.043	8	0.031
R7-2	0.617	0.804	0.742	76.7	12	0.051	6	0.031
R7-3	0.556	0.767	0.708	72.5	13	0.043	5	0.042
R7-4	0.556	0.773	0.714	71.9	13	0.043	5	0.043
R7-5	0.538	0.696	0.642	77.3	10	0.054	7	0.023

Table IV-S2: Annual extension rates (mm/yr) measured for 5 different rhodolith branches over the 1963-2011 period using the combination of major growth banding and Mg/Ca cycles.

Year	BSA1	BSA2	BSA3	MSA1	SSA1
2010				0.71	0.55
2009				1.01	0.72
2008	0.53	0.67	0.48	0.82	0.48
2007	0.46	0.48	0.46	0.46	0.61
2006	0.81	0.57	0.52	0.88	0.59
2005	0.56	0.49	0.59	0.43	0.62
2004	0.68	0.51	0.34	0.42	0.38
2003	0.67	0.35	0.53	0.93	0.60
2002	0.73	0.45	0.33	0.42	0.44
2001	0.72	0.53	0.51	0.87	0.72
2000	0.56	0.42	0.44	0.48	0.81
1999	0.87	0.46	0.81	1.13	0.54
1998	1.10	0.42	0.72	0.69	0.75
1997	1.22	1.04	0.51	0.79	0.88
1996	0.90	0.58	0.71	0.52	0.44
1995	0.57	0.38	1.02	0.66	0.53
1994	0.75	0.39	0.37	0.84	0.40
1993	1.02	0.24	0.66	0.52	0.66
1992	0.67	0.34	0.86	0.96	0.35
1991	0.78	0.19	0.48	0.81	0.69
1990	0.91	0.46	0.65	0.84	0.88
1989	0.65	0.33	0.74	0.82	0.32
1988	1.06	0.20	0.94	0.88	0.62
1987	1.09	0.62	0.37	0.49	0.47
1986	0.77	0.58	0.96	0.61	0.55
1985	0.99	0.30	0.27	0.73	0.53
1984	1.24	0.68	1.15	0.49	0.62
1983	1.03	0.38	0.98	0.99	0.65
1982	0.74	0.31	0.67	0.65	0.64
1981	1.07	0.37	0.71	0.53	0.69
1980	1.19	0.50	0.40	0.43	0.68
1979	0.71	0.53	0.58	0.48	0.58
1978	0.93	0.98	0.89	0.31	0.94
1977	0.76	0.57	0.41	0.52	1.20
1976	1.02	0.58	0.41	0.62	0.54
1975	0.46	0.50	0.52	0.65	0.61
1974	0.41	0.70	0.71	0.80	0.38
1973	0.33	0.28	0.27	0.71	0.76
1972	0.21	0.61	0.65	0.59	0.28
1971	0.31	0.39	0.64	0.41	0.43
1970	0.60	0.52	0.97	0.51	0.49
1969	0.69	0.34	0.61	0.78	0.49
1968	0.99	0.63	0.81	0.28	0.76
1967	0.74	0.63	1.18	0.76	0.29
1966	1.14	0.99	1.21	0.83	0.90
1965	0.73		0.82	0.54	1.11
1964	0.93			0.52	0.63
1963					0.68

CHAPTER V

Seasonal patterns in trace elemental composition of coralline red algae from a tropical lagoon: environmental, biological and anthropogenic influences

Keywords: *Sporolithon durum*, LA-ICPMS, alizarin red S, seasonal pattern, temperature, metabolic activity, sediment resuspension, trace metals

Abstract

From the results of an alizarin red S-staining, growth-monitoring experiment, we used laser ablation inductively coupled plasma mass spectrometry (LA-ICPMS) to investigate seasonal variations of Li, Mg, Al, P, Mn, Fe, Co, Ni, Cu, Zn, Rb, Sr, Ba, Pb and U, all normalised to Ca, in tropical *Sporolithon durum* coralline red algae, over a 21-month period. Pairwise correlation matrices were produced to characterise the reproducibility of each trace elemental record across 43 rhodolith branches. Mg/Ca, Sr/Ca and Li/Ca are the most reproducible, with 74 to 95% significantly cross-correlated records, strongly suggesting that their variations are largely controlled by factors acting uniformly across the Ricaudy Reef rhodolith bed. On the contrary, records of elemental ratios such as Al/Ca, Fe/Ca, Co/Ca or Pb/Ca are essentially dominated by individual variability. Possible causes for trace element variability in *S. durum* rhodoliths are discussed, among which, the critical role played by the organic phase for some trace elements. A hierarchical clustering based on the average rhodolith records was carried out to determine similar patterns in elemental variations at a seasonal scale. Temperature changes are the main driver of Mg/Ca, Sr/Ca and Li/Ca variations, with correlations of $r=0.82$ to $r=0.91$ ($p<0.0001$), over the November 2009-August 2011 period. Monthly variations in U/Ca are also closely related to temperature during the studied period ($r=-0.84$; $p<0.0001$). The faint seasonal pattern in P/Ca, Co/Ca, Cu/Ca, Zn/Ca, Rb/Ca and Ba/Ca was attributed to the result of an increase in biological activity of the benthic community in spring, in association with higher concentrations of these elements in the water column due to wind-driven-current-resuspension of particulate material. Finally, we propose that the higher concentrations in rhodoliths observed for Al/Ca, Mn/Ca, Fe/Ca, Ni/Ca and Pb/Ca may be related to anthropogenic, sediment-removal activities from a nearby area, where high concentrations of these metals in the marine sediment are the result of continuous terrigenous inputs from former mining sites.

V-1 Introduction

In recent years, a new biological archive of extra-tropical environment has arisen in the form of long-lived, encrusting coralline red algae (Halfar et al., 2000; 2007; 2008; 2010; Kamenos et al., 2008; Hetzinger et al., 2009; 2011a,b; Burdett et al., 2010; Williams et al., 2011; Chan et al., 2011). Coralline red algae are calcareous marine organisms that are globally distributed in coastal areas, from the tropics to the poles and from the inter-tidal zone down to the limit of the photic zone (e.g. Bosence 1983b; Foster, 2001; Nelson, 2009). These major carbonate producers (Borowitzka, 1983; Littler and Littler, 1988) have been present in the world's oceans since the Cretaceous (Aguirre et al., 2000), forming thick deposits in the geological record that may have accumulated over thousands of years (Freiwald et al., 1991). Modern representative of coralline red algae occur either as attached forms, encrusted on a hard substratum, or as free-living nodules, called rhodoliths (Steneck, 1986; Foster, 2001). The high-Mg calcite that coralline red algae continuously form as they grow can be up to ~20-cm thick (e.g. Littler et al., 1991, Adey and MacIntyre, 1973). This, in combination with a relatively slow growth rate that ranges from 0.02 to 2.2 mm.yr-1 (Böhm et al., 1978; Foster, 2001; Blake and Maggs, 2003), can lead to the potential retrieval of environmental information from coralline red algae spanning decades to centuries (Frantz et al., 2005; Halfar et al., 2007)

One of the most commonly investigated sources of environmental information from various marine calcifiers is the analysis of the geochemical composition of their calcareous skeletons/shells. In particular, variations in trace elemental ratios such as Mg/Ca or Sr/Ca are reliable seawater temperature proxies in foraminifera (Lear et al., 2000; Eggins et al., 2003), corals (Beck et al., 1992; Alibert and McCulloch, 1997; Corrège, 2006a) or bivalves (Klein et al., 1998). Similarly, temperature-controlled variations in U/Ca and Li/Ca have been demonstrated for corals (Fallon et al., 1999; Marriott et al., 2004). Other trace elements such as P/Ca, Mn/Ca or Ba/Ca can vary according to nutrient levels, biological activity or river runoff (Fallon et al., 1999; Alibert et al., 2003; Montagna et al., 2006). The impact of anthropogenic activities have also been recorded through increases in Mn/Ca, Zn/Ca, Pb/Ca and Cu/Ca concentrations in coral aragonite (Fallon et al., 2002; Runnalls and Coleman, 2003).

A significant number of these studies used laser ablation inductively coupled plasma mass spectrometry (LA-ICPMS) because of the ability to simultaneously measure a wide range of chemical elements at high resolution (e.g. Eggins et al., 1998). For coralline red algae, however, few published studies on the cold-water species have used LA-ICPMS

(Gamboa et al., 2010; Chan et al., 2011; Halfar et al. 2011) and only one aimed at characterising the seasonal pattern of various trace elements (Hetzinger et al., 2011a). This study focused on single crusts of coralline red algae and was limited to the investigation of Mg/Ca, Sr/Ca, Ba/Ca, and U/Ca.

Here, we used LA-ICPMS to investigate high-resolution variations of 15 trace elements (Li, Mg, Al, P, Mn, Fe, Co, Ni, Cu, Zn, Rb, Sr, Ba, Pb and U, all normalised to Ca) in the skeleton of tropical specimens of *Sporolithon durum* rhodoliths. For each of the 43 analysed rhodolith branches, a 21-month trace elemental record was measured. A basic statistical approach was employed to help determine the degree of elemental variability between all records, as well as to characterise common, seasonal pattern between the average records of the studied trace elements. Results were then compared to different environmental parameters recorded during the studied period in an attempt to better understand trace elements behaviour in *S. durum* rhodoliths at a seasonal scale.

V-2 Material and methods

V-2.a Rhodolith collection, staining and environmental dataset

The seven rhodolith specimens studied here were collected by SCUBA diving in early February 2011, from various sites in the Ricaudy Reef rhodolith bed (4-5 m depth), that spans ~1 km^2 at the southern end of the Sainte Marie Bay, on the edge of Nouméa, New Caledonia (22°18'57"S; 166°27'26"E – Figure V-1). Rhodoliths are exclusively formed by *S. durum*, the most abundant coralline red alga species at this site. Individuals range between ~4 and >8 cm in diameter, show spheroidal shapes and a degree IV branching structure (see classification in Bosence, 1983a).

Upon collection, rhodolith specimens were stained onshore using alizarin red S (ARS), at a concentration of 7.5 mg l^{-1} of seawater from the Ricaudy Reef, for a period of 48 h (adapted from Payri, 1997). They were then grouped in a ~1x1 m^2 enclosure in their natural environment, where they were left to grow for 28 weeks prior retrieval at the end of August 2011.

In situ seawater temperature for the rhodolith bed was recorded hourly for the entire period by a TinyTag TG-4100 Aquatic 2 data logger, attached to the enclosure since November 2009, at the beginning of the unsuccessful first attempt at rhodolith growth monitoring. Monthly averages of rainfall, global solar radiation and wind strength were recorded at the Faubourg Blanchot meteorological station of Nouméa (~1-2 km from the Ricaudy Reef) and data for the November 2009-August 2011 period was obtained from Météo France. Photosynthetically Active Radiation (PAR), chlorophyll a (Chl a)

concentrations and coloured, dissolved organic matter (CDOM) data was obtained using the Giovanni online data system, developed and maintained by the NASA GES DISC (Acker and Leptoukh, 2007), from MODIS-AQUA satellite images centred on the Ricaudy Reef area (Figure V-1).

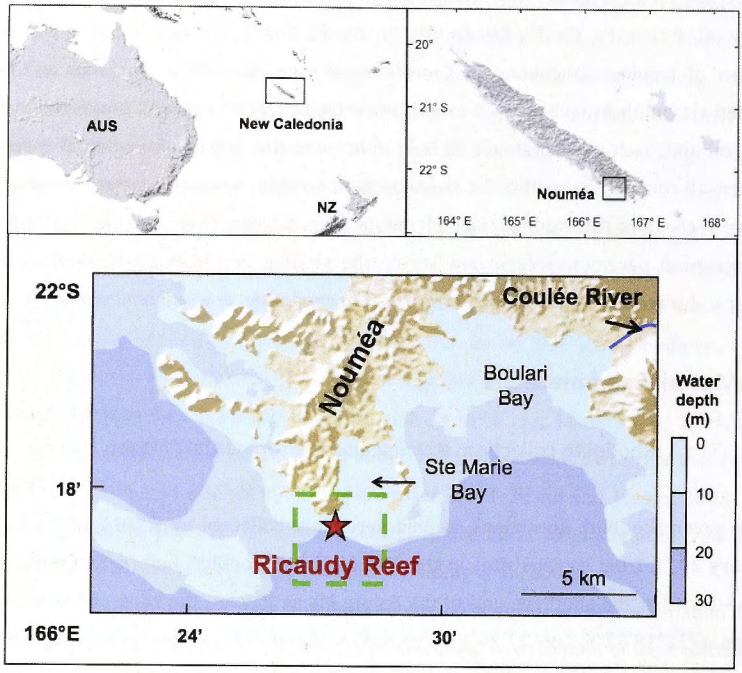

Figure V-1 Location map of the Ricaudy Reef (red star), on the edge of Nouméa, New Caledonia. The Sainte Marie Bay, Boulari Bay and the position of the Coulée River are also indicated on the bottom map. The green rectangle defines the area from which environmental, satellite data was recovered from MODIS images (see text for details).

V-2.b LA-ICPMS analysis

Rhodolith samples were dried, impregnated in araldite resin and cut in half to reveal sections of their branches (Figure V-2). After polishing, branches were photographed at high-resolution using a Digital Sight DS-F1 digital camera attached to a Nikon AZ100 optical microscope, at the Research School of Earth Sciences (RSES) of the Australian National University (ANU).

From the branches where the alizarin stain was clearly determined visually (Figure V-2), 43 were analysed by LA-ICPMS, using the RSES ANU ArF Excimer laser unit (Eggins et al., 1998) combined to a Varian 820 quadrupole ICPMS. A 42-µm diameter laser spot,

associated with a 5 J cm^{-2} energy and a pulse rate of 10 Hz scanned the outermost ~1.5-2 mm of each branch along the axis of main growth, at a speed of 5 µm s^{-1}. A pre-ablation run, using a bigger spot-size and higher speed, was systematically performed before every analytical run so potential surface contamination of the samples was avoided. 17 isotopes were analysed, with individual dwell times adding up to ~1 s per measurement. The analytical procedure followed the one described in Chapter III (this thesis), with a background acquisition and standard measurements bracketing sample measurements. Data reduction followed the one in Longerich et al. (1996). ^{43}Ca was used as an internal standard to correct for the variable amount of material reaching the MS detector and the NIST SRM 612 reference material was used for calibration of the trace elements ratios, except for Mg/Ca, for which a dolomite marble of known composition was used for calibration (see Chapter III – this thesis). Typical detection limits for each analysed isotope were: ^{25}Mg, ^{43}Ca < 20 µg g^{-1}; ^{57}Fe < 10 µg g^{-1}; ^{24}Mg, ^{31}P < 5 µg g^{-1}; ^{55}Mn, ^{60}Ni, ^{66}Zn < 1 µg g^{-1}; ^{63}Cu < 0.5 µg g^{-1}; ^{7}Li, ^{27}Al, ^{59}Co, ^{85}Rb, ^{88}Sr < 0.1 µg g^{-1} and ^{138}Ba, ^{208}Pb, ^{238}U < 0.05 µg g^{-1}.

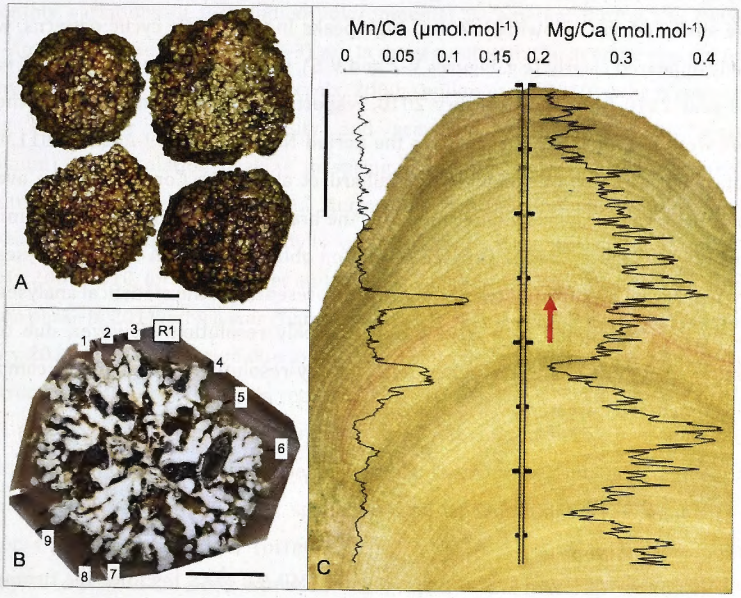

Figure V-2 A: Whole rhodolith specimens of the *Sporolithon durum* species collected in August 2011 from the Ricaudy Reef, New Caledonia. Scale bar: 3 cm. B: Cross-section of a rhodolith (R1) where the branching structure is clearly visible. The branches analysed by LA-ICPMS are numbered (1-9). Scale bar: 2cm. C:Close up on the R1-6 branch tip. The red arrow indicates the position of the alizarin red S stained-layer. The thick vertical bars, for which the major tick marks are 0.5 mm apart, represent the LA-ICPMS track. Full-resolution records of Mn/Ca and Mg/Ca measured by LA-ICPMS (thin black lines) are also displayed. Note the cyclic pattern of the Mg/Ca record and the peak in Mn/Ca corresponding to the alizarin red S stained layer as well as the high concentration in the tissue layer. Scale bar: 0.5 mm.

Two of the 43 branches were reanalysed under the same conditions after the rhodolith specimen was treated with H_2O_2 in order to remove the organic phase from the skeleton. H_2O_2 treatment consisted in the immersion, for ~1 h, of the rhodolith thick section in a 50%-mix solution of H_2O_2 (30%) and 0.1 *N* NaOH (e.g. Stoll et al., 2001), heated at 60°C. When bubbling stopped, the rhodolith thick section was immediately rinsed with distilled water and oven-dried prior to LA-ICPMS reanalysis.

V-2.c Age model determination

We used both the position of the ARS stain layer and the previously observed seasonal character of major Mg/Ca variations in various species of coralline red algae (Halfar et al., 2000; Kamenos et al., 2008; Hetzinger et al., 2009) that was also determined in *S. durum* (Chapter IV – this thesis), to constrain our chronologies. As the rhodoliths were collected alive, the outermost layer of each branch was attributed to August 2011. The position of ARS layer was matched to the starting date of the staining experiment (February 2011), and we anchored the following low and high peaks in the Mg/Ca cyclic patterns, which generally appeared clearly (e.g. Figures V-2 and V-5), to the lowest and highest IST values for the year 2010 (July and February 2010, respectively). Data points between these 4 anchors were extrapolated linearly over the period November 2009-August 2011, using the data analysis software AnalySeries (Paillard et al., 1996). Considering the average annual growth rate previously determined for the branches presented here (~0.6 mm y^{-1}; Chapter IV – this thesis) and the spatial resolution obtained from LA-ICPMS analyses (~5 µm per measurement), the full resolution records presented in the statistical analyses (see below) would correspond to a weekly-to-sub-weekly resolution. However, due to the constraints of our age model, no higher than monthly-resolution data should be compared to environmental parameters.

V-2.d Statistical analyses

Statistical analyses were performed using the JMP 9.0 (SAS Institute Inc.) computer software. From the 43 LA-ICPMS records, pairwise correlation matrices were produced for each elemental ratio, at full as well as monthly resolutions. In each case, the degree of record reproducibility was characterised by the percentage of pairs showing a significant correlation (Figure V-4). A hierarchical clustering at full- and monthly-resolution was performed on the average record of each elemental ratio using the Ward method on

standardised data, and is displayed along with the corresponding pairwise correlation matrices (Figure V-6). Correlation coefficients (r) presented here are Pearson's correlation coefficients obtained from least-square regressions. Their significance is discussed considering a confidence level of 95% (α=0.05).

It has to be noted that the peak in Mn/Ca concentration observed in every branch, and attributed to the use of ARS stain (Figure V-2 – see discussion below), as well as the high elemental concentrations recorded in the living tissue (i.e. outermost cell layers), which could represent 1-to-2 months according to the element and/or the branch's growth rate (see further: Figures V-8 and V-9), were not included in the dataset used for statistical analyses.

V-3 Results and discussion

V-3.a Environmental data

Monthly variations of the studied environmental parameters during the November 2009-August 2011 period (Figure V-3) are in agreement with the average climate pattern of New Caledonia (e.g. Nicet and Delcroix, 2000; Ouillon et al., 2010), which consists of a strong seasonality in light-intensity and seawater temperature, with maximum (minimum) solar radiation peaking in spring (autumn), before the warmest (coldest) seawater temperatures are reached during the austral summer (winter). Average seasonality in rainfall and wind activity was disturbed by the alternation of an El-Nino event in 2009-2010, for which dryer and windier weather was recorded, and the opposite La-Nina phase in 2011, which was characterised by higher precipitation and slower winds. January 2011 was an exception due to the effects of cyclone Vania, bringing heavy rainfall and strong winds over the Nouméa region.

Chl a concentration is generally related to phytoplankton primary production (e.g. Torréton et al., 2007; 2010). While higher plankton productivity in summer/fall is commonly observed, variability is spatial as well as temporal in the lagoon of New Caledonia (Fichez et al., 2010; Torréton et al., 2010). It is probable that the observed January 2011 peak in Chl a corresponds to an abrupt increase in terrigenous nutrients due to high cyclone-related precipitation at that time (Torréton et al., 2010; Le Borgne et al., 2010).

The fact that the CDOM does not seem to respond to the rainfall activity at the site indicates that river runoffs or urban effluents are not the primary source of CDOM in the water column. It therefore suggests that CDOM is more likely to reflect some combination of the intensity of metabolic activity of the benthic community, which may be related to

light intensity, and surface-sediment resuspension, which is somewhat in agreement with the wind strength pattern (Figure V-3; see Boss and Zaneveld, 2003; Otis et al., 2004; Coble, 2007).

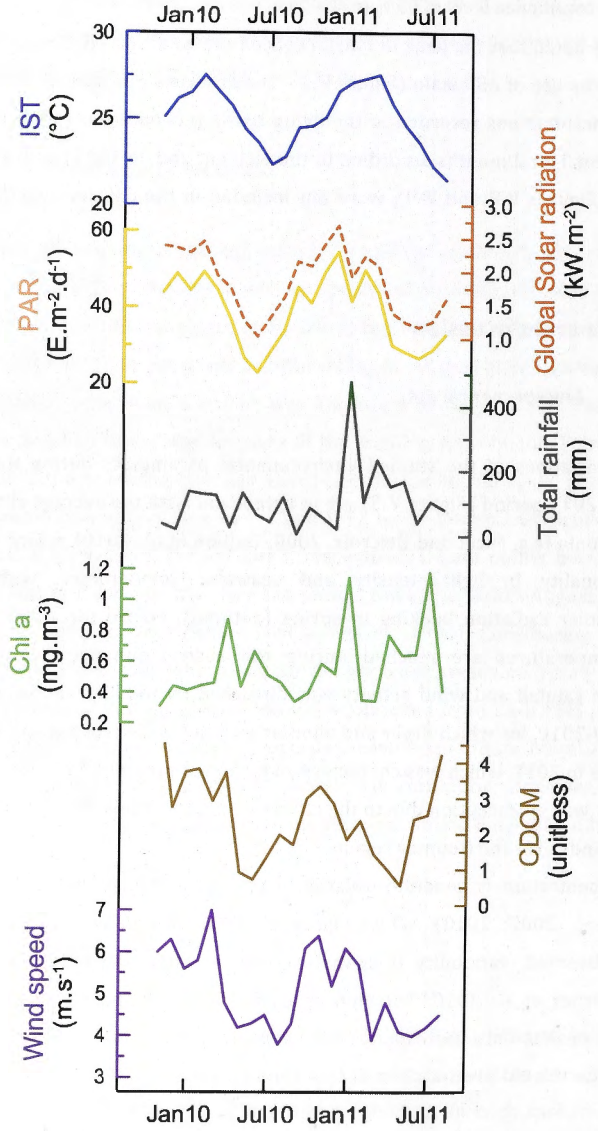

Figure V-3 Monthly variations of *in situ* temperature (IST), photosynthetically active radiation (PAR) and global solar radiation, total amount of rainfall, chlorophyll a (Chl a) concentration, coloured dissolved organic matter (CDOM) concentration and wind speed, over the November 2009-August 2011 period, for the Ricaudy Reef or the local area. See text for sources of the different datasets.

V-3.b Reproducibility of the geochemical records

From the elemental correlation matrices presented in Figure V-4, it appears that monthly data are systematically more reproducible than full-resolution data. This is explained by the reduction of both instrumental and age-model uncertainties when lower-resolution records are considered. Except for Mg/Ca, Sr/Ca and Li/Ca, where at least 78% of the monthly, pairwise correlations are significant, a high degree of variability between individual tracks is observed. P/Ca, Mn/Ca, Ni/Ca and U/Ca are only moderately reproducible and for Al/Ca, Fe/Ca, Co/Ca and Pb/Ca, half of more records are inconsistent and do not significantly correlate with one another (Figure V-4).

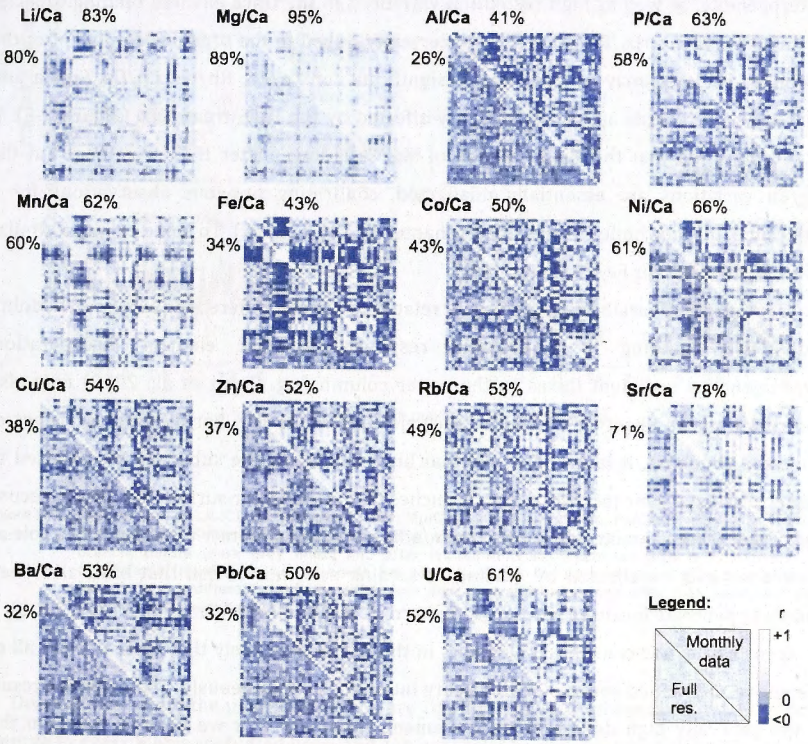

Figure V-4 Cross-correlation matrices for Li/Ca, Mg/Ca, Al/Ca, P/Ca, Mn/Ca, Fe/Ca, Co/Ca, Ni/Ca, Cu/Ca, Zn/Ca, Rb/Ca, Sr/Ca, Ba/Ca, Pb/Ca and U/Ca, based on the individual LA-ICPMS records obtained along the top 1.5-2 mm of the 43 studied rhodolith branches, at full- and monthly-resolutions. The colour scale reflects the degree of correlation between the different records. For each elemental ratio, the proportion of significant (α=0.05) pairwise correlations between the 43 records is displayed for the full-resolution and monthly-resolved datasets.

The reproducibility of the trace elements signals recorded here can be affected by various sources. Uncertainties in the age model will affect every element to the same extent and are due to the linear interpolation of the records between the anchor points chosen to constrain our chronology. This does not take into account the growth rate variability that is likely to occur at higher-than-seasonal resolution and that would be particular to each analysed branch. High-resolution growth rates variations may also add a source of variability for some trace elements for which the incorporation into calcite has been shown to be sensitive to precipitation rate (e.g. Mn, Fe, Co – Lorens, 1981; Dromgoole and Walter, 1990). An association with the organic phase, which could be unevenly distributed throughout the skeleton of *S. durum* as it is the case for some corals (e.g. Allison, 1996 for Rb, Ba or U), may also significantly contribute to the observed heterogeneity, as well as high-resolution variations in the trace element binding capacity of this organic matrix. This source of uncertainty linked to the organic component of the rhodolith skeleton may be particularly significant for Zn/Ca, Rb/Ca, Co/Ca, Cu/Ca and Ba/Ca, which records appear particularly affected by the H_2O_2 treatment (Figure V-5). It has to be noted that the concentration of Mg/Ca is lower after H_2O_2 treatment but the Mg/Ca variations are essentially unaffected, confirming previous observations for a different *S. durum* rhodolith specimen (Chapter III – this thesis). To some extent, a similar effect is observed for Fe/Ca (Figure V-5).

Trace element variability may also be related to genetic differences between rhodolith individuals resulting in a different response to trace element incorporation. Heterogeneous sediment fluxes to the water column (e.g. Grenz et al., 2010) may also contribute to the observed temporal trace-element variability. For different branches of the same rhodolith, it is also possible that branches facing the substrate are exposed to higher dissolved concentrations than branches facing the water surface and hence, record a different trace element signal. The surrounding biotic community may also play a role as rhodoliths may be affected by grazing or feeding activities of fish that have also been shown to generate localised resuspension in coral reef environments (Yahel et al., 2002).

According to the considered elements in this study, it is likely that several if not all of the above-mentioned sources of variability intervene simultaneously. The expected result is the generally high degree of trace element variability that we observe between the analysed transects. This variability is less pronounced for the Mg/Ca, Sr/Ca and Li/Ca records, suggesting that they may respond more reliably to environmental forcing. For those trace elements where individual variability clearly dominates, the analysis of a single branch is very unlikely to reflect representative elemental variations, even at the scale of a rhodolith specimen, over a period of several-months.

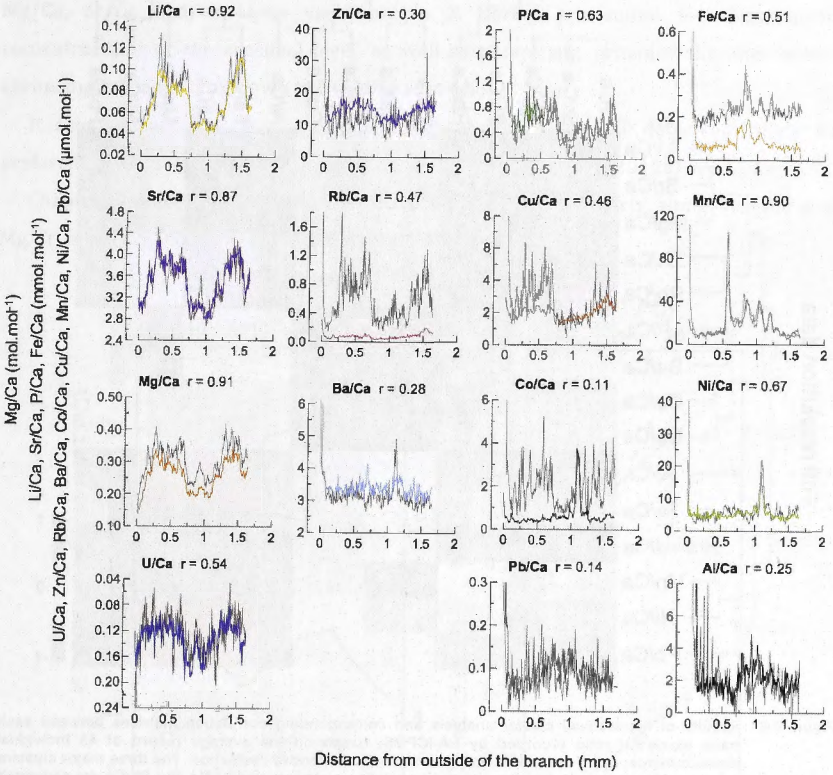

Figure V-5 **Comparison of LA-ICPMS records of Li/Ca, Mg/Ca, Al/Ca, P/Ca, Mn/Ca, Fe/Ca, Co/Ca, Ni/Ca, Cu/Ca, Zn/Ca, Rb/Ca, Sr/Ca, Ba/Ca, Pb/Ca and U/Ca, along the outermost ~2 mm of the R1-3 rhodolith branch, before (dark grey lines) and after (coloured lines) treatment with H_2O_2. Correlation coefficients (r) between both records are also displayed for each element. Note that another branch form a different rhodolith (R7-1) was also analysed before and after H_2O_2 treatment and yielded similar results (not shown here).**

Despite this, when the overall averages are considered, various seasonal patterns still emerge in every element studied here, and can generally be distinguished according to the results of the statistical cluster analysis (Figure V-6).

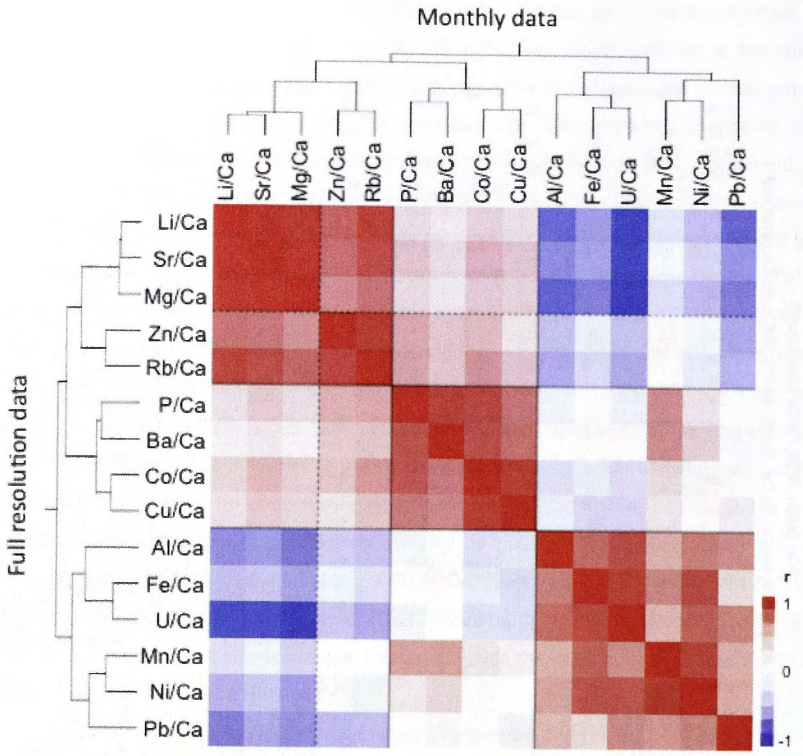

Figure V-6 **Results of hierarchical cluster analysis and corresponding correlation matrices between each trace elemental ratio recorded by LA-ICPMS, based on the average record of 43 individual measurements, at full-resolution and re-sampled to a monthly resolution. The three major clusters are separated by black plain lines in the correlation matrices, and Zn/Ca and Rb/Ca are separated from Li/Ca, Sr/Ca and Mg/Ca by the black dotted line (see text for details). Colouration of the correlation matrix reflects the sign and degree of correlation (r) between trace elements.**

V-3.c Mg/Ca, Sr/Ca and Li/Ca

Average Mg/Ca and Sr/Ca concentrations in *S. durum* rhodoliths are consistent with previous reports for other species of coralline red algae (Halfar et al., 2000; Kamenos et al., 2008; Hetzinger et al., 2009; 2011a) and Li/Ca values are comparable to the ones of various marine organisms (e.g. Delaney et al., 1989; Marriott et al., 2004; Bryan and Marchitto, 2008; Rollion-Bard et al., 2009).

For the average elemental pattern recorded during the November 2009 – September 2011 period, which displays well-defined seasonal variations, it is clear that temperature is of major influence on the incorporation of Mg/Ca, Sr/Ca and Li/Ca into *S. durum*. This is illustrated both by the strong correlation coefficients recorded at monthly resolution

($r>0.82$; $p<0.0001$ – Figure V-7), and by the fact that these elements present the highest degree of reproducibility in the individual record (Figure V-4). We therefore propose that Mg/Ca, Sr/Ca and/or Li/Ca variations in *S. durum* are suited for temperature reconstructions at the seasonal level, as well as potentially, provided the appropriate chronological constrains, down to a weekly resolution.

It also appears that Mg/Ca displays the best fit to the IST data, confirming its preferential use over Sr/Ca (Kamenos et al., 2008; Hetzinger et al., 2011a) and Li/Ca.

Chapter VI of this thesis will further discuss these various aspects, along with the way Mg, Sr and Li are incorporated into the rhodoliths.

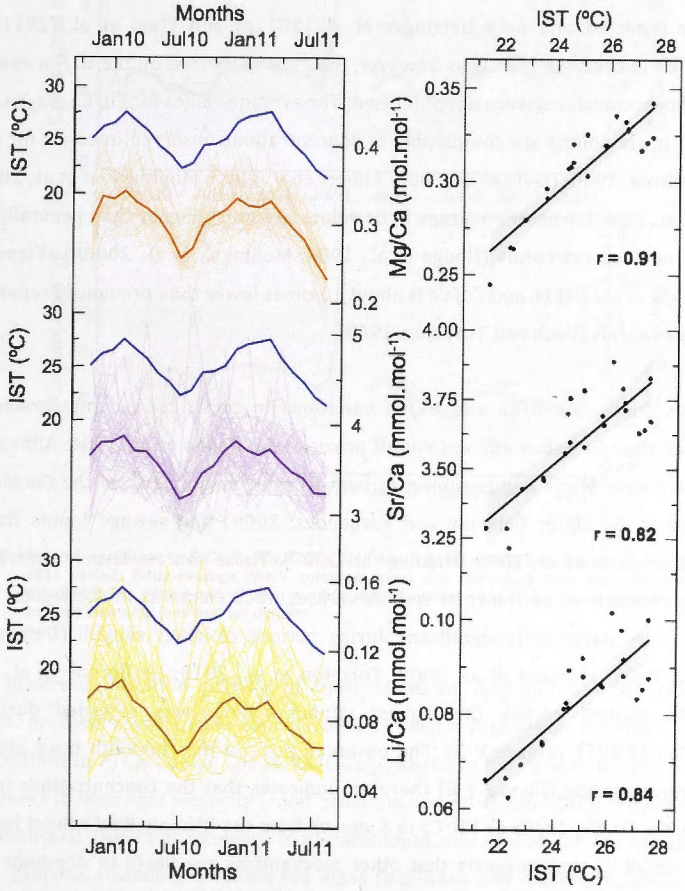

Figure V-7 Right: Monthly variations of Mg/Ca, Sr/Ca and Li/Ca average (thick lines) and individual (thin lines) records, compared to the IST record (thick blue lines) for the November 2009-August 2011 period. Left: Scatter plots showing the linear relationships (black lines) between the IST and the trace elements records over the same period. The corresponding correlation coefficients (r) are also displayed, along with the 95% confidence interval for each linear regression (grey areas).

V-3.d P/Ca, Cu/Ca, Co/Ca, Ba/Ca and Zn/Ca, Rb/Ca

Although the hierarchical clustering gave the average Zn/Ca and Rb/Ca closer to Mg/Ca, Sr/Ca and Li/Ca than to P/Ca, Ba/Ca, Cu/Ca and Co/Ca, we chose to group Zn/Ca and Rb/Ca with the latter, based on the high degree of variability observed at the individual record level (Figure V-4), the influence of the organic phase on their variations (Figure V-5) and the timing of their seasonal patterns (Figure V-8), all of which, are more similar to the ones of P/Ca, Ba/Ca, Cu/Ca and Co/Ca.

Coralline red algae composition in P/Ca, Cu/Ca, Co/Ca, Zn/Ca and Rb/Ca have not been previously reported and only Hetzinger et al. (2011a) and Chan et al. (2011) have measured Ba in coralline red algae, however, their study focused on the Ba/Ca anomalies and actual concentrations were not published. The average values for Cu/Ca, Ba/Ca, Zn/Ca and Rb/Ca in rhodoliths are comparable to concentrations observed in corals for coastal regions (Allison, 1996; David et al., 2003; Alibert et al., 2003; Montaggioni et al., 2006; Al-Rousan et al., 2007), whereas average P/Ca values are much higher than generally found in surface or deep-sea corals (Dodge et al., 1984; Montagna et al., 2006; LaVigne et al., 2008; Mallela et al., 2011), and Co/Ca is about 10 times lower than previously reported for Pacific Ocean corals (Veeh and Turekian, 1968).

Previous studies on P/Ca and Ba/Ca variations in corals have demonstrated their potential as river or urban effluent runoff proxies (e.g. Dodge et al., 1984; Alibert et al., 2003). The Sainte Marie Bay is subject to both freshwater inputs form the Coulée River (Fernandez et al., 2006; Debenay and Fernandez, 2009) and sewage inputs from the Nouméa city (Dalto et al., 2006; Migon et al., 2007). These sources largely contribute to increasing amounts of nutrients as well as various trace elements in the lagoon coastal waters and are particularly significant during periods of heavy rainfall (Debenay and Fernandez, 2009; Moreton et al., 2009; Torréton et al., 2010; Le Borgne et al., 2010). During the studied period, the highest rainfall activity was recorded during the summer/fall of 2011 (Figure V-3). The observed peak in the rhodolith trace elemental records during spring (Figure V-8) therefore indicates that the concentrations in P/Ca, Ba/Ca, Cu/Ca, Co/Ca, Zn/Ca or Rb/Ca in *S. durum* from the Ricaudy Reef cannot be linked to local rainfall. It thus suggests that other mechanisms are likely to dominate at the seasonal scale.

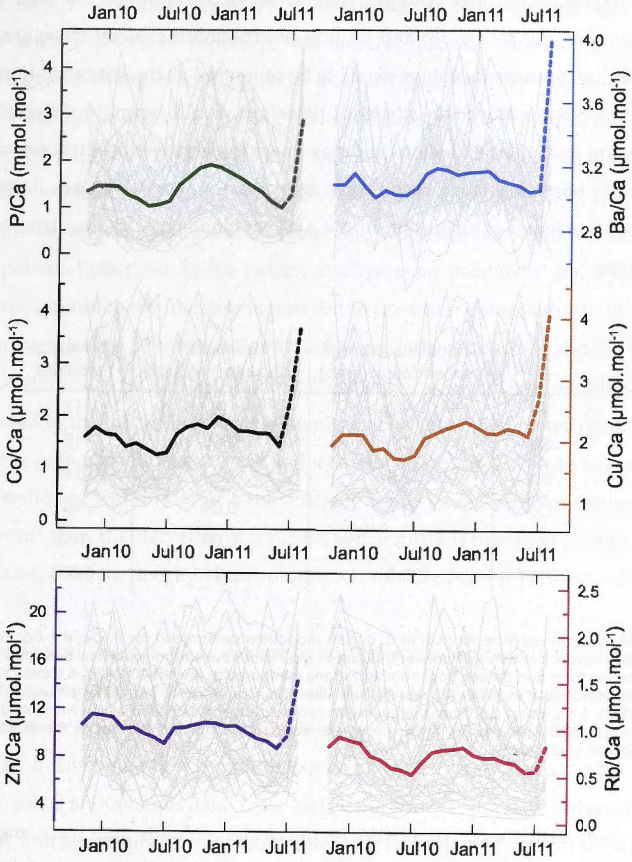

Figure V-8 **Monthly variations of P/Ca, Cu/Ca, Co/Ca, Ba/Ca and Zn/Ca, Rb/Ca over the November 2009-August 2011 period. Both average (thick coloured lines) and individual (thin grey lines) records are displayed. The dotted part of each average record corresponds to the tissue layer that is enriched in trace elements (see text for details).**

The observed variation pattern of these elements may indicate the intensity of metabolic processes, with higher concentrations linked to higher alga activity. The highest concentrations in P/Ca, Cu/Ca, Co/Ca, Zn/Ca and Rb/Ca in the rhodoliths are coeval with spring peaks in both light intensity (solar radiation and PAR) and CDOM (Figure V-3). It is well established that light intensity is of paramount importance for the metabolism of many organisms, including coralline red algae (e.g. Adey and MacIntyre, 1973; Steneck, 1986; Foster, 2001), and CDOM concentrations in similar types of tropical, shallow-water environments, can be related to the intensity of benthic biological activity (Boss and Zaneveld, 2003; Otis et al., 2004). In that respect, the elemental partition coefficients (K_d)

for *S. durum* (Table 1), also strongly suggest an active role of the alga during the incorporation of P, Cu, Zn, Co, Rb and Ba into the rhodolith skeletal structure. However, the interpretation of these K_d values needs to be tempered as the concentration values for seawater were not measured *in situ* and, therefore, could be quite different from the reality. They are particularly likely to underestimate the actual concentration values at the sediment-water boundary layer, resulting in an overestimation of the calculated K_d values and hence, of the actual contribution of the alga metabolism in the incorporation of the trace elements.

	Rhodoliths average concentration (ppm)	Seawater concentration (µg/l)	Kd value in rhodoliths
P	300	18	17
Cu	0.9	0.06	15
Ba	2.9	5	0.6
Co	0.7	0.04	16
Zn	5	0.05	100
Rb	0.5	131	0.004

Table V-1 **Distribution coefficients (Kd) in S. durum rhodoliths determined for P, Cu, Ba, Co, Zn and Rb from their respective average concentrations in the rhodoliths and in seawater. Seawater concentration values for P and Ba are from concentrations measured in the NRCC NASS-5 Open Ocean reference solution (Field et al., 2007); for Rb, from the IGG B1 reference sea water solution (Tonarini et al., 2003); for Cu and Co, from the averages concentrations measured at the Anse Vata site (Moreton et al., 2009); and for Zn, from the concentration measured at the Sainte Marie Bay station N33 (Migon et al., 2007).**

Another potential source of CDOM in the water column and trace metals in the rhodoliths is the resuspension of surficial sediments. This could be driven by higher wind activity recorded in spring during the studied period (Figure V-3), which would favour sediment resuspension through the generation of water currents (Clavier et al., 1995; Douillet et al., 2001). Sediments in the bays surrounding Nouméa are rich in organic matter and various trace metals such as P, Cu, Zn or Co (Dalto et al., 2006; Migon et al., 2007; Torréton et al., 2010; Grenz et al., 2010). Their resuspension would hence contribute to increase the CDOM concentration in the water column. Similarly, trace elements concentrations in the water column would be enhanced by the high capacity for chemical exchange of suspended particles (Ouillon et al., 2010). Spagnoli and Bergamini (1997) for instance, have shown that resuspension favours the release of P through surficial desorption from fine particles and/or dissolution processes. The sediments of the area are also enriched in nutrients compared to the water column (Grenz et al., 2010), therefore, resuspension would also lead to an increase in nutrient availability, particularly at the sediment-water interface, enhancing the biological activity of the benthic

community, in turn increasing the CDOM concentration in the water column. This is also concordant with a previous report of net benthic primary production in the New Caledonian lagoon peaking in spring (Clavier and Garrigue, 1999).

Increased biological processes during spring contrasts with the Chl a pattern for the November 2009-August 2011 period where high concentrations occurred in late fall 2010 and fall/ early winter 2011, with the highest Chl a peak in January 2011 (Figure V-3). If validated, this assumption indicates that metabolic processes in coralline red algae follow a different pattern than those of the pelagic algal primary producers and, specifically, do not appear to respond to the increase in nutrient in the water column due to increase river discharge or higher flow of urban effluent during periods of heavier rainfall (Torréton et al., 2010; Le Borgne et al., 2010). Rather, the biological activity of coralline red algae appears related to that of the benthic community and is controlled by nutrient fluxes from the sediments, enhanced during current-induced resuspension. This also suggests that, at least at the sediment-water interface, the nutrient inputs from sediment resuspension are more important than the decrease in nutrient concentration that is predicted due to the increase mixing with the more oligotrophic waters of the lagoon (Torréton et al., 2007; 2010).

Higher biological activity of *S. durum* in spring is in contradiction with the annual growth pattern recorded for the studied samples, which indicates higher extension rates during the summer/fall period rather than in spring (Chapter IV, this thesis). However, it has previously been shown that rhodolith extension rates can somewhat differ from their calcification pattern (Kamenos and Law, 2010; Burdett et al., 2010). Our results may indicate that annual extension rates and intensity of biological processes in *S. durum* rhodoliths could also be decoupled. Unfortunately, skeleton densities have not been measured here and our observations call for further studies in this area, as well as a growth monitoring experiment at higher resolution to better understand the relationships between extension rates, calcification pattern and intensity of metabolic processes in *S. durum*.

V-3.e Al/Ca, Fe/Ca, Mn/Ca, Ni/Ca, Pb/Ca and U/Ca

Average records of Al/Ca, Fe/Ca, Ni/Ca, Pb/Ca as well as Mn/Ca, if the peak attributed to the use of ARS is not considered, all present higher concentrations in the *S. durum* rhodolith skeleton during winter 2010 (Figure V-9). Lower IST during this period could contribute to a preferential incorporation of some of these metals into the calcite, particularly Pb and, to a lesser extent, Mn (Rimstidt et al., 1998). Similarly, higher Mn, Fe

and Pb concentrations could be explained by possible slower calcification rates in winter (Rimstidt et al., 1998). However, for Ni incorporation into calcite, Lakshtanov and Stipp (2007) found only a weak, negative dependency to calcification rate, and Rimstidt et al. (1998) even predict a contradictory positive correlation between these two parameters. These observations suggest that temperature and/or calcification pattern are not directly responsible for the common increase in the observed metal concentration. As for the other environmental parameters presented here, none could explain the recorded average pattern in the rhodoliths.

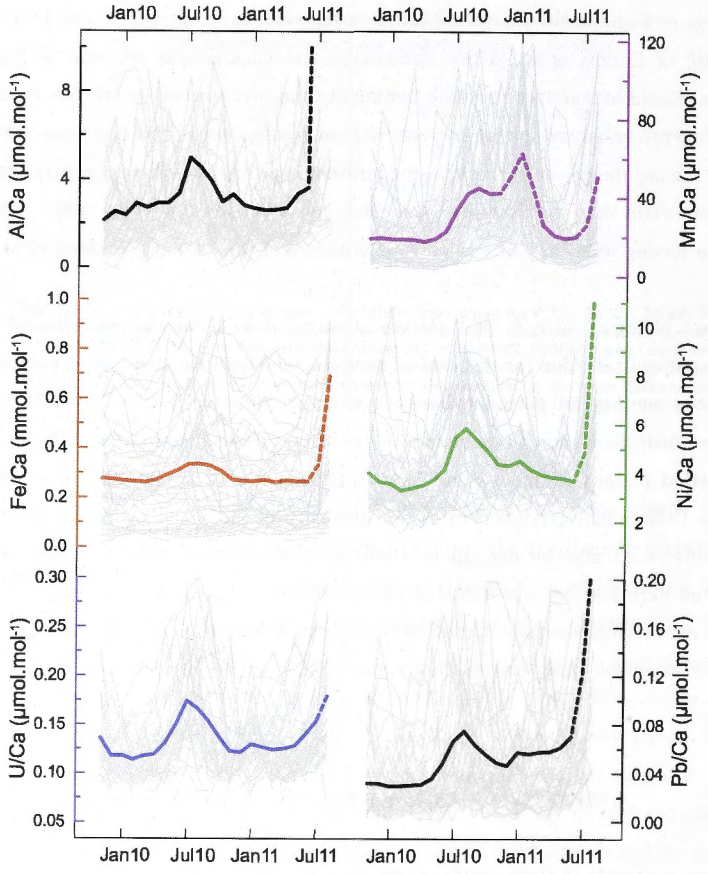

Figure V-9 **Monthly variations of Al/Ca, Fe/Ca, Mn/Ca, Ni/Ca, Pb/Ca and U/Ca over the November 2009-August 2011 period. Both average (thick coloured lines) and individual (thin grey lines) records are displayed. The dotted part of each average record corresponds to the tissue layer that is enriched in trace elements. For Mn/Ca, the part affected by the presence of the alizarin red S stained layer also appears as a dotted line (see text for details).**

In winter 2010, however, maintenance work was carried out in the area, which essentially consisted of the removal of sediments from the Coulée river-mouth, to protect it from silting in (S. Chevalier; Direction du Développement Rural – DDR, Nouméa; personal communication). As a result of this operation, considerable amounts of particles would have been locally resuspended. For similar activities that occurred in the Sainte Marie Bay in 2000, twice the average turbidity levels were recorded (Ouillon et al., 2010). It is most likely that a significant proportion of this material, resuspended at the mouth of the Coulée River, has reached the Sainte Marie Bay and the Ricaudy Reef (see Fernandez et al., 2006). Considering the fact that surficial sediments from the mouth of the Coulée River and the adjacent Boulari Bay present considerably high concentrations in Fe, Ni and Mn as a result of past, opencast mining activities and continuing erosion of abandoned sites (Fernandez et al., 2006; Dalto et al., 2006; Migon et al., 2007; Debenay and Fernandez, 2009), we propose that the dredging in winter 2010 resulted in higher metal concentrations in the water column that were available for the rhodoliths to incorporate into their calcite skeleton. This could be enhanced by higher dissolved metal concentrations in seawater when residence times are longer (see Migon et al., 2007 for Ni), which would have been the case in winter 2010 when wind speed was low. Sediment oxygen consumption is also lower in winter (Grenz et al., 2010), increasing the probability of metal incorporation into the rhodoliths calcite before the dissolved metals are oxidised and trapped into the sediments. Incorporation of Mn, Fe and Ni (as well as Co) into the *S. durum* rhodoliths will be further discussed in another section of this thesis (Chapter VII).

The presence of Al in lateritic layers of the southwest of New Caledonia (Baltzer and Trescases, 1971; Trescases, 1975) suggests that this metal may also be present in relatively high concentration in the sediment of the river mouth, and may have behaved similarly to Fe, Mn and Ni for the period studied, as may have Pb.

The statistical affiliation given by the hierarchical cluster analysis of U/Ca variations with the above-mentioned metals (Figure V-6) may suggest that higher U/Ca concentrations in rhodoliths are also linked to the presence of metal-rich particles resuspended by anthropogenic activities. However, based on the fact that the U/Ca patterns of individual tracks recorded in the analysed *S. durum* branches are quite different than the ones of the other metals, and seems to relate more to the Mg/Ca, Sr/Ca and Li/Ca patterns (see Figure V-5), we propose that U/Ca variations actually reflect IST variations during the studied period. This is supported by the high-level of anti-correlation between the average monthly U/Ca variations and the IST instrumental dataset ($r=-0.84$; $p<0.0001$ – data not shown). It is also consistent with a recent report of U/Ca anti-correlation with SST for a cold-water coralline red algae species (Hetzinger et al., 2011a). Similarly, U/Ca variations were often shown to be linked to seawater temperature, in

marine organisms such as corals, with a decrease in U/Ca as temperature increases (e.g. Corrège et al., 2000; Fallon et al., 2003; Corrège, 2006a).

Naturally, the proposed processes are based solely on the average patterns of the studied metals and have to be tempered by the generally high heterogeneity (particularly Al and Fe), observed both between records for a single element (Figure V-4), and between elements for a single record (Figure V-5).

V-3.f On the influence of the tissue layer and ARS stain on trace element concentrations

For most of the studied trace elemental ratios, very high concentrations are recorded in the first tens of microns of every branch (e.g. Figures V-2 and V-5), which can represent up to 1-to-2 months according to the extension rate (Figures V-8 and V-9), and correspond to the living tissue layer of the rhodolith. This phenomenon is also observed in other marine organisms such as corals where metals can be 10 to 80 times more concentrated in the tissue layer than in the rest of the skeleton (e.g. McConchie and Harriott, 1992; Corrège, 2006b). High concentrations in the tissue layer suggest that these trace elements may play an active role in the calcification processes. Therefore, and although such high concentrations do not translate further down in the skeleton, it is probable that variations in the trace element composition of the tissue layer influence, to some extent, the resulting skeletal composition.

In addition to the high trace-element concentrations recorded in the tissue layer, a distinct peak in Mn/Ca concentration is observed in all the analysed rhodolith branches and systematically matches the position of the ARS-stained layer (e.g. Figure V-2). We attribute this Mn/Ca peak to the formation of Mn-bearing polymeric chelates. Indeed, it has been shown that when ARS is added in a solution, it spontaneously reacts with various bivalent cations, such as Mn, Co, Ni or Cu, to form alizarin complexes (Govil and Banerji, 1973; Al-Janabi et al., 1987). This characteristic is commonly used in separation and preconcentration procedures leading to the analysis of metals in seawater, environmental or biological samples (e.g. Nagahiro et al., 1995; Korn et al., 2004).

No peak similar to the Mn one is observed for other metals in the *S. durum* record, although Ni may show a slight concentration increase corresponding approximately to January 2011 (Figure V-9). This might be explained by (1) the higher O–metal bond of the Mn chelate compared to the Ni chelate (Al-Janabi et al., 1987), resulting in the relative instability of the Ni chelate (Govil and Banerji, 1973); (2) other factors over-powering the trace metals signals in the rhodoliths, particularly for Co and Cu.

The fact that the ARS peak in Mn is lower after H_2O_2 treatment whereas the rest of the signal is essentially unaffected (Figure V-5), implies a different form of Mn incorporation in this particular layer, further suggesting the probable link with the use of ARS.

V-4 Conclusion

In an attempt to characterise the behaviour of trace elemental variations in *S. durum* form the Ricaudy Reef, New Caledonia at the seasonal level, we used high-resolution LA-ICPMS to analyse 43 branches belonging to different rhodoliths specimens.

A 21-month period was studied and ARS staining helped constrain the chronology for every branch. The reproducibility of each of the 15 trace elements considered in this study was assessed using pairwise correlation matrices at both full (i.e. weekly to sub-weekly) and monthly resolution. Except for the Mg/Ca, Sr/Ca and Li/Ca records, a relatively high degree of variability between branches, with, for some trace elements, more than half of the records being inconsistent with each other. Potential explanations for the observed variability were discussed and the re-analysis of a branch after H_2O_2 treatment permitted to better determine the role of the organic component in the distribution of some trace elements in *S. durum* rhodoliths.

Despite the relative inconsistency of some trace elements between individual branches, common patterns in seasonal variations could have been determined through a hierarchical clustering based on the average records. We observed Mg/Ca, Sr/Ca, Li/Ca and potentially U/Ca in *S. durum* being mainly controlled by temperature variations, whereas P/Ca, Cu/Ca, Zn/Ca, Co/Ca, Rb/Ca and Ba/Ca may reflect a higher intensity of biological processes, likely to be coeval with an increase of these elements in seawater due to resuspension related to increased local wind activity. The pattern of Mn/Ca, Ni/Ca, Fe/Ca, Al/Ca and Pb/Ca during the period of study was attributed to the impact of anthropogenic activities that occurred in an nearby area where sediments containing a high proportion of these metals were resuspended and reached the Ricaudy Reef, likely to have caused an increase in the metal concentration of the water column.

Further work is required to better understand the mode of incorporation of the studied trace elements in the rhodoliths. At present, at the exception of Mg/Ca, Sr/Ca and Li/Ca, it appears delicate to use the variations of most trace metals in *S. durum* for environmental reconstruction at high (i.e. monthly) resolution, unless several records can be averaged.

References

Acker, J. G., and Leptoukh, G. 2007. Online analysis enhances use of NASA earth science data. *Eos, Transactions American Geophysical Union* **88**(2), 14.

Adey, W., H., and MacIntyre, I., G. 1973. Crustose Coralline Algae: A Re-evaluation in the Geological Sciences. *Geological Society of America Bulletin* **84**, 883-904.

Aguirre, J., Riding, R., and Braga, J., C. 2000. Diversity of coralline red algae: origination and extinction patterns from the Early Cretaceous to the Pleistocene. *Paleobiology* **26**(4), 651-667.

Al-Janabi, M. Y., Al-Azawe, S. S., and Salman, A. 1987. Alizarine red S complexes of Mn (II), Co (II) and Ni (II). *Thermochimica acta* **113**, 209-215.

Al-Rousan, S. A., Al-Shloul, R. N., Al-Horani, F. A., and Abu-Hilal, A. H. 2007. Heavy metal contents in growth bands of *Porites* corals: Record of anthropogenic and human developments from the Jordanian Gulf of Aqaba. *Marine Pollution Bulletin* **54**(12), 1912-1922.

Alibert, C., Kinsley, L., Fallon, S. J., McCulloch, M. T., Berkelmans, R., and McAllister, F. 2003. Source of trace element variability in Great Barrier Reef corals affected by the Burdekin flood plumes. *Geochimica et Cosmochimica Acta* **67**(2), 231-246.

Alibert, C., and McCulloch, M. T. 1997. Strontium/calcium ratios in modern *Porites* corals from the Great Barrier Reef as a proxy for sea surface temperature: calibration of the thermometer and monitoring of ENSO. *Paleoceanography* **12**(3), 345-363.

Allison, N. 1996. Comparative determinations of trace and minor elements in coral aragonite by ion microprobe analysis, with preliminary results from Phuket, southern Thailand. *Geochimica et Cosmochimica Acta* **60**(18), 3457-3470.

Baltzer, F., and Trescases, J. J. 1971. Erosion, transport et sédimentation liés aux cyclones tropicaux dans les massifs d'ultrabasites de Nouvelle-Calédonie. *Cahiers ORSTOM Série Géologie III* **2**, 221-244.

Beck, J. W., Edwards, R. L., Ito, E., Taylor, F. W., Recy, J., Rougerie, F., Joannot, P., and Henin, C. 1992. Sea-surface temperature from coral skeletal strontium/calcium ratios. *Science* **257**(5070), 644-647.

Blake, C., and Maggs, C. A. 2003. Comparative growth rates and internal banding periodicity of maerl species (Corallinales, Rhodophyta) from northern Europe. *Phycologia* **42**(6), 606-612.

Böhm, L., Schramm, W., and Rabsch, U. 1978. Ecological and physiological aspects of some coralline algae from the western Baltic. Calcium uptake and skeleton formation in *Phymatolithon calcareum*. *Kieler Meeresforschung* **4**, 282-288.

Borowitzka, M. A. 1983. Calcium carbonate deposition by reef algae: morphological and physiological aspects. *Perspectives on Coral Reefs*, 16-28.

Bosence, D., W. J. (1983a). Description and Classification of Rhodoliths (Rhodoids, Rhodolites). *In* "Coated Grains." (T. M. Peryt, Ed.), pp. 217-224. Springer-Verlag, Berlin.

Bosence, D., W., J. (1983b). The Occurence and Ecology of Recent Rhodoliths - A Review. *In* "Coated Grains." (T. M. Peryt, Ed.), pp. 225-242. Springer-Verlag Berlin.

Boss, E., and Zaneveld, J. R. V. 2003. The effect of bottom substrate on inherent optical properties: Evidence of biogeochemical processes. *Limnology and Oceanography* **48**(1), 346-354.

Bryan, S. P., and Marchitto, T. M. 2008. Mg/Ca-temperature proxy in benthic foraminifera: New calibrations from the Florida Straits and a hypothesis regarding Mg/Li. *Paleoceanography* **23**(2), PA2220.

Burdett, H., Kamenos, N. A., and Law, A. 2010. Using coralline algae to understand historic marine cloud cover. *Palaeogeography, Palaeoclimatology, Palaeoecology* **302**, 65-70.

Chan, P., Halfar, J., Williams, B., Hetzinger, S., Steneck, R., Zack, T., and Jacob, D. E. 2011. Freshening of the Alaska Coastal Current recorded by coralline algal Ba/Ca ratios.

Journal of Geophysical Research **116**(G1), G01032.

Clavier, J., Chardy, P., and Chevillon, C. 1995. Sedimentation of particulate matter in the south-west lagoon of New Caledonia: spatial and temporal patterns. *Estuarine, Coastal and Shelf Science* **40**(3), 281-294.

Clavier, J., and Garrigue, C. 1999. Annual sediment primary production and respiration in a large coral reef lagoon (SW New Caledonia). *Marine Ecology Progress Series* **191**, 79-89.

Coble, P. G. 2007. Marine optical biogeochemistry: The chemistry of ocean color. *Chemical Reviews* **107**(2), 402-418.

Corrège, T. 2006a. Sea surface temperature and salinity reconstruction from coral geochemical tracers. *Palaeogeography, Palaeoclimatology, Palaeoecology* **232**(2), 408-428.

Corrège, T. 2006b. Monitoring of terrestrial input by massive corals. *Journal of Geochemical Exploration* **88**(1), 380-383.

Corrège, T., Delcroix, T., Récy, J., Beck, W., and Cabioch, G. 2000. Evidence for stronger El Nino-Southern Oscillation (ENSO) events. *Paleoceanography* **15**(4), 465-470.

Dalto, A. G., Gremare, A., Dinet, A., and Fichet, D. 2006. Muddy-bottom meiofauna responses to metal concentrations and organic enrichment in New Caledonia South-West Lagoon. *Estuarine, Coastal and Shelf Science* **67**(4), 629-644.

David, C. P. 2003. Heavy metal concentrations in growth bands of corals: a record of mine tailings input through time (Marinduque Island, Philippines). *Marine pollution bulletin* **46**(2), 187-196.

Debenay, J. P., and Fernandez, J. M. 2009. Benthic foraminifera records of complex anthropogenic environmental changes combined with geochemical data in a tropical bay of New Caledonia (SW Pacific). *Marine pollution bulletin* **59**(8-12), 311-322.

Delaney, M., Popp, B., Lepzelter, C., and Anderson, T. 1989. Lithium-to-calcium ratios in modern, Cenozoic, and Paleozoic articulate brachiopod shells. *Paleoceanography* **4**(6), 681-691.

Dodge, R. E., Jickells, T. D., Knap, A. H., Boyd, S., and Bak, R. P. M. 1984. Reef-building coral skeletons as chemical pollution (phosphorus) indicators. *Marine Pollution Bulletin* **15**(5), 178-187.

Douillet, P., Ouillon, S., and Cordier, E. 2001. A numerical model for fine suspended sediment transport in the southwest lagoon of New Caledonia. *Coral Reefs* **20**(4), 361-372.

Dromgoole, E. L., and Walter, L. M. 1990. Iron and manganese incorporation into calcite: Effects of growth kinetics, temperature and solution chemistry. *Chemical Geology* **81**(4), 311-336.

Eggins, S., De Deckker, P., and Marshall, J. 2003. Mg/Ca variation in planktonic foraminifera tests: implications for reconstructing palaeo-seawater temperature and habitat migration. *Earth and Planetary Science Letters* **212**(3), 291-306.

Eggins, S. M., Kinsley, L. P. J., and Shelley, J. M. G. 1998. Deposition and element fractionation processes during atmospheric pressure laser sampling for analysis by ICP-MS. *Applied Surface Science* **127**, 278-286.

Fallon, S. J., McCulloch, M. T., and Alibert, C. 2003. Examining water temperature proxies in Porites corals from the Great Barrier Reef: a cross-shelf comparison. *Coral Reefs* **22**(4), 389-404.

Fallon, S. J., McCulloch, M. T., van Woesik, R., and Sinclair, D. J. 1999. Corals at their latitudinal limits: laser ablation trace element systematics in *Porites* from Shirigai Bay, Japan. *Earth and Planetary Science Letters* **172**(3-4), 221-238.

Fallon, S. J., White, J. C., and McCulloch, M. T. 2002. Porites corals as recorders of mining and environmental impacts: Misima Island, Papua New Guinea. *Geochimica et Cosmochimica Acta* **66**(1), 45-62.

Fernandez, J. M., Ouillon, S., Chevillon, C., Douillet, P., Fichez, R., and Gendre, R. L. 2006. A combined modelling and geochemical study of the fate of terrigenous inputs from

mixed natural and mining sources in a coral reef lagoon (New Caledonia). *Marine pollution bulletin* **52**(3), 320-331.

Fichez, R., Chifflet, S., Douillet, P., Gérard, P., Gutierrez, F., Jouon, A., Ouillon, S., and Grenz, C. 2010. Biogeochemical typology and temporal variability of lagoon waters in a coral reef ecosystem subject to terrigeneous and anthropogenic inputs (New Caledonia). *Marine Pollution Bulletin* **61**(7-12), 309-322.

Field, M. P., LaVigne, M., Murphy, K. R., Ruiz, G. M., and Sherrell, R. M. 2007. Direct determination of P, V, Mn, As, Mo, Ba and U in seawater by SF-ICP-MS. *Journal of Analytical Atomic Spectrometry* **22**(9), 1145-1151.

Foster, M., S. 2001. Rhodoliths: Between rocks and soft places. *Journal of Phycology* **37**, 659-667.

Frantz, B. R., Foster, M. S., and Riosmena-Rodrìguez, R. 2005. *Clathromorphum nereostratum* (Corallinales, Rhodophyta): The oldest alga? *Journal of Phycology* **41**(4), 770-773.

Freiwald, A., Henrich, R., Schäfer, P., and Willkomm, H. 1991. The significance of high-boreal to subarctic maerl deposits in northern Norway to reconstruct Holocene climatic changes and sea level oscillations. *Facies* **25**(1), 315-340.

Gamboa, G., Halfar, J., Hetzinger, S., Adey, W., Zack, T., Kunz, B., and Jacob, D. E. 2010. Mg/Ca ratios in coralline algae record northwest Atlantic temperature variations and North Atlantic Oscillation relationships. *Journal of Geophysical Research* **115**(C12), C12044.

Govil, P. K., and Banerji, S. K. 1973. Thermodynamics of some bivalent metal chelates of sodium alizarin sulphonate. *Journal of Inorganic and Nuclear Chemistry* **35**(11), 3932-3935.

Grenz, C., Denis, L., Pringault, O., and Fichez, R. 2010. Spatial and seasonal variability of sediment oxygen consumption and nutrient fluxes at the sediment water interface in a sub-tropical lagoon (New Caledonia). *Marine Pollution Bulletin* **61**(7-12), 399-412.

Halfar, J., Hetzinger, S., Adey, W., Zack, T., Gamboa, G., Kunz, B., Williams, B., and Jacob, D. E. 2010. Coralline algal growth-increment widths archive North Atlantic climate variability. *Palaeogeography, Palaeoclimatology, Palaeoecology*,

Halfar, J., Steneck, R., S., Joachimski, M., Kronz, A., and Wanamaker Jr., A., D. 2008. Coralline red algae as high-resolution climate recorders. *Geology* **36**(6), 463-466.

Halfar, J., Steneck, R., S., Schöne, B., R., Moore, G., W., K., Joachimski, M., Kronz, A., Fietzke, J., and Estes, J. 2007. Coralline alga reveals first marine record of subarctic North Pacific climate change. *Geophysical Research Letters* **34**, L07702.

Halfar, J., Zack, T., Kronz, A., and Zachos, J., C. 2000. Growth and high-resolution paleoenvironmental signals of rhodoliths (coralline red algae): A new biogenic archive. *Journal of Geophysical Research* **105**(C9), 22,107-22,116.

Halfar, J., Williams, B., Hetzinger, S., Steneck, R.S., Lebednik, P., Winsborough, C., Omar, A., Chan, P., Wanamaker, A.D., 2011. 225 years of Bering Sea climate and ecosystem dynamics revealed by coralline algal growth-increment widths. *Geology* **39**(6), 579-582.

Hetzinger, S., Halfar, J., Kronz, A., Steneck, R., Adey, W., H., Lebednik, P., A., and Schöne, B., R. 2009. High-resolution Mg/Ca ratios in a coralline red alga as a proxy for Bering Sea temperature variations from 1902 to 1967. *Palaios* **24**, 406-412.

Hetzinger, S., Halfar, J., Zack, T., Gamboa, G., Jacob, D. E., Kunz, B. E., Kronz, A., Adey, W., Lebednik, P. A., and Steneck, R. S. 2011a. High-resolution analysis of trace elements in crustose coralline algae from the North Atlantic and North Pacific by laser ablation ICP-MS. *Palaeogeography, Palaeoclimatology, Palaeoecology* **302**(1-2), 81-94.

Hetzinger, S., Halfar, J., Mecking, J. V., Keenlyside, N. S., Kronz, A., Steneck, R. S., Adey, W. H., and Lebednik, P. A. 2011b. Marine proxy evidence linking decadal North Pacific and Atlantic climate. *Climate Dynamics*, 1-9.

Kamenos, N., A., Cusack, M., and Moore, P., G. 2008. Coralline algae are global

palaeothermometers with bi-weekly resolution. *Geochimica et Cosmochimica Acta* **72**, 771-779.

Kamenos, N. A., and Law, A. 2010. Temperature controls on coralline algal skeletal growth. *Journal of Phycology* **46**(2), 331-335.

Klein, R. T., Lohmann, K. C., and Thayer, C. W. 1996. Bivalve skeletons record sea-surface temperature and δ18O via Mg/Ca and 18O/16O ratios. *Geology* **24**(5), 415-418.

Korn, M. G. A., Santos Jr, A. F., Jaeger, H. V., Silva, N. M. S., and Costa, A. C. S. 2004. Copper, zinc and manganese determination in saline samples employing faas after separation and preconcentration on Amberlite XAD-7 and Dowex 1x-8 loaded with Alizarin Red S. *Journal of the Brazilian Chemical Society* **15**(2), 212-218.

Lakshtanov, L. Z., and Stipp, S. L. S. 2007. Experimental study of nickel (II) interaction with calcite: Adsorption and coprecipitation. *Geochimica et Cosmochimica Acta* **71**(15), 3686-3697.

LaVigne, M., Field, M. P., Anagnostou, E., Grottoli, A. G., Wellington, G. M., and Sherrell, R. M. 2008. Skeletal P/Ca tracks upwelling in Gulf of Panama coral: Evidence for a new seawater phosphate proxy. *Geophysical Research Letters* **35**(5), L05604.

Le Borgne, R., Douillet, P., Fichez, R., and Torréton, J. P. 2010. Hydrography and plankton temporal variabilities at different time scales in the southwest lagoon of New Caledonia: a review. *Marine Pollution Bulletin* **61**(7-12), 297-308.

Lear, C. H., Elderfield, H., and Wilson, P. A. 2000. Cenozoic deep-sea temperatures and global ice volumes from Mg/Ca in benthic foraminiferal calcite. *Science* **287**, 269-272.

Littler, M. M., and Littler, D. S. (1988). Structure and role of algae in tropical reef communities. *In* "Algae and human affairs." Lembi CA, Waaland JR (eds.). Cambridge University Press, Cambridge, pp 30-56.

Littler, M. M., Littler, D. S., and Dennis Hanisak, M. 1991. Deep-water rhodolith distribution, productivity, and growth history at sites of formation and subsequent degradation. *Journal of Experimental Marine Biology and Ecology* **150**(2), 163-182.

Longerich, H. P., Jackson, S. E., and Günther, D. 1996. Laser ablation inductively coupled plasma mass spectrometric transient signal data acquisition and analyte concentration calculation. *Journal of Analytical Atomic Spectrometry* **11**(9), 899-904.

Lorens, R. B. 1981. Sr, Cd, Mn and Co distribution coefficients in calcite as a function of calcite precipitation rate. *Geochimica et Cosmochimica Acta* **45**(4), 553-561.

Mallela, J., Hermann, J., Rapp, R. P., and Eggins, S. M. 2011. Fine-scale phosphorus distribution in coral skeletons: combining X-ray mapping by electronprobe microanalysis and LA-ICP-MS. *Coral Reefs* **30**, 813-818.

Marriott, C. S., Henderson, G. M., Belshaw, N. S., and Tudhope, A. W. 2004. Temperature dependence of 7Li, 44Ca and Li/Ca during growth of calcium carbonate. *Earth and Planetary Science Letters* **222**(2), 615-624.

McConchie, D., and Harriott, V. J. 1992. The partitioning of metals between tissue and skeletal parts of corals: Application in pollution monitoring. *Proc. 7th Int. Coral Reef Symp., Guam* **1**, 97-103.

Migon, C., Ouillon, S., Mari, X., and Nicolas, E. 2007. Geochemical and hydrodynamic constraints on the distribution of trace metal concentrations in the lagoon of Noumea, New Caledonia. *Estuarine, Coastal and Shelf Science* **74**(4), 756-765.

Montaggioni, L. F., Le Cornec, F., Corrège, T., and Cabioch, G. 2006. Coral barium/calcium record of mid-Holocene upwelling activity in New Caledonia, South-West Pacific. *Palaeogeography, Palaeoclimatology, Palaeoecology* **237**(2), 436-455.

Montagna, P., McCulloch, M., Taviani, M., Mazzoli, C., and Vendrell, B. 2006. Phosphorus in cold-water corals as a proxy for seawater nutrient chemistry. *Science* **312**(5781), 1788-1791.

Moreton, B. M., Fernandez, J. M., and Dolbecq, M. B. D. 2009. Development of a Field Preconcentration/Elution Unit for Routine Determination of Dissolved Metal Concentrations by ICP OES in Marine Waters: Application for Monitoring of the

New Caledonia Lagoon. *Geostandards and Geoanalytical Research* **33**(2), 205-218.

Nagahiro, T., Wang, G. F., and Satake, M. 1995. Column preconcentration of aluminum and copper (II) in alloys, biological samples, and environmental samples with Alizarin Red S and cetyltrimethylammonium-perchlorate adsorbent supported on naphthalene using spectrometry. *Microchemical journal* **52**(3), 247-256.

Nelson, W. A. 2009. Calcified macroalgae - critical to coastal ecosystems and vulnerable to change: a review. *Marine and Freshwater Research* **60**(8), 787-801.

Nicet, J. B., and Delcroix, T. 2000. ENSO-Related Precipitation Changes in New Caledonia, Southwestern Tropical Pacific: 1969-98. *Monthly Weather Review* **128**(8), 3001-3006.

Otis, D. B., Carder, K. L., English, D. C., and Ivey, J. E. 2004. CDOM transport from the Bahamas Banks. *Coral Reefs* **23**(1), 152-160.

Ouillon, S., Douillet, P., Lefebvre, J. P., Le Gendre, R., Jouon, A., Bonneton, P., Fernandez, J. M., and Chevillon, C. 2010. Circulation and suspended sediment transport in a coral reef lagoon: The south-west lagoon of New Caledonia. *Marine Pollution Bulletin* **61**(7-12), 309-322.

Paillard, D., Labeyrie, L., and Yiou, P. 1996. Macintosh program performs time-series analysis. *Eos Transactions AGU* **77**(39), 379.

Payri, C. E. 1997. *Hydrolithon reinboldii* rhodolith distribution, growth and carbon production of a French Polynesian reef. *Proceedings of the 8th International Coral Reef Symposium Panama*, 755-760.

Rimstidt, J. D., Balog, A., and Webb, J. 1998. Distribution of trace elements between carbonate minerals and aqueous solutions. *Geochimica et Cosmochimica Acta* **62**(11), 1851-1863.

Rollion-Bard, C., Vigier, N., Meibom, A., Blamart, D., Reynaud, S., Rodolfo-Metalpa, R., Martin, S., and Gattuso, J. P. 2009. Effect of environmental conditions and skeletal ultrastructure on the Li isotopic composition of scleractinian corals. *Earth and Planetary Science Letters* **286**(1), 63-70.

Runnalls, L. A., and Coleman, M. L. 2003. Record of natural and anthropogenic changes in reef environments (Barbados West Indies) using laser ablation ICP-MS and sclerochronology on coral cores. *Coral Reefs* **22**(4), 416-426.

Spagnoli, F., and Bergamini, M. C. 1997. Water-sediment exchange of nutrients during early diagenesis and resuspension of anoxic sediments from the northern Adriatic Sea shelf. *Water, Air, & Soil Pollution* **99**(1), 541-556.

Steneck, R. S. 1986. The ecology of coralline algal crusts: convergent patterns and adaptative strategies. *Annual Review of Ecology and Systematics* **17**, 273-303.

Stoll, H. M., Encinar, J. R., Garcia Alonso, J. I., Rosenthal, Y., Probert, I., and Klaas, C. 2001. A first look at paleotemperature prospects from Mg in coccolith carbonate: Cleaning techniques and culture measurements. *Geochemistry, Geophysics, Geosystems* **200**, 2GC000144.

Tonarini, S., Pennisi, M., Adorni-Braccesi, A., Dini, A., Ferrara, G., Gonfiantini, R., Wiedenbeck, M., and Gröning, M. 2003. Intercomparison of boron isotope and concentration measurements. Part I: selection, preparation and homogeneity tests of the intercomparison materials. *Geostandards Newsletter* **27**(1), 21-39.

Torréton, J. P., Rochelle-Newall, E., Jouon, A., Faure, V., Jacquet, S., and Douillet, P. 2007. Correspondence between the distribution of hydrodynamic time parameters and the distribution of biological and chemical variables in a semi-enclosed coral reef lagoon. *Estuarine, Coastal and Shelf Science* **74**(4), 766-776.

Torréton, J. P., Rochelle-Newall, E., Pringault, O., Jacquet, S., Faure, V., and Briand, E. 2010. Variability of primary and bacterial production in a coral reef lagoon (New Caledonia). *Marine Pollution Bulletin* **61**(7-12), 335-348.

Trescases, J. J. (1975). "L'évolution geochimique supergène des roches ultrabasiques en zone tropicale. Formation des gisement nickélifères de Nouvelle-Calédonie.", Ph.D. Thesis OA 8708, Université Louis Pasteur, Strasbourg.

Veeh, H. H., and Turekian, K. K. 1968. Cobalt, silver, and uranium concentrations of reef-

building corals in the Pacific Ocean. *Limnology and Oceanography* **13**(2), 304-308.

Williams, B., Halfar, J., Steneck, R. S., Wortmann, U. G., Hetzinger, S., Adey, W., Lebednik, P., and Joachimski, M. 2011. Twentieth century 13 C variability in surface water dissolved inorganic carbon recorded by coralline algae in the northern North Pacific Ocean and the Bering Sea. *Biogeosciences* **8**(1), 165-174.

Yahel, R., Yahel, G., and Genin, A. 2002. Daily cycles of suspended sand at coral reefs: A biological control. *Limnology and Oceanography* **47**(4), 1071-1083.

CHAPTER VI

Sea-surface temperature reconstruction from trace elements variations of tropical coralline red algae

Keywords: rhodoliths, *Sporolithon durum*, laser ablation, Mg/Ca, Sr/Ca, Li/Ca, ENSO

Abstract

We used laser ablation inductively coupled plasma mass spectrometry (LA-ICPMS) to obtain high-resolution variations of the trace elemental composition of free-living forms (i.e. rhodoliths) of the coralline red alga species *Sporolithon durum* in order to test their potential to archive sea surface temperature (SST) information. The consistency of the Mg/Ca, Sr/Ca and Li/Ca composition and variation pattern over a >45 year-long period was assessed by comparing the records of five rhodolith branches from three specimens, collected in various locations across a ~1km^2 rhodolith bed in the vicinity of Nouméa, New Caledonia. Average values of Mg/Ca and Sr/Ca (0.31 ±0.04 mol.mol^{-1} and 3.5 ±0.4 mmol.mol^{-1}, respectively) are comparable to the ones previously reported. Slightly higher Mg/Ca values might be explained by higher SST in the *S. durum* living environment and/or a likely influence of species-specific effects. Similar Sr/Ca values in *S. durum* compared to the ones of cold-water species may indicate a common mode of incorporation of Sr in coralline red algae. It is the first time Li/Ca measurements are presented for coralline red algae. The concentrations observed in *S. durum* rhodoliths are comparable to previously reported Li/Ca values for other calcareous organisms.

Trace elements variations show good reproducibility between the records at both monthly and inter-annual resolutions and are all significantly correlated with local variations of SST for the 1963-2008 period ($0.40<r<0.80$; $p<0.0001$; $n=30$). Mg/Ca systematically displays the best fits to local SST variations, with an average Mg/Ca record-local SST correlation of $r=0.85$ ($p<0.0001$), at monthly resolution. Mg/Ca, Sr/Ca and Li/Ca co-vary closely in all records. We propose that the variation of the Mg/Ca composition is the main factor influencing Sr/Ca and Li/Ca variations in *S. durum* to explain their positive

correlation with local SST (r=0.65 and r=0.66, respectively; p<0.0001) over the studied period. Inter-annual Mg/Ca anomalies show significant correlation with the Oceanic Nino Index (ONI), indicating that *S. durum* rhodoliths also have the ability to record the regional climate pattern in the tropical Pacific. Finally, consistent variations between the average Mg/Ca record in *S. durum* rhodoliths and the Sr/Ca record of a *Porites sp.* coral from the same site, as well as a similar relationships with local SST at both monthly and inter-annual scales (r=0.87; r=-0.79 and r=0.62; r=-0.52, respectively), suggests that *S. durum* rhodoliths may be a tool as reliable as coral for SST reconstruction.

VI-1 Introduction

Future climate change has been a major environmental concern for decades and is still bound to significant uncertainties (IPCC, 2007). A wide array of tools, from tree-rings (e.g. Lara and Villalba, 1993; Shao et al., 2010), ice cores (e.g. Dansgaard et al., 1993, Petit et al., 1999, Wolff et al., 2010), lacustrine sediments (e.g. De Deckker et al., 1991; Brauer et al., 1999; Morellón et al., 2011), or speleothems (e.g. McDermott, 2004) on land, to marine sediment cores (e.g. Charles et al., 1996; Cullen et al., 2000) and various marine organisms as foraminifera (Waelbroeck et al., 2002; Eggins et al., 2003), corals (e.g. Beck et al., 1992; Quinn et al., 1998; Corrège, 2006) or bivalve molluscs (e.g. Klein et al., 1996; Schöne et al., 2005) in the oceans, is available to reconstruct past climates with the aim of improving future climate predictions. High-resolution archives are crucial to understanding the climate variability at seasonal to inter-annual timescales. Scleractinian corals are the most commonly used and reliable climatic archives in the tropics (see Corrège, 2006 for a review) and can provide with reconstructions of some of the main factors influencing global climate, such as the El Nino Southern Oscillation (ENSO) variability pattern, over several centuries (e.g. Dunbar et al., 1994; Fairbanks et al., 1997; Cobb et al., 2003). In the extra-tropical zones, bivalves and gastropods have been the almost exclusive tool for oceanic-environment reconstructions (Wanamaker Jr. et al., 2011) until coralline red algae raised a recent interest as potential climate archives (Halfar et al., 2000).

Coralline red algae are globally-distributed calcareous marine organisms that deposit a high-magnesium calcite skeleton as they grow (e.g. Adey and McIntyre, 1973; Bosence, 1983b). They can occur either as attached form on hard bottoms or as free-living nodules (i.e. rhodoliths), on unstable substrata (Steneck, 1986). With thick crusts and nodules of up to 20 cm in diameter (Adey and McIntyre, 1973; Littler et al., 1991; Frantz et al., 2005), as well as generally slow growth rates (0.015-2.17 $mm.yr^{-1}$ – Foster, 2001; Blake and

Maggs, 2003; Böhm et al., 1978), individual organisms have been found to live for more than 800 years (Halfar et al., 2007), potentially making coralline red algae one of the oldest living marine calcifier (Frantz et al., 2005). As they grow, various climate information is recorded in their skeleton, one aspect of which appears in their annual growth pattern, composed of alternating small cells and heavily calcified cell walls generally produced in winter, and longer cells with less calcified cell walls typically produced in summer (e.g. Halfar et al., 2008; Kamenos and Low, 2010). This commonly occurs as pairs of clear and darker bands on visual examination of the coralline red algae skeleton (Kamenos et al., 2008; Kamenos and Low, 2010; Burdett et al., 2010). Recent studies focusing on the climate information contained both in growth increments and in the geochemical composition of the skeleton, provided the first decades-to-century long reconstructions of cold-water environmental parameters from coralline red algae (Halfar et al., 2007; 2008; 2011; Hetzinger et al., 2009; 2011; Chan et al., 2011; Williams et al., 2011). The ability of the variations in Mg composition in coralline red algae to record seawater temperature at the time of calcite deposition, has been, so far, the most promising tool for palaeo-environmental reconstructions (Halfar et al., 2000; Kamenos et al., 2008; Hetzinger et al., 2009; 2011). Sr/Ca records in coralline red algae are seldom but have been shown to present significant, positive correlations with temperature for various high-latitude species (Kamenos et al., 2008; Hetzinger et al., 2011).

Sporolithon durum is widely distributed in oceanic shallow waters, from tropical to temperate-cold environments (e.g. Townsend et al., 1995; Womersley, 1996; Goldberg and Heine, 2008; Basso et al., 2009) and has been reported to continuously live for several decades (Goldberg and Heine, 2008; This thesis, Chapter IV) at a growth rate of approximately 0.6 $mm.y^{-1}$ (This thesis, Chapter IV). Previous work also determined the presence of annual increments in the growth pattern of *S. durum* rhodoliths in a tropical environment (This thesis, Chapter IV), as well as the close relationship between the Mg/Ca variations of several individuals recorded over a several-months monitoring experiment and in situ temperature at the collection site (This thesis, Chapter V). However, longer term seawater temperature reconstructions are yet to be generated.

Here, we assess the potential of trace elements variations in 5 branches of *S. durum* rhodoliths for sea surface temperature (SST) reconstruction over a 45-year period of continuous algal growth. Laser ablation inductively coupled plasma mass spectrometry (LA-ICPMS) was used to record Mg/Ca, Sr/Ca and Li/Ca variations at a monthly to sub-monthly resolution. Results were compared to the ones obtained from solution ICPMS and ICP atomic emission spectrometry (ICP-AES) techniques to assess the accuracy of the LA-ICPMS calibration. Trace elements variations were compared to local SST monthly and inter-annual variations. The Oceanic Nino Index (ONI) was used to investigate the

potential of inter-annual Mg/Ca anomalies in *S. durum* to record regional scale climate pattern. In addition, the reliability of Mg/Ca as a tool for SST reconstruction was tested against the Sr/Ca record of a *Porites sp.* coral from the same site.

VI-2 Material and methods

VI-2.a Study site and rhodolith collection

New Caledonia is a group of islands located in the tropical Pacific Ocean, ~1500 km offshore Australia. The 8000-km² barrier reef on the west side of the main island defines one of the largest lagoon in the world, with an area of 23400 km² (Dandonneau et al., 1981; Labrosse et al., 2000). The typical, annual climatic pattern in New Caledonia alternates between a warm and wet season in the austral summer (Jan-Mar) and a cooler and humid season in winter (Jul-Sep). Dry conditions are generally observed in spring (Oct-Dec) and fall (Apr-Jun). The inter-annual climatic variations are closely related to the El Nino Southern Oscillation (ENSO) pattern, with cooler and drier conditions during periods of El Nino whereas La Nina periods are generally responsible for warmer temperatures and heavier rainfall (Nicet and Delcroix, 2000).

The Ricaudy Reef (22°18'57"S; 166°27'26"E) is one of the fringing coral reefs bordering of Nouméa, the most populated city in New Caledonia (Figure VI-1). Located at the southern end of the Sainte Marie Bay in the Southwest region of New Caledonia, the Ricaudy Reef is under the influence of both the seawater from the lagoon and episodic fresh water inputs from the nearby Coulée River (e.g. Fernandez et al., 2006).

The rhodoliths studied here were collected on the edge of the Ricaudy Reef, at 4-5 m of depth, by SCUBA diving in October 2009 (for the BSA specimen) and February 2011 (for the MSA and SSA specimens). Three individual rhodoliths were selected as being some of the largest nodules observed, in various places of the same rhodolith bed, which spans ~1 km². The ellipsoidal-shaped organisms range in size from 7.4 cm (SSA) to 8.5 cm (MSA) in diameter and present a degree IV branching structure according to the classification in Bosence (1983a). Rhodoliths are exclusively formed by *S. durum*, which is the most abundant coralline red alga species at the site (Figure VI-2).

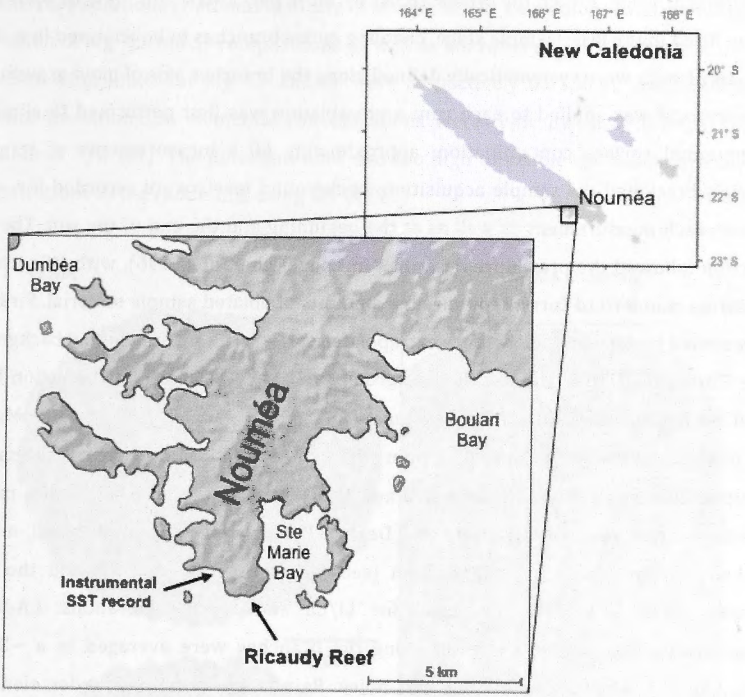

Figure VI-1 Location map showing the Ricaudy Reef study site, at the southern end of the Sainte Marie Bay in the Southwest region of New Caledonia. The site where instrumental SST is recorded daily since 1958 (source: IRD – Institut de Recherche pour le Développement, Nouméa) is also shown.

VI-2.b Trace elements analyses

Upon collection, the rhodoliths were dried and impregnated into araldite resin before being cut into ~5-mm thick sections, parallel to their long axis (Figure VI-2). After polishing and ultrasonic cleaning, the thick sections were oven-dried (40°C) prior to LA-ICPMS analyses and/or sampling for solution ICPMS and ICP-AES analyses.

LA-ICPMS analyses were conducted along 5 rhodolith branches (3 from the BSA specimen and one each from the MSA and SSA specimens) using the ArF excimer laser unit (193 nm wavelength) in combination with a Varian 820 ICPMS, at the Research School of Earth Sciences (RSES) of the Australian National University (ANU). The ablation spot was set to 42 µm in diameter with energy of 5 J.cm^{-2} and a pulse rate of 10 Hz. The laser scanned the branches at a speed of 5 µm.s^{-1}. The ICPMS was set to time-resolved analysis mode at 1 point-per-peak. The isotopes ^{7}Li, ^{24}Mg, ^{25}Mg, ^{43}Ca and ^{88}Sr were analysed, among others, with various dwell times so that the total integration time resulted in ~1 s per

measurement cycle. Either the whole (BSA) or most part (MSA and SSA) of each thick section fitted in the laser sample stage, enabling entire branches to be analysed in a single run. Laser tracks were systematically defined along the branches axis of main growth. The same protocol was applied to each run: a pre-ablation was first performed to eliminate any potential surface contamination; approximately 60 s measurements of standard materials bracketed the sample acquisition; background levels were recorded for ~60 s between each measurement as well as at the beginning and the end of the run. The data reduction followed the procedure described in Longerich et al. (1996), with ^{43}Ca used as an internal standard to correct for variable amounts of ablated sample material. First and last recorded background levels were extrapolated to correct for instrumental background noise. The standard deviation of the background was used to determine detection limits (3σ of the background), which were systematically: <0.19 ppm (^{7}Li), <24 ppm (^{24}Mg), <9 ppm (^{25}Mg), <0.02% (^{43}Ca) and <0.12 ppm (^{88}Sr). The standard bracketing of the sample permitted correction of the linear instrumental drift during the run. A dolomite marble from the Carrara region, Italy (Herz and Dean, 1986), was used as an external, matrix-matched standard for Mg/Ca calibration (see This thesis, Chapter III) and the glass reference NIST 612 SRM, was used for Li/Ca and Sr/Ca calibrations. LA-ICPMS measurements obtained every 5 µm along the branches were averaged to a ~30-µm resolution to minimise the instrumental noise. Results are presented under elemental molar ratios over Ca, against distance from the outside of the rhodoliths branches.

For solution ICPMS and ICP-AES analyses, samples consisting of ~1mg of carbonate powder were hand-drilled (2-3 mm-diameter x ~1 mm-deep holes) along branches of the studied rhodoliths. The same samples (4 for BSA and SSA and 5 for MSA) were analysed by both solution and ICP-AES. Each sample was dissolved into 10-ml, 2% HNO_3 solutions prior to analyses.

Solution ICPMS analyses were performed on the Varian 820 ICPMS (RSES, ANU), also used for LA-ICPMS. Calibration curves were generated from the analysis of four standard solutions of increasing trace metal concentrations (prepared from AccuTrace solutions – National Institute of Standard and Technology) before, during and after the run. A blank solution of pure 2% HNO_3 was used to determine the instrumental background levels as well as the detection limits for Li, Mg, Ca and Sr, which were 0.026 ppm, 2.5 ppm, 59 ppm and 0.03 ppm (3σ of the background), respectively. Instrumental reproducibility was assessed by measuring repeatedly the same sample throughout the run. Reproducibility for Li was 2.8%, for Mg was 2.1%, for Ca was 1.8% for Sr was 1.1% (n=6).

A Varian Vista Pro Axial was used for the ICP-AES analyses at the RSES, ANU, following the method in de Villiers et al. (2002). A matrix-matched standard solution was made out

of AccuTrace solutions (National Institute of Standard and Technology) and permitted the calibration of Mg, Ca and Sr compositions as well as instrumental drift correction through time. Detection limits for Mg, Ca and Sr were respectively 0.01, 0.10 and 0.005 $mg.l^{-1}$. Standard deviations on elemental concentrations were typically <0.74% (Mg), <0.75% (Ca) and <0.70% (Sr). The detection limit was too high to enable the determination of Li concentrations in the rhodoliths using ICP-AES.

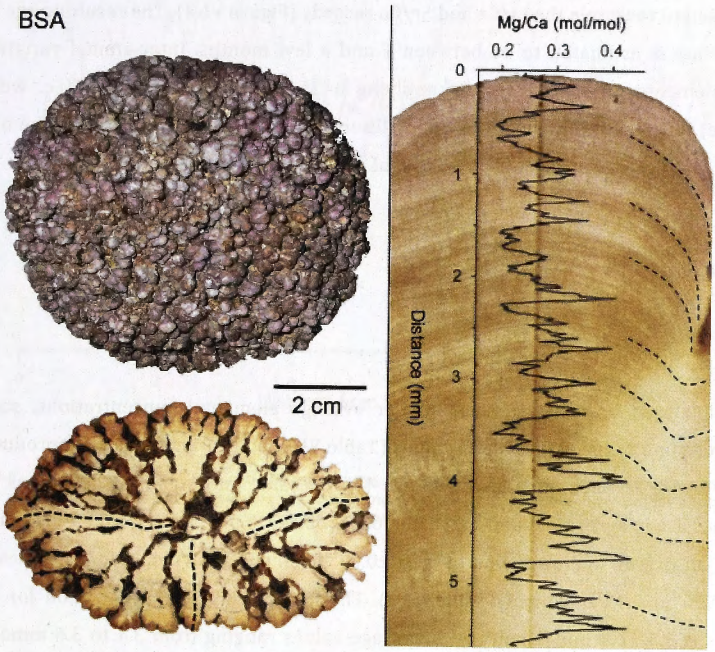

Figure VI-2 Photographs of the whole BSA rhodolith specimen (top left), a section parallel to the long axis of growth (bottom left) showing the path of three laser tracks (dashed lines). Right: Close up on the top part of a rhodolith branch where the Mg/Ca variations measured by LA-ICPMS are shown over the corresponding laser track. Dotted lines correspond to the layers with lowest values in the Mg/Ca cycles, which were used to constrain the chronology (see text for details).

VI-2.c Age model determination

The age models for the rhodoliths presented here were obtained from the establishment of chronologies based on multiple approaches (see details in This thesis, Chapter IV). For the MSA and SSA rhodoliths, the combination of overlapping Mg/Ca cycles from different branches as well as growth band counting was used for the chronology. This approach is commonly used as a reliable chronological tool for other coralline red algae species (e.g. Hetzinger et al., 2009; 2011; Chan et al., 2011). In addition, for two

branches of the BSA rhodolith, radiocarbon dating was performed and gave concordant results with the Mg/Ca cycles and growth band counting approach (This thesis, Chapter IV – Figure VI-2), increasing our confidence in the reliability of the latter for *S. durum* chronology. Using the AnalySeries data analysis software (Paillard et al., 1996), high (low) peaks in the major Mg/Ca cycles along every branch, were tied to months with the highest (lowest) annual SST (Figure VI-3). ~30-µm resolution Mg/Ca data points were, then, linearly extrapolated and resampled to a monthly resolution. The same anchor points were used to resample the Li/Ca and Sr/Ca records (Figure VI-3). The resulting age model uncertainty is estimated to be between 1 and a few months. Inter-annual variations of trace elements were obtained by applying a 25-points Hanning filter (i.e. weighted average) to the monthly data in order to filter the seasonal variations out of the original signals (e.g. Corrège et al., 2000; Le Bec et al., 2000).

VI-3 Results

VI-3.a LA-ICPMS

All analysed branches present similar average elemental concentrations, standard deviations and range of individual values (Table VI-1), indicating the good reproducibility of the LA-ICPMS technique. The average Mg/Ca value and standard deviations for all branches are in agreement and vary from 0.29 (BSA2) to 0.32 (BSA3) ±0.04-0.03 mol.mol^{-1}, with an overall average value of 0.30 ±0.04 mol.mol^{-1}. Individual Mg/Ca values range from 0.20 to 0.47 mol.mol^{-1} (Table VI-1). The average Sr/Ca concentration for all the records is 3.5 ±0.4 mmol.mol^{-1}, with average values ranging from 3.4 to 3.6 mmol.mol^{-1}, according to the analysed branch. The minimum Sr/Ca value recorded is 2.2 mmol.mol^{-1} and the maximum is 4.7 mmol.mol^{-1}. Li/Ca concentrations average 0.08 ±0.02 mmol.mol^{-1} for all branches, with a range of 0.07 to 0.09 mmol.mol^{-1} for the average values of individual branches. The maximum observed range of Li/Ca individual values over the entire dataset is 0.03 to 0.17 mmol.mol^{-1} (Table VI-1).

The high cross-correlation coefficient between each elemental ratio, for each branch as well as for the whole analysis (Table VI-1) illustrates a strong co-variation of Mg/Ca, Sr/Ca and Li/Ca in the *S. durum* rhodoliths (see also Figure VI-3). Sr/Ca and Li/Ca systematically display the strongest bond with correlation coefficients varying from r=0.80 to r=0.90 from branch to branch, and a r-value of 0.87 for the entire dataset. The pairs Mg/Ca-Sr/Ca and Mg/Ca-Li/Ca show very similar correlation coefficients for any particular branch. Mg/Ca and Sr/Ca present correlation coefficients ranging from r=0.62 to r=0.84, with an

overall correlation of r=0.68. Correlation coefficients for Mg/Ca and Li/Ca vary from r=0.76 and r=0.85, with an overall r-value of 0.67 (Table VI-1).

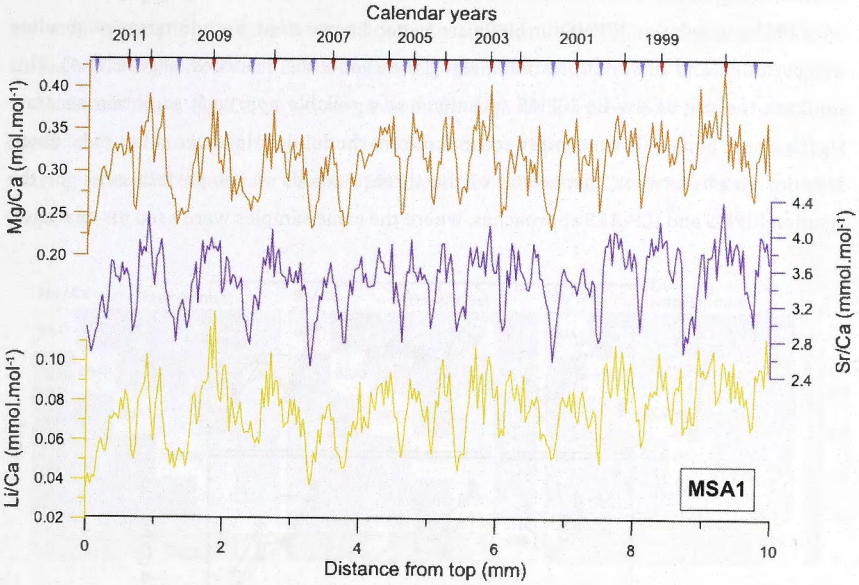

Figure VI-3 **Variation of Mg/Ca, Sr/Ca and Li/Ca along the top 10 cm of the MSA1 branch as recorded by LA-ICPMS. The top axis shows the corresponding chronology with and anchor points attributed to winter (blue triangles) and summer (red triangles) months of every year.**

Rhodolith branch	Average ±1σ *(range)*			Correlation coefficient (r)			n
	Mg/Ca (moi.mol^{-1})	Sr/Ca (mmol.mol^{-1})	Li/Ca (mmol.mol^{-1})	Mg/Ca-Sr/Ca	Mg/Ca-Li/Ca	Sr/Ca-Li/Ca	
BSA1	0.31 ±0.04 *(0.21-0.47)*	3.6 ±0.4 *(2.5-4.7)*	0.09 ±0.02 *(0.05-0.17)*	0,79	0,77	0,90	1143
BSA2	0.29 ±0.04 *(0.20-0.42)*	3.5 ±0.3 (2.7-4.3)	0.08 ±0.02 *(0.04-0.14)*	0,75	0,77	0,85	683
BSA3	0.30 ±0.04 *(0.21-0.44)*	3.6 ±0.3 *(2.6-4.5)*	0.09 ±0.02 *(0.05-0.17)*	0,84	0,85	0,87	913
MSA1	0.31 ±0.04 *(0.22-0.43)*	3.4 ±0.3 *(2.3-4.4)*	0.07 ±0.02 *(0.03-0.13)*	0,62	0,79	0,80	1033
SSA1	0.30 ±0.03 *(0.21-0.40)*	3.5 ±0.4 *(2.2-4.5)*	0.08 ±0.02 *(0.03-0.16)*	0,74	0,76	0,89	974
All	0.30 ±0.04 *(0.20-0.47)*	3.5 ±0.4 *(2.2-4.7)*	0.08 ±0.02 *(0.03-0.17)*	0,68	0,67	0,87	4746

Table VI-1 **Average values, standard deviation and range of LA-ICPMS records of Mg/Ca, Sr/Ca and Li/Ca along the five individual rhodolith branches studied here as well as the entire dataset. Pearson's correlation coefficients (r) obtained for the cross-correlation between every trace element for every branch and for the whole dataset are also displayed along with the number of data points (n) used to establish these correlations.**

VI-3.b Trace elements calibration

Results from LA-ICPMS, solution ICPMS and ICP-AES analyses for Mg/Ca and Sr/Ca, and LA-ICPMS and solution ICPMS for Li/Ca are in good agreement, both in terms of absolute concentration and of variation trends along the rhodoliths branches (Figure VI-4). This confirms the use of the LA-ICPMS technique as a reliable approach to obtain accurate Mg/Ca, Sr/Ca and Li/Ca concentrations in *S. durum* rhodoliths. However, it has to be noted that the match between the results of the three methods is not perfect, even for the solution ICPMS and ICP-AES approaches, where the same samples were used for analysis.

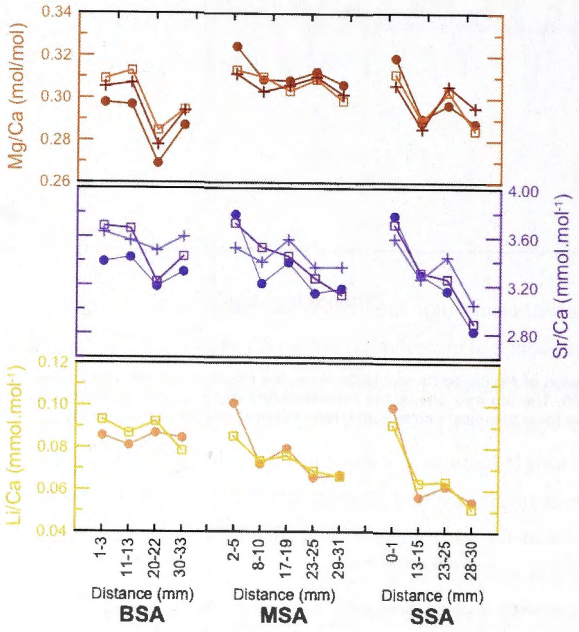

Figure VI-4 Trace elements concentrations along the BSA, MSA and SSA rhodoliths (distances are from the outside toward the center of the nodule) measured by LA-ICPMS (plain dots), solution ICPMS (open squares) and ICPM-AES (crosses). Error bars correspond to the standard error on each measurement for solution ICPMS and ICPAES data point, and to the standard error of the mean of each trace elements values recorded between the corresponding distance, for the LA-ICPMS data points.

VI-3.c Reproducibility of trace elements variations

The reproducibility of trace elemental ratio across the five analysed rhodoliths branches was assessed for both monthly and inter-annual variations (Figure VI-5). All but one correlation coefficients are significant at the 95% confidence level (n=60).

Mg/Ca and Li/Ca are the most reproducible at monthly resolution, with most of the correlation coefficients c between r=0.4 and r=0.6. Sr/Ca is slightly less reproducible at this scale, with half of the r-values between 0.4 and 0.6 and the other half ranging from 0.2 to 0.4. All correlations are, however, statistically significant ($p<0.001$; n=590). At the inter-annual scale, higher correlations are generally observed, with r-values often >0.6 (Figure VI-5). At this scale, Mg/Ca variations present the highest and most consistent correlation coefficients, whereas the correlation coefficients for Sr/Ca are relatively inconsistent, ranging from non-significant at the 95% level (for the pair BSA1-BSA2) to up to r=0.8 (Figure VI-5).

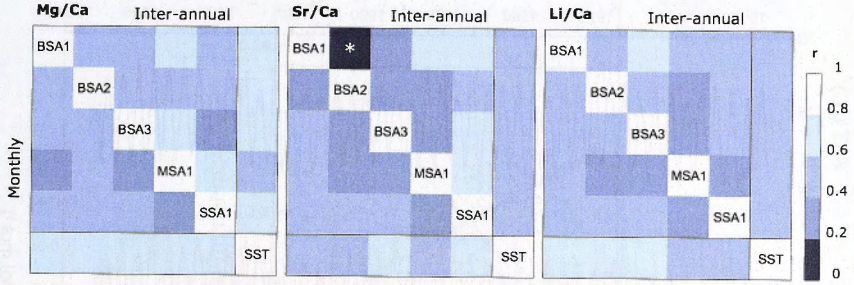

Figure VI-5 **Cross-correlation matrix diagram for the records of Mg/Ca, Sr/Ca and Li/Ca along the five rhodoliths branches analysed with LA-ICPMS, considering both the monthly and inter-annual data. The correlation of each record with the local SST is also displayed. All correlations are statistically significant at the 99.9% and 95% levels for, respectively, monthly and inter-annual datasets, except for *. The scale is such that the clearer the colour, the higher the correlation coefficients.**

VI-3.d Trace element variations and local SST

All monthly variations of Mg/Ca, Sr/Ca and Li/Ca along every rhodolith branch display significant correlations at the 99.9% confidence interval, with local SST ($0.4< r <0.8$ – Figure VI-5). Mg/Ca records show the best fit to SST, with the majority of the correlation coefficients comprised between r=0.6 and r=0.8. Sr/Ca and Li/Ca present slightly lower correlations ($0.4< r <0.6$). The relationship between SST and trace elements variations is generally stronger at the inter-annual level. All the Mg/Ca records are highly correlated with SST variations ($0.6< r <0.8$) as well as the majority of Li/Ca records ($p<0.05$). Sr/Ca-SST correlation coefficients are also slightly improved compared to the monthly resolution (Figure VI-5).

Monthly elemental variations for all the analysed branches are displayed in Figure VI-6, along with the respective average record and the instrumental local SST variations for the 1963-2008 period. The relationship between the average elemental records and SST are

illustrated in Figure VI-7, and Figure VI-8 shows the average and standard deviation of inter-annual variations for each element against the local SST.

Averaging the individual records results in significantly better correlations with local SST. Again, Mg/Ca presents the strongest relationship with SST at monthly and inter-annual resolutions ($r=0.85$; $p<0.001$ and $r=0.83$; $p<0.05$, respectively – Figures VI-7, VI-8). The correlation coefficients for the average Sr/Ca and Li/Ca versus SST are similar at monthly resolution ($r=0.65$ and $r=0.66$, respectively; $p<0.001$ – Figure VI-7) and are improved when inter-annual variations are considered ($r=0.71$ and $r=0.75$, respectively; $p<0.05$ – Figure VI-8).

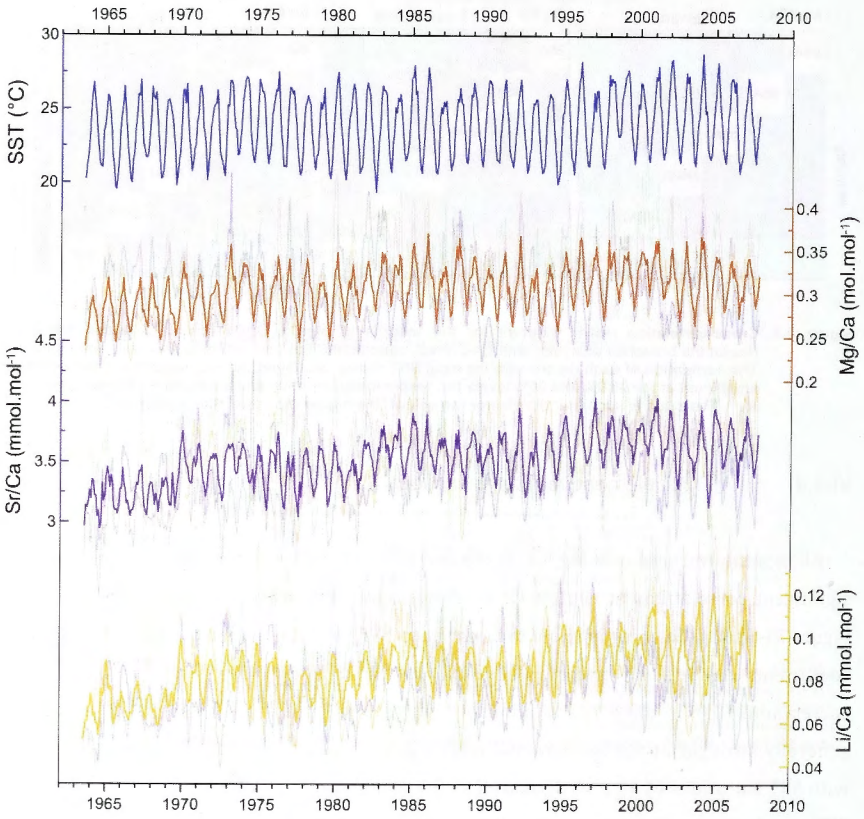

Figure VI-6 Monthly-resolved variations of Mg/Ca, Sr/Ca and Li/Ca recorded along the individual rhodolith branches (thin pale lines) over the 1963-2008 period. Average trace elements records as well as monthly variations of local SST (thick bright lines) are also displayed for the same period.

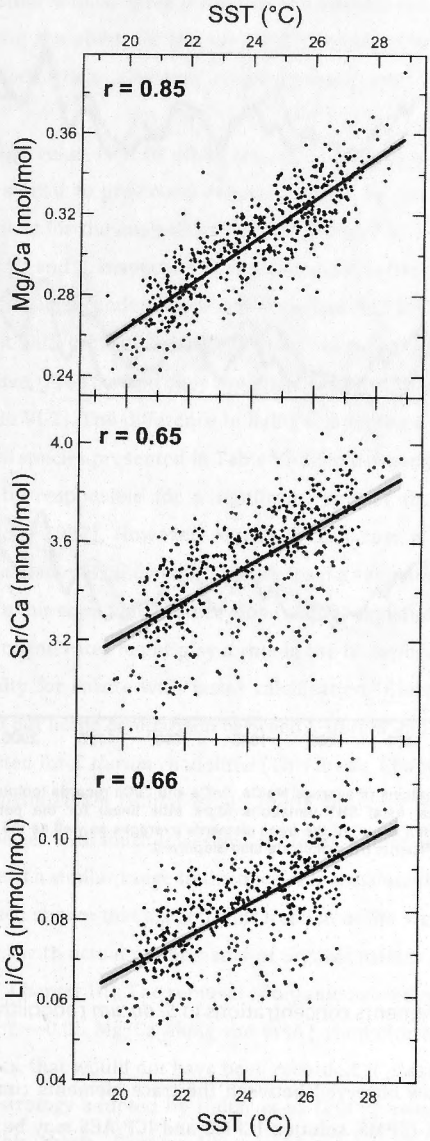

Figure VI-7 Scatter plots of the relationships between monthly data of average Mg/Ca, Sr/Ca and Li/Ca against local SST. Linear regression line (black line) and 95% confidence intervals (shaded areas) are displayed as well as the corresponding Pearson's correlation coefficients (r); $p<0.001$.

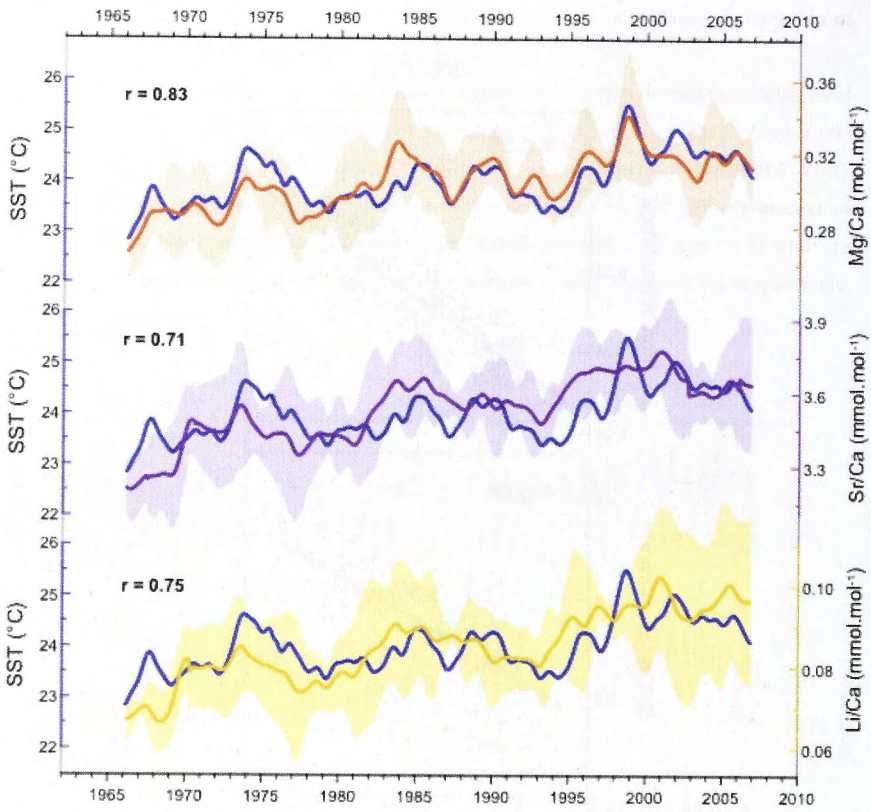

Figure VI-8 Inter-annual variations of average Mg/Ca, Sr/Ca and Li/Ca records (coloured lines), super imposed over inter-annual local SST variations (dark blue lines) for the period 1965-2006. Standard deviations (shaded areas) of the trace elements averages as well as the corresponding Pearson's correlation coefficients (r); $p<0.05$ are also displayed.

VI-4 Discussion

VI-4.a Trace elements concentrations in *S. durum* rhodoliths

The slight differences observed between the trace elements concentrations for each sample analysed by LA-ICPMS, solution ICPMS and ICP-AES may be attributed to (1) the sampling of different branches for the same rhodolith, between LA-ICPMS and both solution ICPMS and ICP-AES, which would result in samples not exactly matching each other's location. This, associated with the inter-branch variability in trace element variations, possibly led to reported trace elements concentration values that may not correspond exactly to the same area along the rhodolith branch; and (2) a slight difference

in trace elements calibration between the solution ICPMS and ICPM-AES methods. Nevertheless, the results of these three independent analytical techniques are still in good agreement, confirming the ability of the LA-ICPMS technique to provide with accurate measurements of both trace elements concentrations and variations in *S. durum* rhodoliths.

The Mg/Ca average value of 0.30 ±0.04 mol.mol^{-1} for entire branches of several *S. durum* rhodoliths is similar to previously reported values for the outermost portion of a single branch, as well as for the analysis of multiple rhodoliths over the 2010-2011 year (This thesis, Chapter III and V, respectively), indicating a consistency in Mg incorporation both across the Ricaudy Reef rhodolith bed and over time. Our Mg/Ca results for *S. durum* are also in agreement with the 0.08-0.40 Mg/Ca (molar) range reported for coralline red algae in general (Chave, 1954), albeit they are slightly higher than for most of the other species studied (Table VI-2). The difference in living temperature range between most of the coralline red algae species presented in Table VI-2 (cold-water) and *S. durum* (tropical water), is likely to be responsible for a significant part of the Mg/Ca concentration difference (e.g. Oomori, 1987). However, Mg/Ca in *S. durum* is also higher than in a specimen of *Lithothamnion crassiusculum* rhodolith from a very similar temperature range (Halfar et al., 2000). In this case, temperature alone cannot explain the difference in Mg/Ca concentration. Calcification rates might play a role in the incorporation of Mg into calcite, with higher Mg affinity for calcite with faster calcification (Rimstidt et al., 1998). This effect cannot be ruled out in the comparison between *S. durum* and *L. crassiusculum* as the extension rates reported for *S. durum* rhodoliths (This thesis, Chapter IV) are significantly higher than for *L. crassiusculum* (Halfar et al., 2000). However for different cold-water coralline red algae species with much lower growth rates, Kamenos et al. (2008) reported Mg/Ca values that are of a similar range to the ones of *L. crassiusculum* (Halfar et al., 2000; Table VI-2). It has been shown that a significant fraction of the Mg content in *S. durum* is likely to be associated with actual or remnants of organic matter present inside the cell structure (This thesis, Chapter III). The removal of organic-related material in *S. durum* led to a constant offset of ~-0.05 Mg/Ca along the MSA1 rhodolith branch. The correction from this Mg/Ca excess, that would not have been recorded, if present, in *L. crassiusculum* due to the sampling strategy adopted by Halfar et al. (2000) using electron microprobe analysis (see also This thesis, Chapter III), would narrow the difference in Mg/Ca concentration between *S. durum* and *L. crassiusculum*, but *S. durum* Mg/Ca values would still be slightly higher. Consequently, as previously suggested (Halfar et al., 2000; Kamenos et al., 2008), our results indicate a most probable role of inter-species variability in the differences in Mg composition of coralline red algae.

Authors	Species	Location	Range of values ($mol.mol^{-1}$)	Temperature relationship Proxy.$°C^{-1}$	r	Technique
Mg/Ca						
Chave, 1954	Various	Various	0.08 - 0.40	0,007	n/a	X-Ray spectrometry
Chave and Wheeler, 1965	*C. compactum*	Gulf of Maine, USA	0.10 - 0.16	0,005	n/a	XRD
Moberly, 1968	*C. compactum*	Quebec, Canada	0.08 - 0.22	0,013	n/a	EPMA
Halfar et al., 2000	*L. crassiusculum*	Gulf of California, Mexico	0.15 - 0.29	0,017	n/a	EPMA
	L. glaciale	Newfoundland, Canada	0.08 - 0.22	0,012	n/a	EPMA
Kamenos et al., 2008	*L. glaciale*	Loch Sween, Scotland	0.15 - 0.33	0,019	0,97	EPMA
				0,034	0,87	Ion probe
	P. calcareum	Isle of Arran, Scotland	0.17 - 0.31	0,019	0,89	EPMA
Hetzinger et al., 2009	*C. nereostratum*	Aleutian Is, USA	0.08 - 0.18	0,015	0,50	EPMA
Hetzinger et al., 2011	*C. nereostratum*	Aleutian Is, USA	0.09 - 0.17	0,015	0,54	LA-ICPMS
	C. compactum	Newfoundland, Canada	0.08 - 0.26	0,012	0,77	LA-ICPMS
This study	*S. durum*	Nouméa, New Caledonia	0.24 - 0.39	0,011	0,85	LA-ICPMS
Sr/Ca						
Kamenos et al., 2008	*L. glaciale*	Loch Sween, Scotland	0.0027 - 0.0055	2.10^{-4}	0,88	Ion probe
	P. calcareum	Isle of Arran, Scotland	0.0024 - 0.0041	1.10^{-4}	0,83	EPMA
Hetzinger et al., 2011	*C. nereostratum*	Aleutian Is, USA	0.0031 - 0.0036	$0.8.10^{-4}$	0,21	LA-ICPMS
	C. compactum	Newfoundland, Canada	0.0031 - 0.0036	$0.6.10^{-4}$	0,31	LA-ICPMS
This study	*S. durum*	Nouméa, New Caledonia	0.0029 - 0.0040	$0.7.10^{-4}$	0,65	LA-ICPMS

Table VI-2 Mg/Ca and Sr/Ca range of values (in mol.mol-1) reported in the literature for various modern species of coralline red algae across the world. Where applicable, the amplitude of variation for each element against temperature (per degree Celsius) is indicated as well as the corresponding Pearson's correlation coefficients (r). The technique used to for trace elemental analysis is also reported. EPMA: electron microprobe analysis; XRD: X-Ray diffraction; LA-ICPMS: Laser ablation inductively coupled plasma mass spectrometry.

The range of Sr/Ca values in *S. durum* is within values reported for cold water species of coralline red algae (2.2-5.5 mmol.mol^{-1}; Kamenos et al., 2008; Hetzinger et al., 2011 - Table VI-2). The temperature difference between the various collection sites is therefore to be excluded as a factor controlling the Sr content of different species of coralline red algae. Kamenos et al. (2008) suggested a role of organic-bound Sr as a potential source of Sr enrichment. However, neither Sr/Ca concentrations nor Sr/Ca variations showed a significant difference after H_2O_2 treament of a *S. durum* rhodolith branch (This thesis, Chapter V), suggesting Sr content in rhodolith's calcite is not significantly affected by the presence of organic matter. Higher calcification rates, as observed in *S. durum* compared to the other specimens studied (This thesis, Chapter IV) should result in higher affinity of Sr with calcite (Carpenter and Lohman, 1992; Rimstidt et al., 1998) and therefore higher Sr/Ca concentrations in *S. durum*. Our results suggest that a significant effect of the growth rate on Sr incorporation in coralline red algae is also unlikely. Sr concentration in calcite would be affected by Sr concentrations in seawater (e.g. Pingitore Jr. and Eastman, 1986). However, Sr/Ca has been shown to only vary by ~2-3% globally, mainly due to salinity differences along latitudinal gradients (de Villiers, 1999). This relative uniformity of Sr in the world oceans may explain similarities between Sr/Ca concentration values between different coralline red algae species from different oceanic environments, hence suggesting that the Sr content in coralline red algae is not species dependant.

Li/Ca concentrations have not yet been reported for coralline red algae. However, average values presented here are comparable to the ones of other calcareous organisms. Li/Ca concentrations for *S. durum* rhodoliths (0.03 to 0.17 mmol.mol^{-1}) are higher than the range reported in corals (0.005 – 0.009 mmol.mol^{-1}; Marriott et al., 2004a; Rollion-Bard et al., 2009) and various species of foraminifera (0.003 – 0.024 mmol.mol^{-1}; Bryan and Marchitto, 2008; see also Delaney and Boyle, 1986; Hall and Chan, 2004, Marriott et al., 2004b; Yu et al., 2005). They are also slightly higher than the ones reported in brachiopods (0.018 – 0.05 mmol.mol^{-1}; Delaney et al., 1989) but lower than lacustrine ostracods Li/Ca concentrations (0.04 – 0.20 mmol.mol^{-1}; Zhu et al., 2012).

VI-4.b Trace elements reproducibility

All trace elements records are significantly cross-correlated at monthly resolution, indicating that common processes are likely to be involved in the variations of Mg/Ca, Sr/Ca and Li/Ca into *S. durum* rhodoliths. However, dissimilarities are also observed and may have different sources of explanation.

The uncertainty of the age model (1 to a few months) could have a significant impact on the reproducibility of the signals. This may explain the generally higher correlations observed at the inter-annual resolution.

Partial diagenesis can also be a potential factor of trace elements variability in coralline red algae, however, it is unlikely here due to the absence, along the sampling tracks set for this study, of visible recrystallisation features (see This thesis, Chapter III), as well as the absence of conceptacles in *S. durum* that could be subject to post-formation infillings (e.g. Moberly Jr., 1968). Furthermore, no mark of cessation of growth has been observed in any of the *S. durum* specimens presented here and it has been shown that abiotic carbonate precipitation is prevented at the algal surface, while coralline red algae are living (Alexandersson, 1974).

The effect of variable growth rates could influence the trace element incorporation into *S. durum*, with Mg, Sr and Li being potentially more easily substituted for Ca with faster growth rates (Rimstidt et al., 1998; Marriott et al., 2004b). As extension rates for the different branches studied here are very variable during the studied period (This thesis, Chapter IV), it is a factor to potentially take into account. However, at the seasonal level, extension rates have been suggested to be of insignificant influence on trace element variations (This thesis, Chapter V).

Non-systematic distribution of organic matter in the rhodoliths may affect the Mg/Ca variability, however, this characteristic has not been documented nor determined here and the H_2O_2 treatment of the MSA branch did not significantly affect the Mg/Ca variations (This thesis, Chapter III), hence, we speculate this hypothesis is unlikely to occur. The composition or variation of Sr/Ca and Li/Ca are not affected by H_2O_2 treatment (This thesis, Chapter V).

Another potential source of trace element variability in rhodoliths resides in fluctuations of trace elements concentrations in the ambient seawater. As rhodoliths are in contact with the sediment, the boundary layer can be crucial to consider, particularly for Mg, which is abundant in the clay material of the surrounding landscape (e.g. Baltzer and Trescases, 1971) and in the surface sediments (Ambatsian et al., 1997). Indeed, oxidation potentials of those sediments could highly vary over a short period of time and/or a short spatial scale, according to various factors such as local hydrodynamics or bioturbation (Grenz et al., 2010). This could result in variable dissolved Mg concentrations in the boundary layer that are likely to translate in Mg/Ca variability between different rhodoliths of the same bed. Sr/Ca and Li/Ca variations in rhodoliths are also possibly subject to changes in dissolved concentrations of their corresponding cations in seawater and the boundary layer. Unfortunately, the extent of this effect is hardly quantifiable due to the nature of the variability sources.

Overall, Mg/Ca shows the highest reproducibility, suggesting that it is the least affected by the above-mentioned sources of variability. Sr/Ca and Li/Ca are closely related o each other and display a similar reproducibility that may indicate that they are both affected in a similar way by variability factors.

VI-4.c Trace elements relationship with SST

All trace elements records show highly significant, positive relationships with local SST at both monthly and inter-annual resolutions (Figure VI-5), suggesting that SST pplays a major role on the variations of Mg/Ca, Sr/Ca and Li/Ca in *S. durum* rhodoliths over the studied period. These trace elements-SST relationships are enhanced when the average records are considered (Figures VI-6, VI-7). It appears that averaging across branches of the same rhodolith specimen as well as across various organisms permits the elimination of a significant fraction of the non-systematic sources of variability affecting the individual signals and, therefore, highlights the common trends related to the environmental influence.

VI-4.c.1 Mg/Ca

Mg/Ca display the strongest correlation with local SST and is considered to be the best candidate for temperature reconstructions from *S. durum* rhodoliths at monthly to inter-annual resolutions. The extent of the Mg/Ca relationship with temperature (average: $r=0.85$; individual records $0.6< r <0.8$) is concordant with previously reported values for cold-water environments (Table VI-2). It is generally higher than for *Clathromorphum nereostratum* and *C. compatum* using electrom microprobe and LA-ICPMS techniques ($0.50< r <0.77$; Hetzinger et al., 2009; 2011) but lower than for *L. glaciale* and *Phymatolithon calcareum* using ion probe and electron microprobe techniques ($0.87< r <0.97$; Kamenos et al., 2008). However, it has to be noted that the studies by Hetzinger et al. (2009; 2011) used satellite-derived regional SST for their comparison, whereas Kamenos et al. (2008), used in situ temperatures. It is expected that the comparison of Mg/Ca variations from both of these studies with local area SST, as it is the case for this study, results in respectively higher and lower correlation coefficients, thus matching up even better with our findings.

It has been proposed that the Mg composition in coralline red algae varies by about 1% $MgCO_3$ (equivalent to 0.013 Mg/Ca mol.mol^{-1}) per degree Celsius (e.g. Halfar et al., 2000). The slope of the linear regression between Mg/Ca variations in *S. durum* and local SST is

0.011, which is in good agreement with this proposition and within the range of previously reported slopes for Mg/Ca variations (Table VI-2). Therefore, it appears that, despite a probable species-specific effect on the absolute Mg concentration in coralline red algae, the range of Mg variations against seawater temperature is consistent between different species and also different environments. A positive, 3.1 ±0.4% variation in Mg composition per degree Celsius was predicted for abiotic calcite (Oomori, 1987). Our results indicate a positive variation of 3.5% per degree Celsius in *S. durum*, hence adding further confidence in the suggestion that there is no significant vital effect on the Mg/Ca variations in the coralline red algae skeleton (Ries, 2006; Kamenos et al., 2008).

VI-4.c.2 Sr/Ca and Li/Ca

Although the Sr/Ca-SST relationship is still significant with r=0.65 for the average monthly record (Figure VI-7), Sr/Ca variations in *S. durum* display weaker correlations with SST than Mg/Ca. This is concordant with the observations of other studies on Sr/Ca variations in coralline red algae (Kamenos et al., 2008; Hetzinger et al., 2011). The correlation coefficients between Sr/Ca and local SST as well as the amplitude of Sr/Ca variations over the range of SST are in agreement with previously reported values (Table VI-2). Indeed, with an average Sr/Ca (mol.mol^{-1}) variation of 0.7 10^{-4} .°C^{-1}, our results match the range of 0.6 10^{-4} - 2 10^{-4} .°C^{-1} obtained by Kamenos et al. (2008) and Hetzinger et al. (2011) for four different coralline red algal species from cold water environments (Table VI-2). Consequently, it appears that Sr/Ca variations with SST are consistent within a wide range of coralline red algae species as well as drastically different environments.

Li/Ca variations show a positive relationship with SST of the same order than the Sr/Ca variations as well as a strong correlation with those Sr/Ca variations in each individual record. This suggests that Li/Ca and Sr/Ca share similar factors influencing their variations.

For abiotic calcite precipitation, negative correlations with temperature are predicted for both Sr/Ca (Kinsman and Holland, 1969) and Li/Ca (e.g. Marriott et al., 2004a). This has been observed in various calcareous organisms (Sr/Ca in corals: see Corrège, 2006 for a review; Li/Ca in foraminifera: e.g. Hall and Chan, 2004; Marriott et al., 2004b; Byan and Marchitto, 2008; in brachiopods: Delaney, 1989; in corals: Marriott et al., 2004a; Montagna et al., 2006; Rollion-Bard et al., 2009; Hathorne et al., 2009). A strong vital effect was suggested by Kamenos et al. (2008) to explain the positive Sr/Ca-SST relationship. Our observations agree with this hypothesis. Indeed, calcite deposition in coralline red algae occurs within the cell walls (Chisholm, 2003), where specific polysaccharide fibrils and alginic acid polymers are thought to intervene at the beginning of the mineralisation

process (Bilan and Usov, 2001). These polymers have been proposed as being responsible for the preferential formation of high-Mg calcite over aragonite in environments where aragonite precipitation should normally occur (Wada et al., 1993). The active role of coralline red algae in precipitating high-Mg calcite over aragonite has also been demonstrated from laboratory experiments (Ries, 2006; 2009). It is therefore possible that the presence of specific organic components, through their high affinity with divalent cations (Bilan and Usov, 2001), favours high concentrations of these cations (and particularly Mg^{2+}) in the restricted cell wall environment, from which calcite crystals mineralise. An increase in Mg^{2+} concentration in the parent solution has been shown to result in an increase of the distribution coefficients of both Sr^{2+} (Carpenter and Lohman, 1992) and Li^{+} (Okumura and Kitano, 1986), which will, therefore, be more easily incorporated into calcite. Okumura and Kitano (1986) also showed a positive linear relationship between the $MgCO_3$ concentration and the Li content in calcite. Consequently, we speculate that the variations of Sr/Ca and Li/Ca in coralline red algae may be primarily controlled by the variations in Mg incorporation into the calcite skeleton. This could explain (1) the fact that Sr/Ca and Li/Ca variations are positively correlated to SST, despite the fact that abiotic calcite precipitation and observations in other calcareous organisms predict negative correlations; (2) the lower extent of the Sr/Ca-SST and Li/Ca-SST relationships compared to the one of Mg/Ca-SST. Indeed, for Sr/Ca and Li/Ca, SST variations may only be an indirect control, the major influential factor being the Mg/Ca variations, itself being directly controlled by SST variations.

Further investigations should focus on Sr and Li isotopes measurements in order to gain more insight into the extent of the algal influence on Sr and Li incorporation into the coralline red algae calcite.

VI-4.d Regional climate record

Mg/Ca variations in *S. durum* from the Ricaudy Reef reliably record local SST variations at monthly to inter-annual timescales. When compared to the Oceanic Nino Index (ONI), which is a climate index of ENSO variability in the tropical Pacific (http://ggweather.com/enso/oni.htm), it appears that the average inter-annual Mg/Ca anomaly signal is significantly correlated with ONI variations over the studied period, with the best fit obtained using a 4-month lag (Figure VI-9A). This 4-month lag also gives the best correlation between ONI and the local SST anomalies (Figure VI-9A). Delcroix and Lenormand (1997) obtained the best response of the SST in the lagoon of New Caledonia to the ENSO variability with a 3-month lag. Considering that the Ricaudy Reef, as well as

the nearby site of instrumental SST measurements are located near shore, and therefore, can be subject to specific hydrodynamical conditions as, for instance, longer residence times of the waters that approximate 15 days (Jouon et al., 2006; Ouillon et al., 2010), a month difference between the New Caledonian lagoon in general and our study site, is not incoherent.

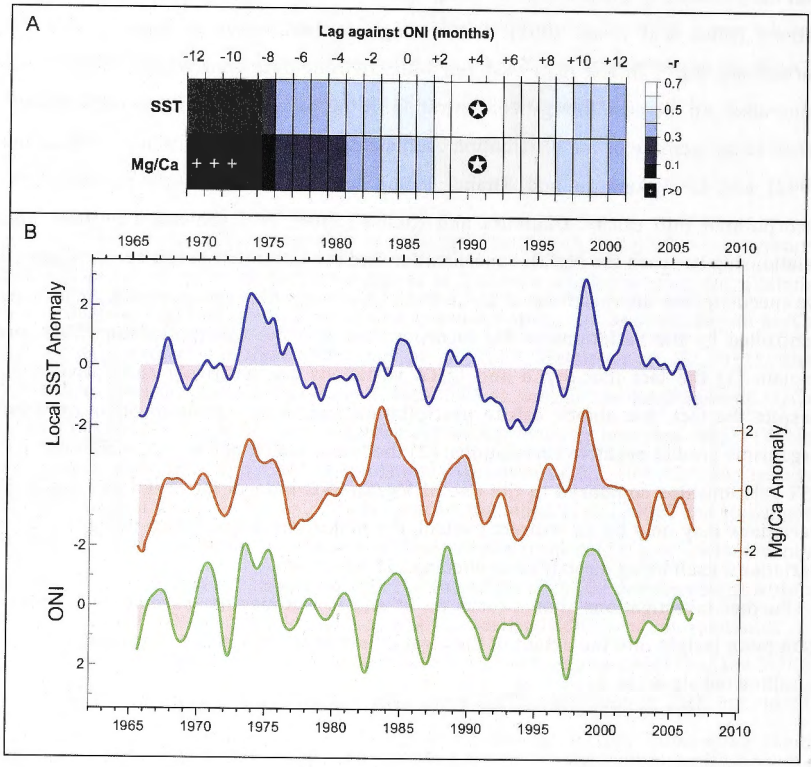

Figure VI-9 **A: Lagged cross-correlation diagram between inter-annual local SST and average Mg/Ca anomalies and the Oceanic Nino Index (ONI). The scale is such that lighter colours correspond to stronger anti-correlations. A '+' symbol stands for a positive correlation coefficient and the stars highlights the +4 months lag, for which the highest correlation was obtained. Correlations are significant for $|r|>0.3$; $p<0.05$. B: Variations of inter-annual local SST anomaly, average Mg/Ca anomaly and ONI for the 1965-2007 period. Positive anomalies in the ONI record (red areas) represent El Nino periods and negative anomalies (blue areas) are characteristic of La Nina periods. Note: the ONI representation takes into account the 4-month lag discussed in the text.**

Mg/Ca anomalies in *S. durum* from the Ricaudy Reef are able to record the extent of the regional climatic variability in the Pacific (Figure VI-9B). In particular, the majority of the La Nina periods (i.e. negative ONI values associated with higher SST in New Caledonia) appear clearly as positive Mg/Ca anomalies. The El Nino periods (i.e. positive ONI and lower SST), however, are less visible in the *S. durum* record. Specifically, the 1982-83 and

1997-98 strong El Nino events (Caviedes, 1984; McPhaden, 1999) are missing from the Mg/Ca anomalies (Figure VI-9B). It has to be noted though, that these events resulted in only very slight decreases in the local SST near the Ricaudy Reef.

VI-4.e Mg/Ca in rhodoliths vs. Sr/Ca in corals

It is only recently that coralline red algae have been assessed as high-resolution archives of the environment (e.g. Kamenos et al., 2008; Hetzinger et al., 2009). The essential part of these studies focused on high-latitudes species where the reliability of the environmental reconstruction can almost exclusively be compared to the ones of bivalve molluscs that are well-known to present adverse limitations for these types of study due to an ontogenic effect as they grow (Wanamaker et al., 2011). One of the mostly used and accurate tools in high-resolution palaeo-environmental studies is schleractinian corals (e.g. Corrège, 2006) that are, however, mostly limited to tropical regions. The comparison between coralline red algae and corals for high-resolution temperature reconstruction will enable further assessment of the reliability and potential of coralline red algae for palaeo-temperature reconstructions.

A high-resolution Sr/Ca record from a *Porites sp.* coral has been generated from the Ricaudy Reef and covers 17 years of SST variations from 1975 to 1992 (Montaggioni et al., 2006). The correlation between these two variables is strong (r=-0.72). The SST relationships obtained from the Sr/Ca variations of the *Porites sp.* coral and the average Mg/Ca variations in the *S. durum* rhodoliths are in good agreement at monthly resolution and lead to highly significant correlation coefficients (r=-0.79 and r=0.87, respectively for the coral and rhodolith records, respectively – Figure VI-10). This suggests that the high-resolution Mg/Ca reconstruction of SST from *S. durum* rhodoliths is as reliable as the Sr/Ca reconstruction from a *Porites sp.* coral from the same site. It has to be noted that the correlation associated with the average rhodolith Mg/Ca even exceeds the one of coral Sr/Ca for the 1975-1992 period, however, if the individual rhodolith records are considered, The Mg/Ca-SST correlations are slightly lower than the ones of the Sr/Ca-SST of a single coral colony. This indicates that the Mg/Ca variations in a single rhodolith branch may be more affected by factors other than SST than the Sr/Ca of a single coral colony. Averaging the Mg/Ca records of rhodoliths permits removal of most of the variability factors and achieve better SST reconstructions. Similar conclusions can be drown from the inter-annual variations of Mg/Ca in *S. durum* rhodoliths and Sr/Ca in *Porites sp.* coral against local SST (Table VI-3), with a slightly better SST reconstruction from the average rhodolith Mg/Ca.

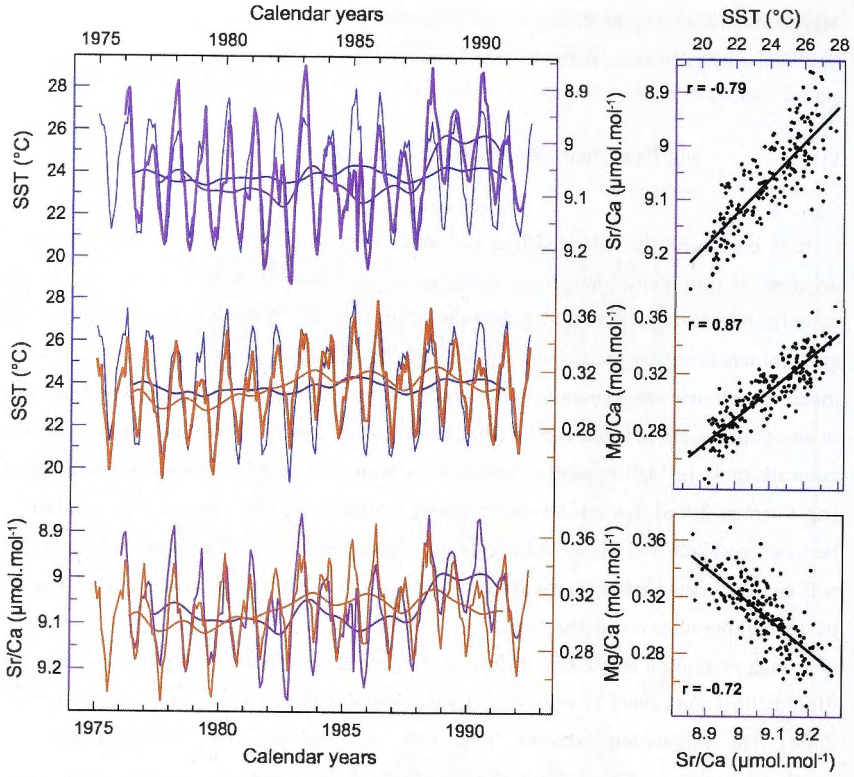

Figure VI-10 Left, top 2 plots: Sr/Ca from *Porites* sp. and Mg/Ca from *S. durum* (purple and orange lines, respectively) compared to the monthly and inter annual variations of local SST (blue lines) over the same period. Bottom plot: Monthly variations of the Sr/Ca record from a *Porites* sp. coral (purple line – Montaggioni et al., 2006) compared against the average Mg/Ca record from the *S. durum* rhodoliths (orange line – this study) over the 1975-1992 period. Right: Scattered plots of the relationships between monthly data of the above-mentioned parameters. Corresponding linear regression lines (black lines) and 95% confidence intervals (shaded areas) are displayed as well as Pearson's correlation coefficients (r); p<0.001.

r		SST	Coral Sr/Ca	Rhodolith Mg/Ca
SST	Monthly		-0.52	0.62
Coral Sr/Ca		-0.79		-0.28
Rhodolith Mg/Ca		0.87	-0.72	Inter-annual

Table VI-3 Cross correlation matrix between the records of Sr/Ca in *Porites* sp. coral (Montaggioni et al., 2006), average Mg/Ca in *S. durum* (this study) and the local SST at the monthly (p<0.001) and inter annual (p<0.05) resolutions;.

VI-5 Conclusion

High-resolution trace elements records in *S. durum* tropical rhodoliths were accurately measured using LA-ICPMS. Records from different rhodolith branches all show consistent average absolute values and a similar range of variation for each trace element.

Mg/Ca concentration slightly exceeds most of the previously reported values for other coralline red algae species, likely resulting from higher living temperatures. It also appears that a species-specific effect may be crucial in the incorporation of Mg in *S. durum*. Sr/Ca concentrations are similar to those previously reported, suggesting a common mode of Sr incorporation shared between different coralline red algae species. It is the first time Li/Ca concentrations are reported in coralline red algae and the range of values is within previous reports for other calcareous organisms.

Trace elements variations over the 1963-2008 period display significant cross-correlations between every branch, however, a non-systematic variability is observed. Mg/Ca is the most reproducible of the analysed trace elements, indicating a lesser effect of non-environmental factors on its variations in *S. durum* rhodoliths.

The average records of Mg/Ca, Sr/Ca and Li/Ca are significantly correlated to the local SST at both monthly and inter-annual timescales. Mg/Ca variations show the best fit with local SST, confirming previous suggestions on the preferential use of Mg/Ca over other trace elements for SST reconstructions. Sr/Ca and Li/Ca are thought to primarily reflect the variations in Mg incorporation into the rhodoliths rather than being directly influenced by the SST.

S. durum rhodoliths are able to record the regional climate pattern as shown by the significant correlation between inter-annual Mg/Ca anomalies and the ONI over the entire studied period.

A comparison of Mg/Ca variations in *S. durum* with Sr/Ca variations in a *Porites sp.* coral from the same site suggests that coralline red algae have the potential to be a proxy as reliable as corals in terms of SST reconstruction.

References

Adey, W., H., MacIntyre, I., G., 1973. Crustose Coralline Algae: A Re-evaluation in the Geological Sciences. *Geological Society of America Bulletin* **84**, 883-904.

Alexandersson, T., 1974. Carbonate cementation in coralline algal nodules in the Skagerrak, North Sea; biochemical precipitation in undersaturated waters. *Journal of Sedimentary Research* **44**(1), 7-26.

Ambatsian, P., Fernex, F., Bernat, M., Parron, C., Lecolle, J., 1997. High metal inputs to closed seas: the New Caledonian lagoon. *Journal of Geochemical Exploration* **59**(1), 59-74.

Baltzer, F., Trescases, J.J., 1971. Erosion, transport et sédimentation liés aux cyclones tropicaux dans les massifs d'ultrabasites de Nouvelle-Calédonie. *Cahiers ORSTOM Série Géologie III* **2**, 221-244.

Basso, D., Nalin, R., Nelson, C., S, 2009. Shallow-water *Sporolithon* rhodoliths from North Island (New Zealand). *Palaios* **24**, 92-103.

Beck, J.W., Edwards, R.L., Ito, E., Taylor, F.W., Recy, J., Rougerie, F., Joannot, P., Henin, C., 1992. Sea-surface temperature from coral skeletal strontium/calcium ratios. *Science* **257**(5070), 644-647.

Bilan, M.I., Usov, A.I., 2001. Polysaccharides of calcareous algae and their effect on the calcification process. *Russian Journal of Bioorganic Chemistry* **27**(1), 2-16.

Blake, C., Maggs, C.A., 2003. Comparative growth rates and internal banding periodicity of maerl species (Corallinales, Rhodophyta) from northern Europe. *Phycologia* **42**(6), 606-612.

Böhm, L., Schramm, W., Rabsch, U., 1978. Ecological and physiological aspects of some coralline algae from the western Baltic. Calcium uptake and skeleton formation in *Phymatolithon calcareum*. *Kieler Meeresforschung* **4**, 282-288.

Bosence, D., W. J., 1983a. Description and Classification of Rhodoliths (Rhodoids, Rhodolites), in: Peryt, T.M. (Ed.), Coated Grains. Springer-Verlag, Berlin, pp. 217-224.

Bosence, D., W., J., 1983b. The Occurence and Ecology of Recent Rhodoliths - A Review, in: Peryt, T.M. (Ed.), Coated Grains. Springer-Verlag Berlin, pp. 225-242.

Brauer, A., Endres, C., Günter, C., Litt, T., Stebich, M., Negendank, J.F.W., 1999. High resolution sediment and vegetation responses to Younger Dryas climate change in varved lake sediments from Meerfelder Maar, Germany. *Quaternary Science Reviews* **18**(3), 321-329.

Bryan, S.P., Marchitto, T.M., 2008. Mg/Ca-temperature proxy in benthic foraminifera: New calibrations from the Florida Straits and a hypothesis regarding Mg/Li. *Paleoceanography* **23**(2), PA2220.

Burdett, H., Kamenos, N.A., Law, A., 2010. Using coralline algae to understand historic marine cloud cover. *Palaeogeography, Palaeoclimatology, Palaeoecology* **302**, 65-70.

Carpenter, S.J., Lohmann, K.C., 1992. Sr/Mg ratios of modern marine calcite: Empirical indicators of ocean chemistry and precipitation rate. *Geochimica et Cosmochimica Acta* **56**(5), 1837-1849.

Caviedes, C.N., 1984. El Nino 1982-83. *Geographical Review* **74**(3), 267-290.

Chan, P., Halfar, J., Williams, B., Hetzinger, S., Steneck, R., Zack, T., Jacob, D.E., 2011. Freshening of the Alaska Coastal Current recorded by coralline algal Ba/Ca ratios. *Journal of Geophysical Research* **116**(G1), G01032.

Charles, C.D., Lynch-Stieglitz, J., Ninnemann, U.S., Fairbanks, R.G., 1996. Climate connections between the hemisphere revealed by deep sea sediment core/ice core correlations. *Earth and Planetary Science Letters* **142**(1), 19-27.

Chave, K.E., 1954. Aspects of the biogeochemistry of magnesium 1. Calcareous marine organisms. *The Journal of Geology* **62**(3), 266-283.

Chave, K., E., Wheeler, B., D., Jr., 1965. Mineralogic changes during growth in the red alga, *Clathromorphum compactum*. *Science* **147**, 621.

Cobb, K.M., Charles, C.D., Cheng, H., Edwards, R.L., 2003. El Nino/Southern Oscillation and

tropical Pacific climate during the last millennium. *Nature* **424**, 271-276.

Corrège, T., 2006. Sea surface temperature and salinity reconstruction from coral geochemical tracers. *Palaeogeography, Palaeoclimatology, Palaeoecology* **232**(2), 408-428.

Corrège, T., Delcroix, T., Récy, J., Beck, W., Cabioch, G., 2000. Evidence for stronger El Nino-Southern Oscillation (ENSO) events. *Paleoceanography* **15**(4), 465-470.

Cullen, H., Hemming, S., Hemming, G., Brown, F., Guilderson, T., Sirocko, F., 2000. Climate change and the collapse of the Akkadian empire: Evidence from the deep sea. *Geology* **28**(4), 379-382.

Dandonneau, Y., Debenay, J., Dugas, F., Fourmanoir, P., Magnier, Y., Rougerie, F., 1981. Le lagon de la Grande Terre, Présentation d'ensemble, Sédimentologie et hydrologie du sud-ouest. *Atlas de Nouvelle-Calédonie et dépendances. ORSTOM, Paris*, 21-24.

Dansgaard, W., Johnsen, S., Clausen, H., Dahl-Jensen, D., Gundestrup, N., Hammer, C., Hvidberg, C., Steffensen, J., Sveinbjörnsdottir, A., Jouzel, J., 1993. Evidence for general instability of past climate from a 250-kyr ice-core record. *Nature* **364**, 218-220.

De Deckker, P., Corrège, T., Head, J., 1991. Late Pleistocene record of cyclic eolian activity from tropical Australia suggesting the Younger Dryas is not an unusual climatic event. *Geology* **19**(6), 602-605.

de Villiers, S., 1999. Seawater strontium and Sr/Ca variability in the Atlantic and Pacific oceans. *Earth and Planetary Science Letters* **171**(4), 623-634.

de Villiers, S., Greaves, M., Elderfield, H., 2002. An intensity ratio calibration method for the accurate determination of Mg/Ca and Sr/Ca of marine carbonates by ICP-AES. *Geochemistry, Geophysics, Geosystems* **3**(1), 1001.

Delaney, M., Popp, B., Lepzelter, C., Anderson, T., 1989. Lithium-to-calcium ratios in modern, Cenozoic, and Paleozoic articulate brachiopod shells. *Paleoceanography* **4**(6), 681-691.

Delaney, M.L., Boyle, E.A., 1986. Lithium in foraminiferal shells: implications for high-temperature hydrothermal circulation fluxes and oceanic crustal generation rates. *Earth and Planetary Science Letters* **80**(1-2), 91-105.

Delcroix, T., Lenormand, O., 1997. ENSO signals in the vicinity of New Caledonia, South Western Pacific. *Oceanologica acta* **20**(3), 481-491.

Dunbar, R.B., Wellington, G.M., Colgan, M.W., Glynn, P.W., 1994. Eastern Pacific sea surface temperature since 1600 AD: Thed18O record of climate variability in Galapagos corals. *Paleoceanography* **9**(2), 291-315.

Eggins, S., De Deckker, P., Marshall, J., 2003. Mg/Ca variation in planktonic foraminifera tests: implications for reconstructing palaeo-seawater temperature and habitat migration. *Earth and Planetary Science Letters* **212**(3), 291-306.

Fairbanks, R., Evans, M., Rubenstone, J., Mortlock, R., Broad, K., Moore, M., Charles, C., 1997. Evaluating climate indices and their geochemical proxies measured in corals. *Coral Reefs* **16**(5), 93-100.

Fernandez, J.M., Ouillon, S., Chevillon, C., Douillet, P., Fichez, R., Gendre, R.L., 2006. A combined modelling and geochemical study of the fate of terrigenous inputs from mixed natural and mining sources in a coral reef lagoon (New Caledonia). *Marine pollution bulletin* **52**(3), 320-331.

Foster, M., S., 2001. Rhodoliths: Between rocks and soft places. *Journal of Phycology* **37**, 659-667.

Frantz, B.R., Foster, M.S., Riosmena-Rodrìguez, R., 2005. *Clathromorphum nereostratum* (Corallinales, Rhodophyta): The oldest alga? *Journal of Phycology* **41**(4), 770-773.

Goldberg, N., Heine, J., N., 2008. Age estimates of *Sporolithon durum* (Corallinales, Rhodophyta) from Rottnest Island, Western Australia, based on radiocarbon-dating methods. *Journal of the Royal Society of Western Australia* **91**, 27-30.

Grenz, C., Denis, L., Pringault, O., Fichez, R., 2010. Spatial and seasonal variability of sediment oxygen consumption and nutrient fluxes at the sediment water interface in a sub-tropical lagoon (New Caledonia). *Marine pollution bulletin* **61**(7-12), 399-412.

Halfar, J., Steneck, R., S., Joachimski, M., Kronz, A., Wanamaker Jr., A., D., 2008. Coralline red

algae as high-resolution climate recorders. *Geology* **36**(6), 463-466.

Halfar, J., Steneck, R., S., Schöne, B., R., Moore, G., W., K., Joachimski, M., Kronz, A., Fietzke, J., Estes, J., 2007. Coralline alga reveals first marine record of subarctic North Pacific climate change. *Geophysical Research Letters* **34**, L07702.

Halfar, J., Williams, B., Hetzinger, S., Steneck, R.S., Lebednik, P., Winsborough, C., Omar, A., Chan, P., Wanamaker, A.D., 2011. 225 years of Bering Sea climate and ecosystem dynamics revealed by coralline algal growth-increment widths. *Geology* **39**(6), 579-582.

Halfar, J., Zack, T., Kronz, A., Zachos, J., C., 2000. Growth and high-resolution paleoenvironmental signals of rhodoliths (coralline red algae): A new biogenic archive. *Journal of Geophysical Research* **105**(C9), 22,107-122,116.

Hall, J.M., Chan, L.H., 2004. Li/Ca in multiple species of benthic and planktonic foraminifera: thermocline, latitudinal, and glacial-interglacial variation. *Geochimica et Cosmochimica Acta* **68**(3), 529-545.

Hathorne, E., Felis, T., Suzuki, A., Kawahata, H., 2009. Lithium content of the aragonitic skeletons of massive Porites corals: a new tool to reconstruct tropical sea surface temperatures?, American Geophysical Union, Fall Meeting 2009, abstract #PP34B-05.

Herz, N., Dean, N.E., 1986. Stable isotopes and archaeological geology: the Carrara marble, northern Italy. *Applied geochemistry* **1**(1), 139-151.

Hetzinger, S., Halfar, J., Kronz, A., Steneck, R., Adey, W., H., Lebednik, P., A., Schöne, B., R., 2009. High-resolution Mg/Ca ratios in a coralline red alga as a proxy for Bering Sea temperature variations from 1902 to 1967. *Palaios* **24**, 406-412.

Hetzinger, S., Halfar, J., Zack, T., Gamboa, G., Jacob, D.E., Kunz, B.E., Kronz, A., Adey, W., Lebednik, P.A., Steneck, R.S., 2011. High-resolution analysis of trace elements in crustose coralline algae from the North Atlantic and North Pacific by laser ablation ICP-MS. *Palaeogeography, Palaeoclimatology, Palaeoecology* **302**(1-2), 81-94.

IPCC, 2007. Fourth assessment report (AR4), climate change 2007: the physical science basis. Contribution of Working Group I to the Fourth Assessment Report of the Intergovernmental Panel on Climate Change, Cambridge, United Kingdom and New York, NY, USA. 996 pp.

Jouon, A., Douillet, P., Ouillon, S., Fraunié, P., 2006. Calculations of hydrodynamic time parameters in a semi-opened coastal zone using a 3D hydrodynamic model. *Continental Shelf Research* **26**(12-13), 1395-1415.

Kamenos, N., A., Cusack, M., Moore, P., G., 2008. Coralline algae are global palaeothermometers with bi-weekly resolution. *Geochimica et Cosmochimica Acta* **72**, 771-779.

Kamenos, N.A., Law, A., 2010. Temperature controls on coralline algal skeletal growth. *Journal of Phycology* **46**(2), 331-335.

Kinsman, D.J.J., Holland, H.D., 1969. The co-precipitation of cations with CaCO3--IV. The co-precipitation of Sr2+ with aragonite between 16* and 96* C. *Geochimica et Cosmochimica Acta* **33**(1), 1-17.

Klein, R.T., Lohmann, K.C., Thayer, C.W., 1996. Bivalve skeletons record sea-surface temperature and d18O via Mg/Ca and 18O/16O ratios. *Geology* **24**(5), 415-418.

Labrosse, P., Fichez, R., Farman, R., Adams, T., 2000. New Caledonia, in: Sheppard, C.R.C.E. (Ed.), Seas at the millennium: an environmental evaluation, pp. 723-736.

Lara, A., Villalba, R., 1993. A 3620-year temperature record from Fitzroya cupressoides tree rings in southern South America. *Science* **260**, 1104-1106.

Le Bec, N., Juillet-Leclerc, A., Corrège, T., Blamart, D., Delcroix, T., 2000. A coral δ18O record of ENSO driven sea surface salinity variability in Fiji (south-western tropical Pacific). *Geophysical Research Letters* **27**(23), 3897-3900.

Littler, M.M., Littler, D.S., Dennis Hanisak, M., 1991. Deep-water rhodolith distribution, productivity, and growth history at sites of formation and subsequent degradation. *Journal of Experimental Marine Biology and Ecology* **150**(2), 163-182.

Longerich, H.P., Jackson, S.E., G¸nther, D., 1996. Laser ablation inductively coupled plasma

mass spectrometric transient signal data acquisition and analyte concentration calculation. *Journal of Analytical Atomic Spectrometry* **11**(9), 899-904.

Marriott, C.S., Henderson, G.M., Belshaw, N.S., Tudhope, A.W., 2004a. Temperature dependence of 7Li, 44Ca and Li/Ca during growth of calcium carbonate. *Earth and Planetary Science Letters* **222**(2), 615-624.

Marriott, C.S., Henderson, G.M., Crompton, R., Staubwasser, M., Shaw, S., 2004b. Effect of mineralogy, salinity, and temperature on Li/Ca and Li isotope composition of calcium carbonate. *Chemical geology* **212**(1), 5-15.

McDermott, F., 2004. Palaeo-climate reconstruction from stable isotope variations in speleothems: a review. *Quaternary Science Reviews* **23**(7-8), 901-918.

McPhaden, M.J., 1999. Genesis and evolution of the 1997-98 El Nino. *Science* **283**, 950.

Moberly Jr, R., 1968. Composition of Magnesian Calcites of Algae and Pelecypods by Electron Microprobe analysis. *Sedimentology* **11**(1 2), 61-82.

Montaggioni, L.F., Le Cornec, F., Corrège, T., Cabioch, G., 2006. Coral barium/calcium record of mid-Holocene upwelling activity in New Caledonia, South-West Pacific. *Palaeogeography, Palaeoclimatology, Palaeoecology* **237**(2), 436-455.

Montagna, P., McCulloch, M., Mazzoli, C., Silenzi, S., Schiaparelli, S., 2006. Li/Ca ratios in the Mediterranean non-tropical coral Cladocora caespitosa as a potential paleothermometer, Geophysical Research Abstracts, Vol. 8, 03695.

Morellón, M., Valero-Garces, B., Gonzalez-Samperiz, P.I., Vegas-Vilarrubia, T., Rubio, E., Rieradevall, M., Delgado-Huertas, A., Mata, P., Romero, O., Engstrom, D.R., 2011. Climate changes and human activities recorded in the sediments of Lake Estanya (NE Spain) during the Medieval Warm Period and Little Ice Age. *Journal of Paleolimnology* **46** (3), 423-452.

Nicet, J.B., Delcroix, T., 2000. ENSO-Related Precipitation Changes in New Caledonia, Southwestern Tropical Pacific: 1969-98. *Monthly Weather Review* **128**(8), 3001-3006.

Okumura, M., Kitano, Y., 1986. Coprecipitation of alkali metal ions with calcium carbonate. *Geochimica et Cosmochimica Acta* **50**(1), 49-58.

Oomori, T., Kaneshima, H., Maezato, Y., Kitano, Y., 1987. Distribution coefficient of Mg2+ ions between calcite and solution at 10-50 C. *Marine Chemistry* **20**(4), 327-336.

Ouillon, S., Douillet, P., Lefebvre, J.P., Le Gendre, R., Jouon, A., Bonneton, P., Fernandez, J.M., Chevillon, C., 2010. Circulation and suspended sediment transport in a coral reef lagoon: The south-west lagoon of New Caledonia. *Marine pollution bulletin* **61**(7-12), 309-322.

Paillard, D., Labeyrie, L., Yiou, P., 1996. Macintosh program performs time-series analysis. *Eos Transactions AGU* **77**(39), 379.

Petit, J.R., Jouzel, J., Raynaud, D., Barkov, N., Barnola, J., Basile, I., Bender, M., Chappellaz, J., Davis, M., Delaygue, G., 1999. Climate and atmospheric history of the past 420,000 years from the Vostok ice core, Antarctica. *Nature* **399**, 429-436.

Pingitore Jr, N.E., Eastman, M.P., 1986. The coprecipitation of Sr2+ with calcite at 25°C and 1 atm. *Geochimica et Cosmochimica Acta* **50**(10), 2195-2203.

Quinn, T.M., Crowley, T.J., Taylor, F.W., Henin, C., 1998. A multicentury stable isotope record from a New Caledonia coral: Interannual and decadal sea surface temperature variability in the. *Paleoceanography* **13**(4), 412-426.

Ries, J., B., 2006. Mg fractionation in crustose coralline algae: Geochemical, biological, and sedimentological implications of secular variation in the Mg/Ca ratio of seawater. *Geochimica et Cosmochimica Acta* **70**, 891-900.

Ries, J., B., 2009. Review: The effects of secular variation in seawater Mg/Ca on marine biocalcification. *Biogeosciences Discussions* **6**, 7359-7367.

Rimstidt, J.D., Balog, A., Webb, J., 1998. Distribution of trace elements between carbonate minerals and aqueous solutions. *Geochimica et Cosmochimica Acta* **62**(11), 1851-1863.

Rollion-Bard, C., Vigier, N., Meibom, A., Blamart, D., Reynaud, S., Rodolfo-Metalpa, R., Martin, S., Gattuso, J.P., 2009. Effect of environmental conditions and skeletal

ultrastructure on the Li isotopic composition of scleractinian corals. *Earth and Planetary Science Letters* **286**(1), 63-70.

Shao, X., Xu, Y., Yin, Z.Y., Liang, E., Zhu, H., Wang, S., 2010. Climatic implications of a 3585-year tree-ring width chronology from the northeastern Qinghai-Tibetan Plateau. *Quaternary Science Reviews* **29**(17), 2111-2122.

Schöne, B.R., Fiebig, J., Pfeiffer, M., Gleh, R., Hickson, J., Johnson, A.L.A., Dreyer, W., Oschmann, W., 2005. Climate records from a bivalved Methuselah (*Arctica islandica*, Mollusca; Iceland). *Palaeogeography, Palaeoclimatology, Palaeoecology* **228**, 130-148.

Steneck, R.S., 1986. The ecology of coralline algal crusts: convergent patterns and adaptative strategies. *Annual Review of Ecology and Systematics* **17**, 273-303.

Townsend, R.A., Woelkerling, W.J., Harvey, A.S., Borowitzka, M., 1995. An account of the red algal genus *Sporolithon* (Sporolithaceae, Corallinales) in southern Australia. *Australian Systematic Botany* **8**(1), 85-121.

Wada, N., Okazaki, M., Tachikawa, S., 1993. Effects of calcium-binding polysaccharides from calcareous algae on calcium carbonate polymorphs under conditions of double diffusion. *Journal of Crystal Growth* **132**(1-2), 115-121.

Waelbroeck, C., Labeyrie, L., Michel, E., Duplessy, J.C., McManus, J., Lambeck, K., Balbon, E., Labracherie, M., 2002. Sea-level and deep water temperature changes derived from benthic foraminifera isotopic records. *Quaternary Science Reviews* **21**(1-3), 295-305.

Wanamaker Jr, A.D., Hetzinger, S., Halfar, J., 2011. Reconstructing mid-to high-latitude marine climate and ocean variability using bivalves, coralline algae, and marine sediment cores from the Northern Hemisphere. *Palaeogeography, Palaeoclimatology, Palaeoecology* **302**(1-2), 1-9.

Williams, B., Halfar, J., Steneck, R.S., Wortmann, U.G., Hetzinger, S., Adey, W., Lebednik, P., Joachimski, M., 2011. Twentieth century 13 C variability in surface water dissolved inorganic carbon recorded by coralline algae in the northern North Pacific Ocean and the Bering Sea. *Biogeosciences* **8**(1), 165-174.

Wolff, E.W., Barbante, C., Becagli, S., Bigler, M., Boutron, C.F., Castellano, E., De Angelis, M., Federer, U., Fischer, H., Fundel, F., Changes in environment over the last 800,000 years from chemical analysis of the EPICA Dome C ice core. *Quaternary Science Reviews* **29** (1), 285-295.

Womersley, H.B.S., 1996. The marine benthic flora of southern Australia, Part III B: Gracilariales, Rhodymeniales, Corallinales and Bonnemaisoniales. Australian Biological Resources Study, Canberra.

Yu, J., Day, J., Greaves, M., Elderfield, H., 2005. Determination of multiple element/calcium ratios in foraminiferal calcite by quadrupole ICP-MS. *Geochem. Geophys. Geosyst* **6**(10), 1029.

Zhu, Z., Chen, J., Li, D., Ren, S., Liu, F., Li/Ca ratios of ostracod shells at Lake Qinghai, NE Tibetan Plateau, China: a potential temperature indicator. *Environmental Earth Sciences*, 1-8.

CHAPTER VII

A record of mining and industrial activities in New Caledonia based on trace elements in rhodolith-forming coralline red algae

Keywords: CCA, *Sporolithon durum*, laser ablation, metals, pollution

Abstract

We investigate the ability of coralline red algae to record historical mining activities in the southwest region of New Caledonia. From the early 1960s until 1981, industrial nickel mining took place in the Coulée River watershed, drastically modifying the landscape of the area as well as the depositional regime in the adjacent bays. We have used laser ablation inductively coupled plasma mass spectrometry (LA-ICPMS) to generate high-resolution variations of trace metal (Mn/Ca, Fe/Ca, Ni/Ca and Co/Ca) concentrations in three ~45 years old, free-living forms (i.e. rhodoliths) of the coralline red alga *Sporolithon durum* from the Ricaudy Reef in the inner lagoon of New Caledonia. Absolute metal concentrations as well as monthly-resolution trace metal records are quite variable and we identified a significant role of the algae in the uptake of Fe, as well as an strong association of Co with the organic component of the rhodolith, to potentially explain some of this variability. In spite of this, all three rhodoliths show elevated Mn/Ca, Fe/Ca and Ni/Ca concentrations during the industrial mining period (Mn/Ca: 31-86 $\mu mol.mol^{-1}$; Fe/Ca: 0.3-0.8 $mmol.mol^{-1}$; Ni/Ca: 6-10 $\mu mol.mol^{-1}$ – 1963-1977) relative to their respective present-day values (Mn/Ca: 14-30 $\mu mol.mol^{-1}$; Fe/Ca: 0.1-0.3 $mmol.mol^{-1}$; Ni/Ca: 4-6 $\mu mol.mol^{-1}$ – 1993-2008). Mn/Ca and Fe/Ca concentrations track the intensity of mining whereas Ni/Ca concentrations appear more sensitive to the type of material being targeted during two separate stages of mining activity. Mn/Ca, Fe/Ca and Ni/Ca decrease rapidly following the cessation of mining in 1981, although, the equivalent of current values were not reached until more than 10 years after that date. Co/Ca variations do not correlate with mining activity but rather increase steadily through the recorded period (from 0.1 to 3 $\mu mol.mol^{-1}$). We attribute this to the expansion of the city of Nouméa and of industrial activities linked to the nickel refining and smelting over the past half century. Our results also suggest that the local, inter-annual rainfall variability may have influenced the metal concentrations recorded in the rhodoliths during the period of intense mining activity.

VII-1 Introduction

Rhodoliths are free-living forms of coralline red algae that are globally distributed in the shallow-water oceans from the tropics to the poles (Foster, 2001). Coralline red algae play a significant role as carbonate reef builders (e.g. Freiwald and Heinrich, 1994; Steneck et al., 2003). They secrete a cement of high-Mg calcite at a relatively slow growth rate varying from 0.015 to more than 1 $mm.y^{-1}$ (Foster, 2001), depending on the species and environmental factors. Their slow growth rates, combined with the thick crusts that they generally form (often >10 cm, see e.g. Bosence, 1983b), offer the potential to retrieve specimens that have grown continuously for decades to centuries (e.g. Frantz et al., 2005; Halfar et al., 2007).

Coralline red algae have attracted the interest of the palaeoclimate community due to their potential to act as climate archives. Variations in growth rates and geochemical composition of their high-Mg calcite skeleton have been observed to relate to various environmental parameters. Mg/Ca variations in different species have been shown to correlate with *in situ* and regional sea surface temperature (SST) (e.g. Halfar et al., 2000; Kamenos et al.,2008; Hetzinger et al., 2009; 2011), through the incorporation of magnesium into the calcite lattice (Kamenos et al., 2009). $\delta^{18}O$, Sr/Ca and U/Ca variations have also been linked to oceanic temperature (Halfar et al., 2000; 2007; 2008; Kamenos et al., 2008; Hetzinger et al., 2011), while Ba/Ca variations were recently linked to salinity changes in the Northwest Pacific (Chan et al., 2011). Changing oceanic conditions and circulation have also been shown to be recorded in coralline red algae through the variations of $\delta^{18}O$, $\delta^{13}C$ and $\Delta^{14}C$ (Halfar et al., 2007; Williams et al., 2011; Frantz et al., 2000). Growth rate and calcification pattern studies also led to several environmental reconstructions, including temperature variations and cloud cover (e.g. Halfar et al., 2010; 2011; Burdett et al., 2011).

Anthropogenic input of carbon, nutrients and toxins into the oceans *via* terrestrial runoff is one of the major environmental concerns for the sustainability of the marine biota. Monitoring studies have used various types of marine organisms to determine their sensitivity to anthropogenic effects (e.g. Fichez et al., 2005; Silva et al., 2006). However, only a few of these "biomonitors" can record such effects with high resolution (subannual) over relatively long periods of time (several decades to centuries). Corals are the most widely used archives of environmental pollution in the tropical waters (e.g. Fallon et al., 2002; McCulloch et al., 2003; David, 2003; Alibert et al., 2003). Adding coralline red algae to the list of potential high-resolution bio-indicators of anthropogenic impact could extend the geographical boundaries of which such studies could be conducted to the extra-

tropical and high-latitude regions, as well as broaden the use of coralline red algae as a high-resolution archive of environmental conditions.

In this study, we analysed three rhodolith specimens of the species *Sporolithon durum* to assess their ability to record historical industrial mining activities in southwest New Caledonia. A record of over 45 years of trace metals (Mn/Ca, Fe/Ca, Ni/Ca and Co/Ca) variations was obtained at high-resolution along five rhodolith branches using laser ablation inductively coupled plasma (LA-ICPMS) technique. Reproducibility of the metal records along five different rhodolith branches is assessed and pathways leading to the incorporation of these metals into the rhodolith structure are also investigated.

VII-2 Study site and associated mining activities

New Caledonia is located in the South West Pacific, near the tropic of Capricorn, about 1500 km east of Australia (Figure VII-1). The main island is ringed by the world's second largest barrier reef. It encloses a lagoon of ~23,400 km^2 and up to 50 m deep (Labrosse et al., 2000). The Ricaudy Reef is adjacent to one of the most populated area of Nouméa, the capital city of the main island and is located at the southern end of Sainte Marie Bay (Figure VII-1). An approximately 3-m deep, 500-m wide channel connects the Sainte Marie Bay to the Boulari Bay, which is under the direct influence of terrigenous input transported by the Coulée River (as shown by Fernandez et al., 2006). Fernandez et al. (2006) demonstrated that, as a consequence of its direct connection to the Boulari Bay, the Sainte Marie Bay receives a significant input of material from the Coulée River. Discharge from the Coulée River is closely linked to seasonal variations in local rainfall and displays a torrential-type of hydrological regime. During dry periods, the Coulée River has reduced discharge (1-3 $m^3.s^{-1}$) and carries a minimal sediment load, whereas during intense rainfall events, discharge values can be more than a hundred times higher (e.g. ~850 $m^3.s^{-1}$ during cyclone Erica in 2003; Alric, 2009) and river waters are then loaded with sediment eroded from the catchment (Fernandez et al., 2006). The Coulée River basin rises up to about 500 m above sea level (Alric, 2009) and the steep slopes of the upper watershed have promoted the intense weathering of the silica- and magnesium-rich peridotite bedrock and the development Ni-rich laterite and saprolite ore deposits (Trescases, 1975). Erosion of these weathered profiles results in the transport of particles with high transition metal (Ni, Co, Cr, Fe, Mn) concentrations into the lagoon.

Ni-ore extraction is the main economic resource in New Caledonia, which ranks as the 3rd largest Ni producer in the world. In addition to Ni-ores, mining activities also focus on Co, Cr and Mn extractions using open-cast mining methods that involve an initial

deforestation of the extraction site, followed by the removal of the surficial layers of the regolith before reaching the exploitable saprolite and enriched laterite profiles. This leads to drastic changes in the natural landscape and leaves the mined sites exposed to the direct influence of erosion and weathering (Labrosse, 2000; Fernandez et al., 2006).

Mining in the Coulée River watershed started at the beginning of the 20th century with a relatively small scale Ni-extraction period from 1904 to 1965 during which ~64,000 tons of Ni were produced – P. Maurizot, *pers. comm.*). Large-scale industrial mining followed, and resulted in the extraction of more than five times the pre-mechanisation production of Ni (~362,000 tons) between 1966 and 1980. Mining activities in the Coulée region ceased in 1981 and since that time, despite attempts at landscape rehabilitation, significant erosion and weathering of the original mining sites have continued to supply silica- and metal-enriched material to the Coulée River (e.g. Fernandez et al., 2006).

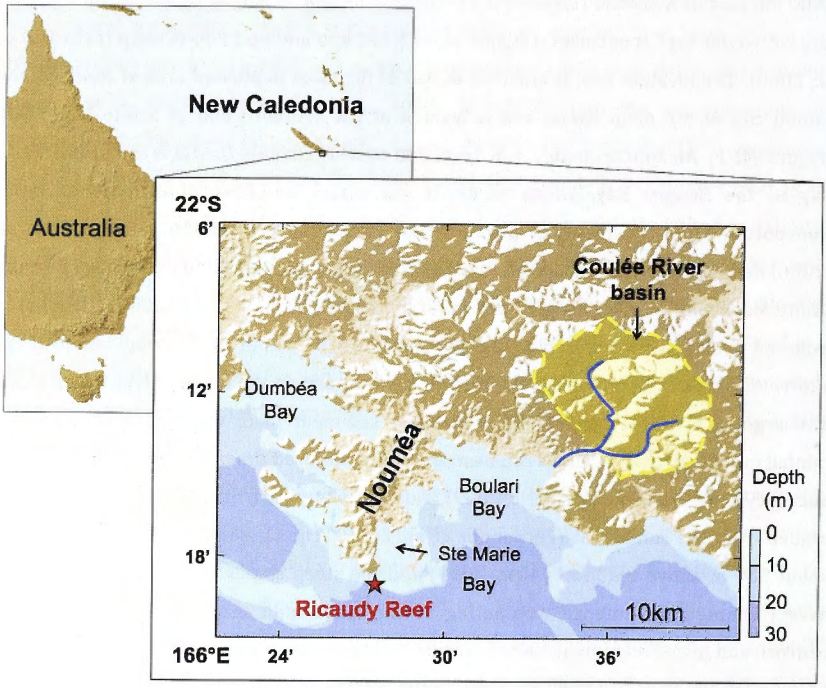

Figure VII-1 Map of the studied area showing the Ricaudy Reef (red star) in New Caledonia, offshore the city of Nouméa and the extent of the Coulée River basin (yellow-shaded area).

VII-3 Material and methods

VII-3.a Rhodolith collection and samples studied

Three rhodolith specimens have been the subjects of detailed study. These rhodoliths, formed by the coralline red algal species *Sporolithon durum* (Sporolithaceae family), were collected live in waters between 4 and 5 m deep by SCUBA divers on the edge of the Ricaudy Reef (22°18'57"S; 166°27'26"E), New Caledonia, in October 2009 (rhodolith labelled as BSA) and February 2011 (rhodoliths labelled as MSA and SSA). *S. durum* is the most abundant species in this low-slope, moderate-energy environment and reach concentrations of more than 50 individuals per square meter, often entirely covering the substrate.

The rhodoliths collected for analysis are of spheroidal shape and are larger than the average rhodolith size at the site. The lengths of their long axes are, respectively, 8.1 cm, 8.5 cm and 7.4 cm for the BSA, MSA and SSA specimens. All three rhodoliths present a dense branching structure (degree IV in the classification of Bosence, 1983a) determined from the thick and very dense visible branches, which is representative of most *S. durum* at this site (Figure VII-2).

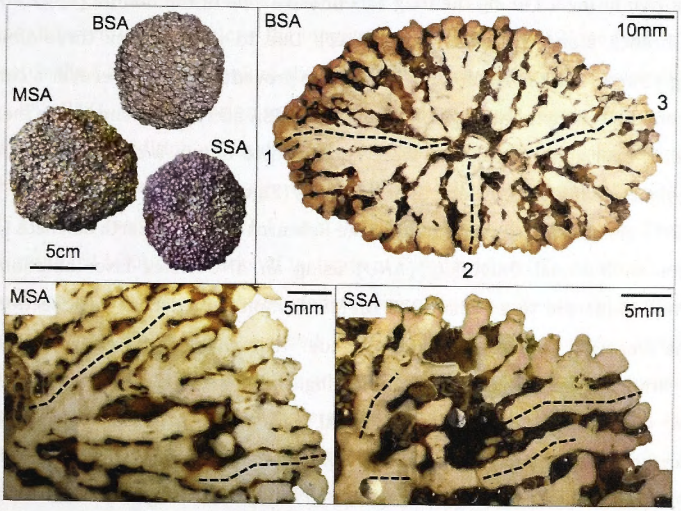

Figure VII-2 Photographs of the rhodolith samples studied. Top-left: Whole rhodoliths after collection from the Ricaudy Reef. Note the high branch density. Top-right and bottom: photos of transverse sections across the BSA, MSA and SSA rhodoliths. The dashed lines display the laser ablation tracks. The dark colouration surrounding the branches represents empty space or organic stains that are not derived from the coralline red algae.

The three rhodoliths specimens were oven dried (40°C) before being set in hard resin (araldite) blocks and sectioned along their long axes using a diamond rock saw. This procedure preserves the dense and fragile branch network during the sawing. Polished thick sections (2-5 mm-thick) were then cut parallel to each rhodolith' long axis-short axis plane, so as to obtain transverse branch sections for analysis (Figure VII-2).

The transverse sections reveal each rhodolith to be monospecific and to have grown continuously over its living periods (as evidenced by the absence of hiatuses or signs of growth discontinuity along branches such as the presence of green algae bands. Growth increments can be clearly seen with the naked eye as well as on high-definition digital images of the samples. Reproductive structures (conceptacles) could not be seen by either method and are considered not to be present in any of the studied rhodoliths.

Prior to laser ablation and solution ICPMS analyses, the thick sections were cleaned of any material that had been redeposited in the pores of the skeleton structure during the cutting process by ultrasonic probe in milli-Q water. The sections were then dried in an oven at 40°C overnight.

VII-3.b LA-ICPMS

Three separate, continuous branches were selected for detailed analysis on the BSA specimen: two branches along the long axis on each side of the nodule (BSA1 and BSA3) and one branch along the short axis (BSA2). Due to the complex three-dimensional branching structure of the rhodoliths, the cutting procedure did not recover a continuous branch from the centre to the edge of either of the MSA and SSA specimens. In these cases, two parallel, overlapping branches were combined to obtain a complete record of the coralline algae's living period along their long axes (Figure VII-2).

LA-ICPMS analyses were carried out at the Research School of Earth Sciences (RSES) of the Australian National University (ANU) using an ANU Helex laser ablation system (λ=193 nm) connected to a Varian 820 ICPMS. Complete or partial thick sections of the rhodoliths were placed into the sample holder that enabled the entire length of the targeted branches to be measured in a single analytical run. The same analytical procedure was used for every run. Analytical tracks were pre-cleaned by ablating the sample surface prior to analysis in order to eliminate any potential surface contamination effect. A 42-µm-diameter laser spot was scanned at 5 $\mu m.s^{-1}$ along the branch main axis of growth to analyse the sample surface with energy of 5 $J.cm^{-2}$, at a repetition rate of 10 Hz. This ablation procedure produces a trough of <20 µm-deep in the rhodolith's skeleton. The calcite material is ablated in a helium atmosphere and transferred via a combined He-Ar gas flow to the ICPMS (Eggins et al., 1998). The isotopes ^{24}Mg, ^{25}Mg, ^{43}Ca, ^{55}Mn, ^{57}Fe,

^{59}Co and ^{60}Ni were measured among others, resulting in a total integration time of about 1 s per measurement cycle. The NIST SRM 612 standard glass was used for external calibration of trace metals. Calculation of detection limits (3σ of the background) for each elements were based on the NIST SRM 612 GeoReM preferred concentration values (after Jochum et al., 2011) and were typically: Ca=0.02 %, Mn=0.5 $\mu g.g^{-1}$, Fe=5 $\mu g.g^{-1}$, Co= 0.3 $\mu g.g^{-1}$ and Ni=1 $\mu g.g^{-1}$. The data reduction method followed the one described in Longerich et al. (1996), using ^{43}Ca as the reference isotope to normalise for varying ablation yield due to the variable porosity of the sample surface. Results of the LA-ICPMS analysis are presented element/Ca molar ratios (e.g. Mn/Ca, Fe/Ca – $\mu mol.mol^{-1}$). Backgrounds with laser off and external standards were analysed before and after every rhodolith branch scan and used to correct for any instrument drift during the analytical run. The combination of the laser ablation speed and the ICPMS integration time provided a resolution of ~5 µm per data point that was averaged to ~30 µm per data point, which corresponds to monthly to sub-monthly resolution in the rhodoliths, considering an average extension rate of 0.6 $mm.yr^{-1}$ for the specimens analysed (see below – section VII-3.d).

VII-3.c Solution ICPMS

Approximately 1 mg samples of calcite powder was hand drilled from the rhodolith skeleton at different locations along the long axis of the BSA and MSA nodule, in order to closely match the LA-ICPMS sampling strategy. Calcite powder samples were diluted (10 times) in 2% HNO_3 solution prior to solution ICPMS analysis. Samples were weighed before and after the addition of the dilute HNO_3 for precise determination of the dilution factor. The same elements were analysed and ICPMS dwell times settings were used as for LA-ICPMS analyses (section VII-3.b). Four standard solutions, prepared from "AccuTrace" reference standard solutions (National Institute of Standards and Technology) containing known concentrations of each analysed element, were used to generate calibration curves. A solution of pure 2% HNO_3 was used as a blank. Three calibration curves were established, before, during and after the analytical run to correct for instrumental drift. Repeats of a single sample and blanks were measured throughout the run to assess the instrument reproducibility and the detection limits for each element. Detection limits (3σ of the blanks, n=6) were as follows: Ca=59 $\mu g.g^{-1}$, Mn=49 $ng.g^{-1}$, Fe=16 $\mu g.g^{-1}$, Ni=85 $ng.g^{-1}$, Co=8 $ng.g^{-1}$. All measured concentrations in the samples were at least 17 times higher than the corresponding detection limit. The analytical reproducibility was estimated by repeat analyses of one sample and found to be 1.8% (Ca), 0.9% (Mn), 3.6% (Fe), 2.8% (Ni) and 3.9% (Co).

VII-3.d Chronology: Radiocarbon and Mg/Ca cycles - annual bands counting

The chronologies on the different analysed branches were established using a combination of radiocarbon dating and an association of seasonal growth band counting and periodic Mg/Ca cycles determination. Both methods gave concordant results (Chapter IV, This thesis) and the latter method has previously been used with success to derive age models for various species of coralline red algae (e.g. Hetzinger et al., 2009; 2011; Brudett et al., 2010; Gamboa et al., 2010). We used an easily identifiable match between overlapping Mg/Ca signals from different branches of the MSA and SSA specimens to construct a single Mg/Ca record for each whole specimen. Radiocarbon dating was carried out using the single stage accelerator mass spectrometer (SSAMS) at RSES, ANU (see Fallon et al., 2010 and Chapter IV, This thesis, for further details). The resulting chronologies for each branch were employed with the data analysis software AnalySeries (Paillard et al., 1996) to convert the LA-ICPMS records to a common temporal scale with monthly resolution.

VII-4 Results

VII-4.a Trace elements records

VII-4.a.1 LA-ICPMS signals

The trace elements concentrations measured by LA-ICPMS for the five rhodolith branches are presented in Figure VII-3. The chronology applied to each branch and used to convert distances along the laser tracks to calendar years is also shown in Figure VII-3. The reproducibility of the profiles was tested by running two parallel tracks under the same experimental conditions along the BSA2 branch (Figure VII-4). A close match is observed for each elemental ratio (Mn/Ca, Fe/Ca, Ni/Ca and Co/Ca) measured on the two parallel tracks ($0.77<r<0.83$; $p<0.0001$), therefore, the record for the BSA2 branch presented in Figure VII-3 represents the average of these two parallel tracks.

Next page:

Figure VII-3 LA-ICPMS records of Mn/Ca, Fe/Ca, Ni/Ca and Co/Ca variations obtained along 5 different branches of 3 individual rhodoliths. Original, raw data have been smoothed with a 6-points average and are represented on the bottom axes of each profile against distance from the outside (most recent) layer of the branches (in mm). The chronology for each branch is also displayed above each plot and permits the correlation of the original distances with any particular year. Note the varying annual growth rates recorded for each profile. The BSA2 record and some parts of the SSA record correspond to the average signal of two parallel tracks (for BSA2) and parts of two overlapping branches (for SSA).

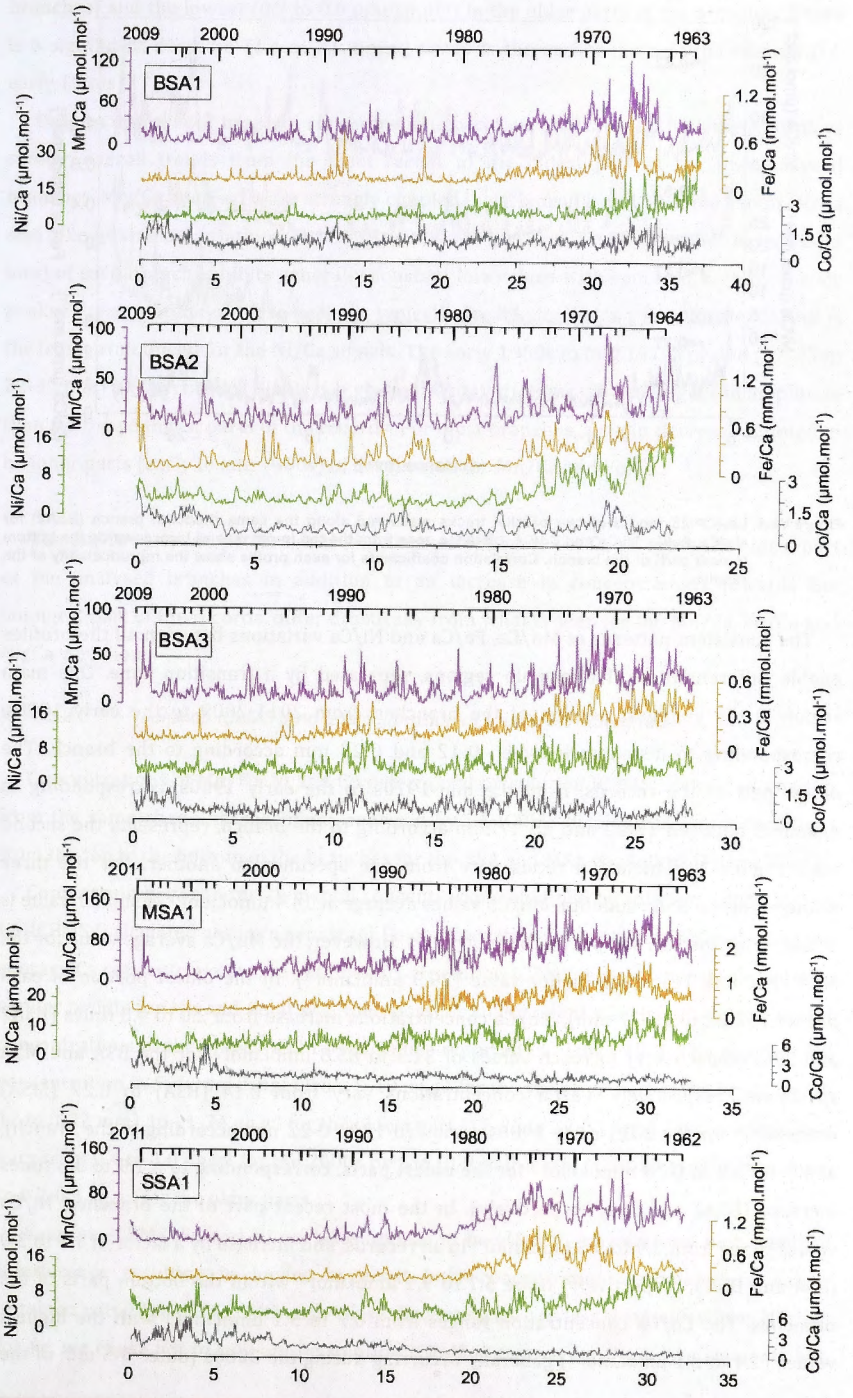
BSA1
2009 2000 1990 1980 1970 1963
Mn/Ca (µmol.mol-1)
Ni/Ca (µmol.mol-1)
Fe/Ca (mmol.mol-1)
Co/Ca (µmol.mol-1)
BSA2
2009 2000 1990 1980 1970 1964
BSA3
2009 2000 1990 1980 1970 1963
MSA1
2011 2000 1990 1980 1970 1963
SSA1
2011 2000 1990 1980 1970 1962

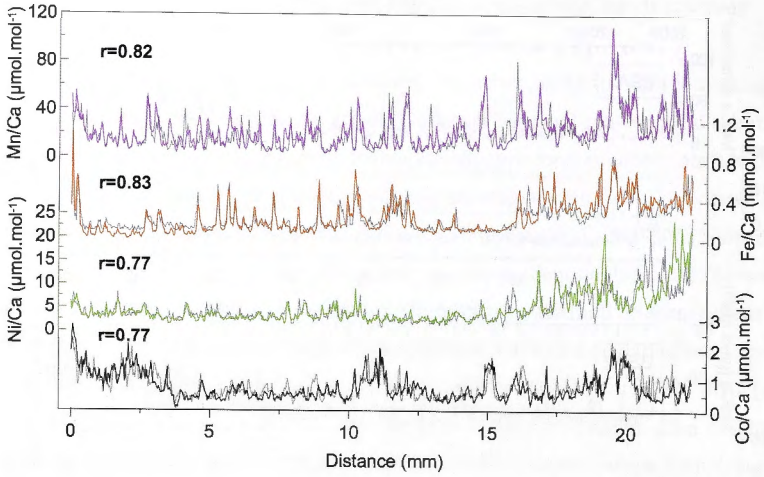

Figure VII-4 LA-ICPMS record of two parallel tracks measured along the same rhodolith branch (BSA2) for Mn/Ca, Fe/Ca, Ni/Ca and Co/Ca. Distance goes from the top (most recent) layer towards the bottom (oldest part) of the branch. Correlation coefficients for each profile show the reproducibility of the results.

The consistent patterns of Mn/Ca, Fe/Ca and Ni/Ca variations between all the profiles enable differentiation of two main regions, separated by a transition zone. One main region is the youngest portion of the branches, from 2011-2009 to the early 1980s, corresponding to distances between 0-12 and 0-22 mm according to the branch. The oldest part of the records, from the mid-1970s to the early 1960s, corresponding to distances between 17-22 and 25-37 mm according to the branch, represents the second main region. The metal/Ca ratios vary from one specimen to another. For the three branches of the BSA rhodolith, Mn/Ca values average at 14.4 µmol.mol^{-1}. A similar value is obtained for the SSA sample (13.6 µmol.mol^{-1}). However, the Mn/Ca average value for the MSA rhodolith reaches a higher value (29.9 µmol.mol^{-1}). In the oldest portion of each branch (17-22 to 25-37 mm), Mn/Ca concentrations increase from 2.0 to 4.8 times (BSA2 and SSA, respectively) to reach values of 31.3 to 85.8 µmol.mol^{-1} for the BSA and MSA specimens, respectively. Fe/Ca concentrations vary from 0.14 (BSA) to 0.27 (MSA) mmol.mol^{-1} for the 2011-early 1980s period (0-12 to 0-22 mm according to the branch), and from 0.3 to 0.78 mmol.mol^{-1} for the oldest parts, corresponding to a 1.9 to 3.6 times increase (BSA2 and SSA, respectively). In the most recent part of the branches, Ni/Ca values range from 3.9 to 5.6 µmol.mol^{-1} in all records, and increase by a factor of 1.3 to 3.0 (SSA and BSA3, respectively) to be 5.7 to 9.9 µmol.mol^{-1} within the bottom parts of the branches. The Co/Ca concentration ranges from 0.7 to 3.1 µmol.mol^{-1} with the highest values (1.4 to 3.1 µmol.mol^{-1}) generally occurring during the 2000s (outer 3-5 mm of the

branches) and the lowest (0.7 to 0.9 µmol.mol^{-1}) in the older parts of the branches. There is a significant decrease (1.4 to 3.6 times) towards the earlier parts of the records (i.e. early 1960s).

Despite differences in metal concentrations between branches, each element displays similar overall trends from the most recent to the oldest part of the five analysed branches. Mn/Ca and Fe/Ca are strongly coupled in each profile and, to some extent Ni/Ca also follows similar variations. For these metals, the 2011-early 1980s period (outer 12-22 mm) of each branch exhibits generally constant low values with sporadic, high-frequency peaks. The amplitude of these peaks is typically greater for Mn/Ca than for Fe/Ca and is the least pronounced for the Ni/Ca signals. The early 1960s to mid 1970s period (17-25 to 22-37 mm) of each branch displays high-frequency variations that are higher in amplitude than for the youngest parts of the records. For most branches, a slight decrease is noted in he inner parts (early to late 1960s) of the records for Mn/Ca and Fe/Ca.

The Co/Ca variation pattern, with the absence of higher Co/Ca values in the oldest part of the analysed branches in addition to an increase in concentrations towards the youngest part of the records, differ drastically from what is seen for the Mn/Ca, Fe/Ca and Ni/Ca variations.

VII-4.a.2 Solution ICPMS data and calibration of the LA-ICPMS signals

Concentrations of Mn, Fe, Ni and Co determined by solution ICPMS analysis of samples from the same rhodolith specimens analysed by LA-ICPMS display consistent variations from the top to the bottom of the branches for the BSA and MSA rhodoliths (Figure VII-5).

Comparison between the elemental concentrations obtained by solution ICPMS and by LA-ICPMS (calculated assuming constant Ca concentration for every sample and using the average Ca concentration value obtained from solution ICPMS measurements) shows very similar results for Mn and Co. It was then possible to confidently assign absolute element concentrations to the Mn/Ca and Co/Ca values reported in Figure VII-3. The absolute Mn concentration in *S. durum* ranges from 5-10 µg.g^{-1} for the youngest part of the branches (0-12 to 0-22 mm), to 11-34 µg.g^{-1} for the oldest part (17-25 to 22-35 mm). Co concentrations vary from 0.4 to 1.0 µg.g^{-1} for the 2000s period (0-3 to 0-5 mm according to the branches) to 0.2-0.4 µg.g^{-1} for the older parts.

Solution ICPMS, Fe and Ni analyses appear to be affected by relatively high levels of interference resulting in higher apparent bulk concentrations compared to values obtained using LA-ICPMS. Although these discrepancies are less pronounced for Ni than for Fe, we chose not to rely on the solution ICPMS outcomes for these two elements but,

rather, keep the concentration values calibrated and derived from the LA-ICPMS measurements. The concentrations of Fe (Ni) along the rhodolith branches range from 48-77 (1.5-2) $\mu g.g^{-1}$ for the 2011-early 1980s period (0-12 to 0-22 mm of the records) to 130-350 (2-5) $\mu g.g^{-1}$ in the earliest period (17-25 to 22-35 mm).

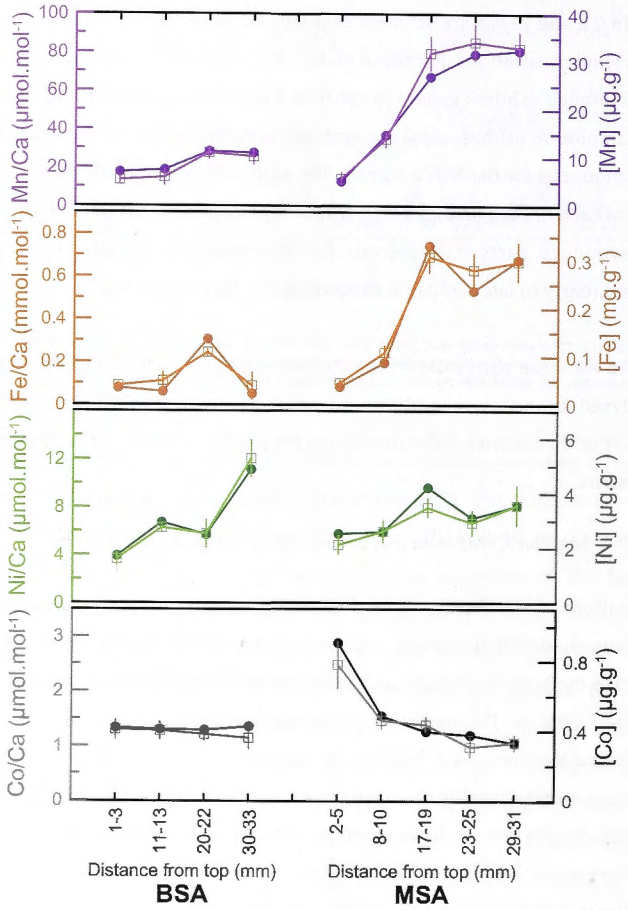

Figure VII-5 Comparison and calibration plots between metal concentration data obtained from solution ICPMS and elemental molar ratios over Ca recorded by LA-ICPMS for Mn, Fe, Ni and Co from the BSA and MSA rhodoliths. Solution ICPMS data points represent individual samples drilled along different branches for each rhodolith (dots). LA-ICPMS values (squares) were obtained by averaging the record corresponding to the same distance interval as the solution ICPMS samples for each rhodolith. For the BSA individual, the LA-ICPMS values were obtained from the average signal of the 3 branches analysed for that same rhodolith. Vertical error bars for the LA-ICPMS data points corresponds to 2σ for any particular distance interval. Vertical error bars for the solution ICPMS data points are too small to be displayed. Note that absolute concentrations displayed here for Fe and Ni are derived from the LA-ICPMS results and do not correspond to the solution ICPMS results (see text for details).

VII-4.b Trace elements reproducibility

The reproducibility of trace elements in the rhodoliths skeleton is based on monthly data for each LA-ICPMS record and was tested at three different scales: intra-branch, intra-rhodolith and inter-rhodolith. The distribution of trace elements across a single rhodolith branch is shown by comparing the two parallel LA-ICPMS profiles along the BSA2 branch (Figure VII-4). The variability between different branches of the same rhodolith is assessed using the profiles obtained for three branches from the BSA specimen. The reproducibility between rhodoliths is based on the average profile obtained from the BSA, MSA and SSA rhodoliths. Correlation coefficients are based on the monthly data for the 1963-2009 period and are presented in Table VII-1.

Within the BSA2 branch, Mn/Ca and Fe/Ca variations follow very similar patterns and show a high degree of reproducibility (r=0.82 and r=0.83, respectively; p<0.0001). Good reproducibility is also obtained for the parallel Ni/Ca and Co/Ca profiles along the same rhodolith branch (r=0.77; p<0.0001, for both signals).

r	Mn/Ca		Fe/Ca		Ni/Ca		Co/Ca	
Single branch	BSA2b		BSA2b		BSA2b		BSA2b	
BSA2a	0.82		0.83		0.77		0.77	
Single rhodolith	BSA1	BSA2	BSA1	BSA2	BSA1	BSA2	BSA1	BSA2
BSA2	0.32		0.41		0.61		0.10*	
BSA3	0.47	0.51	0.60	0.63	0.55	0.43	0.12*	0.21
Inter-rhodoliths	SSA	BSA	SSA	BSA	SSA	BSA	SSA	BSA
BSA	0.69		0.74		0.59		0.22	
MSA	0.70	0.62	0.82	0.78	0.43	0.56	0.66	0.32

Table VII-1 **Correlation matrix of the reproducibility of metal variations based on monthly data from a single branch to an inter-rhodolith scale. All coefficients are significant for a 95% confidence interval, except for *.**

The reproducibility of metal/Ca profiles between branches of the same rhodolith is generally much weaker. Mn/Ca and Fe/Ca in different branches display correlation coefficients that vary from r=0.28 to r=0.63. The lowest correlation coefficients are between the two branches that are perpendicular to each other, thus correspond to the long (BSA1) and short axes (BSA2) of the rhodolith's growth. Nevertheless, these correlation coefficients are significant at the 95% confidence interval (r=0.28 for Mn/Ca and r=0.41 for Fe/Ca). Correlation coefficients for Ni/Ca within the three branches of the BSA rhodolith range from r=0.42 to r=0.61 and are also statistically significant. This contrasts with the correlation coefficients for Co/Ca, which are not statistically significant,

except for the BSA2-BSA3 branch comparison that is only weakly significant ($r=0.21$; $p<0.05$).

Between rhodoliths, both Mn/Ca and Fe/Ca display good reproducibility between the three studied rhodoliths ($0.62<r<0.70$ for Mn/Ca and $0.74<r<0.83$ for Fe/Ca; $p<0.0001$). Ni/Ca variations are more weakly correlated ($0.43<r<0.59$; $p<0.0001$) and are comparable to the intra-specimen values. In the case of Co/Ca, the profiles from SSA and MSA are in good agreement ($r=0.60$; $p<0.0001$) but, when compared with the BSA profiles, the reproducibility is weaker, although still significant at the 95% confidence interval (Table VII-1).

VII-5 Discussion

VII-5.a Trace metal variability and incorporation into the rhodoliths

The agreement between the trace elements profiles along parallel tracks on the same branch indicates Mn, Fe, Ni and Co are consistently incorporated into the rhodoliths at the branch scale. However, some variability is observed between records at the intra-rhodolith and inter-rhodolith scales.

Dissolution or recrystallisation processes are unlikely to contribute significantly to the metal concentration variability as back scattered electron images of different parts of branches show consistent and apparently unmodified cell structures from the margin to the centre of the studied rhodoliths (Figure VII-6). One cause of this variability may be linked to the uncertainties with the age model, which is determined for each branch individually. Indeed, the linear interpolation of the trace element signals between every summer and winter peak would result in a mismatch in the monthly data across branches when the sub-annual extension rates differ.

Within an individual rhodolith, the greatest variability occurs between the long and short axes of growth profiles (particularly for Mn/Ca and Fe/Ca). This might be due to a combination of physical parameters. The surface sediments in the Sainte Marie Bay are enriched in trace metals (Dalto et al., 2006; Debenay and Fernandez, 2009) therefore diffusive fluxes from the sediments to the water column are likely to occur (see Grenz et al., 2010). This would create a boundary layer at the water-sediment interface, where rhodoliths live, with dissolved metal concentrations decreasing very rapidly from the sediments upwards. It is thus possible that, at any time, different parts of a rhodolith are exposed to seawater with different metal concentrations, therefore contributing to the variability recorded in the profiles. The regular overturning of the rhodoliths is also likely to enhance this observed variability.

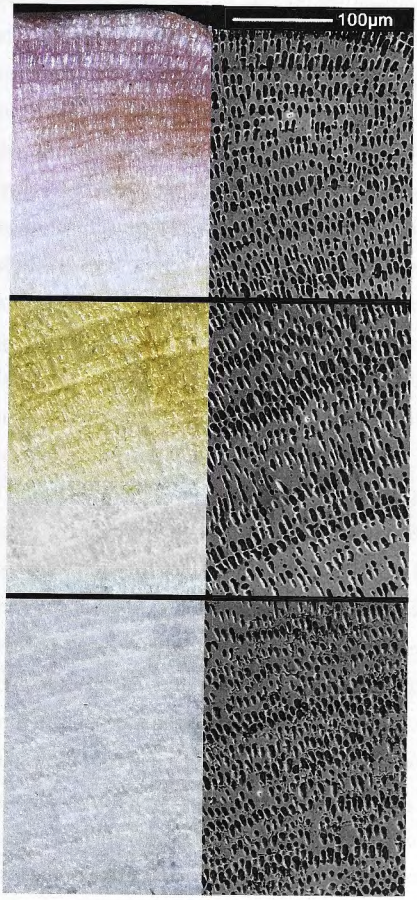

Figure VII-6 Light microscope (left) and back-scattered electron (BSE) (right) images of different parts of a branch for the BSA specimen from the youngest portion of the branch (top) to the oldest part of the rhodolith (bottom), with an intermediate step in between (middle). Note the similar cell structure and alignment for each of the three parts of the branch, suggesting that no major dissolution/recrystallisation process occurred.

In the New Caledonian lagoon, oxygen and nutrient fluxes from the sediments can be highly spatially variable (Grenz et al., 2010). If trace metals present a similar characteristic, it could also explain some of the inter-rhodolith heterogeneity. Local fish feeding or grazing activities that can generate sediment resuspension in reefal environments (Yahel et al., 2002) may also contribute to variable amounts of available trace metals in the water column, across the rhodolith bed.

For different rhodoliths, an active role of the alga in the incorporation of trace metals may explain some of the observed variability. Table VII-2 presents the distribution coefficients (K_D) of the corresponding divalent cations (Mn^{2+}, Fe^{2+}, Ni^{2+} and Co^{2+}) into the high-Mg calcite of rhodoliths. Published K_D values for Mn^{2+}, Fe^{2+}, Ni^{2+} and Co^{2+} for abiotic calcite are also displayed for comparison. Although the absence of any symbiont-mediated feeding process in coralline red algae (as it is the case, for example, in corals through

zooxanthellae - e.g. Harland and Nganro, 1990; Harland et al., 1990; Fallon et al., 2002) eliminates a potential source of biological intervention in the metal incorporation into the rhodoliths, the K_D for Fe in the rhodoliths is ~100 times higher than for abiotic calcite (Table VII-2) and indicates a strong contribution of the coralline red alga in the uptake of Fe from the dissolved phase of seawater. We can speculate that the intensity of this biological effect is variable from one rhodolith to another and thus, might explain differences in the average Fe concentration recorded between specimens (see Figures VII-3 and VII-5). A potential role of the alga is also suggested for Mn, Ni and Co (Table VII-2), however, the intensity of the biological processes in the incorporation of these trace metals into the rhodoliths appears of less significance than for Fe. It is important to note that the K_D values analysed here for the rhodoliths are only an indication of what may be happening at the site and are subject to various sources of uncertainty. Indeed, trace metal concentrations in seawater used here were not measured exactly at the Ricaudy Reef but at the Anse Vata Bay, a few kilometres from the rhodolith bed (Moreton et al., 2009). Due to the high spatial variability of trace metal concentrations in the SW lagoon of New Caledonia (Migon et al., 2007), this can have a significant effect on the actual K_D value calculated for the study site. Also, considering that the water-sediment boundary layer is enriched in trace metals would result in lower K_D values than calculated here. The rapid average extension rate of *S. durum* (Chapter IV, This thesis) is another factor that may influence to some extent the K_D values in the rhodoliths (Rimstidt et al., 1998). Therefore, although a vital effect in Fe incorporation seems to stand out in our results, a more reliable quantification of the distribution coefficients of Mn^{2+}, Ni^{2+} and Co^{2+} in *S. durum* rhodoliths, potentially using culture experiments, appears critical in order to better understand the role of the alga in the incorporation of these metals.

	Rhodolith concentration ($\mu mol.mol^{-1}$)	Seawater concentration ($\mu mol.mol^{-1}$)		K_D rhodoliths	K_D' calcite
Mn/Ca	15	2.29	Mn^{2+}	7	13-17
Fe/Ca	153	0.34	Fe^{2+}	450	4
Ni/Ca	4.1	1.62	Ni^{2+}	2.5	0.2
Co/Ca	1.8	0.065	Co^{2+}	28	8

Table VII-2 **Left: Average Mn/Ca, Fe/Ca, Ni/Ca and Co/Ca concentrations (in $\mu mol.mol^{-1}$) in the modern part of the rhodoliths (1993-2008, except for Co: 2008-2005) and the corresponding concentrations in seawater calculated from the data in Moreton et al. (2009) for the Anse Vata site. Note Ca concentration value was calculated as the average of 9 solution ICPMS measurements of seawater samples collected bi-monthly at the Ricaudy Reef between October 2009 and February 2011 (unpublished data). Right: Distribution coefficients (K_D) for the divalent cations $Mn2^+$, Fe^{2+}, Ni^{2+} and Co^{2+} calculated for the rhodoliths as K_D = Rhodolith conc. / Seawater conc., compared to corresponding published K_D' values for calcite (Mn^{2+}: Mucci, 1988; Pingitore et al., 1988; Fe^{2+}: Dromgoole and Walter, 1989; Ni^{2+}: Rimstidt et al., 1998; Co^{2+}: Lorens, 1981).**

The significance of the living component of the *S. durum* rhodoliths in the Co distribution is illustrated by the decrease in Co/Ca concentration in the outermost part of the MSA branch after H_2O_2 treatment (Figure VII-7). This indicates that approximately 60% of Co in the modern part of the branch was bound to actual or remnants of organic matter, which is a potential source of variability for Co/Ca distribution between rhodolith branches as well as rhodolith specimens. H_2O_2 treatment had no significant effect on the average Mn/Ca, Fe/Ca and Ni/Ca concentrations along the MSA branch (Figure VII-7), suggesting that these elements are not controlled by organic matter distribution in the rhodoliths and are likely to be incorporated in the calcite structure.

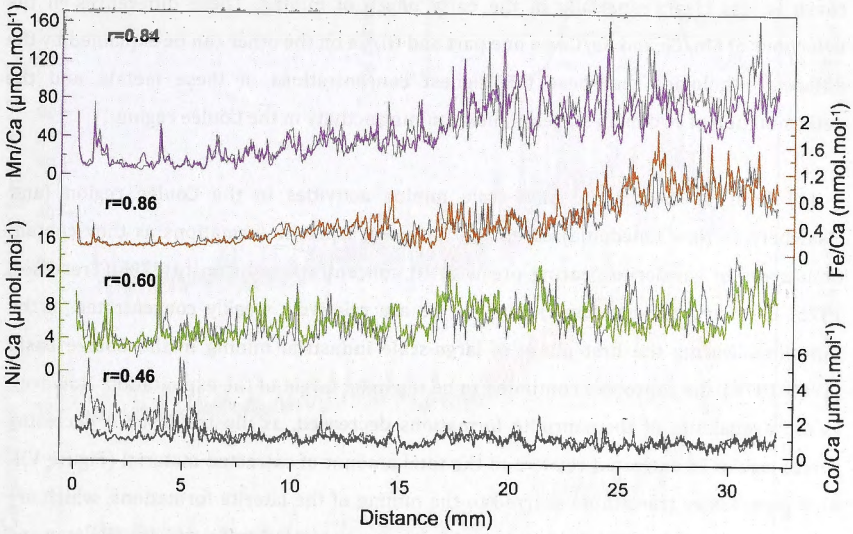

Figure VII-7 LA-ICPMS record of Mn/Ca, Fe/Ca, Ni/Ca and Co/Ca from two parallel tracks carried out along the same rhodolith branch (MSA1). Grey records are before the 15% H_2O_2 treatment aimed at removing the organic matter from the branch, and the coloured records are after the 15% H_2O_2 treatment was applied. Correlation coefficients for each profile show the reproducibility of the results).

In summary, variations of Mn/Ca, Fe/Ca, Ni/Ca and Co/Ca concentrations in *S. durum* rhodoliths are subject to various sources of uncertainties that would have a particularly evident effect on the monthly-resolution data. Therefore, although the reproducibility of monthly data at every level (from a single branch to inter-rhodolith) is statistically significant at he 95% confidence interval (except for two Co/Ca profiles), for the purpose of environmental studies, it seems more reasonable to focus on the annual to inter-annual resolution patterns of metal variations as well as on the average records of several rhodolith branches.

VII-5.b Rhodoliths as a proxy for mining activities: Mn/Ca, Fe/Ca and Ni/Ca

Figure VII-8 presents the rhodoliths average metal variations for the 1965-2008 period, compared to the intensity of the mining activities (total extracted material and Ni concentration in extracted material) in the Coulée River watershed as well as an inter-annual pattern of rainfall over Nouméa city for the same period.

The average Mn/Ca and Fe/Ca variations are closely related to each other and broadly track the intensity of mining production from the Coulée River watershed for the 1965-1981 period. Ni/Ca variations show a similar pattern but the fit to the mining production curve is less clear, especially in the early phase of mining. These differences in the behaviour of Mn/Ca and Fe/Ca on one part and Ni/Ca on the other can be explained by the different lithologies that bear the highest concentrations of these metals, and the determination of two main stages of nickel mining activity in the Coulée region.

(1) Prior to the 1960s, small-scale mining activities in the Coulée region (and elsewhere in New Caledonia) essentially targeted saprolite formations as they contain thin layers of garnierite bearing ore with Ni concentrations of up to 37% (Trescases, 1975; P. Maurizot, *pers. comm*). Mn and Fe are relatively weakly concentrated in the saprolites. During the first phase of large-scale industrial mining in the Coulée basin (1960-1970), the saprolites continued to be the main target of the exploitation. However, as the availability of the saprolite formations decreased, as illustrated by a decresing percentage of Ni extracted relative to the total amount of extracted material (Figure VII-8), a progressive transition occurred to the mining of the laterite formations, which are less concentrated in Ni (1-2%) and much more concentrated in Fe and Mn (Baltzer and Trescaes, 1971; Trescases, 1975). The transition between different types of material targeted by mining is matched in the geochemical composition of the rhodoliths over that 1960-1970 period, Concentrations of Mn/Ca and Fe/Ca increase with the overall extracted material (and extracted laterites) whereas Ni/Ca concentrations drop simultaneously with the decrease in saprolite excavation (Figure VII-8).

(2) From the peak of mining activity (late 1960s-early 1970s), laterite formations of the Coulée region were most probably exclusively extracted as shown by the low Ni percentage of extracted material. In the rhodoliths, this translates to the highest concentrations in Mn/Ca and Fe/Ca as well as lower, but still high, Ni/Ca concentrations. From this period on, Mn/Ca, Fe/Ca and Ni/Ca show similar trends, in accordance with the laterite-derived type of material coming to the lagoon.

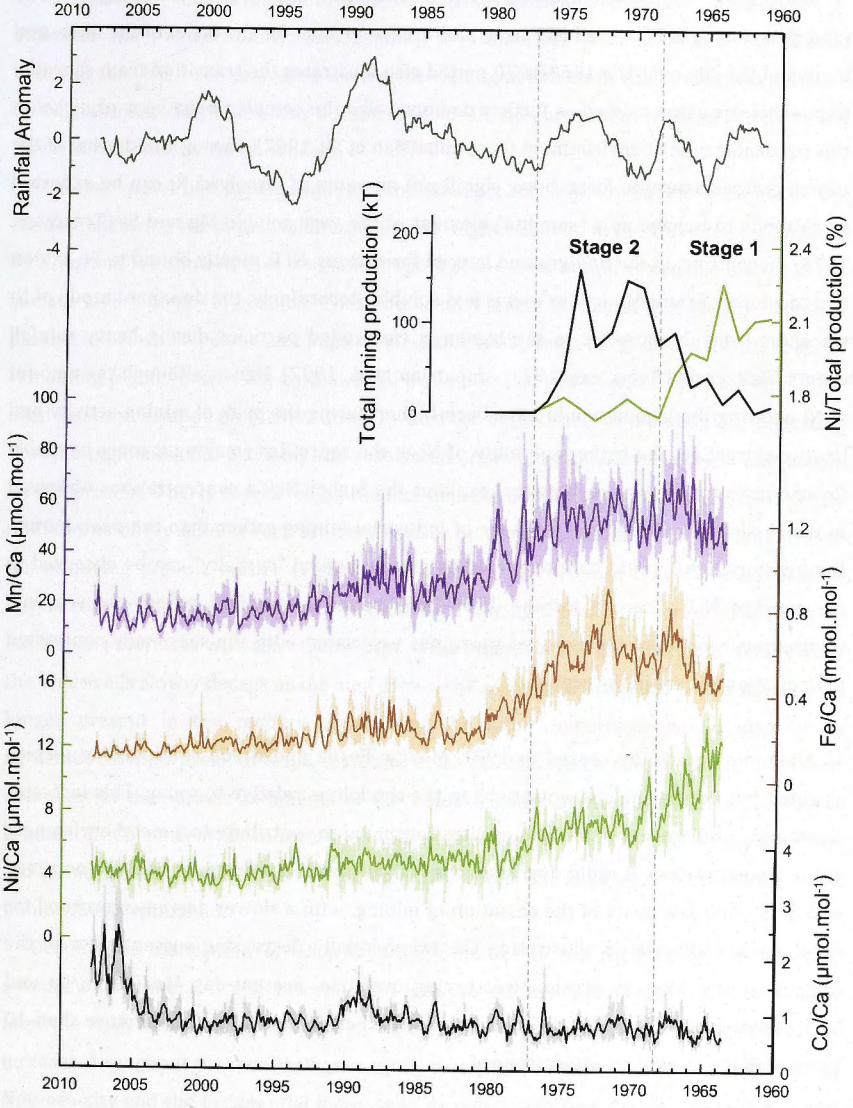

Figure VII-8 Variations in average Mn/Ca, Fe/Ca, Ni/Ca and Co/Ca for the 1963-2008 period compared to annual total mining production and percentage of nickel extracted over the total amount of material extracted in the Coulée area between 1961 and 1981 (data from the Direction des Mines et de l'Energie de Nouvelle Calédonie – DIMENC) and 3-years smoothed rainfall anomaly over Nouméa from 1961 (monthly data obtained from Météo France). The average metal variations (thick lines) were obtained using the mean of monthly-resolved values for each branch analysed with LA-ICPMS. The shaded area surrounding the average signals is $2\sigma_M$ (std err) for each mean value. The different stages of mining activity in the Coulée region are separated by the vertical dotted lines.

The fact that Ni/Ca concentrations in the rhodoliths during the peak of mining activities (and thus, the peak of overall Ni extraction) are lower than for the onset of the industrial mining at the site over the 1960-1970 period also illustrates the transition from saprolite to laterite extraction as well as further demonstrates the complex behaviour of nickel in this particular type of environment (see Ambatsian et al., 1997). During weathering of the coarse-grained saprolite formations, significant amounts of dissolved Ni can be exported as Ni tends to behave as a "satellite" element of the very soluble Mg and Si (Trescases, 1975). In contrast, in the fine-grained laterite formations, Ni is mostly bound to Fe oxides, and to a lesser extent Mn oxides and is less soluble. Accordingly, the dominant mode of Ni transport from the laterites to the lagoon is *via* eroded particles during heavy rainfall events (Baltzer and Trescases, 1971; Ambatsian et al., 1997). Hence, although the amount of Ni entering the lagoon would have been higher during the peak of mining activity and laterite extraction, the higher solubility of Ni in the saprolites (making it more available for co-precipitation with carbonates) explains the higher Ni/Ca concentrations observed in the rhodoliths during the first stage of industrial mining rather than the peak period. Furthermore, what could be interpreted as pseudo-annual "cyclicity" can be observed in the average Ni/Ca record for the 1965-1970 period and might reflect the seasonal weathering/erosion of the exposed saprolites associated with the seasonally contrasted precipitation regime in the region.

After mining activity ceased in 1981, Mn/Ca, Fe/Ca and Ni/Ca continued to display elevated but decreasing concentrations in the rhodoliths relative to today. This indicates weathering and erosion of the mining sites continued to contribute to a metal enrichment of the lagoon waters. A rapid decrease in metal concentration in the rhodoliths occurred within the first few years of the cessation of mining, with a slower decrease recorded for several years afterwards, illustrating the exponentially decreasing susceptibility of the original mining sites to erosion/weathering overtime. Present-day Mn/Ca, Fe/Ca and Ni/Ca concentrations in the rhodoliths were reached in the early 1990s, more than 10 years after the mining activities stopped.

VII-5.c The case of cobalt

Surprisingly, Co/Ca does not follow the mining activity pattern although it has been shown to be generally closely related to Mn in laterite formations (Trescases, 1975; Ambatsian et al., 1997). One explanation might be that Co is only highly concentrated in transitional absolane formations located between the saprolites and laterites (Trescases,

1975). However, that formation is not systematically present everywhere in the region (P. Maurizot and J-M Fernandez, *pers comm.*). It is therefore possible that in the laterite material that has been extracted during the mining activities in the Coulée watershed, a Co-rich absolane formation was absent. As a result, no enrichment in dissolved Co in the Bay was recorded by the rhodoliths.

Another potential explanation for the absence of any Co/Ca enrichment in the rhodoliths during the industrial mining period might be found in the way Co is assimilated by *S. durum*. We showed that a significant part of the Co is bound to organic matter in the surface layers of the organisms. These outermost layers almost systematically display a pinkish to brownish colour (see Figures VII-2 and VII-7), most likely due to the presence of remaining pigments that the coralline red algae possess. However, this colouration of the algal skeleton disappears further down toward the oldest parts of the nodules, suggesting that the pigments, and probably the associated organic matter, have decayed and are no longer present. This is supported by the fact that the Co/Ca variations below the first few millimetres of the MSA branch are very similar before and after the H_2O_2 treatment used for removing organic matter (Figure VII-6). Hence, we propose that, if an increase in Co/Ca concentration did occur in the rhodoliths during the mining period, it is likely to have been associated with the organic part of the organism and as the organic matter from the older cells slowly decays as the alga grows, the associated historical Co/Ca signal is no longer present in the modern rhodoliths. The latter hypothesis would also be in agreement with a previous study by Dalto et al. (2006), which shows that Co is indeed abundant in the surface sediments of the Boulari/Sainte Marie Bays with a decreasing gradient in Co concentration from the Coulée River mouth outward into the lagoon, thus indicating that a significant part of the Co reaching this site is likely to originate from the Coulée River watershed.

Despite the association of Co with organic matter in the rhodoliths, a measurable amount of that metal is also incorporated into the calcite skeleton and is recorded even after the H_2O_2 treatment. The Co/Ca signal derived from the calcite shows a steady, slow increase throughout the record (Figure VII-7) that might be explained by the expansion of Nouméa city and the exponential increase in its population (see Figure 2 in Debenay and Fernandez, 2009). This demographic shift is closely related to an increase of the number of vehicles in the area. As the Ricaudy Reef is very close to the shore of a populated area and as car exhaust products have been shown to contribute to higher environmental Co concentrations in high-density population areas (Hamilton, 1994), it is possible that an enrichment in the seawater Co concentration originates from the wind-driven motorised-vehicle exhausts to the lagoon and appears in the rhodoliths skeleton. Another potential source of Co to the Ricaudy site is the proximity of the major nickel-smelting factory (SLN

– Société Le Nickel). Indeed, Macholz (1982) measured the highest concentrations of Co in the atmosphere near a nickel refinery in Wales and demonstrated that Co was a by-product of Ni-smelting. Salmon et al. (1978) also reported enrichment in Co in the atmosphere around industrial sites compared to rural areas. Due to the ever-expanding nickel production in New Caledonia, this potential source of Co to the atmosphere is most likely to have increased in the last decades.

In conclusion, even though Co/Ca variations in the rhodoliths do not record the historical mining activity in the Coulée region, other anthropogenic effects such as the industrial expansion of Nouméa city might be evidenced by the long-term trend in the Co/Ca concentrations.

VII-5.d Metal records and the local rainfall pattern

The local, inter-annual rainfall pattern can be associated with some of the variations observed in the metal concentrations, especially during the period of mining activities. Between 1963 and 1969, Mn/Ca and Fe/Ca show a steady increase in their concentration in the rhodoliths. Although we mentioned that an increase in excavated laterite material is likely to be the main driver in the rise of Mn/Ca and Fe/Ca, it also appears that the 1965-1968 period saw elevated rainfall over Nouméa, which will be consistent with higher erosion processes in the Coulée watershed, therefore likely to contribute to more Mn and Fe being incorporated into the rhodoliths. Rainfall variability may also be reflected in the metal records during the 1969-1971 period, when a drop in the precipitation was observed. Although the mining production continued to increase during this time of low precipitation, a slight decrease is recorded in the Mn/Ca and Fe/Ca concentrations, suggesting a net reduced supply of these dissolved metals into the lagoon. This is followed, over the next few years, by higher Mn/Ca and Fe/Ca values concordant with a higher rate of rainfall during a period of active mining activity.

After mining stopped, Mn/Ca and Fe/Ca concentrations in the rhodoliths steeply decreased and the influence of the local rainfall pattern is more difficult to discern in the metal records, although a slight increase in Mn/Ca, Fe/Ca and Co/Ca between 1986 and 1990 does correspond to a high precipitation period. However, the inter-annual rainfall pattern does not appear to exert much influence on the rhodoliths trace metal concentrations after 1993. Different hypotheses may be drawn from this. Firstly, one may expect a close coupling between precipitation and dissolved metal concentration when rain was falling on a bare landscape, as it would have been the case during the period of mining. Nevertheless, after mining activities stopped and available loose sediment was

cleared away and/or a weathering rind develops, it is probable that the strength of precipitation became less of a dominant influence over the amount of metal carried by the river into the lagoon. The metal records in the rhodoliths might then reflect these contrasted periods of rainfall influence, between the mining (late 1960s – late 1970s) and the post-1993, modern-day weathering conditions. Secondly, trace metals from the weathered profiles of the Coulée region are transported into the lagoon essentially as particulates in their oxidised form (i.e. MnO, Fe_2O_3, CoO, NiO; Ambastian et al., 1997). Dissolution can occur either as desorption from particles (Ouillon et al., 2010) or by reduction in the upper layers of the sediment (Ambastian et al., 1997), surface sediments thus acting as a source of dissolved metals for the water column. Therefore, the fate of particles entering the lagoon can be crucial to consider. From the 1950s, major structural modifications have been undertaken around Sainte Marie Bay (e.g. new embankments) that may have contributed to a gradual reduction of the connection between sediments from the Boulari and Sainte Marie bays (Debenay and Fernandez, 2009). Also, despite the fact that Sainte Marie Bay is directly influenced by river inputs (Fernandez et al., 2006), Clavier et al. (1995) have shown that about 80% of the sedimentation in the area is due to resuspension as opposed to direct deposition. Therefore, during their journey from the Coulée River mouth to the south end of Sainte Marie Bay, the sediments are likely to have undergone several phases of sedimentation, current-driven resuspension and re-sedimentation. This may spread the signal of river runoffs over longer periods of time, especially when the input of particulate material is reduced since the mining closure, and explain why the rainfall pattern is absent from the rhodolith record after 1993.

VII-6 Conclusion

This study reports for the first time Mn/Ca, Fe/Ca, Ni/Ca and Co/Ca concentrations and variations in coralline red algae and might serve as a baseline for future work. Comparing the distribution coefficients of the trace metals in the rhodoliths to the ones for abiotic calcite helped determined a major role of the alga in the uptake of Fe from the water column. For the other trace metals, the vital effect is unclear and calls for further studies. H_2O_2 treatment of a rhodolith branch revealed that a significant part of the Co present in the outermost regions of the rhodolith is associated with actual or remnants of organic matter. This association was not shown for Mn, Fe or Ni, suggesting these metals are rather likely to be incorporated in the calcite structure of the rhodoliths.

The observed variability of trace metals, both in absolute concentrations and in the LA-ICPMS profiles makes the use of monthly resolution data from a single *S. durum* rhodolith

branch unreliable for obtaining environmental information. However, considering inter-annual variations of averaged trace metals profiles enables us to record historical mining activities in the Coulée region of New Caledonia. Increased Mn/Ca and Fe/Ca concentrations reflect the intensity of the mining activity from 1965 to 1977, while Ni/Ca variations appear sensitive to the type of excavated material (Ni-rich saprolites versus relatively Ni-poor laterites). Concentrations in Mn/Ca, Fe/Ca and Ni/Ca steeply decrease in the rhodoliths after the cessation of mining. However, present-day values are not reached until 1993, indicating a response-time of the system of more than ten years. Co/Ca in the rhodoliths is not associated with mining activity but, instead, shows a slight steady increase over the last five decades that is possibly related to the rapid expansion of Nouméa city through different ways of contamination (e.g. car exhausts, rubber tyres residue, hospital waste, building material), and the ever increasing nickel-related industrial activities in the area.

We also suggest that trace metal variations in *S. durum*, especially Mn/Ca and Fe/Ca, may be sensitive, to some extent, to local rainfall variability. However, further work is required to establish why this sensitivity only appears when metal concentrations in the rhodoliths are relatively high. Studies at sites more prone to have a quicker rainfall/metal concentration response (e.g. closer to a river mouth) would be critical to assess this characteristic.

References

Alibert, C., Kinsley, L., Fallon, S. J., McCulloch, M. T., Berkelmans, R., and McAllister, F. 2003. Source of trace element variability in Great Barrier Reef corals affected by the Burdekin flood plumes. *Geochimica et Cosmochimica Acta* **67**(2), 231-246.

Alric, R. 2009. Recueil des débits caractéristiques de la Nouvelle Calédonie. Direction des Affaires Veterinaires Alimentaires et Rurales (DAVAR), Service de l'eau des statistiques et études rurales, Observatoire de la ressource en eau, Nouméa, 314pp.

Ambatsian, P., Fernex, F., Bernat, M., Parron, C., and Lecolle, J. 1997. High metal inputs to closed seas: the New Caledonian lagoon. *Journal of Geochemical Exploration* **59**(1), 59-74.

Baltzer, F., and Trescases, J. J. 1971. Erosion, transport et sédimentation liés aux cyclones tropicaux dans les massifs d'ultrabasites de Nouvelle-Calédonie. *Cahiers ORSTOM Série Géologie III* **2**, 221-244.

Bosence, D., W. J. (1983a). Description and Classification of Rhodoliths (Rhodoids, Rhodolites). *In* "Coated Grains." (T. M. Peryt, Ed.), pp. 217-224. Springer-Verlag, Berlin.

Bosence, D., W., J. (1983b). The Occurence and Ecology of Recent Rhodoliths - A Review. *In* "Coated Grains." (T. M. Peryt, Ed.), pp. 225-242. Springer-Verlag Berlin.

Burdett, H., Kamenos, N. A., and Law, A. 2011. Using coralline algae to understand historic marine cloud cover. *Palaeogeography, Palaeoclimatology, Palaeoecology* **302**, 65-70.

Chan, P., Halfar, J., Williams, B., Hetzinger, S., Steneck, R., Zack, T., and Jacob, D. E. 2011. Freshening of the Alaska Coastal Current recorded by coralline algal Ba/Ca ratios. *Journal of Geophysical Research* **116**(G1), G01032.

Clavier, J., Chardy, P., and Chevillon, C. 1995. Sedimentation of particulate matter in the south-west lagoon of New Caledonia: spatial and temporal patterns. *Estuarine, Coastal and Shelf Science* **40**(3), 281-294.

Dalto, A. G., Gremare, A., Dinet, A., and Fichet, D. 2006. Muddy-bottom meiofauna responses to metal concentrations and organic enrichment in New Caledonia South-West Lagoon. *Estuarine, Coastal and Shelf Science* **67**(4), 629-644.

David, C. P. 2003. Heavy metal concentrations in growth bands of corals: a record of mine tailings input through time (Marinduque Island, Philippines). *Marine pollution bulletin* **46**(2), 187-196.

Debenay, J. P., and Fernandez, J. M. 2009. Benthic foraminifera records of complex anthropogenic environmental changes combined with geochemical data in a tropical bay of New Caledonia (SW Pacific). *Marine pollution bulletin* **59**(8-12), 311-322.

Eggins, S. M., Kinsley, L. P. J., and Shelley, J. M. G. 1998. Deposition and element fractionation processes during atmospheric pressure laser sampling for analysis by ICP-MS. *Applied Surface Science* **127**, 278-286.

Fallon, S. J., Fifield, L. K., and Chappell, J. M. 2010. The next chapter in radiocarbon dating at the Australian National University: Status report on the single stage AMS. *Nuclear Instruments and Methods in Physics Research Section B: Beam Interactions with Materials and Atoms* **268**(7-8), 898-901.

Fallon, S. J., White, J. C., and McCulloch, M. T. 2002. Porites corals as recorders of mining and environmental impacts: Misima Island, Papua New Guinea. *Geochimica et Cosmochimica Acta* **66**(1), 45-62.

Fernandez, J. M., Ouillon, S., Chevillon, C., Douillet, P., Fichez, R., and Gendre, R. L. 2006. A combined modelling and geochemical study of the fate of terrigenous inputs from mixed natural and mining sources in a coral reef lagoon (New Caledonia). *Marine pollution bulletin* **52**(3), 320-331.

Fichez, R., Harris, P. A., Fernandez, J. M., Chevillon, C., and Badie, C. 2005. Sediment records of past anthropogenic environmental changes in a barrier reef lagoon (Papeete, Tahiti, French Polynesia). *Marine pollution bulletin* **50**(5), 599-608.

Foster, M., S. 2001. Rhodoliths: Between rocks and soft places. *Journal of Phycology* **37**, 659-667.

Frantz, B., R., Kashgarian, M., Coale, K., H., and Foster, M., S. 2000. Growth rate and potential climate record from a rhodolith using ^{14}C accelerator mass spectrometry. *Limnology and Oceanography* **45**(8), 1773-1777.

Frantz, B. R., Foster, M. S., and Riosmena-RodrÌguez, R. 2005. *Clathromorphum nereostratum* (Corallinales, Rhodophyta): The oldest alga? *Journal of Phycology* **41**(4), 770-773.

Freiwald, A., and Henrich, R. 1994. Reefal coralline algal build ups within the Arctic Circle: morphology and sedimentary dynamics under extreme environmental seasonality. *Sedimentology* **41**(5), 963-984.

Gamboa, G., Halfar, J., Hetzinger, S., Adey, W., Zack, T., Kunz, B., and Jacob, D. E. 2010. Mg/Ca ratios in coralline algae record northwest Atlantic temperature variations and North Atlantic Oscillation relationships. *Journal of Geophysical Research* **115**(C12), C12044.

Grenz, C., Denis, L., Pringault, O., and Fichez, R. 2010. Spatial and seasonal variability of sediment oxygen consumption and nutrient fluxes at the sediment water interface in a sub-tropical lagoon (New Caledonia). *Marine pollution bulletin* **61**(7-12), 399-412.

Halfar, J., Hetzinger, S., Adey, W., Zack, T., Gamboa, G., Kunz, B., Williams, B., and Jacob, D. E. 2010. Coralline algal growth-increment widths archive North Atlantic climate variability. *Palaeogeography, Palaeoclimatology, Palaeoecology*,

Halfar, J., Steneck, R., S., Joachimski, M., Kronz, A., and Wanamaker Jr., A., D. 2008. Coralline red algae as high-resolution climate recorders. *Geology* **36**(6), 463-466.

Halfar, J., Steneck, R., S., Schöne, B., R., Moore, G., W., K., Joachimski, M., Kronz, A., Fietzke, J., and Estes, J. 2007. Coralline alga reveals first marine record of subarctic North Pacific climate change. *Geophysical Research Letters* **34**, L07702.

Halfar, J., Williams, B., Hetzinger, S., Steneck, R. S., Lebednik, P., Winsborough, C., Omar, A., Chan, P., and Wanamaker, A. D. 2011. 225 years of Bering Sea climate and ecosystem dynamics revealed by coralline algal growth-increment widths. *Geology* **39**(6), 579.

Halfar, J., Zack, T., Kronz, A., and Zachos, J., C. 2000. Growth and high-resolution paleoenvironmental signals of rhodoliths (coralline red algae): A new biogenic archive. *Journal of Geophysical Research* **105**(C9), 22,107-22,116.

Hamilton, E. I. 1994. The geobiochemistry of cobalt. *Science of the total environment* **150**(1-3), 7-39.

Harland, A. D., Bryan, G. W., and Brown, B. E. 1990. Zinc and cadmium absorption in the symbiotic anemone Anemonia viridis and the non-symbiotic anemone Actinia equina. *Journal of the Marine Biological Association of the United Kingdom. Plymouth* **70**(4), 789-802.

Harland, A. D., and Nganro, N. R. 1990. Copper uptake by the sea anemoneAnemonia viridis and the role of zooxanthellae in metal regulation. *Marine Biology* **104**(2), 297-301.

Hetzinger, S., Halfar, J., Kronz, A., Steneck, R., Adey, W., H., Lebednik, P., A., and Schöne, B., R. 2009. High-resolution Mg/Ca ratios in a coralline red alga as a proxy for Bering Sea temperature variations from 1902 to 1967. *Palaios* **24**, 406-412.

Hetzinger, S., Halfar, J., Zack, T., Gamboa, G., Jacob, D. E., Kunz, B. E., Kronz, A., Adey, W., Lebednik, P. A., and Steneck, R. S. 2011. High-resolution analysis of trace elements in crustose coralline algae from the North Atlantic and North Pacific by laser ablation ICP-MS. *Palaeogeography, Palaeoclimatology, Palaeoecology* **302**(1-2), 81-94.

Jochum, K. P., Weis, U., Stoll, B., Kuzmin, D., Yang, Q., Raczek, I., Jacob, D. E., Stracke, A., Birbaum, K., Frick, D. A., Günther, D., and Enzweiler, J. 2011. Determination of Reference Values for NIST SRM 610–617 Glasses Following ISO Guidelines. *Geostandards and Geoanalytical Research* **35**(4), 397-429.

Kamenos, N., A., Cusack, M., Huthwelker, T., Lagarde, P., and Scheibling, R., E. 2009. Mg-lattice associations in red coralline algae. *Geochimica et Cosmochimica Acta* **73**, 1901-1907.

Kamenos, N., A., Cusack, M., and Moore, P., G. 2008. Coralline algae are global palaeothermometers with bi-weekly resolution. *Geochimica et Cosmochimica Acta* **72**, 771-779.

Labrosse, P., Fichez, R., Farman, R., and Adams, T. (2000). New Caledonia. *In* "Seas at the millennium: an environmental evaluation." (C. R. C. E. Sheppard, Ed.), pp. 723-736.

Longerich, H. P., Jackson, S. E., and G¸nther, D. 1996. Laser ablation inductively coupled plasma mass spectrometric transient signal data acquisition and analyte concentration calculation. *Journal of Analytical Atomic Spectrometry* **11**(9), 899-904.

Macholz, R. M. (1982). "Trace metals in the environment. Volume 6: Cobalt. An appraisal of environmental exposure." Ann Arbor Science.

McCulloch, M., Fallon, S., Wyndham, T., Hendy, E., Lough, J., and Barnes, D. 2003. Coral record of increased sediment flux to the inner Great Barrier Reef since European settlement. *Nature* **421**(6924), 727-730.

Migon, C., Ouillon, S., Mari, X., and Nicolas, E. 2007. Geochemical and hydrodynamic constraints on the distribution of trace metal concentrations in the lagoon of Noumea, New Caledonia. *Estuarine, Coastal and Shelf Science* **74**(4), 756-765.

Moreton, B. M., Fernandez, J. M., and Dolbecq, M. B. D. 2009. Development of a Field Preconcentration/Elution Unit for Routine Determination of Dissolved Metal Concentrations by ICP OES in Marine Waters: Application for Monitoring of the New Caledonia Lagoon. *Geostandards and Geoanalytical Research* **33**(2), 205-218.

Ouillon, S., Douillet, P., Lefebvre, J. P., Le Gendre, R., Jouon, A., Bonneton, P., Fernandez, J. M., and Chevillon, C. 2010. Circulation and suspended sediment transport in a coral reef lagoon: The south-west lagoon of New Caledonia. *Marine Pollution Bulletin* **61**(7-12), 309-322.

Paillard, D., Labeyrie, L., and Yiou, P. 1996. Macintosh program performs time-series analysis. *Eos Transactions AGU* **77**(39), 379.

Rimstidt, J. D., Balog, A., and Webb, J. 1998. Distribution of trace elements between carbonate minerals and aqueous solutions. *Geochimica et Cosmochimica Acta* **62**(11), 1851-1863.

Salmon, L., Atkins, D. H. F., Fisher, E. M. R., Healy, C., and Law, D. V. 1978. Retrospective trend analysis of the content of UK air particulate material 1957-1974. *The Science of The Total Environment* **9**(2), 161-199.

Silva, C. A. R., Smith, B. D., and Rainbow, P. S. 2006. Comparative biomonitors of coastal trace metal contamination in tropical South America (N. Brazil). *Marine Environmental Research* **61**(4), 439-455.

Steneck, R. S., Kramer, P. A., and Loreto, R. M. 2003. The Caribbean's western-most algal ridges in Cozumel, Mexico. *Coral Reefs* **22**(1), 27-28.

Trescases, J. J. (1975). "L'évolution geochimique supergène des roches ultrabasiques en zone tropicale. Formation des gisement nickélifères de Nouvelle-Calédonie.", Ph.D. Thesis OA 8708, Université Louis Pasteur, Strasbourg.

Williams, B., Halfar, J., Steneck, R. S., Wortmann, U. G., Hetzinger, S., Adey, W., Lebednik, P., and Joachimski, M. 2011. Twentieth century 13 C variability in surface water dissolved inorganic carbon recorded by coralline algae in the northern North Pacific Ocean and the Bering Sea. *Biogeosciences* **8**(1), 165-174.

Yahel, R., Yahel, G., and Genin, A. 2002. Daily cycles of suspended sand at coral reefs: A biological control. *Limnology and oceanography* **47**(4), 1071-1083.

CHAPTER VIII

Oxygen isotopic composition of tropical coralline red algae using a sensitive, high-resolution ion microprobe (SHRIMP II)

Keywords: *Sporolithon durum*, rhodolith, instrumental mass fractionation, vital effect, sea-surface temperature, sea-surface salinity

Abstract

We report sensitive, high-resolution ion microprobe (SHRIMP) oxygen isotope analyses carried out for the first time on a coralline red alga in the form of a *Sporolithon durum* rhodolith. The magnesium content of carbonate samples was found to significantly affect the SHRIMP instrumental mass fractionation (IMF) and for the high-Mg-calcite, tropical specimen of free-living *S. durum*, the extent of this IMF on the $\delta^{18}O$ values is 1-2‰. The sample porosity and/or the presence of organic matter in the skeletal structure of *S. durum* may be responsible for another type of IMF related to variable secondary ion intensities. Whilst the correction for IMF may induce additional uncertainties to the SHRIMP $\delta^{18}O$ measurements, it improved their accuracy. The resulting, average SHRIMP $\delta^{18}O$ value for the *S. durum* rhodolith collected live from New Caledonia is -4.9 ±0.1‰, in agreement with conventional $\delta^{18}O$ mass spectrometry (MS) measurements of the same organism, and within the range of $\delta^{18}O$ values for various species of coralline red algae. The distance of *S. durum* $\delta^{18}O$ average value from equilibrium is also comparable to those reported in the literature. A range of 10.4‰ is observed over only hundreds of microns along the rhodolith branch and cannot be explained solely by variations in environmental parameters such as sea-surface temperature (SST) or salinity (SSS). A similar range of $\delta^{18}O$ values at the micrometer scale had previously been observed in a *Porites lutea* coral from the same region. We discuss various factors potentially controlling the $\delta^{18}O$ variation in *S. durum* at high resolution and propose that a pH-related oxygen fractionation is likely to occur during the calcification process. Therefore, we suggest that SHRIMP analyses may potentially contribute to a better characterisation of metabolic processes and vital effects in coralline red algae. A poor but significant anti-correlation with SST ($r=-0.32$; $p<0.001$) is, however, observed for the detrended, monthly variations of $\delta^{18}O$ in *S. durum* during the 1984-2008 period, as well as a match between the SST and $\delta^{18}O$ average seasonal patterns.

A decrease of ~2‰ per increasing degree Celsius, was found to be in agreement with predictions for abiotic calcite. In addition, inter-annual $\delta^{18}O$ variations showed a significant correlation ($r=0.64$; $p<0.0001$) with the SSS pattern over a 20-year period, suggesting that environmental information can be extracted from the $\delta^{18}O$ signal of *S. durum* rhodoliths. However, due to the various sources of uncertainty connected with the high-resolution analyses, we propose that the SHRIMP approach might not be the most suitable one for environmental reconstructions.

VIII-1 Introduction

Coralline red algae are encrusting marine organisms that form a high-magnesium calcite structure as they grow (Adey and McIntyre, 1973; Steneck, 1986; Foster, 2001). They are ubiquitous in the oceans, from the tropics to the poles, over the entire depth of the photic zone (Bosence, 1983), occurring either as crusts on a hard substrate or as free-living nodules, called rhodoliths (Foster, 2001). The last decade has seen the expansion of geochemical studies on long-lived coralline red algae, with the aim of generating decadal- to century-long environmental records (Halfar et al., 2000; 2007; 2008; Hetzinger et al., 2009; 2011a;b; Burdett et al., 2010; Williams et al., 2011; Chan et al., 2011).

The oxygen isotopic composition ($\delta^{18}O$) of coralline red algae skeletons was one of the first proxies to be investigated (e.g. Milliman, 1974; Wefer and Berger, 1991; Rahimpour-Banoab, 1997; Halfar et al., 2000) due to its common and successful application in palaeo-environmental reconstructions in other marine organisms (e.g. Chappell and Shackleton, 1986; Gagan et al., 2000). However, $\delta^{18}O$ values in coralline red algae, as for other organisms, appear to be influenced by biological processes, commonly termed the "vital effect" (Urey, 1951). The extent of this vital effect in coralline red algae, which has been proposed to be either dependent upon environmental factors (Rahimpour-Bonab et al., 1997) or species-dependent (Halfar et al., 2000), was recognised in earlier studies to potentially dominate the $\delta^{18}O$ signal, hence rendering difficult any attempt at palaeo-environmental reconstructions (e.g. Wefer and Berger, 1991). Most recently, however, $\delta^{18}O$ records were found to be significantly influenced by sea-surface temperature (SST) variations (Halfar et al., 2000; 2007; 2008; Hetzinger et al., 2009). These studies generally used conventional mass spectrometry (MS) to obtain sub-annual to annually resolved $\delta^{18}O$ records.

Secondary ion microprobe spectrometry (SIMS) enables high-resolution *in situ* measurements of $\delta^{18}O$ values at the sample surface and has previously been successfully used for the reconstruction of environmental parameters in materials of marine origin

(e.g. Trotter et al., 2008; Rigo et al., 2012). Micrometer-scale SIMS analyses were also proven to provide critical insights into biomineralisation processes of zooxanthellate and deep-sea corals (Rollion-Bard et al., 2003a). Instrumental mass fractionation (IMF) is inherent to any type of SIMS measurement due to the nature of the analysis that involves a sputtering of the sample surface. This process results in an energy-based differentiation of ion emission from the sample, where light ions (i.e. with higher energy) are preferentially emitted, and therefore, preferentially recorded by the SIMS detectors. This causes a systematic offset in the isotopic values measured by SIMS, compared to the natural composition of the sample (Slodzian et al., 1980; Shimizu and Hart, 1982). The analysis of standards of known isotopic composition, along with any sample, is generally used to calibrate the SIMS values and overcome this effect. However, as the IMF can be due to various factors depending on the chemical and structural environment of the considered element (Shimizu and Hart, 1982), if the reference material used for calibration does not precisely match the "matrix" of the sample (which is often the case for biogenic samples), the IMF needs to be independently characterised in order to adequately correct for it and obtain accurate measurements of the sample composition. A recent study reported, for instance, a significant effect of the Mg composition of the carbonate material on the IMF during SIMS analyses (Rollion-Bard and Marin-Carbonne, 2011). These authors suggested, however, that the extent of this type of IMF could vary according to different instrumental settings.

In the present study, we used a different type of SIMS instrument, a sensitive, high-resolution ion microprobe (SHRIMP), to assess the influence of Mg content in carbonate samples as being configuration-dependant, or rather, related to the sputtering process, which implies that this will occur in any type of SIMS analysis. After characterisation of other sources of IMF, the corrected $\delta^{18}O$ values obtained for a *Sporolithon durum* rhodolith are compared to conventional $\delta^{18}O$ MS analyses and equilibrium $\delta^{18}O$ values for abiotic high-Mg calcite over the temperature range observed at the collection site. Factors responsible for the $\delta^{18}O$ variations in *S. durum* are discussed, and monthly and inter-annual variations of the $\delta^{18}O$ signal are compared to local SST and SSS records over the 1984-2008 period.

VIII-2 Material and methods

VIII-2.a Samples characteristics and description

Different materials (3 calcites ranging from almost pure calcite to relatively high-Mg calcite, and 4 dolomites) were used to determine the SHRIMP mass fractionation of oxygen

isotopes according to the Mg-content of the carbonate samples. The calcite sample (C1) was from the rock museum at the Research School of Earth Sciences (RSES) of the Australian National University (ANU) and was labelled as collected in England, with no further indication. The 2 high-Mg calcites (HMg C2 and HMg C3) are from different layers of the same Famennian (Devonian) limestone formation, collected in the Emmanuel Range (Canning Basin), Western Australia. The dolomite materials consisted in 2 different dolomites from the Carrara region, Italy (D1 and D2), another sample was collected in the Thornwood area, New York, USA (D3) and one is from the Landegode Island dolomite quarry, in the Bodo region, Norway (D4).

The rhodolith branch analysed here was located along the short axis of a ~8 cm-diameter coralline red algae spheroidal nodule, collected by SCUBA diving in October 2009 in the shallow waters of the Ricaudy Reef (22°18'57"S; 166°27'26"E), New Caledonia (Figure VIII-1). It is formed exclusively by the *S. durum* species.

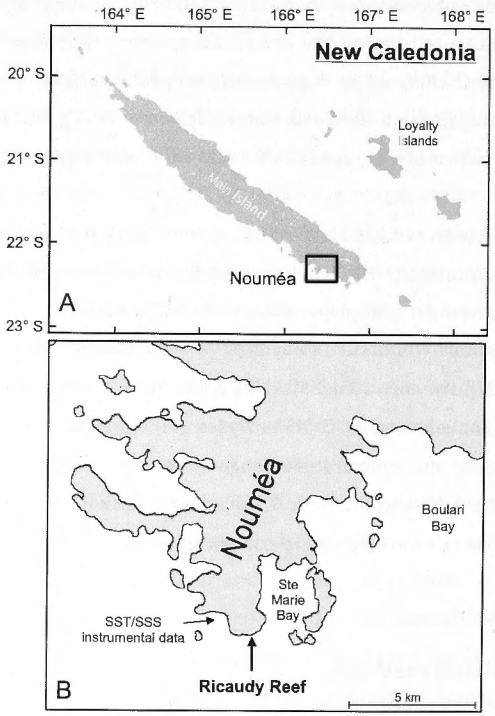

Figure VIII-1 **Location map of New Caledonia (A) and the Ricaudy Reef (B) at the southern end of the Sainte Marie Bay, on the edge of Nouméa. The site of instrumental SST and SSS recording is also shown.**

VIII-2.b Sample preparation

All carbonate materials that were used to assess the Mg-related IMF were crushed down to ~100 µm-diameter grains and mounted in clusters of 10 to 20 grains in the same 35-mm, epoxy resin "megamount", along with NBS18 and NBS19 $CaCO_3$ reference materials. The resin mount was rough cut, then polished with 1 µm diamond, Al-coated and dried out in a vacuum-oven for over 24h prior to SHRIMP analysis. Preparation of the rhodolith branch followed a similar procedure. The entire rhodolith specimen was put into an araldite resin before being cut in half along its long axis. Subsequently, a branch along the short axis of the nodule was separated from the rest and reimpregnated into a 35 mm-diameter resin "megamount", along with grains of the NBS18 and NBS19 reference materials. A 1-µm polishing, Al-coating and vacuum-oven drying preceded the SHRIMP analysis.

For conventional mass spectrometer $\delta^{18}O$ analyses, the carbonate materials were crushed into fine powder and homogenised. Four rhodolith samples were hand-drilled from the back of the "megamount" used for SHRIMP analysis. They represent 4-5 mm-wide holes along the rhodolith branch and were evenly spaced from the outside to the inner part of the branch. About 50 µg of each powder-sample was weighed before proceeding with the MS analysis.

The same "megamounts" as for the SHRIMP analysis were also used for the laser ablation inductively coupled plasma mass spectrometry (LA-ICPMS) measurements.

VIII-2.c SHRIMP operating conditions

High-resolution oxygen isotopic analyses presented herein were performed using the SHRIMPII at the RSES, ANU. The instrument configuration and settings used for oxygen isotope measurements are detailed in Ickert et al. (2008). A positive caesium (Cs^+) primary ion beam is generated, with an impact potential of 15keV and a beam current of ~3nA. Kohler illumination is used to focus and homogenise the primary Cs^+ ion beam that hits the sample surface with a 45° incidence, producing a ~30x40 µm sputtering spot. This configuration leads to a typical production of about 250pA of O^- secondary ions. A medium energy, focused electron gun of oblique incidence (45° from sample surface, 90° from Cs^+ primary beam) maintains the charge neutrality of the sample during the analysis. $^{16}O^-$ and $^{18}O^-$ were measured simultaneously (multi-collector mode) by two, off-axis Faraday cups connected to temperature-regulated, high-vacuum electrometers with ~10^{11} ohms input resistors. Mass resolution at 1% was 1950, which is sufficient to resolve potential isobaric interferences on ^{18}O from $^{16}OH_2$ and ^{16}OD, but not the interference from ^{17}OH (mass resolution of 2300). That resolution was achieved using a 150-µm mass spectrometer

entrance slit, truncating the secondary beam by about 5%, and 300-µm collector slits. The resulting measured $^{18}O^-$ intensity was typically around 5.10^6 cps (counts per second) for the carbonate materials analysis and ranged from ~2 to 5.10^6 cps for the rhodolith branch. The analytical procedure consisted of a 3-min sputtering of the sample surface, which allowed the secondary ion isotopic composition to stabilise. It was then followed by two sets of 6 measurements separated by auto-refocusing. Each measurement lasted 10 s, resulting in a total acquisition time for a single analysis of approximately 2 min.

The various carbonate materials used for IMF correction of Mg content were analysed in clusters of five measurements for each sample, consisting of one measurement on five different grains. This procedure enabled us to test the homogeneity of each material as well as the reproducibility of the instrument. Before and after each series of measurements, a NBS18 standard grain was analysed as a reference to correct for any instrumental drift during the session. For the rhodolith analysis, SHRIMP spots were located along the pre-existing, LA-ICPMS track that followed the branch axis of main growth. Successive measurements were separated by approximately the size of the analytical spot, hence, giving an almost continuous coverage along the branch, at a 30- to 40-µm resolution, with no overlapping measurement (Figure VIII-2). The instrumental drift through time was corrected by the analysis of the NBS19 reference material every 5 to 6 sample measurements. A total of 320 isotopic measurements were carried out along the ~3 cm-long rhodolith branch. Two transects, perpendicular to the axis of main growth, were also performed to assess the reproducibility of the oxygen isotopic composition along single rows of cells.

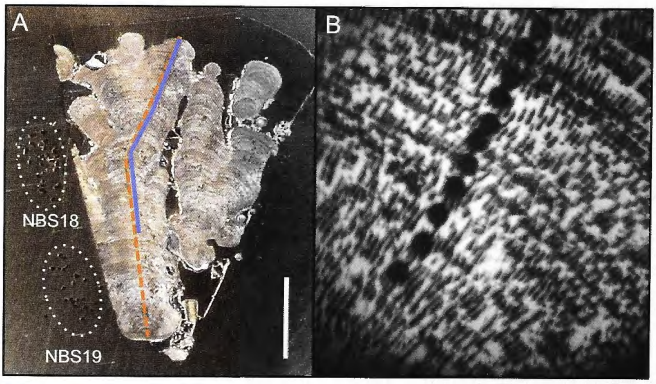

Figure VIII-2 **A: *Sporolithon durum* rhodolith branch impregnated in the SHRIMP araldite "megamount" and coated with aluminium. The track generated by the SHRIMP spots along the branch (thick blue line) is parallel to the LA-ICPMS track (dotted orange line) set to measure the Mg/Ca composition of the sample. The location of the reference materials NBS 18 and NBS 19, near the rhodolith branch is also indicated (dotted ellipses). Scale bar is 500 µm. B: Close up on SHRIMP spots (dark) along the rhodolith branch. Individual spot diameter is ~30 µm.**

VIII-2.d Conventional mass spectrometer $\delta^{18}O$ analysis

The MS analyses of the oxygen isotopic composition of the different carbonate materials and rhodolith samples were carried out at the RSES, ANU, on a Finnigan MAT 251 with a Kiel carbonate device, using 105% phosphoric acid at 90°C. The working gas used (2009-2) has the following isotopic composition: $\delta^{18}O_{VPDB}$=+0.19‰. Data were corrected for ^{17}O interference using the method of Santrock et al. (1985) and normalised such that samples of solid NBS 18 and NBS 19 analysed by this method would yield $\delta^{18}O_{VPDB}$=-23.00‰ and $\delta^{18}O_{VPDB}$=-2.20‰, respectively.

A fractionation factor was applied to the oxygen isotopic values in order to take into account the relative Mg content of each analysed material. Except for the almost pure calcite sample, corrected values were calculated as follow:

$$\delta^{18}O_{corr} = \delta^{18}O_i + 1000 \ln(\alpha_C) - 1000 \ln(\alpha_M) \quad (1)$$

where $\delta^{18}O_i$ is the initial, measured $\delta^{18}O$ value, for which the regular Kiel correction had been applied (see method by Santrock et al., 1985); α_C is the fractionation factor for calcite at 90°C, calculated from equation (1) in Sharma et al. (2002); α_M is the fractionation factor specific to each analysed material according to its Mg content. For dolomites, α_M at 90°C was calculated from equation (3) in Rosenbaum and Sheppard (1986). For the high-Mg calcite materials and the rhodolith, α_M was calculated from equation (4) in Rosenbaum and Sheppard (1986), which takes into account the mole percent of Ca and Mg in the carbonate. Note that this equation was established for a 100°C reaction temperature but is the best approximation available in the literature. The consistency of both the temperature- and composition-dependant equations (i.e. equations (3) and (4) in Rosenbaum and Sheppard, 1986) was tested on the dolomite samples. The resulting fractionation factors are consistent within 4% of their values.

The oxygen isotopic compositions are expressed in per mil notation, relative to the Vienna Pee Dee Belemnite (VPDB) standard ($\delta^{18}O_{VPDB}$) and are presented in Table VIII-1.

VIII-2.e Analysis of Mg/Ca composition

The RSES, ANU, LA-ICPMS (see Eggins et al., 1998; Chapter III, This thesis), composed of an Excimer ArF laser (192 nm wave length) combined with a Varian 820 ICPMS, was used to characterise the Mg/Ca composition of the carbonate materials and the rhodolith branch.

The carbonate materials were analysed by LA-ICPMS after the SHRIMP analyses. 42 µm-diameter laser-spots were focused directly over the sites of previous SHRIMP measurements, which were determined visually at the surface of each analysed grain. Each measurement consisted in ~40 s ablation time at a rate of 10 Hz and energy of 5 J.cm^{-2}. The ICPMS settings were similar to those used for the N4 configuration detailed in Chapter III (This thesis), which involves the measurement of the ^{24}Mg, ^{25}Mg and ^{43}Ca isotopes, with dwell times adding up to ~0.75 s per measurement. All grains (n=35) were successively measured during the same analytical run. At the beginning and end of each run, approximately 60 s of NIST SRM 610 reference material was measured. The NIST SRM 610 was used as external standard for calibration of the carbonate materials Mg/Ca composition, following the data reduction method of Longerich et al. (1996), with ^{43}Ca as the internal standard (see also Chapters III, V, VI, VII, This thesis). In addition, the Mg/Ca composition of the 2 dolomites from the Carrara region (D1-2) was independently determined using electron probe microanalysis (EPMA), ICP atomic emission spectrometry (ICP-AES) and solution ICPMS (see Chapter III, This thesis), which all gave consistent results. These results were used to adjust the values of the NIST SRM 610 calibration that slightly under-estimated the Mg/Ca ratio of the dolomite samples (Chapter III, This thesis; see also Craig et al., 2000). The average of the LA-ICPMS results was taken to characterise the Mg/Ca ratio of each grain and is reported in Table VIII-1, along with the standard deviation corresponding to each series of individual Mg/Ca data points.

For the rhodolith sample, two parallel tracks were analysed, separated by approximately 300 µm. A 42-µm-diameter laser spot was used to scan the branch, from the outside in, at a speed of 5 µm.s^{-1}, a rate of 10 Hz and energy of 5 J.cm^{-2} (N4 configuration in Chapter III, This thesis; see also Chapters V, VI, VII). The ICPMS settings were similar to the ones described above and so was the data reduction method, with the exception of the external standard. In this case, the D2 dolomite from the Carrara region, Italy, was used as external standard for calibration of the Mg/Ca in the rhodolith (Chapter III, This thesis). Results of the two parallel tracks, which presented a good reproducibility ($r=0.76$; $p<0.0001$), were averaged between one another as well as down to a ~30 µm-resolution.

VIII-2.f Chronology and age model determination

The chronology for the rhodolith branch was obtained by combining the determination of seasonal cycles from the LA-ICPMS results, with the counting of annual growth bands

from high-resolution digitised images. This approach is commonly used to establish chronologies in coralline red algal studies (e.g. Hetzinger et al., 2009; 2011a; Chan et al., 2011) and yielded results in agreement with radiocarbon dating for different branches of the rhodolith specimen presented here (see Chapter IV, This thesis). An average extension rate of 0.52 ±0.20 mm.yr^{-1} was obtained for the studied branch, which is concordant with the average extension rate reported for other branches located along the short axis of the same rhodolith (Chapter IV, This thesis). The seasonal variations of Mg/Ca linked to seawater temperature were used to convert geochemical data from a distance- to a time-relative scale using the AnalySeries data analysis software (Paillard et al., 1996) with high (low) peaks in Mg/Ca cycles matching the month of highest (lowest) instrumental SST for each annual cycle. Data points between these anchor points were linearly interpolated and resampled at a monthly resolution. An estimated uncertainty of one to a few months is generally associated with this chronological approach (Hetzinger et al., 2009; 2011a).

Inter-annual variations for the various studied parameters were obtained by applying a 25-point Hanning filter to the monthly data (e.g. as done by Corrège et al., 2000; Le Bec et al., 2000).

VIII-3 Results

VIII-3.a Original SHRIMP results

Three different analytical sessions on the SHRIMP gave an overall internal error of 0.1-0.2‰ on any measurement, associated with a precision of ±0.5‰ based on repeated measurements of standards (n=50; 3 sessions). The range of isotopic values ($\delta^{18}O_{VPDB}$) for the various carbonate materials goes from -3.3 ±0.2‰ for C1 to -15.3 ±0.2‰ for D4 (Table VIII-1). The homogeneity of each material was assessed by the concordance of the $\delta^{18}O$ values recorded on five different grains that are within 1‰ for C1 and D1 to 4 and within 1.5-2‰ for the less homogenous HMg C2 to 3. The $\delta^{18}O_{VPDB}$ values along the rhodolith branch average -12.0 ±2.3‰ and are associated with a wide range of 11.8‰, from a very negative -18.5 to -6.7‰ (Figure VIII-3; Tables VIII-1; VIII-2). The two sets of measurements across the branch, representing ~120-150 µm (i.e. 4 data points) on each side of the main growth direction, are reproducible within 1‰ (<7% variation) in each case.

Sample	Description	Mg/Ca (mol.mol^{-1})	MS $\delta^{18}O$ (‰ VPDB)	SHRIMP $\delta^{18}O$ (‰ VPDB)	$\Delta\ \delta^{18}O$ (‰ VPDB)
NBS18	NIST SRM #8543	0.02 [a]	-23.0 [b]	-23.3 – -22.8	-0.3 – 0.2
C1	Calcite England	0.01 – 0.02	-3,9	-3.9 – -3.3	0.0 – 0.5
HMg C2	High-Mg calcite upper	0.05 – 0.07	-5,8	-5.8 – -3.9	-0.8 – 1.2
HMg C3	High-Mg calcite lower	0.05 – 0.12	-4,9	-5.4 – -3.9	-0.9 – 0.6
D1	Dolomite Carrara 1	0.99 – 1.00	-5,1	-10.0 – -9.1	-6.0 – -5.1
D2	Dolomite Carrara 2	0.98 – 1.00	-8,9	-14.1 – -13.5	-6.2 – -5.7
D3	Dolomite, New York	0.98 – 1.00	-10,2	-14.6 – -13.9	-5.5 – -4.8
D4	Dolomite Bodo, Norway	0.99 – 1.00	-10,6	-15.3 – -14.8	-5.3 – -5.8
Rhodolith	*S. durum*, New Caledonia	0.23 – 0.42	-4.8 ±0.1	-18.5 – -6.7	-13.6 – -1.8

Table VIII-1 **Ranges of LA-ICPMS Mg/Ca content, conventional mass spectrometry (MS) and SHRIMP $\delta^{18}O$ composition and difference between SHRIMP and MS $\delta^{18}O$ composition ($\Delta\ \delta^{18}O$) for the different carbonate samples analysed in this study (see text for more information). Note for NBS18 sample: a: Mg/Ca content calculated from Crowley (2010); b: $\delta^{18}O$ value from Graser et al. (2008).**

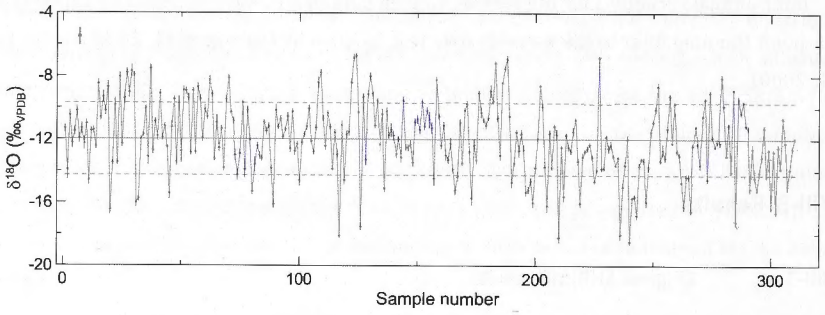

Figure VIII-3 **Original SHRIMP $\delta^{18}O$ dataset. Horizontal plain line represents the average value and dotted lines are ±1 standard deviation. Error bars are instrumental uncertainties for each measurement except for the spot in the top left corner where the error bar represents the extent of $\delta^{18}O$ variation for two sets of four measurements following single rows of cells across the rhodolith branch. Total length: ~13 mm.**

VIII-3.b Instrumental mass fractionation (IMF)

VIII-3.b.1 Effect of the Mg content

Conventional MS oxygen isotope analyses of the carbonate materials resulted in values ranging from -3.9‰ for C1 to -10.6‰ for D4, which is well above the one obtained from the SHRIMP for the same material (Table VIII-1). The difference between the $\delta^{18}O$ values measured from these two methods ($\Delta\ \delta^{18}O$) is linked to the proportion of Mg present in the different carbonate materials (Table VIII-1; Figure VIII-4) and is due to the SHRIMP fractionation in favour of the light oxygen isotope (^{16}O) resulting in lower $\delta^{18}O$ values with

increasing Mg content in the carbonate. The IMF due to the Mg composition of the sample does not depend on the original oxygen isotopic composition of the material and is ~0‰ for pure calcite (Mg/Ca ~0) and up to -5 – -6‰ for the dolomites (Mg/Ca ~1), giving a fractionation factor of ~ -0.6‰ per increasing Mg/Ca molar percent.

The rhodolith samples do not align on this fractionation trend line indicating that other factors must explain the differences observed between the conventional MS and the SHRIMP $\delta^{18}O$ measurements. However, with a Mg/Ca composition varying between ~0.20 and ~0.42, the extent of the Mg-content IMF on the rhodolith $\delta^{18}O$ values measured with the SHRIMP is between -1.0 and -2.2‰.

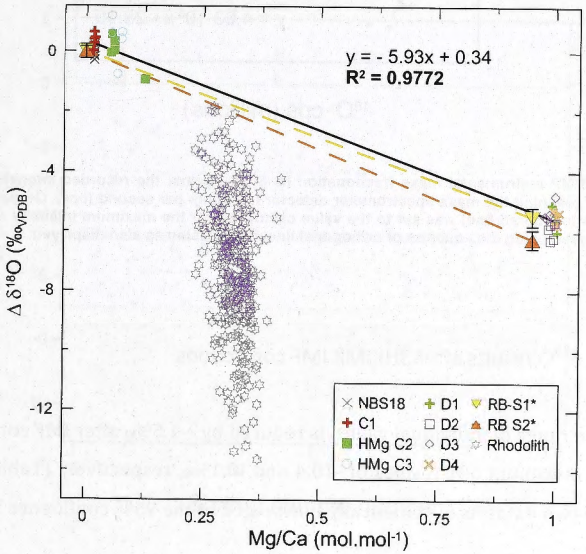

Figure VIII-4 **Instrumental mass fractionation (IMF) calculated as the difference between SHRIMP $\delta^{18}O$ measurements and conventional mass spectrometry $\delta^{18}O$ results ($\Delta\ \delta^{18}O$) represented against the Mg/Ca concentration of the analysed samples. The equation and correlation coefficient of linear regression from the materials analysed in this study (except for the rhodolith samples) are displayed (p<0.0001). Triangle symbols are from Rollion-Bard and Marin-Carbonne (2011).**

VIII-3.b.2 Recorded signal intensity

A significant positive correlation (r=0.50; p<0.001) is observed between the intensity of the recorded secondary oxygen ion signals (cps) and the resulting $\delta^{18}O$ value of the rhodolith samples (Figure VIII-5). In this case, the IMF can reach up to -10‰ for values associated with the lowest cps, compared to the ones for which maximum secondary ion intensities are recorded. The slope of the orthogonal linear fit gives an IMF of -4.6‰ per decreasing million cps on the secondary $^{18}O^-$ ion intensity.

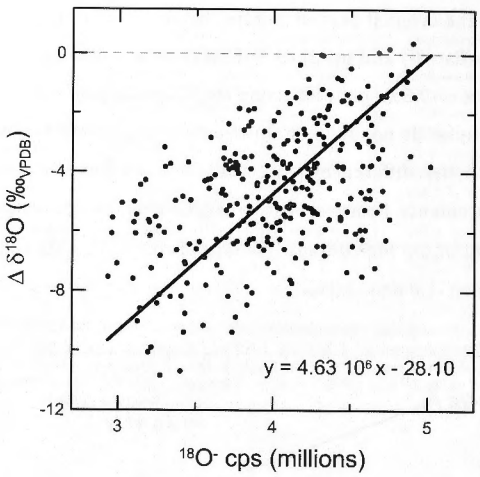

Figure VIII-5 **SHRIMP instrumental mass fractionation (Δ $\delta^{18}O$) against the recorded intensity of secondary $^{18}O^-$ reaching the mass spectrometer detector in counts per second (cps). Origin of the ordinate axis (scattered line) was set to the value calculated for the maximum intensity recorded for the dataset, using the equation of orthogonal linear regression, is also displayed.**

VIII-3.c $\delta^{18}O$ results after SHRIMP IMF corrections

Although the range of individual values is reduced by ~1.5‰ after IMF correction, with minimum and maximum $\delta^{18}O$ values of -10.4 and -0.1‰, respectively (Table VIII-2), the variance of the two datasets is statistically unchanged at the 95% confidence level (F-Test; p=0.10).

Correcting the original $\delta^{18}O$ dataset for the SHRIMP IMF drastically increased the rhodolith average $\delta^{18}O$, to a value of -4.9 ±2.1‰ (~7‰ increase – see Table VIII-2). This corrected $\delta^{18}O$ value is identical, within error, to the one obtained by the conventional MS analysis (Figure VIII-6; Table VIII-1). By comparing the calculated average and range of $\delta^{18}O$ values for inorganic high-Mg calcite at equilibrium in a similar environment (Figure VIII-6 – $\delta^{18}O_{VPDB}$ ~0.0 ±0.8‰), it appears that the vital effect of *S. durum* upon oxygen isotopes incorporation into the skeleton is relatively strong and results in a reduction in $\delta^{18}O$ of 4.1 to 5.7‰. We also observed that the range of $\delta^{18}O$ variation in *S. durum* rhodoliths is ~6.5 times higher than for the high-Mg calcite at equilibrium based on the same temperature range (Figure VIII-6).

Summary satistics	Original $\delta^{18}O$ (‰)	IMF-corrected $\delta^{18}O$ (‰)
Average	-12.0	-4.9
Std Err	0.1	0.1
Std Dev	2.3	2.1
Variance	5.2	4.5
Range	11.8	10.3
Min	-18,5	-10,4
Max	-6.7	-0.1

Table VIII-2 **Summary statistics for SHRIMP $\delta^{18}O$ values, before and after correction for instrumental mass fractionation (IMF – see text for details).**

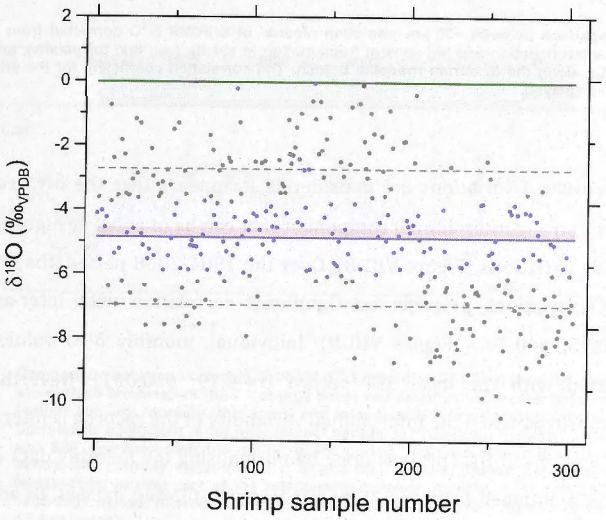

Figure VIII-6 **Range of SHRIMP $\delta^{18}O$ values after instrumental mass fractionation corrections (blue dots). The average value (blue line) and the standard deviation (dotted lines: ±1σ) are also represented, along with the range of $\delta^{18}O$ values measured by conventional mass spectrometry analysis (light red area). The equilibrium $\delta^{18}O$ average value for inorganic high-Mg calcite (green line) was calculated for an average of 22 $MgCO_3$ mol% from Jimenez-Lopez et al. (2004), using a $\delta^{18}O_{sw}$ of ~0.5‰ (LeGrande and Schmidt, 2006). The range of equilibrium values (light green area) was calculated from Kim and O'Neil (1997) for temperatures varying from 20 to 29 °C.**

VIII-3.d $\delta^{18}O$ variation in *S. durum*

SHRIMP $\delta^{18}O$ values show a significant negative correlation ($r=-0.34$; $p<0.001$) with the Mg/Ca record along the rhodolith branch (Figure VIII-7), after correction for IMF and the Mg-content effect on $\delta^{18}O$ variations (see Discussion below).

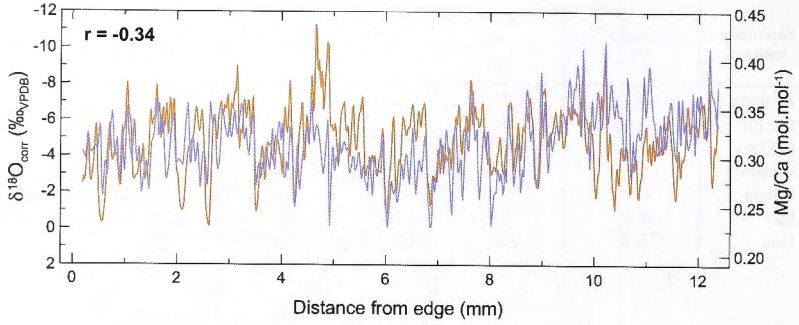

Figure VIII-7 **Comparison between ~30 µm-resolution records of SHRIMP $\delta^{18}O$ corrected from instrumental mass fractionation and Mg-content fractionation in calcite (see text for details), and LA-ICPMS Mg/Ca along the *S. durum* rhodolith branch. The correlation coefficient for the entire series is also displayed.**

When time-resolved variations are considered, it appears that the $\delta^{18}O$ record in *S. durum* presents a strong inter-annual component that can be of equal or higher amplitude than the monthly variations (Figure VIII-8). Over the 1984-2008 period, the inter-annual pattern of $\delta^{18}O$ variations presents no significant correlation with inter-annual SST variations ($r=0.05$; $p=0.39$ – Figure VIII-8). Individual, monthly $\delta^{18}O$ values are only weakly correlated with the local SST record ($r=-0.19$; $p=0.001$). Nevertheless, this correlation is improved when the inter-annual variability of the records is filtered out ($r=-0.33$; $p<0.05$ – Figure VIII-8). This was done by normalising the monthly data against the inter-annual trend obtained from the 25-points Hanning-filtered dataset. In addition, the average annual pattern of $\delta^{18}O$ variations in *S. durum* over the 1984-2008 period is concordant with the local SST, with more negative $\delta^{18}O$ values during the austral summer and higher $\delta^{18}O$ values in winter (Figure VIII-8). The range of $\delta^{18}O$ variations against local SST for the average annual pattern as well as the slope of the linear fit between the SST and $\delta^{18}O$ monthly data (filtered out from inter-annual variability), give comparable values of -0.19 and -0.21‰.°C^{-1}, respectively.

The comparison between the $\delta^{18}O$ record in *S. durum* and SSS variations shows a significant, positive relationship ($r=0.64$; $p<0.05$) at the inter-annual level (Figure VIII-8), whereas when these variations are filtered out, the correlation between the respective monthly datasets is insignificant at the 95% confidence level ($r=-0.10$; $p=0.14$ – data not shown). This is also illustrated by the misfit between the $\delta^{18}O$ and SSS average annual patterns (Figure VIII-8).

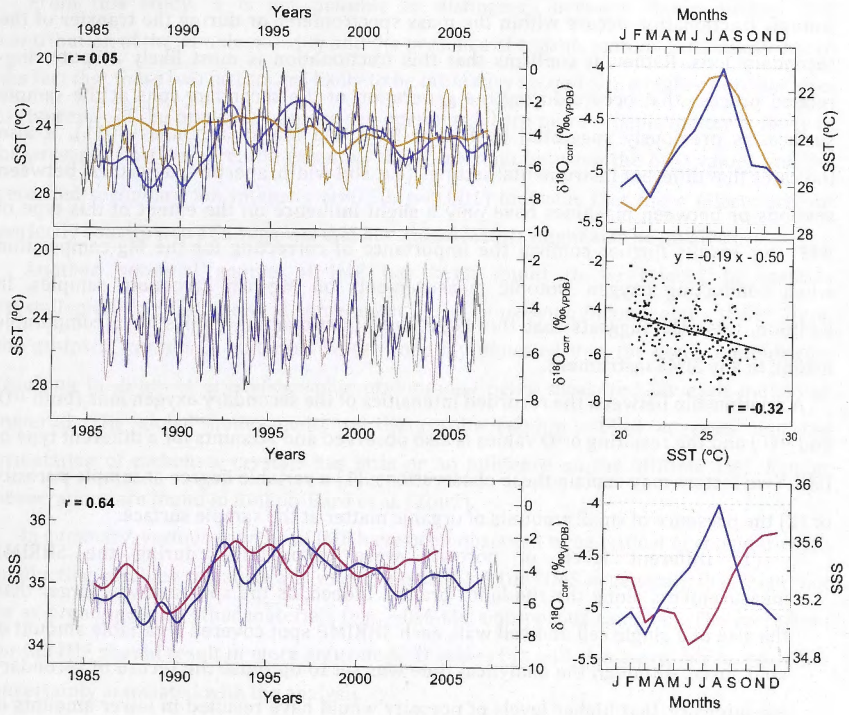

Figure VIII-8 Comparison between corrected SHRIMP $\delta^{18}O$ record in *S. durum* rhodolith (blue lines) and local sea-surface temperature (SST – orange lines) and salinity (SSS – pink lines), over the 1984-2008 period. Top-left: monthly (thin lines) and inter-annual (thick lines) variations of $\delta^{18}O$ and SST. Correlation coefficient is for inter-annual variations. Top-right: monthly, annual pattern of $\delta^{18}O$ and SST averaged over the entire record period. Note the reversed scale of SST variations. Middle-left: monthly variations of $\delta^{18}O$ and SST signals, filtered from inter-annual variations. Middle-right: scatter plot of the relationship between monthly $\delta^{18}O$ and SST signals over the 1985-2007 period, filtered from inter-annual variations. Bottom figures as for top ones but for SSS variations.

VIII-4 Discussion

VIII-4.a SHRIMP IMF

A significant SHRIMP IMF was found to be related to the Mg-content of the analysed carbonate samples. This is in agreement with the results of a recent study (Rollion-Bard and Marin-Carbonne, 2011) carried out using another SIMS instrument (Cameca 1270), in which the secondary ion extraction optics are very different from the SHRIMP (Ireland, 1995). The fact that the slope of the IMF versus Mg-content reported in our study and the ones in Rollion-Bard and Marin-Carbonne (2011) are very similar (-5.9‰ and -5.8‰; -6.7‰. Mg/Ca mol%$^{-1}$, respectively – Figure VIII-4) eliminates the possibility that oxygen

isotopic fractionation occurs within the mass spectrometer or during the transfer of the secondary ions. Rather, it confirms that this fractionation is most likely a sputtering-related process that occurs during the generation of the secondary ions at the sample surface, as previously suggested by Rollion-Bard and Marin-Carbonne (2011). It also indicates that different instrumental settings (e.g. slid width, aperture, detectors) between sessions or between machines have only a slight influence on the extent of this type of IMF. Our results further confirm the importance of correcting for the Mg-composition when conducting oxygen isotopic measurements on Mg-rich carbonate samples. In addition, this also suggests that this Mg-related fractionation applies, to a comparable extent, to any SIMS instrument.

A relationship between the recorded intensities of the secondary oxygen ions (both $^{18}O^-$ and $^{16}O^-$) and the resulting $\delta^{18}O$ values is also observed and accounts for a different type of IMF. Two factors may explain these observations: (1) a variable degree of sample porosity or (2) the presence of small amounts of organic matter at the sample surface.

(1) Different levels of porosity were encountered during the SHRIMP measurements along the rhodolith branch. Indeed, as the spot size was larger than the size of a single cell and cell wall, each SHRIMP spot covered a variable amount of void space. Although the analytical time was set to optimise the record of secondary ion intensity, that higher levels of porosity would have resulted in lower amounts of secondary ions reaching the spectrometer's detector. As light isotopes are preferentially emitted during the sputtering process (Slodzian et al., 1980; Shimizu and Hart, 1982), it is possible that, when maximum levels of secondary ion intensity are not reached, a higher proportion of $^{16}O^-$ is recorded, resulting in depleted $\delta^{18}O$ values. Rollion-Bard et al. (2007), however, recorded no significant effect of porosity on the secondary ion intensities (or the resulting $\delta^{18}O$ values) for a SIMS analysis of corals.

(2) SIMS measurements of organic matter using a similar procedure to the one for carbonate samples have yielded drastically lower oxygen secondary ions intensities (i.e. a 5000-times decrease in secondary $^{16}O^-$ cps) and a very important $\delta^{18}O$ depletion ($\Delta\ \delta^{18}O$=-95‰ for araldite, uncorrected – Rollion-Bard et al., 2003b). Although the results of our analysis are far from these extreme values (i.e. maximum of 2-times decrease in $^{16}O^-$ cps and a maximum $\Delta\ \delta^{18}O$ of ~ -11‰), it is possible that the presence of a small amount organic matter in our sample may explain the trend in IMF observed here. In this respect, it has to be noted that small quantities of organic matter are suspected inside the cell structure of *S. durum* (Chapter III, This thesis).

From this study, it is not possible to distinguish between the respective IMF contribution of the sample porosity and the presence of organic matter, particularly due to the fact that these two factors are likely to be intimately related (i.e. a higher porosity level is the result of the presence of more cell openings where more organic matter is likely to be present). Furthermore, the extent of the correlation between the $\delta^{18}O$ values and the recorded secondary ion intensity ($r=0.50$; $p<0.001$) indicates that these effects are not perfectly constrained and suggests that additional factors might also be involved.

Another potential source of IMF has been found to be related to variable crystallographic orientations in some material (i.e. muscovite, Deloule et al., 1992). Here, the grains of carbonate materials were randomly mounted into the resin, undoubtedly resulting in different crystallographic orientations being measured for each individual material. The global homogeneity of the results (within ~1‰) suggests that the orientation of carbonate crystals has little or no influence on the SHRIMP IMF. Similar observations are found in Rollion-Bard et al. (2007).

In summary, various sources of IMF have been observed to be critical to consider when conducting coralline red algae analyses using SHRIMP (or SIMS in general), that might not be as pronounced in other materials (e.g. ~0%-Mg, non-porous samples). The correction for the IMF should result in more accurate $\delta^{18}O$ values but will also inevitably increase the uncertainty associated with the analysis.

VIII-4.b Rhodolith $\delta^{18}O$ composition

The SHRIMP $\delta^{18}O_{VPDB}$ values for the *S. durum* rhodolith branch, corrected for the IMF, give an average value of -4.9‰ that is within the range of previously reported $\delta^{18}O$ values for coralline red algae (-6 – 0‰; Milliman, 1974; Morrisson and Brand, 1986; Halfar et al., 2000). This value for a tropical rhodolith specimen is lower than recently published values for other coralline red algae species from cold environments (Halfar et al., 2000; 2008). In agreement with Rahimpour-Bonab et al. (1997), we attribute this difference to temperature, rather than differences in seawater $\delta^{18}O$ ($\delta^{18}O_{sw}$) that might exist between the different environments. These authors, however, along with Halfar et al. (2000), proposed that the lower $\delta^{18}O$ value recorded in tropical coralline red algae compared to their cold-environment counterparts, might also be due to a higher degree of vital effect, as higher temperatures would result in higher metabolic activity (Rahimpour-Bonab et al., 1997). Similarly, the $\delta^{18}O$ disequilibrium recorded here in *S. durum* compared to the $\delta^{18}O$ values for abiotic high-Mg calcite (i.e. vital effect), is more important than for cold-water species (e.g Halfar et al., 2000; 2008), although it is still comparable to the ones reported

in the literature (e.g. Milliman, 1974; Wefer and Berger, 1991). Higher extension rates in *S. durum* (Chapter IV, This thesis) might also contribute to the more negative $\delta^{18}O$ values observed here (Dietzel et al., 2009). A species-specific vital effect on oxygen isotopic fractionation in coralline red algae is also likely to exist and should not be ignored when trying to explain the observed differences.

VIII-4.c Range of $\delta^{18}O$ values

The range of $\delta^{18}O$ values (10.4‰) obtained from the SHRIMP analyses of the rhodolith branch at high resolution is very similar to that recorded for a *Porites lutea* coral, also from New Caledonia (Rollion-Bard et al., 2003a;b), possibly suggesting comparable oxygen isotope fractionation processes between tropical coralline red algae and corals. To explain this large range of $\delta^{18}O$ values, seasonal SST variations at the Ricaudy Reef (~9°C) are not sufficient. The $\delta^{18}O$ variability potentially linked to SST, calculated from Kim and O'Neill (1997), is ~1.8‰. Salinity changes may also account for some of the $\delta^{18}O$ variability, through changes in the $\delta^{18}O_{sw}$. The value of 0.4‰.psu^{-1} has been reported by Morimoto et al. (2002) as a maximum fractionation factor attributable to salinity changes. At the collection site, the SSS variations reached approximately 2 psu over the 1984-2008 period, resulting in a maximum of ~0.8‰ variation in $\delta^{18}O_{sw}$. Both of these environmental parameters, even if combined, cannot explain the $\delta^{18}O$ variability in *S. durum*. Other factors need, therefore, to be considered. A fractionation of the oxygen isotopes in carbonates, linked to the Mg-content of the material and independent from the IMF discussed above, translates as an increase of 0.13‰ per $MgCO_3$ mol% (Jimenez-Lopez et al., 2004). In our case, to correct for this fractionation would affect the range of $\delta^{18}O$ values by less than 2‰. The effect of the carbonate calcification rate has also been reported as potentially significant (e.g. McConnaughey, 1989a;b; Dietzel et al., 2009). Based on Dietzel et al. (2009) findings, we calculated a possible $\delta^{18}O$ range reduction of ~0.6‰, based on the annual extension rates recorded for the *S. durum* rhodolith branch over the studied period (0.2-0.8 mm.yr^{-1}). A very simplified and rough estimation of the reality would be to consider that all of these factors are intimately related and that the correction for the relative fractionations acts toward an overall reduction of the $\delta^{18}O$ range in *S. durum*. Even under this unlikely, ideal scenario, a $\delta^{18}O$ range of ~5.2‰ would still remain unexplained.

Variations in pH explain, to some extent, the $\delta^{18}O$ fractionation in foraminifera (Spero et al., 1997; Zeebe, 1999) as well as a >10‰ $\delta^{18}O$ range in corals (Rollion-Bard et al., 2003a; 2007). We propose that pH variations also most likely explain a significant part of

the observed $\delta^{18}O$ range in the *S. durum* rhodolith as pH controls the proportion of the carbonate species in any solution (i.e. H_2CO_3; HCO_3^-; CO_3^{2-}). For each of the carbonate species possessing a different $\delta^{18}O$ signature, the $\delta^{18}O$ value measured in a solution, therefore reflects the proportion of each carbonate species and, thus, contains pH information (McCrea, 1950; Usdowski and Hoefs, 1993; Zeebe, 1999). According to Usdowski and Hoefs (1993), a variation of ~5‰ in $\delta^{18}O$ corresponds to a pH variation of ~5 units (see also Rollion-Bard et al., 2003b). Although pH>9.5 can result from high photosynthetic activity of the seagrass beds in shallow, tropical lagoons (Semesi et al., 2009), we consider that a pH variation of 5 units is unlikely to occur in the natural environment. However, it may be possible that high pH variations occur in the coralline red alga calcifying fluids. Although direct pH measurements in corals' calcifying structures showed variations of ~1 unit (Al-Horani et al., 2003a;b), as processes of calcification between corals and coralline red algae are somewhat different (e.g. corals: Gattuzo et al., 1999; coralline algae: Bilan and Usov, 2001) and no direct (micro electrode or microsensor) or indirect (e.g. boron isotopes) measurements of pH in coralline red algae are so far available in the literature, a variation of ~5 pH units in the calcifying fluid of *S. durum* cannot be ruled out.

Another potential pH-related explanation for the wide range of $\delta^{18}O$ values observed in the rhodolith resides in the kinetics of the calcification process. Indeed, as described in Rollion-Bard et al. (2003a), the pH of the solution also controls the way HCO_3^- ions are produced, either by CO_2 hydration or hydroxylation. These two reactions have different equilibrium times in seawater as well as different $\delta^{18}O$ fractionation factors (Johnson, 1982; Rollion-Bard et al., 2003a). Therefore, for a defined pH range, differences in the kinetics of calcification may result in different levels of oxygen isotope fractionation that could translate in the precipitated carbonate mineral (Rollion-Bard et al., 2003a).

It was beyond the scope of this study to provide precise, quantitative information on the extent of each discussed factor. However, it appears that the $\delta^{18}O$ composition of *S. durum* rhodoliths at high resolution is the result of more than only environmental variability. Therefore, the use of SHRIMP methodology for $\delta^{18}O$ analyses may have the potential to provide critical insights into biologically-related processes in coralline red algae.

VIII-4.d $\delta^{18}O$ variations in rhodoliths

Both the anti-correlations between $\delta^{18}O$ and Mg/Ca along the rhodolith branch and between $\delta^{18}O$ filtered from inter-annual variations and the local SST at monthly resolution

suggest that a seasonal temperature signal may be recovered from $\delta^{18}O$ measurements in *S. durum*. Furthermore, the extent of $\delta^{18}O$ variations against the range of SST (determined by the slope of the linear fit at monthly resolution as well as by the average annual patterns for the 1984-2008 period) matches the one for abiotic calcite (-0.2‰.°C^{-1} – Kim and O'Neil, 1997) and is comparable to previously reported values for other coralline red algal species (Halfar et al., 2000; 2008). However, the poor correlation coefficients also indicate that the environmental signal present in the high-resolution $\delta^{18}O$ variations recorded from SHRIMP analyses is likely to be altered by significant sources of uncertainties, which can be:

(1) instrumental: when undertaking SIMS analyses, the nature of the coralline red algae inevitably results in a necessity for IMF corrections;

(2) methodological: associated with the fit between the Mg/Ca, LA-ICPMS dataset and the $\delta^{18}O$, SHRIMP spots, as well as with age model uncertainties;

(3) biological: linked to the hardly quantifiable, high-resolution heterogeneity of coralline red algae metabolic processes that potentially affect the $\delta^{18}O$ fractionation.

Considering the inter-annual variations enables us to overcome the methodological sources of uncertainty as well as to reduce the dominance of high-resolution vital effects (see also Rollion-Bard et al., 2003a). At this particular scale, the $\delta^{18}O$ variations in *S. durum* do not show any significant relationship with the local SST but, rather, significantly correlate with the SSS pattern, particularly recording the abrupt increase in salinity at the site in the early 1990s (Figure VIII-8). This correlation is not surprising as in New Caledonia, and in the tropics in general, SST patterns have limited inter-annual variability whereas the SSS signal is mostly dominated by an inter-annual pattern (e.g. Nicet and Delcroix, 2000). Furthermore, monthly-filtered $\delta^{18}O$ records are commonly used in other calcareous marine organisms (e.g. corals) to reconstruct inter-annual $\delta^{18}O_{sw}$ variations that are related to SSS changes (Corrège et al., 2000; Le Bec et al., 2000; Kilbourne et al., 2004; Corrège, 2006). However, in our case, the range of $\delta^{18}O$ variation against SSS (+3.3‰.psu^{-1}) considerably exceeds the maximum predicted $\delta^{18}O_{sw}$ variations (~0.4‰.psu^{-1}). Consequently, we speculate that instead of directly recording $\delta^{18}O_{sw}$ variations, the inter-annual SHRIMP $\delta^{18}O$ signal in *S. durum* is either still biased by undetermined IMF factors that have not been corrected for and appear to control the amplitude of $\delta^{18}O$ variations, or is primarily affected by other parameters that are, themselves, related to the local SSS pattern.

In any case, it appears that $\delta^{18}O$ analyses in tropical coralline red algae could possibly lead to the reconstruction of environmental signals at monthly to inter-annual resolutions. However, due to the multiple sources of uncertainty that are likely to bias the $\delta^{18}O$ record,

we are reserved concerning the use of high-resolution SIMS as the ideal analytical approach to achieve such a goal.

VIII-5 Conclusion

Oxygen isotopic analyses of coralline red algae were conducted for the first time using the SHRIMP technique.

An Mg-content-related IMF for carbonate samples was found to be of comparable extent to the one recently reported using a different SIMS instrumentation, confirming that the oxygen fractionation occurs during the sputtering process. Another type of IMF was related to the intensity of secondary oxygen ion beam reaching the MS detector and might be attributed to the sample porosity, the presence of a small amount of organic matter or a combination of both.

Correcting for the IMF led to an increase of ~7‰ in the average $\delta^{18}O$ value that was, then, similar to the $\delta^{18}O$ measurements from conventional MS, as well as within the range of previously published values for other species of coralline red algae.

The range of $\delta^{18}O$ variations at high-resolution could not be explained by environmental factors such as SST or SSS alone. Other potential factors were discussed, one of the most probable being the effect of pH on the oxygen isotopic fractionation occurring during calcification processes. We therefore suggest that future $\delta^{18}O$ SHRIMP analyses associated, for example, with carbon and boron isotopic measurements, may considerably improve our understanding of the metabolic behaviour and vital effects of coralline red algae, as has been the case previously for other marine organisms.

Environmental signals might, nevertheless, still be recovered from the *S. durum* $\delta^{18}O$ variations at monthly to inter-annual timescales using SHRIMP analyses. However, due to the multiple sources of uncertainty associated both with the nature of the sample and the instrumentation, further developments of the method are required.

References

Adey, W., H., and MacIntyre, I., G. 1973. Crustose Coralline Algae: A Re-evaluation in the Geological Sciences. *Geological Society of America Bulletin* **84**, 883-904

Al-Horani, F. A., Al-Moghrabi, S. M., and de Beer, D. 2003a. Microsensor study of photosynthesis and calcification in the scleractinian coral *Galaxea fascicularis*: active internal carbon cycle. *Journal of experimental marine biology and ecology* **288**(1), 1-15

Al-Horani, F. A., Al-Moghrabi, S. M., and De Beer, D. 2003b. The mechanism of calcification and its relation to photosynthesis and respiration in the scleractinian coral *Galaxea fascicularis*. *Marine Biology* **142**(3), 419-426

Bilan, M. I., and Usov, A. I. 2001. Polysaccharides of calcareous algae and their effect on the calcification process. *Russian Journal of Bioorganic Chemistry* **27**(1), 2-16

Bosence, D., W., J. (1983). The Occurence and Ecology of Recent Rhodoliths - A Review. *In* "Coated Grains." (T. M. Peryt, Ed.), pp. 225-242. Springer-Verlag Berlin.

Burdett, H., Kamenos, N. A., and Law, A. 2010. Using coralline algae to understand historic marine cloud cover. *Palaeogeography, Palaeoclimatology, Palaeoecology* **302**, 65-70

Chan, P., Halfar, J., Williams, B., Hetzinger, S., Steneck, R., Zack, T., and Jacob, D. E. 2011. Freshening of the Alaska Coastal Current recorded by coralline algal Ba/Ca ratios. *Journal of Geophysical Research* **116**(G1), G01032

Chappell, J., and Shackleton, N. J. 1986. Oxygen isotopes and sea level. *Nature* **324**, 137-140

Corrège, T. 2006. Sea surface temperature and salinity reconstruction from coral geochemical tracers. *Palaeogeography, Palaeoclimatology, Palaeoecology* **232**(2), 408-428

Corrège, T., Delcroix, T., Récy, J., Beck, W., and Cabioch, G. 2000. Evidence for stronger El Nino-Southern Oscillation (ENSO) events. *Paleoceanography* **15**(4), 465-470

Craig, C. A., Jarvis, K. E., and Clarke, L. J. 2000. An assessment of calibration strategies for the quantitative and semi-quantitative analysis of calcium carbonate matrices by laser ablation-inductively coupled plasma-mass spectrometry (LA-ICP-MS). *Journal of Analytical Aomic Spectrometry* **15**(8), 1001-1008

Crowley, S. F. 2010. Mineralogical and Chemical Composition of International Carbon and Oxygen Isotope Calibration Material NBS 19, and Reference Materials NBS 18, IAEA-CO-1 and IAEA-CO-8. *Geostandards and Geoanalytical Research* **34**(2), 193-206

Deloule, E., Chaussidon, M., and Allé, P. 1992. Instrumental limitations for isotope measurements with a Caméca® ims-3f ion microprobe: Example of H, B, S and Sr. *Chemical Geology: Isotope Geoscience section* **101**(1-2), 187-192

Dietzel, M., Tang, J., Leis, A., and Köhler, S. J. 2009. Oxygen isotopic fractionation during inorganic calcite precipitation - Effects of temperature, precipitation rate and pH. *Chemical Geology* **268**(1), 107-115

Eggins, S. M., Kinsley, L. P. J., and Shelley, J. M. G. 1998. Deposition and element fractionation processes during atmospheric pressure laser sampling for analysis by ICP-MS. *Applied Surface Science* **127**, 278-286

Foster, M., S. 2001. Rhodoliths: Between rocks and soft places. *Journal of Phycology* **37**, 659-667

Gagan, M. K., Ayliffe, L. K., Beck, J. W., Cole, J. E., Druffel, E. R. M., Dunbar, R. B., and Schrag, D. P. 2000. New views of tropical paleoclimates from corals. *Quaternary Science Reviews* **19**(1-5), 45-64

Gattuso, J. P., Allemand, D., and Frankignoulle, M. 1999. Photosynthesis and calcification at cellular, organismal and community levels in coral reefs: a review on interactions and control by carbonate chemistry. *American Zoologist* **39**(1), 160-183

Graser, G., Potter, J., Köhler, J., and Markl, G. 2008. Isotope, major, minor and trace element geochemistry of late-magmatic fluids in the peralkaline Ilímaussaq intrusion, South Greenland. *Lithos* **106**(3-4), 207-221

Halfar, J., Steneck, R., S., Joachimski, M., Kronz, A., and Wanamaker Jr., A., D. 2008. Coralline red algae as high-resolution climate recorders. *Geology* **36**(6), 463-466

Halfar, J., Steneck, R., S., Schöne, B., R., Moore, G., W., K., Joachimski, M., Kronz, A., Fietzke, J., and Estes, J. 2007. Coralline alga reveals first marine record of subarctic North Pacific climate change. *Geophysical Research Letters* **34**, L07702

Halfar, J., Zack, T., Kronz, A., and Zachos, J., C. 2000. Growth and high-resolution paleoenvironmental signals of rhodoliths (coralline red algae): A new biogenic archive. *Journal of Geophysical Research* **105**(C9), 22,107-22,116

Hetzinger, S., Halfar, J., Kronz, A., Steneck, R., Adey, W., H., Lebednik, P., A., and Schöne, B., R. 2009. High-resolution Mg/Ca ratios in a coralline red alga as a proxy for Bering Sea temperature variations from 1902 to 1967. *Palaios* **24**, 406-412

Hetzinger, S., Halfar, J., Zack, T., Gamboa, G., Jacob, D. E., Kunz, B. E., Kronz, A., Adey, W., Lebednik, P. A., and Steneck, R. S. 2011a. High-resolution analysis of trace elements in crustose coralline algae from the North Atlantic and North Pacific by laser ablation ICP-MS. *Palaeogeography, Palaeoclimatology, Palaeoecology* **302**(1-2), 81-94

Hetzinger, S., Halfar, J., Mecking, J. V., Keenlyside, N. S., Kronz, A., Steneck, R. S., Adey, W. H., and Lebednik, P. A. 2011b. Marine proxy evidence linking decadal North Pacific and Atlantic climate. *Climate Dynamics*, 10.1007/s00382-011-1229-4

Ickert, R. B., Hiess, J., Williams, I. S., Holden, P., Ireland, T. R., Lanc, P., Schram, N., Foster, J. J., and Clement, S. W. 2008. Determining high precision, in situ, oxygen isotope ratios with a SHRIMP II: analyses of MPI-DING silicate-glass reference materials and zircon from contrasting granites. *Chemical Geology* **257**(1-2), 114-128

Ireland T. R. 1995. Ion microprobe mass spectrometry: Techniques and applications in cosmochemistry, geochemistry and geochronology. In *Advances in Analytical Geochemistry (ed. M. Hyman and M. Row), pp. 1–118. JAI Press*

Johnson, K. S. 1982. Carbon dioxide hydration and dehydration kinetics in seawater. *Limnology and Oceanography* **27**(5), 849-855

Kilbourne, K. H., Quinn, T. M., Taylor, F. W., Delcroix, T., and Gouriou, Y. 2004. El Nino Southern Oscillation-Related Salinity Variations Recorded in the Skeletal Geochemistry of a *Porites* Coral from Espiritu Santo, Vanuatu. *Paleoceanography* **19**(4), PA4002

Kim, S. T., and O'Neil, J. R. 1997. Equilibrium and nonequilibrium oxygen isotope effects in synthetic carbonates. *Geochimica et cosmochimica acta* **61**(16), 3461-3475

Le Bec, N., Juillet-Leclerc, A., Corrège, T., Blamart, D., and Delcroix, T. 2000. A coral δ18O record of ENSO driven sea surface salinity variability in Fiji (south-western tropical Pacific). *Geophysical research letters* **27**(23), 3897-3900

LeGrande, A. N., and Schmidt, G. A. 2006. Global gridded data set of the oxygen isotopic composition in seawater. *Geophysical Research Letters* **33**(12), L12604

Longerich, H. P., Jackson, S. E., and Gunther, D. 1996. Laser ablation inductively coupled plasma mass spectrometric transient signal data acquisition and analyte concentration calculation. *Journal of Analytical Atomic Spectrometry* **11**(9), 899-904

McConnaughey, T. 1989a. 13C and 18O isotopic disequilibrium in biological carbonates: I. Patterns. *Geochimica et cosmochimica acta* **53**(1), 151-162

McConnaughey, T. 1989b. 13C and 18O isotopic disequilibrium in biological carbonates: II. In vitro simulation of kinetic isotope effects. *Geochimica et cosmochimica acta* **53**(1), 163-171

McCrea, J. M. 1950. On the isotopic chemistry of carbonates and a paleotemperature scale. *The Journal of Chemical Physics* **18**, 849

Milliman, J. D. 1974. Marine carbonates. Part 1: recent sedimentary carbonates. *Springer-Verlag*, 375pp

Morimoto, M., Abe, O., Kayanne, H., Kurita, N., Matsumoto, E., and Yoshida, N. 2002. Salinity records for the 1997-98 El-Nino from Western Pacific corals. *Geophysical Research Letters* **29**(11), 35-1

Morrison, J. O., and Brand, U. 1986. Paleoscene# 5. Geochemistry of recent marine invertebrates. *Geoscience Canada* **13**(4), 237-254

Nicet, J. B., and Delcroix, T. 2000. ENSO-Related Precipitation Changes in New Caledonia, Southwestern Tropical Pacific: 1969-98. *Monthly Weather Review* **128**(8), 3001-3006

Paillard, D., Labeyrie, L., and Yiou, P. 1996. Macintosh program performs time-series analysis. *Eos Transactions AGU* **77**(39), 379

Rahimpour-Bonab, H., Bone, Y., and Moussavi-Harami, R. 1997. Stable isotope aspects of modern molluscs, brachiopods, and marine cements from cool-water carbonates, Lacepede Shelf, South Australia. *Geochimica et cosmochimica acta* **61**(1), 207-218

Rigo, M., Trotter, J. A., Preto, N., and Williams, I. S. 2012. Oxygen isotopic evidence for Late Triassic monsoonal upwelling in the northwestern Tethys. *Geology*, published online 10 April 2012. doi: 10.1130/G32792.1

Rollion-Bard, C., Blamart, D., Cuif, J. P., and Juillet-Leclerc, A. 2003b. Microanalysis of C and O isotopes of azooxanthellate and zooxanthellate corals by ion microprobe. *Coral Reefs* **22**(4), 405-415

Rollion-Bard, C., Chaussidon, M., and France-Lanord, C. 2003a. pH control on oxygen isotopic composition of symbiotic corals. *Earth and Planetary Science Letters* **215**(1), 275-288

Rollion-Bard, C., and Marin-Carbonne, J. 2011. Determination of SIMS matrix effects on oxygen isotopic compositions in carbonates. *Journal of Analytical Atomic Spectrometry* **26**(6), 1285-1289

Rollion-Bard, C., Vigier, N., and Spezzaferri, S. 2007. In situ measurements of calcium isotopes by ion microprobe in carbonates and application to foraminifera. *Chemical Geology* **244**(3-4), 679-690

Rosenbaum, J., and Sheppard, S. M. F. 1986. An isotopic study of siderites, dolomites and ankerites at high temperatures. *Geochimica et cosmochimica acta* **50**(6), 1147-1150

Santrock, J., Studley, S. A., and Hayes, J. M. 1985. Isotopic analyses based on the mass spectra of carbon dioxide. *Analytical chemistry* **57**(7), 1444-1448

Semesi, I. S., Kangwe, J., and Björk, M. 2009. Alterations in seawater pH and CO2 affect calcification and photosynthesis in the tropical coralline alga, *Hydrolithon* sp.(Rhodophyta). *Estuarine, Coastal and Shelf Science* **84**(3), 337-341

Sharma, S. D., Patil, D. J., and Gopalan, K. 2002. Temperature dependence of oxygen isotope fractionation of CO2 from magnesite-phosphoric acid reaction. *Geochimica et cosmochimica acta* **66**(4), 589-593

Shimizu, N., and Hart, S. R. 1982. Applications of the ion microprobe to geochemistry and cosmochemistry. *Annual Review of Earth and Planetary Sciences* **10**, 483

Slodzian, G., Lorin, J. C., and Havette, A. 1980. Isotopic effect on the ionization probabilities in secondary ion emission. *Journal de Physique Lettres* **41**(23), 555-558

Spero, H. J., Bijma, J., Lea, D. W., and Bemis, B. E. 1997. Effect of seawater carbonate concentration on foraminiferal carbon and oxygen isotopes. *Nature* **390**, 497-500

Steneck, R. S. 1986. The ecology of coralline algal crusts: convergent patterns and adaptative strategies. *Annual Review of Ecology and Systematics* **17**, 273-303

Trotter, J. A., Williams, I. S., Barnes, C. R., Lécuyer, C., and Nicoll, R. S. 2008. Did cooling oceans trigger Ordovician biodiversification? Evidence from conodont thermometry. *Science* **321**(5888), 550-554

Urey, H. C., Lowenstam, H. A., Epstein, S., and McKinney, C. R. 1951. Measurement of paleotemperatures and temperatures of the Upper Cretaceous of England, Denmark, and the southeastern United States. *Geological Society of America Bulletin* **62**(4), 399-416

Usdowski, E., and Hoefs, J. 1993. Oxygen isotope exchange between carbonic acid, bicarbonate, carbonate, and water: A re-examination of the data of McCrea (1950) and an expression for the overall partitioning of oxygen isotopes between the carbonate species and water. *Geochimica et cosmochimica acta* **57**(15), 3815-3818

Wefer, G., and Berger, W. H. 1991. Isotope paleontology: growth and composition of extant calcareous species. *Marine Geology* **100**(1-4), 207-248

Williams, B., Halfar, J., Steneck, R. S., Wortmann, U. G., Hetzinger, S., Adey, W., Lebednik, P., and Joachimski, M. 2011. Twentieth century 13 C variability in surface water dissolved inorganic carbon recorded by coralline algae in the northern North Pacific Ocean and the Bering Sea. *Biogeosciences* **8**(1), 165-174

Zeebe, R. E. 1999. An explanation of the effect of seawater carbonate concentration on foraminiferal oxygen isotopes. *Geochimica et cosmochimica acta* **63**(13-14), 2001-2007

CHAPTER IX

Conclusions and future directions

IX-1 On *Sporolithon durum* rhodoliths from the Ricaudy Reef, New Caledonia

This work on *Sporolithon durum* rhodoliths from the Ricaudy Reef, New Caledonia represents a further development of projects conducted around the world that are based on the study of the geochemical composition of long-lived coralline red algae and their ability to provide insights into past environmental conditions. In that respect, previous findings were confirmed, others completed, and new outcomes were provided.

The existence of major growth bands in *S. durum*, attributed to a seasonal cyclicity, as well as the minor, sub-annual banding, appear to be a feature shared between several coralline red algal species. Similarly, the average annual extension rate recorded here for *S. durum* rhodoliths is in good agreement with those previously reported in the literature. In this regard, it has to be noted that we did not record any effect of seawater temperature on the extension rate variations or growth pattern of *S. durum* rhodoliths from the Ricaudy Reef, as has previously been recognised for other species of encrusting coralline red algae from various locations from the high latitudes. However, this absence of relationship has already been reported in the case of rhodoliths.

Our investigations on the variations of Mg composition of *S. durum* skeleton further assessed the pronounced seasonal cyclicity already observed for different species and confirmed the potential use of major Mg cycles for chronological development. The previously reported close relationship between Mg variations in coralline red algae from high latitudes of the Northern Hemisphere and seawater temperature changes was similarly observed in *S. durum* rhodoliths from the tropical Western Pacific. The ability of Mg/Ca variations to record both local sea-surface temperature (SST) changes at monthly

to sub-monthly resolution and regional, inter-annual climate patterns was also confirmed. Among the various trace elements studied, Mg was found to be the most suited for temperature reconstruction, as previously suggested. Nonetheless, variations in Sr composition were also linked to temperature changes, showing appositive correlation as recently reported.

Finally, the analysis of the oxygen isotopic composition in *S. durum* revealed a strong vital effect resulting in more negative $\delta^{18}O$ values than expected for abiotic, high-Mg calcite precipitation. The extent of the $\delta^{18}O$ discrimination recorded in *S. durum* is comparable to the one published for other coralline red algal species.

This study also expanded some of the aspects treated in previous coralline red algal research. The use of laser ablation inductively coupled plasmas mass spectrometry (LA-ICPMS) as a technique to obtain geochemical information from coralline red algae was further assessed and developed here. We demonstrated, for instance, that the use of a matrix-matched external standard is critical for calibration of the Mg/Ca composition. Modifying the LA-ICPMS instrumental settings, and especially the laser spot size, enables to highlight different components of the Mg/Ca signal. Lower-frequency, environmentally controlled Mg/Ca variations are better recorded using a bigger laser spot, whereas higher-frequency, biologically influenced Mg/Ca changes can be best observed using smaller spot sizes.

The observed positive relationship between Sr/Ca and seawater temperature in coralline red algae has been attributed to a biological influence in previous studies. Here, we suggest that rather than an algal control on Sr incorporation, thermodynamics may explain the observed positive relationship and that it is linked to the varying high-concentrations of Mg in the calcifying fluid. As a consequence, Sr may be considered as an indirect proxy of seawater temperature, which would explain the lesser extent of the temperature control on Sr compared to Mg. This project also extended the array of geochemical temperature proxies in coralline red algae, now including Li/Ca variations, which appear to behave similarly to Sr/Ca variations.

Since the use of X-ray absorption near edge structure (XANES) technology to demonstrate the association of Mg in the calcite lattice of *Lithothamnion glaciale*, it has been widely accepted that Mg in coralline red algae was quasi-exclusively incorporated into the calcite mineral. However, here, we demonstrated that, for *S. durum* from the Ricaudy Reef, a significant part of the Mg is likely to be associated with the organic component of the alga that is mainly located inside the cell structure. Therefore, as already suggested, there may be a need to investigate the distribution of Mg into coralline red algae on a species-to-species basis. Nevertheless, for *S. durum*, the presence of organic-

matter-associated Mg does not seem to significantly affect the cyclicity of the Mg/Ca signal, and therefore, does not compromise the temperature changes reconstructions.

In addition to the previous findings, the present project provides new results for coralline red algae geochemistry research and stands as a pioneer one in several aspects of the discipline. First of all, this type of high-resolution (i.e. monthly to sub-monthly resolution) geochemical study conducted on the species *S. durum* represents a first for the coralline red algal order Sporolithales. It is also the first time that specimens from the Southern Hemisphere, moreover from the tropics, were investigated for such purpose. The fact that the conclusions drawn here on the potential of these organisms for palaeoenvironmental reconstruction confirm the ones from previous studies on different species/order from high-latitudes represents a step further in the assessment of coralline red algae as a global environmental proxy.

Furthermore, we provide the first coral-coralline red algae comparison for SST reconstruction. The favourable comparison of the Mg/Ca proxy in the rhodoliths against the Sr/Ca proxy in corals, which is one of the most commonly used and reliable archive of seawater temperature thus far available, adds another level of credibility to our data and reinforces the potential of palaeoenvironmental research using coralline red algae.

The extensive use of LA-ICPMS enabled the study of the composition of 15 trace elements in our rhodoliths, 11 of which have never been reported so far for coralline red algae. Although the variability of the majority of trace elements was too pronounced to expect any direct implication for palaeoenvironmental use, the data presented here may serve as a baseline for future studies. The variations of other trace elements such as Mn, Fe, Ni and Co successfully recorded environmental disturbances linked to local anthropogenic activities over several decades and added a new aspect to the potential of coralline red algae as bio-monitors of the environment.

Finally, this study pioneered in the use of the sensitive, high-resolution ion microprobe (SHRIMP) to determine the coralline red algal oxygen isotopic composition at high-resolution, and although straightforward interpretations of the SHRIMP data were not achieved, it is beyond doubt that further analyses may provide critical information on various aspects of coralline red algal research, from ecology- and biology-related parameters, such as vital effect or calcification processes, to potential high-resolution environmental reconstructions.

IX-2 Future directions

Although the present study further assessed previous suggestions and contains several novelties for coralline red algal and rhodolith research, it still represents a modest contribution to the state of knowledge necessary to fully understand if and how coralline red algae may be used as global environmental recorders. Further investigations are critical in order to establish coralline red algae as reliable and widespread tools for palaeoenvironmental reconstructions.

Future research should involve attempts at environmental reconstructions from more locations around the globe, using the same or additional coralline red algal species from a wider array of environments. This way, the potential of these organisms to be a worldwide archive would be more thoroughly assessed. For example, additional tropical locations should be explored and the presence of known rhodolith beds in French Polynesia, Indonesia, Zanzibar or Brazil should render this task achievable. Records from temperate waters would also be greatly beneficial and the coasts of Australia, New Zealand, the Gulf of California, Spain and the Mediterranean are promising locations for this type of study. It is also crucial to continue expanding coralline red algal records from the high latitudes in the Northern Hemisphere, but also possibly commence studying Southern Hemisphere specimens off Southern Chile or Antarctica for instance, where the presence of coralline red algae has been reported. This type of study may provide invaluable information about the past climatic variability of the Southern Ocean.

It is also critical to generate additional environmental records that go beyond the instrumental records in order to provide significant data for climate models. Depending on the study location, several decade- to century-long records would be needed if modern samples were used. This may be achieved by using long-lived specimens collected alive or by coring through a rhodolith bed and thus, use a compilation of multiple crusts/rhodoliths to obtain a composite, longer record (e.g. Kamenos, 2010). The use of reliably dated, fossil specimens may also contribute to extend environmental records from coralline red algae further back in time. It still remains to be seen how far back in time one can go to reconstruct past conditions of the environments in which coralline red algae grew. Advances in this domain will only be possible when a better characterisation of diagenesis within the specimens, commonly but not exclusively seen as infills in the cell structure, could be achieved.

We saw in this study that the growth pattern of *S. durum* may play a significant role in the observed variability of trace elements in the rhodoliths. Although an attempt at characterising the growth pattern of *S. durum* has been made here, questions still remain.

For instance, what causes the annual extension pattern to be asymmetrical? or, do the minor bands effectively form according to lunar cycles? Parts of the answer may be revealed by future studies, some ongoing (J. Mallela, personal communication), involving growth-monitoring experiments at higher resolution than carried out here. Repetitive staining of rhodoliths or red algal crusts at a fortnightly or even a weekly resolution ought to be envisaged for *in situ* or culture experiments. Nevertheless, we need to keep in mind the potential adverse effect on the algal metabolism of the use of Alizarin Red S stain. Experimenting with other staining techniques such as calceine stain or seawater isotopic (e.g. ^{43}Ca; ^{84}Sr) enrichment may also be beneficial.

Culture experiments also appear critical for further assessment of the mode of incorporation and the distribution of trace elements within coralline red algae. Better knowledge of these two aspects is essential in order to be able to reliably use specific trace elements such as the metals studied here (Mn, Fe, Ni and Co) as proxies of environmental changes. The use of XANES technology as well as the selective extraction technique may represent other ways to contribute to advances in this area.

Finally, although the SHRIMP analyses conducted during this project were originally focused on high-resolution environmental reconstructions using the oxygen isotopic composition of *S. durum*, this pioneer approach seems to offer a welcomed opportunity to further investigate calcification and metabolic processes in coralline red algae. We suggest that future studies involving SHRIMP $\delta^{18}O$ analyses should be carried out in combination with $\delta^{13}C$ measurements in order to obtain insights into the extent of vital effects in the incorporation of oxygen isotopes into the calcite structure. In addition, $\delta^{11}B$ analyses would be greatly beneficial so as to be able to better characterise the role of pH variations during the calcification process on the oxygen isotopic composition recorded in coralline red algae.

In summary, with the pioneer study carried out in 2000, followed by the first applications in the late 2000s-early 2010s, the geochemistry of coralline red algae used for palaeoenvironmental reconstruction is only emerging among the scientific community. As an inevitable comparison, coral geochemistry has been commonly (and almost routinely) used for the same purpose for at least 20 years and is now logically, well in front in terms of technique and state of knowledge. However, coralline red algal geochemistry can greatly benefit from previous advances in this similar (in many ways) discipline, and the results obtained so far are very promising for the recognition of coralline red algae as environmental archives in the marine realm, across all latitudes.

List of appendices

(provided on digital support)

General appendices

_ Environmental dataset
_ Results of ICP-AES, solution and laser ablation ICPMS analyses for the Carrara marble, the BSA, SSA and MSA rhodoliths as well as other carbonate materials

Chapter-specific appendices

CHAPTER III - An investigation of Mg/Ca distribution in *Sporolithon durum* coralline red algae

III_1_EPMA dataset
III_2_LA-ICPMS dataset of the 11 profiles carried out along the tip of the studied rhodolith branch

CHAPTER V - Seasonal patterns in trace elemental composition of coralline red algae from a tropical lagoon: environmental, biological and anthropogenic influences

V_1_Full resolution trace elements variations analysed using LA-ICPMS along the outermost ~2mm of the stained rhodolith branches
V_2_LA-ICPMS trace elements results obtained before and after treatment of a stained rhodolith branch with H_2O_2
V_3_Monthly-resolution trace elements variations along the 43 different stained rhodolith branches, analysed by LA-ICPMS

CHAPTER VI - Sea-surface temperature reconstruction from trace elements variations of tropical coralline red algae

VI_1_LA-ICPMS dataset of Mg/Ca variations recorded along five different rhodolith branches and the corresponding chronological transformation to monthly- and interannual-resolution variations

CHAPTER VII - A record of mining and industrial activities in New Caledonia based on trace elements in rhodolith-forming coralline red algae

VII_1_LA-ICPMS dataset of trace elements variations recorded along five different rhodolith branches and the corresponding chronological transformation to monthly-resolution, of the Mn/Ca, Fe/Ca, Ni/Ca and Co/Ca variations
VII_2_LA-ICPMS trace metals results of two parralel profiles recorded along the BSA3 rhodolith branch
VII_3_LA-ICPMS trace metals results obtained before and after treatment of the MSA1 rhodolith branch with H_2O_2

CHAPTER VIII - Oxygen isotopic composition of tropical coralline red algae using a sensitive, high-resolution ion microprobe (SHRIMP II)

VIII_1_Average Mg/Ca concentrations in the carbonate materials studied, as well as their corresponding $\delta^{18}O$ composition measured by SHRIMP and conventional mass spectrometry
VIII_2_Full LA-ICPMS dataset for the Mg/Ca concentrations of the studied carbonate materials
VIII_3_Original and corrected-for-IMF SHRIMP $\delta^{18}O$ dataset for the rhodolith branch as well as the corresponding LA-ICPMS Mg/Ca measurements

References

Adey, W., H., and MacIntyre, I., G. (1973). Crustose Coralline Algae: A Re-evaluation in the Geological Sciences. *Geological Society of America Bulletin* **84,** 883-904.

Basso, D., Nalin, R., and Nelson, C., S. (2009). Shallow-water *Sporolithon* rhodoliths from North Island (New Zealand). *Palaios* **24,** 92-103.

Bosence, D., W. J. (1983a). Description and Classification of Rhodoliths (Rhodoids, Rhodolites). *In* "Coated Grains." (T. M. Peryt, Ed.), pp. 217-224. Springer-Verlag, Berlin.

Bosence, D., W., J. (1983b). The Occurence and Ecology of Recent Rhodoliths - A Review. *In* "Coated Grains." (T. M. Peryt, Ed.), pp. 225-242. Springer-Verlag Berlin.

Burdett, H., Kamenos, N. A., and Law, A. (2010). Using coralline algae to understand historic marine cloud cover. *Palaeogeography, Palaeoclimatology, Palaeoecology* **302,** 65-70.

Chan, P., Halfar, J., Williams, B., Hetzinger, S., Steneck, R., Zack, T., and Jacob, D. E. (2011). Freshening of the Alaska Coastal Current recorded by coralline algal Ba/Ca ratios. *Journal of Geophysical Research* **116,** G01032.

Chave, K. E. (1954). Aspects of the biogeochemistry of magnesium 1. Calcareous marine organisms. *The Journal of Geology* **62,** 266-283.

Craig, C. A., Jarvis, K. E., and Clarke, L. J. (2000). An assessment of calibration strategies for the quantitative and semi-quantitative analysis of calcium carbonate matrices by laser ablation-inductively coupled plasma-mass spectrometry (LA-ICP-MS). *Journal of Analytical Aomic Spectrometry* **15,** 1001-1008.

de Villiers, S., Greaves, M., and Elderfield, H. (2002). An intensity ratio calibration method for the accurate determination of Mg/Ca and Sr/Ca of marine carbonates by ICP-AES. *Geochemistry, Geophysics, Geosystems* **3,** 1001.

Dickson, J. A. D. (1965). A modified staining technique for carbonates in thin section. *Nature* **205,** 587.

Eggins, S., De Deckker, P., and Marshall, J. (2003). Mg/Ca variation in planktonic foraminifera tests: implications for reconstructing palaeo-seawater temperature and habitat migration. *Earth and Planetary Science Letters* **212,** 291-306.

Fallon, S. J., McCulloch, M. T., van Woesik, R., and Sinclair, D. J. (1999). Corals at their latitudinal limits: laser ablation trace element systematics in *Porites* from Shirigai Bay, Japan. *Earth and Planetary Science Letters* **172,** 221-238.

Foster, M., S. (2001). Rhodoliths: Between rocks and soft places. *Journal of Phycology* **37,** 659-667.

Frantz, B. R., Foster, M. S., and Riosmena-Rodrìguez, R. (2005). *Clathromorphum nereostratum* (Corallinales, Rhodophyta): The oldest alga? *Journal of Phycology* **41,** 770-773.

Gamboa, G., Halfar, J., Hetzinger, S., Adey, W., Zack, T., Kunz, B., and Jacob, D. E. (2010). Mg/Ca ratios in coralline algae record northwest Atlantic temperature variations and North Atlantic Oscillation relationships. *Journal of Geophysical Research* **115,** C12044.

Goldberg, N. (2006). Age estimates and description of rhodoliths from Esperance Bay, Western Australia. *Journal of the Marine Biological Association of the United Kingdom* **86,** 1291-1296.

Halfar, J., Steneck, R., S., Schöne, B., R., Moore, G., W., K., Joachimski, M., Kronz, A., Fietzke, J., and Estes, J. (2007). Coralline alga reveals first marine record of subarctic North Pacific climate change. *Geophysical Research Letters* **34,** L07702.

Halfar, J., Zack, T., Kronz, A., and Zachos, J., C. (2000). Growth and high-resolution paleoenvironmental signals of rhodoliths (coralline red algae): A new biogenic archive. *Journal of Geophysical Research* **105,** 22,107-22,116.

Harris, P., J., Tsuji, Y., Marshall, J., F., Davies, P., J., Honda, N., and Matsuda, H. (1996). Sand and rhodolith-gravel entrainment on the mid- to outer-shelf under a western

boundary current: Fraser Island continental shelf, eastern Australia. *Marine Geology* **129,** 313-330.

Hathorne, E. C., Alard, O., James, R. H., and Rogers, N. W. (2003). Determination of intratest variability of trace elements in foraminifera by laser ablation inductively coupled plasma-mass spectrometry. *Geochemistry, Geophysics, Geosystems* **4,** 8408.

Hetzinger, S., Halfar, J., Kronz, A., Steneck, R., Adey, W., H., Lebednik, P., A., and Schöne, B., R. (2009). High-resolution Mg/Ca ratios in a coralline red alga as a proxy for Bering Sea temperature variations from 1902 to 1967. *Palaios* **24,** 406-412.

Hetzinger, S., Halfar, J., Zack, T., Gamboa, G., Jacob, D. E., Kunz, B. E., Kronz, A., Adey, W., Lebednik, P. A., and Steneck, R. S. (2011a). High-resolution analysis of trace elements in crustose coralline algae from the North Atlantic and North Pacific by laser ablation ICP-MS. *Palaeogeography, Palaeoclimatology, Palaeoecology* **302**(1-2), 81-94.

Hetzinger, S., Halfar, J., Mecking, J. V., Keenlyside, N. S., Kronz, A., Steneck, R. S., Adey, W. H., and Lebednik, P. A. (2011b). Marine proxy evidence linking decadal North Pacific and Atlantic climate. *Climate Dynamics,* 1-9.

Kamenos, N., A., Cusack, M., Huthwelker, T., Lagarde, P., and Scheibling, R., E. (2009). Mg-lattice associations in red coralline algae. *Geochimica et Cosmochimica Acta* **73,** 1901-1907.

Kamenos, N., A., Cusack, M., and Moore, P., G. (2008). Coralline algae are global palaeothermometers with bi-weekly resolution. *Geochimica et Cosmochimica Acta* **72,** 771-779.

Kamenos, N. A., and Law, A. (2010). Temperature controls on coralline algal skeletal growth. *Journal of Phycology* **46,** 331-335.

Longerich, H. P., Jackson, S. E., and G¸nther, D. (1996). Laser ablation inductively coupled plasma mass spectrometric transient signal data acquisition and analyte concentration calculation. *Journal of Analytical Atomic Spectrometry* **11,** 899-904.

Love, K. M., and Woronow, A. (1991). Chemical changes induced in aragonite using treatments for the destruction of organic material. *Chemical geology* **93,** 291-301.

Martin, P. A., and Lea, D. W. (2002). A simple evaluation of cleaning procedures on fossil benthic foraminiferal Mg/Ca. *Geochemistry, Geophysics, Geosystems* **3,** 8401.

Milliman, J. D., Gastner, M., and Müller, J. (1971). Utilization of magnesium in coralline algae. *Geological Society of America Bulletin* **82,** 573-580.

Moberly Jr, R. (1968). Composition of Magnesian Calcites of Algae and Pelecypods by Electron Microprobe analysis. *Sedimentology* **11,** 61-82.

Nash, M. C., Troitzsch, U., Opdyke, B. N., Trafford, J. M., Russell, B. D., and Kline, D. I. (2011). First discovery of dolomite and magnesite in living coralline algae and its geobiological implications. *Biogeosciences* **8,** 3331-3340.

Nelson, W. A. (2009). Calcified macroalgae - critical to coastal ecosystems and vulnerable to change: a review. *Marine and Freshwater Research* **60,** 787-801.

Paillard, D., Labeyrie, L., and Yiou, P. (1996). Macintosh program performs time-series analysis. *Eos Transactions AGU* **77,** 379.

Schöne, B. R., Zhang, Z., Radermacher, P., Thébault, J., Jacob, D. E., Nunn, E. V., and Maurer, A. F. (2011). Sr/Ca and Mg/Ca ratios of ontogenetically old, long-lived bivalve shells (*Arctica islandica*) and their function as paleotemperature proxies. *Palaeogeography, Palaeoclimatology, Palaeoecology* **302,** 52-64.

Sinclair, D. J., Kinsley, L. P. J., and McCulloch, M. T. (1998). High resolution analysis of trace elements in corals by laser ablation ICP-MS. *Geochimica et Cosmochimica Acta* **62,** 1889-1901.

Steneck, R. S. (1986). The ecology of coralline algal crusts: convergent patterns and adaptative strategies. *Annual Review of Ecology and Systematics* **17,** 273-303.

Stoll, H. M., Encinar, J. R., Garcia Alonso, J. I., Rosenthal, Y., Probert, I., and Klaas, C. (2001). A first look at paleotemperature prospects from Mg in coccolith carbonate: Cleaning techniques and culture measurements. *Geochemistry, Geophysics, Geosystems* **200,** 2GC000144.

References

Adey, W., H., and MacIntyre, I., G. (1973). Crustose Coralline Algae: A Re-evaluation in the Geological Sciences. *Geological Society of America Bulletin* **84,** 883-904.

Basso, D., Nalin, R., and Nelson, C., S. (2009). Shallow-water *Sporolithon* rhodoliths from North Island (New Zealand). *Palaios* **24,** 92-103.

Bosence, D., W. J. (1983a). Description and Classification of Rhodoliths (Rhodoids, Rhodolites). *In* "Coated Grains." (T. M. Peryt, Ed.), pp. 217-224. Springer-Verlag, Berlin.

Bosence, D., W., J. (1983b). The Occurence and Ecology of Recent Rhodoliths - A Review. *In* "Coated Grains." (T. M. Peryt, Ed.), pp. 225-242. Springer-Verlag Berlin.

Burdett, H., Kamenos, N. A., and Law, A. (2010). Using coralline algae to understand historic marine cloud cover. *Palaeogeography, Palaeoclimatology, Palaeoecology* **302,** 65-70.

Chan, P., Halfar, J., Williams, B., Hetzinger, S., Steneck, R., Zack, T., and Jacob, D. E. (2011). Freshening of the Alaska Coastal Current recorded by coralline algal Ba/Ca ratios. *Journal of Geophysical Research* **116,** G01032.

Chave, K. E. (1954). Aspects of the biogeochemistry of magnesium 1. Calcareous marine organisms. *The Journal of Geology* **62,** 266-283.

Craig, C. A., Jarvis, K. E., and Clarke, L. J. (2000). An assessment of calibration strategies for the quantitative and semi-quantitative analysis of calcium carbonate matrices by laser ablation-inductively coupled plasma-mass spectrometry (LA-ICP-MS). *Journal of Analytical Aomic Spectrometry* **15,** 1001-1008.

de Villiers, S., Greaves, M., and Elderfield, H. (2002). An intensity ratio calibration method for the accurate determination of Mg/Ca and Sr/Ca of marine carbonates by ICP-AES. *Geochemistry, Geophysics, Geosystems* **3,** 1001.

Dickson, J. A. D. (1965). A modified staining technique for carbonates in thin section. *Nature* **205,** 587.

Eggins, S., De Deckker, P., and Marshall, J. (2003). Mg/Ca variation in planktonic foraminifera tests: implications for reconstructing palaeo-seawater temperature and habitat migration. *Earth and Planetary Science Letters* **212,** 291-306.

Fallon, S. J., McCulloch, M. T., van Woesik, R., and Sinclair, D. J. (1999). Corals at their latitudinal limits: laser ablation trace element systematics in *Porites* from Shirigai Bay, Japan. *Earth and Planetary Science Letters* **172,** 221-238.

Foster, M., S. (2001). Rhodoliths: Between rocks and soft places. *Journal of Phycology* **37,** 659-667.

Frantz, B. R., Foster, M. S., and Riosmena-Rodrìguez, R. (2005). *Clathromorphum nereostratum* (Corallinales, Rhodophyta): The oldest alga? *Journal of Phycology* **41,** 770-773.

Gamboa, G., Halfar, J., Hetzinger, S., Adey, W., Zack, T., Kunz, B., and Jacob, D. E. (2010). Mg/Ca ratios in coralline algae record northwest Atlantic temperature variations and North Atlantic Oscillation relationships. *Journal of Geophysical Research* **115,** C12044.

Goldberg, N. (2006). Age estimates and description of rhodoliths from Esperance Bay, Western Australia. *Journal of the Marine Biological Association of the United Kingdom* **86,** 1291-1296.

Halfar, J., Steneck, R., S., Schöne, B., R., Moore, G., W., K., Joachimski, M., Kronz, A., Fietzke, J., and Estes, J. (2007). Coralline alga reveals first marine record of subarctic North Pacific climate change. *Geophysical Research Letters* **34,** L07702.

Halfar, J., Zack, T., Kronz, A., and Zachos, J., C. (2000). Growth and high-resolution paleoenvironmental signals of rhodoliths (coralline red algae): A new biogenic archive. *Journal of Geophysical Research* **105,** 22,107-22,116.

Harris, P., J., Tsuji, Y., Marshall, J., F., Davies, P., J., Honda, N., and Matsuda, H. (1996). Sand and rhodolith-gravel entrainment on the mid- to outer-shelf under a western

boundary current: Fraser Island continental shelf, eastern Australia. *Marine Geology* **129,** 313-330.

Hathorne, E. C., Alard, O., James, R. H., and Rogers, N. W. (2003). Determination of intratest variability of trace elements in foraminifera by laser ablation inductively coupled plasma-mass spectrometry. *Geochemistry, Geophysics, Geosystems* **4,** 8408.

Hetzinger, S., Halfar, J., Kronz, A., Steneck, R., Adey, W., H., Lebednik, P., A., and Schöne, B., R. (2009). High-resolution Mg/Ca ratios in a coralline red alga as a proxy for Bering Sea temperature variations from 1902 to 1967. *Palaios* **24,** 406-412.

Hetzinger, S., Halfar, J., Zack, T., Gamboa, G., Jacob, D. E., Kunz, B. E., Kronz, A., Adey, W., Lebednik, P. A., and Steneck, R. S. (2011a). High-resolution analysis of trace elements in crustose coralline algae from the North Atlantic and North Pacific by laser ablation ICP-MS. *Palaeogeography, Palaeoclimatology, Palaeoecology* **302**(1-2), 81-94.

Hetzinger, S., Halfar, J., Mecking, J. V., Keenlyside, N. S., Kronz, A., Steneck, R. S., Adey, W. H., and Lebednik, P. A. (2011b). Marine proxy evidence linking decadal North Pacific and Atlantic climate. *Climate Dynamics*, 1-9.

Kamenos, N., A., Cusack, M., Huthwelker, T., Lagarde, P., and Scheibling, R., E. (2009). Mg-lattice associations in red coralline algae. *Geochimica et Cosmochimica Acta* **73,** 1901-1907.

Kamenos, N., A., Cusack, M., and Moore, P., G. (2008). Coralline algae are global palaeothermometers with bi-weekly resolution. *Geochimica et Cosmochimica Acta* **72,** 771-779.

Kamenos, N. A., and Law, A. (2010). Temperature controls on coralline algal skeletal growth. *Journal of Phycology* **46,** 331-335.

Longerich, H. P., Jackson, S. E., and G¸nther, D. (1996). Laser ablation inductively coupled plasma mass spectrometric transient signal data acquisition and analyte concentration calculation. *Journal of Analytical Atomic Spectrometry* **11,** 899-904.

Love, K. M., and Woronow, A. (1991). Chemical changes induced in aragonite using treatments for the destruction of organic material. *Chemical geology* **93,** 291-301.

Martin, P. A., and Lea, D. W. (2002). A simple evaluation of cleaning procedures on fossil benthic foraminiferal Mg/Ca. *Geochemistry, Geophysics, Geosystems* **3,** 8401.

Milliman, J. D., Gastner, M., and Müller, J. (1971). Utilization of magnesium in coralline algae. *Geological Society of America Bulletin* **82,** 573-580.

Moberly Jr, R. (1968). Composition of Magnesian Calcites of Algae and Pelecypods by Electron Microprobe analysis. *Sedimentology* **11,** 61-82.

Nash, M. C., Troitzsch, U., Opdyke, B. N., Trafford, J. M., Russell, B. D., and Kline, D. I. (2011). First discovery of dolomite and magnesite in living coralline algae and its geobiological implications. *Biogeosciences* **8,** 3331-3340.

Nelson, W. A. (2009). Calcified macroalgae - critical to coastal ecosystems and vulnerable to change: a review. *Marine and Freshwater Research* **60,** 787-801.

Paillard, D., Labeyrie, L., and Yiou, P. (1996). Macintosh program performs time-series analysis. *Eos Transactions AGU* **77,** 379.

Schöne, B. R., Zhang, Z., Radermacher, P., Thébault, J., Jacob, D. E., Nunn, E. V., and Maurer, A. F. (2011). Sr/Ca and Mg/Ca ratios of ontogenetically old, long-lived bivalve shells (*Arctica islandica*) and their function as paleotemperature proxies. *Palaeogeography, Palaeoclimatology, Palaeoecology* **302,** 52-64.

Sinclair, D. J., Kinsley, L. P. J., and McCulloch, M. T. (1998). High resolution analysis of trace elements in corals by laser ablation ICP-MS. *Geochimica et Cosmochimica Acta* **62,** 1889-1901.

Steneck, R. S. (1986). The ecology of coralline algal crusts: convergent patterns and adaptative strategies. *Annual Review of Ecology and Systematics* **17,** 273-303.

Stoll, H. M., Encinar, J. R., Garcia Alonso, J. I., Rosenthal, Y., Probert, I., and Klaas, C. (2001). A first look at paleotemperature prospects from Mg in coccolith carbonate: Cleaning techniques and culture measurements. *Geochemistry, Geophysics, Geosystems* **200,** 2GC000144.

References

Adey, W., H., and MacIntyre, I., G. (1973). Crustose Coralline Algae: A Re-evaluation in the Geological Sciences. *Geological Society of America Bulletin* **84,** 883-904.

Basso, D., Nalin, R., and Nelson, C., S. (2009). Shallow-water *Sporolithon* rhodoliths from North Island (New Zealand). *Palaios* **24,** 92-103.

Bosence, D., W. J. (1983a). Description and Classification of Rhodoliths (Rhodoids, Rhodolites). *In* "Coated Grains." (T. M. Peryt, Ed.), pp. 217-224. Springer-Verlag, Berlin.

Bosence, D., W., J. (1983b). The Occurence and Ecology of Recent Rhodoliths - A Review. *In* "Coated Grains." (T. M. Peryt, Ed.), pp. 225-242. Springer-Verlag Berlin.

Burdett, H., Kamenos, N. A., and Law, A. (2010). Using coralline algae to understand historic marine cloud cover. *Palaeogeography, Palaeoclimatology, Palaeoecology* **302,** 65-70.

Chan, P., Halfar, J., Williams, B., Hetzinger, S., Steneck, R., Zack, T., and Jacob, D. E. (2011). Freshening of the Alaska Coastal Current recorded by coralline algal Ba/Ca ratios. *Journal of Geophysical Research* **116,** G01032.

Chave, K. E. (1954). Aspects of the biogeochemistry of magnesium 1. Calcareous marine organisms. *The Journal of Geology* **62,** 266-283.

Craig, C. A., Jarvis, K. E., and Clarke, L. J. (2000). An assessment of calibration strategies for the quantitative and semi-quantitative analysis of calcium carbonate matrices by laser ablation-inductively coupled plasma-mass spectrometry (LA-ICP-MS). *Journal of Analytical Aomic Spectrometry* **15,** 1001-1008.

de Villiers, S., Greaves, M., and Elderfield, H. (2002). An intensity ratio calibration method for the accurate determination of Mg/Ca and Sr/Ca of marine carbonates by ICP-AES. *Geochemistry, Geophysics, Geosystems* **3,** 1001.

Dickson, J. A. D. (1965). A modified staining technique for carbonates in thin section. *Nature* **205,** 587.

Eggins, S., De Deckker, P., and Marshall, J. (2003). Mg/Ca variation in planktonic foraminifera tests: implications for reconstructing palaeo-seawater temperature and habitat migration. *Earth and Planetary Science Letters* **212,** 291-306.

Fallon, S. J., McCulloch, M. T., van Woesik, R., and Sinclair, D. J. (1999). Corals at their latitudinal limits: laser ablation trace element systematics in *Porites* from Shirigai Bay, Japan. *Earth and Planetary Science Letters* **172,** 221-238.

Foster, M., S. (2001). Rhodoliths: Between rocks and soft places. *Journal of Phycology* **37,** 659-667.

Frantz, B. R., Foster, M. S., and Riosmena-Rodrìguez, R. (2005). *Clathromorphum nereostratum* (Corallinales, Rhodophyta): The oldest alga? *Journal of Phycology* **41,** 770-773.

Gamboa, G., Halfar, J., Hetzinger, S., Adey, W., Zack, T., Kunz, B., and Jacob, D. E. (2010). Mg/Ca ratios in coralline algae record northwest Atlantic temperature variations and North Atlantic Oscillation relationships. *Journal of Geophysical Research* **115,** C12044.

Goldberg, N. (2006). Age estimates and description of rhodoliths from Esperance Bay, Western Australia. *Journal of the Marine Biological Association of the United Kingdom* **86,** 1291-1296.

Halfar, J., Steneck, R., S., Schöne, B., R., Moore, G., W., K., Joachimski, M., Kronz, A., Fietzke, J., and Estes, J. (2007). Coralline alga reveals first marine record of subarctic North Pacific climate change. *Geophysical Research Letters* **34,** L07702.

Halfar, J., Zack, T., Kronz, A., and Zachos, J., C. (2000). Growth and high-resolution paleoenvironmental signals of rhodoliths (coralline red algae): A new biogenic archive. *Journal of Geophysical Research* **105,** 22,107-22,116.

Harris, P., J., Tsuji, Y., Marshall, J., F., Davies, P., J., Honda, N., and Matsuda, H. (1996). Sand and rhodolith-gravel entrainment on the mid- to outer-shelf under a western

boundary current: Fraser Island continental shelf, eastern Australia. *Marine Geology* **129,** 313-330.

Hathorne, E. C., Alard, O., James, R. H., and Rogers, N. W. (2003). Determination of intratest variability of trace elements in foraminifera by laser ablation inductively coupled plasma-mass spectrometry. *Geochemistry, Geophysics, Geosystems* **4,** 8408.

Hetzinger, S., Halfar, J., Kronz, A., Steneck, R., Adey, W., H., Lebednik, P., A., and Schöne, B., R. (2009). High-resolution Mg/Ca ratios in a coralline red alga as a proxy for Bering Sea temperature variations from 1902 to 1967. *Palaios* **24,** 406-412.

Hetzinger, S., Halfar, J., Zack, T., Gamboa, G., Jacob, D. E., Kunz, B. E., Kronz, A., Adey, W., Lebednik, P. A., and Steneck, R. S. (2011a). High-resolution analysis of trace elements in crustose coralline algae from the North Atlantic and North Pacific by laser ablation ICP-MS. *Palaeogeography, Palaeoclimatology, Palaeoecology* **302**(1-2), 81-94.

Hetzinger, S., Halfar, J., Mecking, J. V., Keenlyside, N. S., Kronz, A., Steneck, R. S., Adey, W. H., and Lebednik, P. A. (2011b). Marine proxy evidence linking decadal North Pacific and Atlantic climate. *Climate Dynamics*, 1-9.

Kamenos, N., A., Cusack, M., Huthwelker, T., Lagarde, P., and Scheibling, R., E. (2009). Mg-lattice associations in red coralline algae. *Geochimica et Cosmochimica Acta* **73,** 1901-1907.

Kamenos, N., A., Cusack, M., and Moore, P., G. (2008). Coralline algae are global palaeothermometers with bi-weekly resolution. *Geochimica et Cosmochimica Acta* **72,** 771-779.

Kamenos, N. A., and Law, A. (2010). Temperature controls on coralline algal skeletal growth. *Journal of Phycology* **46,** 331-335.

Longerich, H. P., Jackson, S. E., and G¸nther, D. (1996). Laser ablation inductively coupled plasma mass spectrometric transient signal data acquisition and analyte concentration calculation. *Journal of Analytical Atomic Spectrometry* **11,** 899-904.

Love, K. M., and Woronow, A. (1991). Chemical changes induced in aragonite using treatments for the destruction of organic material. *Chemical geology* **93,** 291-301.

Martin, P. A., and Lea, D. W. (2002). A simple evaluation of cleaning procedures on fossil benthic foraminiferal Mg/Ca. *Geochemistry, Geophysics, Geosystems* **3,** 8401.

Milliman, J. D., Gastner, M., and Müller, J. (1971). Utilization of magnesium in coralline algae. *Geological Society of America Bulletin* **82,** 573-580.

Moberly Jr, R. (1968). Composition of Magnesian Calcites of Algae and Pelecypods by Electron Microprobe analysis. *Sedimentology* **11,** 61-82.

Nash, M. C., Troitzsch, U., Opdyke, B. N., Trafford, J. M., Russell, B. D., and Kline, D. I. (2011). First discovery of dolomite and magnesite in living coralline algae and its geobiological implications. *Biogeosciences* **8,** 3331-3340.

Nelson, W. A. (2009). Calcified macroalgae - critical to coastal ecosystems and vulnerable to change: a review. *Marine and Freshwater Research* **60,** 787-801.

Paillard, D., Labeyrie, L., and Yiou, P. (1996). Macintosh program performs time-series analysis. *Eos Transactions AGU* **77,** 379.

Schöne, B. R., Zhang, Z., Radermacher, P., Thébault, J., Jacob, D. E., Nunn, E. V., and Maurer, A. F. (2011). Sr/Ca and Mg/Ca ratios of ontogenetically old, long-lived bivalve shells (*Arctica islandica*) and their function as paleotemperature proxies. *Palaeogeography, Palaeoclimatology, Palaeoecology* **302,** 52-64.

Sinclair, D. J., Kinsley, L. P. J., and McCulloch, M. T. (1998). High resolution analysis of trace elements in corals by laser ablation ICP-MS. *Geochimica et Cosmochimica Acta* **62,** 1889-1901.

Steneck, R. S. (1986). The ecology of coralline algal crusts: convergent patterns and adaptative strategies. *Annual Review of Ecology and Systematics* **17,** 273-303.

Stoll, H. M., Encinar, J. R., Garcia Alonso, J. I., Rosenthal, Y., Probert, I., and Klaas, C. (2001). A first look at paleotemperature prospects from Mg in coccolith carbonate: Cleaning techniques and culture measurements. *Geochemistry, Geophysics, Geosystems* **200,** 2GC000144.

References

Adey, W., H., and MacIntyre, I., G. (1973). Crustose Coralline Algae: A Re-evaluation in the Geological Sciences. *Geological Society of America Bulletin* **84,** 883-904.

Basso, D., Nalin, R., and Nelson, C., S. (2009). Shallow-water *Sporolithon* rhodoliths from North Island (New Zealand). *Palaios* **24,** 92-103.

Bosence, D., W. J. (1983a). Description and Classification of Rhodoliths (Rhodoids, Rhodolites). *In* "Coated Grains." (T. M. Peryt, Ed.), pp. 217-224. Springer-Verlag, Berlin.

Bosence, D., W., J. (1983b). The Occurence and Ecology of Recent Rhodoliths - A Review. *In* "Coated Grains." (T. M. Peryt, Ed.), pp. 225-242. Springer-Verlag Berlin.

Burdett, H., Kamenos, N. A., and Law, A. (2010). Using coralline algae to understand historic marine cloud cover. *Palaeogeography, Palaeoclimatology, Palaeoecology* **302,** 65-70.

Chan, P., Halfar, J., Williams, B., Hetzinger, S., Steneck, R., Zack, T., and Jacob, D. E. (2011). Freshening of the Alaska Coastal Current recorded by coralline algal Ba/Ca ratios. *Journal of Geophysical Research* **116,** G01032.

Chave, K. E. (1954). Aspects of the biogeochemistry of magnesium 1. Calcareous marine organisms. *The Journal of Geology* **62,** 266-283.

Craig, C. A., Jarvis, K. E., and Clarke, L. J. (2000). An assessment of calibration strategies for the quantitative and semi-quantitative analysis of calcium carbonate matrices by laser ablation-inductively coupled plasma-mass spectrometry (LA-ICP-MS). *Journal of Analytical Aomic Spectrometry* **15,** 1001-1008.

de Villiers, S., Greaves, M., and Elderfield, H. (2002). An intensity ratio calibration method for the accurate determination of Mg/Ca and Sr/Ca of marine carbonates by ICP-AES. *Geochemistry, Geophysics, Geosystems* **3,** 1001.

Dickson, J. A. D. (1965). A modified staining technique for carbonates in thin section. *Nature* **205,** 587.

Eggins, S., De Deckker, P., and Marshall, J. (2003). Mg/Ca variation in planktonic foraminifera tests: implications for reconstructing palaeo-seawater temperature and habitat migration. *Earth and Planetary Science Letters* **212,** 291-306.

Fallon, S. J., McCulloch, M. T., van Woesik, R., and Sinclair, D. J. (1999). Corals at their latitudinal limits: laser ablation trace element systematics in *Porites* from Shirigai Bay, Japan. *Earth and Planetary Science Letters* **172,** 221-238.

Foster, M., S. (2001). Rhodoliths: Between rocks and soft places. *Journal of Phycology* **37,** 659-667.

Frantz, B. R., Foster, M. S., and Riosmena-Rodrìguez, R. (2005). *Clathromorphum nereostratum* (Corallinales, Rhodophyta): The oldest alga? *Journal of Phycology* **41,** 770-773.

Gamboa, G., Halfar, J., Hetzinger, S., Adey, W., Zack, T., Kunz, B., and Jacob, D. E. (2010). Mg/Ca ratios in coralline algae record northwest Atlantic temperature variations and North Atlantic Oscillation relationships. *Journal of Geophysical Research* **115,** C12044.

Goldberg, N. (2006). Age estimates and description of rhodoliths from Esperance Bay, Western Australia. *Journal of the Marine Biological Association of the United Kingdom* **86,** 1291-1296.

Halfar, J., Steneck, R., S., Schöne, B., R., Moore, G., W., K., Joachimski, M., Kronz, A., Fietzke, J., and Estes, J. (2007). Coralline alga reveals first marine record of subarctic North Pacific climate change. *Geophysical Research Letters* **34,** L07702.

Halfar, J., Zack, T., Kronz, A., and Zachos, J., C. (2000). Growth and high-resolution paleoenvironmental signals of rhodoliths (coralline red algae): A new biogenic archive. *Journal of Geophysical Research* **105,** 22,107-22,116.

Harris, P., J., Tsuji, Y., Marshall, J., F., Davies, P., J., Honda, N., and Matsuda, H. (1996). Sand and rhodolith-gravel entrainment on the mid- to outer-shelf under a western

boundary current: Fraser Island continental shelf, eastern Australia. *Marine Geology* **129,** 313-330.

Hathorne, E. C., Alard, O., James, R. H., and Rogers, N. W. (2003). Determination of intratest variability of trace elements in foraminifera by laser ablation inductively coupled plasma-mass spectrometry. *Geochemistry, Geophysics, Geosystems* **4,** 8408.

Hetzinger, S., Halfar, J., Kronz, A., Steneck, R., Adey, W., H., Lebednik, P., A., and Schöne, B., R. (2009). High-resolution Mg/Ca ratios in a coralline red alga as a proxy for Bering Sea temperature variations from 1902 to 1967. *Palaios* **24,** 406-412.

Hetzinger, S., Halfar, J., Zack, T., Gamboa, G., Jacob, D. E., Kunz, B. E., Kronz, A., Adey, W., Lebednik, P. A., and Steneck, R. S. (2011a). High-resolution analysis of trace elements in crustose coralline algae from the North Atlantic and North Pacific by laser ablation ICP-MS. *Palaeogeography, Palaeoclimatology, Palaeoecology* **302**(1-2), 81-94.

Hetzinger, S., Halfar, J., Mecking, J. V., Keenlyside, N. S., Kronz, A., Steneck, R. S., Adey, W. H., and Lebednik, P. A. (2011b). Marine proxy evidence linking decadal North Pacific and Atlantic climate. *Climate Dynamics*, 1-9.

Kamenos, N., A., Cusack, M., Huthwelker, T., Lagarde, P., and Scheibling, R., E. (2009). Mg-lattice associations in red coralline algae. *Geochimica et Cosmochimica Acta* **73,** 1901-1907.

Kamenos, N., A., Cusack, M., and Moore, P., G. (2008). Coralline algae are global palaeothermometers with bi-weekly resolution. *Geochimica et Cosmochimica Acta* **72,** 771-779.

Kamenos, N. A., and Law, A. (2010). Temperature controls on coralline algal skeletal growth. *Journal of Phycology* **46,** 331-335.

Longerich, H. P., Jackson, S. E., and G¸nther, D. (1996). Laser ablation inductively coupled plasma mass spectrometric transient signal data acquisition and analyte concentration calculation. *Journal of Analytical Atomic Spectrometry* **11,** 899-904.

Love, K. M., and Woronow, A. (1991). Chemical changes induced in aragonite using treatments for the destruction of organic material. *Chemical geology* **93,** 291-301.

Martin, P. A., and Lea, D. W. (2002). A simple evaluation of cleaning procedures on fossil benthic foraminiferal Mg/Ca. *Geochemistry, Geophysics, Geosystems* **3,** 8401.

Milliman, J. D., Gastner, M., and Müller, J. (1971). Utilization of magnesium in coralline algae. *Geological Society of America Bulletin* **82,** 573-580.

Moberly Jr, R. (1968). Composition of Magnesian Calcites of Algae and Pelecypods by Electron Microprobe analysis. *Sedimentology* **11,** 61-82.

Nash, M. C., Troitzsch, U., Opdyke, B. N., Trafford, J. M., Russell, B. D., and Kline, D. I. (2011). First discovery of dolomite and magnesite in living coralline algae and its geobiological implications. *Biogeosciences* **8,** 3331-3340.

Nelson, W. A. (2009). Calcified macroalgae - critical to coastal ecosystems and vulnerable to change: a review. *Marine and Freshwater Research* **60,** 787-801.

Paillard, D., Labeyrie, L., and Yiou, P. (1996). Macintosh program performs time-series analysis. *Eos Transactions AGU* **77,** 379.

Schöne, B. R., Zhang, Z., Radermacher, P., Thébault, J., Jacob, D. E., Nunn, E. V., and Maurer, A. F. (2011). Sr/Ca and Mg/Ca ratios of ontogenetically old, long-lived bivalve shells (*Arctica islandica*) and their function as paleotemperature proxies. *Palaeogeography, Palaeoclimatology, Palaeoecology* **302,** 52-64.

Sinclair, D. J., Kinsley, L. P. J., and McCulloch, M. T. (1998). High resolution analysis of trace elements in corals by laser ablation ICP-MS. *Geochimica et Cosmochimica Acta* **62,** 1889-1901.

Steneck, R. S. (1986). The ecology of coralline algal crusts: convergent patterns and adaptative strategies. *Annual Review of Ecology and Systematics* **17,** 273-303.

Stoll, H. M., Encinar, J. R., Garcia Alonso, J. I., Rosenthal, Y., Probert, I., and Klaas, C. (2001). A first look at paleotemperature prospects from Mg in coccolith carbonate: Cleaning techniques and culture measurements. *Geochemistry, Geophysics, Geosystems* **200,** 2GC000144.

References

Adey, W., H., and MacIntyre, I., G. (1973). Crustose Coralline Algae: A Re-evaluation in the Geological Sciences. *Geological Society of America Bulletin* **84,** 883-904.

Basso, D., Nalin, R., and Nelson, C., S. (2009). Shallow-water *Sporolithon* rhodoliths from North Island (New Zealand). *Palaios* **24,** 92-103.

Bosence, D., W. J. (1983a). Description and Classification of Rhodoliths (Rhodoids, Rhodolites). *In* "Coated Grains." (T. M. Peryt, Ed.), pp. 217-224. Springer-Verlag, Berlin.

Bosence, D., W., J. (1983b). The Occurence and Ecology of Recent Rhodoliths - A Review. *In* "Coated Grains." (T. M. Peryt, Ed.), pp. 225-242. Springer-Verlag Berlin.

Burdett, H., Kamenos, N. A., and Law, A. (2010). Using coralline algae to understand historic marine cloud cover. *Palaeogeography, Palaeoclimatology, Palaeoecology* **302,** 65-70.

Chan, P., Halfar, J., Williams, B., Hetzinger, S., Steneck, R., Zack, T., and Jacob, D. E. (2011). Freshening of the Alaska Coastal Current recorded by coralline algal Ba/Ca ratios. *Journal of Geophysical Research* **116,** G01032.

Chave, K. E. (1954). Aspects of the biogeochemistry of magnesium 1. Calcareous marine organisms. *The Journal of Geology* **62,** 266-283.

Craig, C. A., Jarvis, K. E., and Clarke, L. J. (2000). An assessment of calibration strategies for the quantitative and semi-quantitative analysis of calcium carbonate matrices by laser ablation-inductively coupled plasma-mass spectrometry (LA-ICP-MS). *Journal of Analytical Aomic Spectrometry* **15,** 1001-1008.

de Villiers, S., Greaves, M., and Elderfield, H. (2002). An intensity ratio calibration method for the accurate determination of Mg/Ca and Sr/Ca of marine carbonates by ICP-AES. *Geochemistry, Geophysics, Geosystems* **3,** 1001.

Dickson, J. A. D. (1965). A modified staining technique for carbonates in thin section. *Nature* **205,** 587.

Eggins, S., De Deckker, P., and Marshall, J. (2003). Mg/Ca variation in planktonic foraminifera tests: implications for reconstructing palaeo-seawater temperature and habitat migration. *Earth and Planetary Science Letters* **212,** 291-306.

Fallon, S. J., McCulloch, M. T., van Woesik, R., and Sinclair, D. J. (1999). Corals at their latitudinal limits: laser ablation trace element systematics in *Porites* from Shirigai Bay, Japan. *Earth and Planetary Science Letters* **172,** 221-238.

Foster, M., S. (2001). Rhodoliths: Between rocks and soft places. *Journal of Phycology* **37,** 659-667.

Frantz, B. R., Foster, M. S., and Riosmena-Rodrìguez, R. (2005). *Clathromorphum nereostratum* (Corallinales, Rhodophyta): The oldest alga? *Journal of Phycology* **41,** 770-773.

Gamboa, G., Halfar, J., Hetzinger, S., Adey, W., Zack, T., Kunz, B., and Jacob, D. E. (2010). Mg/Ca ratios in coralline algae record northwest Atlantic temperature variations and North Atlantic Oscillation relationships. *Journal of Geophysical Research* **115,** C12044.

Goldberg, N. (2006). Age estimates and description of rhodoliths from Esperance Bay, Western Australia. *Journal of the Marine Biological Association of the United Kingdom* **86,** 1291-1296.

Halfar, J., Steneck, R., S., Schöne, B., R., Moore, G., W., K., Joachimski, M., Kronz, A., Fietzke, J., and Estes, J. (2007). Coralline alga reveals first marine record of subarctic North Pacific climate change. *Geophysical Research Letters* **34,** L07702.

Halfar, J., Zack, T., Kronz, A., and Zachos, J., C. (2000). Growth and high-resolution paleoenvironmental signals of rhodoliths (coralline red algae): A new biogenic archive. *Journal of Geophysical Research* **105,** 22,107-22,116.

Harris, P., J., Tsuji, Y., Marshall, J., F., Davies, P., J., Honda, N., and Matsuda, H. (1996). Sand and rhodolith-gravel entrainment on the mid- to outer-shelf under a western

boundary current: Fraser Island continental shelf, eastern Australia. *Marine Geology* **129,** 313-330.

Hathorne, E. C., Alard, O., James, R. H., and Rogers, N. W. (2003). Determination of intratest variability of trace elements in foraminifera by laser ablation inductively coupled plasma-mass spectrometry. *Geochemistry, Geophysics, Geosystems* **4,** 8408.

Hetzinger, S., Halfar, J., Kronz, A., Steneck, R., Adey, W., H., Lebednik, P., A., and Schöne, B., R. (2009). High-resolution Mg/Ca ratios in a coralline red alga as a proxy for Bering Sea temperature variations from 1902 to 1967. *Palaios* **24,** 406-412.

Hetzinger, S., Halfar, J., Zack, T., Gamboa, G., Jacob, D. E., Kunz, B. E., Kronz, A., Adey, W., Lebednik, P. A., and Steneck, R. S. (2011a). High-resolution analysis of trace elements in crustose coralline algae from the North Atlantic and North Pacific by laser ablation ICP-MS. *Palaeogeography, Palaeoclimatology, Palaeoecology* **302**(1-2), 81-94.

Hetzinger, S., Halfar, J., Mecking, J. V., Keenlyside, N. S., Kronz, A., Steneck, R. S., Adey, W. H., and Lebednik, P. A. (2011b). Marine proxy evidence linking decadal North Pacific and Atlantic climate. *Climate Dynamics*, 1-9.

Kamenos, N., A., Cusack, M., Huthwelker, T., Lagarde, P., and Scheibling, R., E. (2009). Mg-lattice associations in red coralline algae. *Geochimica et Cosmochimica Acta* **73,** 1901-1907.

Kamenos, N., A., Cusack, M., and Moore, P., G. (2008). Coralline algae are global palaeothermometers with bi-weekly resolution. *Geochimica et Cosmochimica Acta* **72,** 771-779.

Kamenos, N. A., and Law, A. (2010). Temperature controls on coralline algal skeletal growth. *Journal of Phycology* **46,** 331-335.

Longerich, H. P., Jackson, S. E., and G¸nther, D. (1996). Laser ablation inductively coupled plasma mass spectrometric transient signal data acquisition and analyte concentration calculation. *Journal of Analytical Atomic Spectrometry* **11,** 899-904.

Love, K. M., and Woronow, A. (1991). Chemical changes induced in aragonite using treatments for the destruction of organic material. *Chemical geology* **93,** 291-301.

Martin, P. A., and Lea, D. W. (2002). A simple evaluation of cleaning procedures on fossil benthic foraminiferal Mg/Ca. *Geochemistry, Geophysics, Geosystems* **3,** 8401.

Milliman, J. D., Gastner, M., and Müller, J. (1971). Utilization of magnesium in coralline algae. *Geological Society of America Bulletin* **82,** 573-580.

Moberly Jr, R. (1968). Composition of Magnesian Calcites of Algae and Pelecypods by Electron Microprobe analysis. *Sedimentology* **11,** 61-82.

Nash, M. C., Troitzsch, U., Opdyke, B. N., Trafford, J. M., Russell, B. D., and Kline, D. I. (2011). First discovery of dolomite and magnesite in living coralline algae and its geobiological implications. *Biogeosciences* **8,** 3331-3340.

Nelson, W. A. (2009). Calcified macroalgae - critical to coastal ecosystems and vulnerable to change: a review. *Marine and Freshwater Research* **60,** 787-801.

Paillard, D., Labeyrie, L., and Yiou, P. (1996). Macintosh program performs time-series analysis. *Eos Transactions AGU* **77,** 379.

Schöne, B. R., Zhang, Z., Radermacher, P., Thébault, J., Jacob, D. E., Nunn, E. V., and Maurer, A. F. (2011). Sr/Ca and Mg/Ca ratios of ontogenetically old, long-lived bivalve shells (*Arctica islandica*) and their function as paleotemperature proxies. *Palaeogeography, Palaeoclimatology, Palaeoecology* **302,** 52-64.

Sinclair, D. J., Kinsley, L. P. J., and McCulloch, M. T. (1998). High resolution analysis of trace elements in corals by laser ablation ICP-MS. *Geochimica et Cosmochimica Acta* **62,** 1889-1901.

Steneck, R. S. (1986). The ecology of coralline algal crusts: convergent patterns and adaptative strategies. *Annual Review of Ecology and Systematics* **17,** 273-303.

Stoll, H. M., Encinar, J. R., Garcia Alonso, J. I., Rosenthal, Y., Probert, I., and Klaas, C. (2001). A first look at paleotemperature prospects from Mg in coccolith carbonate: Cleaning techniques and culture measurements. *Geochemistry, Geophysics, Geosystems* **200,** 2GC000144.

References

Adey, W., H., and MacIntyre, I., G. (1973). Crustose Coralline Algae: A Re-evaluation in the Geological Sciences. *Geological Society of America Bulletin* **84,** 883-904.

Basso, D., Nalin, R., and Nelson, C., S. (2009). Shallow-water *Sporolithon* rhodoliths from North Island (New Zealand). *Palaios* **24,** 92-103.

Bosence, D., W. J. (1983a). Description and Classification of Rhodoliths (Rhodoids, Rhodolites). *In* "Coated Grains." (T. M. Peryt, Ed.), pp. 217-224. Springer-Verlag, Berlin.

Bosence, D., W., J. (1983b). The Occurence and Ecology of Recent Rhodoliths - A Review. *In* "Coated Grains." (T. M. Peryt, Ed.), pp. 225-242. Springer-Verlag Berlin.

Burdett, H., Kamenos, N. A., and Law, A. (2010). Using coralline algae to understand historic marine cloud cover. *Palaeogeography, Palaeoclimatology, Palaeoecology* **302,** 65-70.

Chan, P., Halfar, J., Williams, B., Hetzinger, S., Steneck, R., Zack, T., and Jacob, D. E. (2011). Freshening of the Alaska Coastal Current recorded by coralline algal Ba/Ca ratios. *Journal of Geophysical Research* **116,** G01032.

Chave, K. E. (1954). Aspects of the biogeochemistry of magnesium 1. Calcareous marine organisms. *The Journal of Geology* **62,** 266-283.

Craig, C. A., Jarvis, K. E., and Clarke, L. J. (2000). An assessment of calibration strategies for the quantitative and semi-quantitative analysis of calcium carbonate matrices by laser ablation-inductively coupled plasma-mass spectrometry (LA-ICP-MS). *Journal of Analytical Aomic Spectrometry* **15,** 1001-1008.

de Villiers, S., Greaves, M., and Elderfield, H. (2002). An intensity ratio calibration method for the accurate determination of Mg/Ca and Sr/Ca of marine carbonates by ICP-AES. *Geochemistry, Geophysics, Geosystems* **3,** 1001.

Dickson, J. A. D. (1965). A modified staining technique for carbonates in thin section. *Nature* **205,** 587.

Eggins, S., De Deckker, P., and Marshall, J. (2003). Mg/Ca variation in planktonic foraminifera tests: implications for reconstructing palaeo-seawater temperature and habitat migration. *Earth and Planetary Science Letters* **212,** 291-306.

Fallon, S. J., McCulloch, M. T., van Woesik, R., and Sinclair, D. J. (1999). Corals at their latitudinal limits: laser ablation trace element systematics in *Porites* from Shirigai Bay, Japan. *Earth and Planetary Science Letters* **172,** 221-238.

Foster, M., S. (2001). Rhodoliths: Between rocks and soft places. *Journal of Phycology* **37,** 659-667.

Frantz, B. R., Foster, M. S., and Riosmena-Rodrìguez, R. (2005). *Clathromorphum nereostratum* (Corallinales, Rhodophyta): The oldest alga? *Journal of Phycology* **41,** 770-773.

Gamboa, G., Halfar, J., Hetzinger, S., Adey, W., Zack, T., Kunz, B., and Jacob, D. E. (2010). Mg/Ca ratios in coralline algae record northwest Atlantic temperature variations and North Atlantic Oscillation relationships. *Journal of Geophysical Research* **115,** C12044.

Goldberg, N. (2006). Age estimates and description of rhodoliths from Esperance Bay, Western Australia. *Journal of the Marine Biological Association of the United Kingdom* **86,** 1291-1296.

Halfar, J., Steneck, R., S., Schöne, B., R., Moore, G., W., K., Joachimski, M., Kronz, A., Fietzke, J., and Estes, J. (2007). Coralline alga reveals first marine record of subarctic North Pacific climate change. *Geophysical Research Letters* **34,** L07702.

Halfar, J., Zack, T., Kronz, A., and Zachos, J., C. (2000). Growth and high-resolution paleoenvironmental signals of rhodoliths (coralline red algae): A new biogenic archive. *Journal of Geophysical Research* **105,** 22,107-22,116.

Harris, P., J., Tsuji, Y., Marshall, J., F., Davies, P., J., Honda, N., and Matsuda, H. (1996). Sand and rhodolith-gravel entrainment on the mid- to outer-shelf under a western

boundary current: Fraser Island continental shelf, eastern Australia. *Marine Geology* **129,** 313-330.

Hathorne, E. C., Alard, O., James, R. H., and Rogers, N. W. (2003). Determination of intratest variability of trace elements in foraminifera by laser ablation inductively coupled plasma-mass spectrometry. *Geochemistry, Geophysics, Geosystems* **4,** 8408.

Hetzinger, S., Halfar, J., Kronz, A., Steneck, R., Adey, W., H., Lebednik, P., A., and Schöne, B., R. (2009). High-resolution Mg/Ca ratios in a coralline red alga as a proxy for Bering Sea temperature variations from 1902 to 1967. *Palaios* **24,** 406-412.

Hetzinger, S., Halfar, J., Zack, T., Gamboa, G., Jacob, D. E., Kunz, B. E., Kronz, A., Adey, W., Lebednik, P. A., and Steneck, R. S. (2011a). High-resolution analysis of trace elements in crustose coralline algae from the North Atlantic and North Pacific by laser ablation ICP-MS. *Palaeogeography, Palaeoclimatology, Palaeoecology* **302**(1-2), 81-94.

Hetzinger, S., Halfar, J., Mecking, J. V., Keenlyside, N. S., Kronz, A., Steneck, R. S., Adey, W. H., and Lebednik, P. A. (2011b). Marine proxy evidence linking decadal North Pacific and Atlantic climate. *Climate Dynamics,* 1-9.

Kamenos, N., A., Cusack, M., Huthwelker, T., Lagarde, P., and Scheibling, R., E. (2009). Mg-lattice associations in red coralline algae. *Geochimica et Cosmochimica Acta* **73,** 1901-1907.

Kamenos, N., A., Cusack, M., and Moore, P., G. (2008). Coralline algae are global palaeothermometers with bi-weekly resolution. *Geochimica et Cosmochimica Acta* **72,** 771-779.

Kamenos, N. A., and Law, A. (2010). Temperature controls on coralline algal skeletal growth. *Journal of Phycology* **46,** 331-335.

Longerich, H. P., Jackson, S. E., and G¸nther, D. (1996). Laser ablation inductively coupled plasma mass spectrometric transient signal data acquisition and analyte concentration calculation. *Journal of Analytical Atomic Spectrometry* **11,** 899-904.

Love, K. M., and Woronow, A. (1991). Chemical changes induced in aragonite using treatments for the destruction of organic material. *Chemical geology* **93,** 291-301.

Martin, P. A., and Lea, D. W. (2002). A simple evaluation of cleaning procedures on fossil benthic foraminiferal Mg/Ca. *Geochemistry, Geophysics, Geosystems* **3,** 8401.

Milliman, J. D., Gastner, M., and Müller, J. (1971). Utilization of magnesium in coralline algae. *Geological Society of America Bulletin* **82,** 573-580.

Moberly Jr, R. (1968). Composition of Magnesian Calcites of Algae and Pelecypods by Electron Microprobe analysis. *Sedimentology* **11,** 61-82.

Nash, M. C., Troitzsch, U., Opdyke, B. N., Trafford, J. M., Russell, B. D., and Kline, D. I. (2011). First discovery of dolomite and magnesite in living coralline algae and its geobiological implications. *Biogeosciences* **8,** 3331-3340.

Nelson, W. A. (2009). Calcified macroalgae - critical to coastal ecosystems and vulnerable to change: a review. *Marine and Freshwater Research* **60,** 787-801.

Paillard, D., Labeyrie, L., and Yiou, P. (1996). Macintosh program performs time-series analysis. *Eos Transactions AGU* **77,** 379.

Schöne, B. R., Zhang, Z., Radermacher, P., Thébault, J., Jacob, D. E., Nunn, E. V., and Maurer, A. F. (2011). Sr/Ca and Mg/Ca ratios of ontogenetically old, long-lived bivalve shells (*Arctica islandica*) and their function as paleotemperature proxies. *Palaeogeography, Palaeoclimatology, Palaeoecology* **302,** 52-64.

Sinclair, D. J., Kinsley, L. P. J., and McCulloch, M. T. (1998). High resolution analysis of trace elements in corals by laser ablation ICP-MS. *Geochimica et Cosmochimica Acta* **62,** 1889-1901.

Steneck, R. S. (1986). The ecology of coralline algal crusts: convergent patterns and adaptative strategies. *Annual Review of Ecology and Systematics* **17,** 273-303.

Stoll, H. M., Encinar, J. R., Garcia Alonso, J. I., Rosenthal, Y., Probert, I., and Klaas, C. (2001). A first look at paleotemperature prospects from Mg in coccolith carbonate: Cleaning techniques and culture measurements. *Geochemistry, Geophysics, Geosystems* **200,** 2GC000144.

References

Adey, W., H., and MacIntyre, I., G. (1973). Crustose Coralline Algae: A Re-evaluation in the Geological Sciences. *Geological Society of America Bulletin* **84,** 883-904.

Basso, D., Nalin, R., and Nelson, C., S. (2009). Shallow-water *Sporolithon* rhodoliths from North Island (New Zealand). *Palaios* **24,** 92-103.

Bosence, D., W. J. (1983a). Description and Classification of Rhodoliths (Rhodoids, Rhodolites). *In* "Coated Grains." (T. M. Peryt, Ed.), pp. 217-224. Springer-Verlag, Berlin.

Bosence, D., W., J. (1983b). The Occurence and Ecology of Recent Rhodoliths - A Review. *In* "Coated Grains." (T. M. Peryt, Ed.), pp. 225-242. Springer-Verlag Berlin.

Burdett, H., Kamenos, N. A., and Law, A. (2010). Using coralline algae to understand historic marine cloud cover. *Palaeogeography, Palaeoclimatology, Palaeoecology* **302,** 65-70.

Chan, P., Halfar, J., Williams, B., Hetzinger, S., Steneck, R., Zack, T., and Jacob, D. E. (2011). Freshening of the Alaska Coastal Current recorded by coralline algal Ba/Ca ratios. *Journal of Geophysical Research* **116,** G01032.

Chave, K. E. (1954). Aspects of the biogeochemistry of magnesium 1. Calcareous marine organisms. *The Journal of Geology* **62,** 266-283.

Craig, C. A., Jarvis, K. E., and Clarke, L. J. (2000). An assessment of calibration strategies for the quantitative and semi-quantitative analysis of calcium carbonate matrices by laser ablation-inductively coupled plasma-mass spectrometry (LA-ICP-MS). *Journal of Analytical Aomic Spectrometry* **15,** 1001-1008.

de Villiers, S., Greaves, M., and Elderfield, H. (2002). An intensity ratio calibration method for the accurate determination of Mg/Ca and Sr/Ca of marine carbonates by ICP-AES. *Geochemistry, Geophysics, Geosystems* **3,** 1001.

Dickson, J. A. D. (1965). A modified staining technique for carbonates in thin section. *Nature* **205,** 587.

Eggins, S., De Deckker, P., and Marshall, J. (2003). Mg/Ca variation in planktonic foraminifera tests: implications for reconstructing palaeo-seawater temperature and habitat migration. *Earth and Planetary Science Letters* **212,** 291-306.

Fallon, S. J., McCulloch, M. T., van Woesik, R., and Sinclair, D. J. (1999). Corals at their latitudinal limits: laser ablation trace element systematics in *Porites* from Shirigai Bay, Japan. *Earth and Planetary Science Letters* **172,** 221-238.

Foster, M., S. (2001). Rhodoliths: Between rocks and soft places. *Journal of Phycology* **37,** 659-667.

Frantz, B. R., Foster, M. S., and Riosmena-Rodrìguez, R. (2005). *Clathromorphum nereostratum* (Corallinales, Rhodophyta): The oldest alga? *Journal of Phycology* **41,** 770-773.

Gamboa, G., Halfar, J., Hetzinger, S., Adey, W., Zack, T., Kunz, B., and Jacob, D. E. (2010). Mg/Ca ratios in coralline algae record northwest Atlantic temperature variations and North Atlantic Oscillation relationships. *Journal of Geophysical Research* **115,** C12044.

Goldberg, N. (2006). Age estimates and description of rhodoliths from Esperance Bay, Western Australia. *Journal of the Marine Biological Association of the United Kingdom* **86,** 1291-1296.

Halfar, J., Steneck, R., S., Schöne, B., R., Moore, G., W., K., Joachimski, M., Kronz, A., Fietzke, J., and Estes, J. (2007). Coralline alga reveals first marine record of subarctic North Pacific climate change. *Geophysical Research Letters* **34,** L07702.

Halfar, J., Zack, T., Kronz, A., and Zachos, J., C. (2000). Growth and high-resolution paleoenvironmental signals of rhodoliths (coralline red algae): A new biogenic archive. *Journal of Geophysical Research* **105,** 22,107-22,116.

Harris, P., J., Tsuji, Y., Marshall, J., F., Davies, P., J., Honda, N., and Matsuda, H. (1996). Sand and rhodolith-gravel entrainment on the mid- to outer-shelf under a western

boundary current: Fraser Island continental shelf, eastern Australia. *Marine Geology* **129,** 313-330.

Hathorne, E. C., Alard, O., James, R. H., and Rogers, N. W. (2003). Determination of intratest variability of trace elements in foraminifera by laser ablation inductively coupled plasma-mass spectrometry. *Geochemistry, Geophysics, Geosystems* **4,** 8408.

Hetzinger, S., Halfar, J., Kronz, A., Steneck, R., Adey, W., H., Lebednik, P., A., and Schöne, B., R. (2009). High-resolution Mg/Ca ratios in a coralline red alga as a proxy for Bering Sea temperature variations from 1902 to 1967. *Palaios* **24,** 406-412.

Hetzinger, S., Halfar, J., Zack, T., Gamboa, G., Jacob, D. E., Kunz, B. E., Kronz, A., Adey, W., Lebednik, P. A., and Steneck, R. S. (2011a). High-resolution analysis of trace elements in crustose coralline algae from the North Atlantic and North Pacific by laser ablation ICP-MS. *Palaeogeography, Palaeoclimatology, Palaeoecology* **302**(1-2), 81-94.

Hetzinger, S., Halfar, J., Mecking, J. V., Keenlyside, N. S., Kronz, A., Steneck, R. S., Adey, W. H., and Lebednik, P. A. (2011b). Marine proxy evidence linking decadal North Pacific and Atlantic climate. *Climate Dynamics,* 1-9.

Kamenos, N., A., Cusack, M., Huthwelker, T., Lagarde, P., and Scheibling, R., E. (2009). Mg-lattice associations in red coralline algae. *Geochimica et Cosmochimica Acta* **73,** 1901-1907.

Kamenos, N., A., Cusack, M., and Moore, P., G. (2008). Coralline algae are global palaeothermometers with bi-weekly resolution. *Geochimica et Cosmochimica Acta* **72,** 771-779.

Kamenos, N. A., and Law, A. (2010). Temperature controls on coralline algal skeletal growth. *Journal of Phycology* **46,** 331-335.

Longerich, H. P., Jackson, S. E., and G¸nther, D. (1996). Laser ablation inductively coupled plasma mass spectrometric transient signal data acquisition and analyte concentration calculation. *Journal of Analytical Atomic Spectrometry* **11,** 899-904.

Love, K. M., and Woronow, A. (1991). Chemical changes induced in aragonite using treatments for the destruction of organic material. *Chemical geology* **93,** 291-301.

Martin, P. A., and Lea, D. W. (2002). A simple evaluation of cleaning procedures on fossil benthic foraminiferal Mg/Ca. *Geochemistry, Geophysics, Geosystems* **3,** 8401.

Milliman, J. D., Gastner, M., and Müller, J. (1971). Utilization of magnesium in coralline algae. *Geological Society of America Bulletin* **82,** 573-580.

Moberly Jr, R. (1968). Composition of Magnesian Calcites of Algae and Pelecypods by Electron Microprobe analysis. *Sedimentology* **11,** 61-82.

Nash, M. C., Troitzsch, U., Opdyke, B. N., Trafford, J. M., Russell, B. D., and Kline, D. I. (2011). First discovery of dolomite and magnesite in living coralline algae and its geobiological implications. *Biogeosciences* **8,** 3331-3340.

Nelson, W. A. (2009). Calcified macroalgae - critical to coastal ecosystems and vulnerable to change: a review. *Marine and Freshwater Research* **60,** 787-801.

Paillard, D., Labeyrie, L., and Yiou, P. (1996). Macintosh program performs time-series analysis. *Eos Transactions AGU* **77,** 379.

Schöne, B. R., Zhang, Z., Radermacher, P., Thébault, J., Jacob, D. E., Nunn, E. V., and Maurer, A. F. (2011). Sr/Ca and Mg/Ca ratios of ontogenetically old, long-lived bivalve shells (*Arctica islandica*) and their function as paleotemperature proxies. *Palaeogeography, Palaeoclimatology, Palaeoecology* **302,** 52-64.

Sinclair, D. J., Kinsley, L. P. J., and McCulloch, M. T. (1998). High resolution analysis of trace elements in corals by laser ablation ICP-MS. *Geochimica et Cosmochimica Acta* **62,** 1889-1901.

Steneck, R. S. (1986). The ecology of coralline algal crusts: convergent patterns and adaptative strategies. *Annual Review of Ecology and Systematics* **17,** 273-303.

Stoll, H. M., Encinar, J. R., Garcia Alonso, J. I., Rosenthal, Y., Probert, I., and Klaas, C. (2001). A first look at paleotemperature prospects from Mg in coccolith carbonate: Cleaning techniques and culture measurements. *Geochemistry, Geophysics, Geosystems* **200,** 2GC000144.

References

Adey, W., H., and MacIntyre, I., G. (1973). Crustose Coralline Algae: A Re-evaluation in the Geological Sciences. *Geological Society of America Bulletin* **84,** 883-904.

Basso, D., Nalin, R., and Nelson, C., S. (2009). Shallow-water *Sporolithon* rhodoliths from North Island (New Zealand). *Palaios* **24,** 92-103.

Bosence, D., W. J. (1983a). Description and Classification of Rhodoliths (Rhodoids, Rhodolites). *In* "Coated Grains." (T. M. Peryt, Ed.), pp. 217-224. Springer-Verlag, Berlin.

Bosence, D., W., J. (1983b). The Occurence and Ecology of Recent Rhodoliths - A Review. *In* "Coated Grains." (T. M. Peryt, Ed.), pp. 225-242. Springer-Verlag Berlin.

Burdett, H., Kamenos, N. A., and Law, A. (2010). Using coralline algae to understand historic marine cloud cover. *Palaeogeography, Palaeoclimatology, Palaeoecology* **302,** 65-70.

Chan, P., Halfar, J., Williams, B., Hetzinger, S., Steneck, R., Zack, T., and Jacob, D. E. (2011). Freshening of the Alaska Coastal Current recorded by coralline algal Ba/Ca ratios. *Journal of Geophysical Research* **116,** G01032.

Chave, K. E. (1954). Aspects of the biogeochemistry of magnesium 1. Calcareous marine organisms. *The Journal of Geology* **62,** 266-283.

Craig, C. A., Jarvis, K. E., and Clarke, L. J. (2000). An assessment of calibration strategies for the quantitative and semi-quantitative analysis of calcium carbonate matrices by laser ablation-inductively coupled plasma-mass spectrometry (LA-ICP-MS). *Journal of Analytical Aomic Spectrometry* **15,** 1001-1008.

de Villiers, S., Greaves, M., and Elderfield, H. (2002). An intensity ratio calibration method for the accurate determination of Mg/Ca and Sr/Ca of marine carbonates by ICP-AES. *Geochemistry, Geophysics, Geosystems* **3,** 1001.

Dickson, J. A. D. (1965). A modified staining technique for carbonates in thin section. *Nature* **205,** 587.

Eggins, S., De Deckker, P., and Marshall, J. (2003). Mg/Ca variation in planktonic foraminifera tests: implications for reconstructing palaeo-seawater temperature and habitat migration. *Earth and Planetary Science Letters* **212,** 291-306.

Fallon, S. J., McCulloch, M. T., van Woesik, R., and Sinclair, D. J. (1999). Corals at their latitudinal limits: laser ablation trace element systematics in *Porites* from Shirigai Bay, Japan. *Earth and Planetary Science Letters* **172,** 221-238.

Foster, M., S. (2001). Rhodoliths: Between rocks and soft places. *Journal of Phycology* **37,** 659-667.

Frantz, B. R., Foster, M. S., and Riosmena-Rodrìguez, R. (2005). *Clathromorphum nereostratum* (Corallinales, Rhodophyta): The oldest alga? *Journal of Phycology* **41,** 770-773.

Gamboa, G., Halfar, J., Hetzinger, S., Adey, W., Zack, T., Kunz, B., and Jacob, D. E. (2010). Mg/Ca ratios in coralline algae record northwest Atlantic temperature variations and North Atlantic Oscillation relationships. *Journal of Geophysical Research* **115,** C12044.

Goldberg, N. (2006). Age estimates and description of rhodoliths from Esperance Bay, Western Australia. *Journal of the Marine Biological Association of the United Kingdom* **86,** 1291-1296.

Halfar, J., Steneck, R., S., Schöne, B., R., Moore, G., W., K., Joachimski, M., Kronz, A., Fietzke, J., and Estes, J. (2007). Coralline alga reveals first marine record of subarctic North Pacific climate change. *Geophysical Research Letters* **34,** L07702.

Halfar, J., Zack, T., Kronz, A., and Zachos, J., C. (2000). Growth and high-resolution paleoenvironmental signals of rhodoliths (coralline red algae): A new biogenic archive. *Journal of Geophysical Research* **105,** 22,107-22,116.

Harris, P., J., Tsuji, Y., Marshall, J., F., Davies, P., J., Honda, N., and Matsuda, H. (1996). Sand and rhodolith-gravel entrainment on the mid- to outer-shelf under a western

boundary current: Fraser Island continental shelf, eastern Australia. *Marine Geology* **129,** 313-330.

Hathorne, E. C., Alard, O., James, R. H., and Rogers, N. W. (2003). Determination of intratest variability of trace elements in foraminifera by laser ablation inductively coupled plasma-mass spectrometry. *Geochemistry, Geophysics, Geosystems* **4,** 8408.

Hetzinger, S., Halfar, J., Kronz, A., Steneck, R., Adey, W., H., Lebednik, P., A., and Schöne, B., R. (2009). High-resolution Mg/Ca ratios in a coralline red alga as a proxy for Bering Sea temperature variations from 1902 to 1967. *Palaios* **24,** 406-412.

Hetzinger, S., Halfar, J., Zack, T., Gamboa, G., Jacob, D. E., Kunz, B. E., Kronz, A., Adey, W., Lebednik, P. A., and Steneck, R. S. (2011a). High-resolution analysis of trace elements in crustose coralline algae from the North Atlantic and North Pacific by laser ablation ICP-MS. *Palaeogeography, Palaeoclimatology, Palaeoecology* **302**(1-2), 81-94.

Hetzinger, S., Halfar, J., Mecking, J. V., Keenlyside, N. S., Kronz, A., Steneck, R. S., Adey, W. H., and Lebednik, P. A. (2011b). Marine proxy evidence linking decadal North Pacific and Atlantic climate. *Climate Dynamics,* 1-9.

Kamenos, N., A., Cusack, M., Huthwelker, T., Lagarde, P., and Scheibling, R., E. (2009). Mg-lattice associations in red coralline algae. *Geochimica et Cosmochimica Acta* **73,** 1901-1907.

Kamenos, N., A., Cusack, M., and Moore, P., G. (2008). Coralline algae are global palaeothermometers with bi-weekly resolution. *Geochimica et Cosmochimica Acta* **72,** 771-779.

Kamenos, N. A., and Law, A. (2010). Temperature controls on coralline algal skeletal growth. *Journal of Phycology* **46,** 331-335.

Longerich, H. P., Jackson, S. E., and G¸nther, D. (1996). Laser ablation inductively coupled plasma mass spectrometric transient signal data acquisition and analyte concentration calculation. *Journal of Analytical Atomic Spectrometry* **11,** 899-904.

Love, K. M., and Woronow, A. (1991). Chemical changes induced in aragonite using treatments for the destruction of organic material. *Chemical geology* **93,** 291-301.

Martin, P. A., and Lea, D. W. (2002). A simple evaluation of cleaning procedures on fossil benthic foraminiferal Mg/Ca. *Geochemistry, Geophysics, Geosystems* **3,** 8401.

Milliman, J. D., Gastner, M., and Müller, J. (1971). Utilization of magnesium in coralline algae. *Geological Society of America Bulletin* **82,** 573-580.

Moberly Jr, R. (1968). Composition of Magnesian Calcites of Algae and Pelecypods by Electron Microprobe analysis. *Sedimentology* **11,** 61-82.

Nash, M. C., Troitzsch, U., Opdyke, B. N., Trafford, J. M., Russell, B. D., and Kline, D. I. (2011). First discovery of dolomite and magnesite in living coralline algae and its geobiological implications. *Biogeosciences* **8,** 3331-3340.

Nelson, W. A. (2009). Calcified macroalgae - critical to coastal ecosystems and vulnerable to change: a review. *Marine and Freshwater Research* **60,** 787-801.

Paillard, D., Labeyrie, L., and Yiou, P. (1996). Macintosh program performs time-series analysis. *Eos Transactions AGU* **77,** 379.

Schöne, B. R., Zhang, Z., Radermacher, P., Thébault, J., Jacob, D. E., Nunn, E. V., and Maurer, A. F. (2011). Sr/Ca and Mg/Ca ratios of ontogenetically old, long-lived bivalve shells (*Arctica islandica*) and their function as paleotemperature proxies. *Palaeogeography, Palaeoclimatology, Palaeoecology* **302,** 52-64.

Sinclair, D. J., Kinsley, L. P. J., and McCulloch, M. T. (1998). High resolution analysis of trace elements in corals by laser ablation ICP-MS. *Geochimica et Cosmochimica Acta* **62,** 1889-1901.

Steneck, R. S. (1986). The ecology of coralline algal crusts: convergent patterns and adaptative strategies. *Annual Review of Ecology and Systematics* **17,** 273-303.

Stoll, H. M., Encinar, J. R., Garcia Alonso, J. I., Rosenthal, Y., Probert, I., and Klaas, C. (2001). A first look at paleotemperature prospects from Mg in coccolith carbonate: Cleaning techniques and culture measurements. *Geochemistry, Geophysics, Geosystems* **200,** 2GC000144.

References

Adey, W., H., and MacIntyre, I., G. (1973). Crustose Coralline Algae: A Re-evaluation in the Geological Sciences. *Geological Society of America Bulletin* **84,** 883-904.

Basso, D., Nalin, R., and Nelson, C., S. (2009). Shallow-water *Sporolithon* rhodoliths from North Island (New Zealand). *Palaios* **24,** 92-103.

Bosence, D., W. J. (1983a). Description and Classification of Rhodoliths (Rhodoids, Rhodolites). *In* "Coated Grains." (T. M. Peryt, Ed.), pp. 217-224. Springer-Verlag, Berlin.

Bosence, D., W., J. (1983b). The Occurence and Ecology of Recent Rhodoliths - A Review. *In* "Coated Grains." (T. M. Peryt, Ed.), pp. 225-242. Springer-Verlag Berlin.

Burdett, H., Kamenos, N. A., and Law, A. (2010). Using coralline algae to understand historic marine cloud cover. *Palaeogeography, Palaeoclimatology, Palaeoecology* **302,** 65-70.

Chan, P., Halfar, J., Williams, B., Hetzinger, S., Steneck, R., Zack, T., and Jacob, D. E. (2011). Freshening of the Alaska Coastal Current recorded by coralline algal Ba/Ca ratios. *Journal of Geophysical Research* **116,** G01032.

Chave, K. E. (1954). Aspects of the biogeochemistry of magnesium 1. Calcareous marine organisms. *The Journal of Geology* **62,** 266-283.

Craig, C. A., Jarvis, K. E., and Clarke, L. J. (2000). An assessment of calibration strategies for the quantitative and semi-quantitative analysis of calcium carbonate matrices by laser ablation-inductively coupled plasma-mass spectrometry (LA-ICP-MS). *Journal of Analytical Aomic Spectrometry* **15,** 1001-1008.

de Villiers, S., Greaves, M., and Elderfield, H. (2002). An intensity ratio calibration method for the accurate determination of Mg/Ca and Sr/Ca of marine carbonates by ICP-AES. *Geochemistry, Geophysics, Geosystems* **3,** 1001.

Dickson, J. A. D. (1965). A modified staining technique for carbonates in thin section. *Nature* **205,** 587.

Eggins, S., De Deckker, P., and Marshall, J. (2003). Mg/Ca variation in planktonic foraminifera tests: implications for reconstructing palaeo-seawater temperature and habitat migration. *Earth and Planetary Science Letters* **212,** 291-306.

Fallon, S. J., McCulloch, M. T., van Woesik, R., and Sinclair, D. J. (1999). Corals at their latitudinal limits: laser ablation trace element systematics in *Porites* from Shirigai Bay, Japan. *Earth and Planetary Science Letters* **172,** 221-238.

Foster, M., S. (2001). Rhodoliths: Between rocks and soft places. *Journal of Phycology* **37,** 659-667.

Frantz, B. R., Foster, M. S., and Riosmena-Rodrìguez, R. (2005). *Clathromorphum nereostratum* (Corallinales, Rhodophyta): The oldest alga? *Journal of Phycology* **41,** 770-773.

Gamboa, G., Halfar, J., Hetzinger, S., Adey, W., Zack, T., Kunz, B., and Jacob, D. E. (2010). Mg/Ca ratios in coralline algae record northwest Atlantic temperature variations and North Atlantic Oscillation relationships. *Journal of Geophysical Research* **115,** C12044.

Goldberg, N. (2006). Age estimates and description of rhodoliths from Esperance Bay, Western Australia. *Journal of the Marine Biological Association of the United Kingdom* **86,** 1291-1296.

Halfar, J., Steneck, R., S., Schöne, B., R., Moore, G., W., K., Joachimski, M., Kronz, A., Fietzke, J., and Estes, J. (2007). Coralline alga reveals first marine record of subarctic North Pacific climate change. *Geophysical Research Letters* **34,** L07702.

Halfar, J., Zack, T., Kronz, A., and Zachos, J., C. (2000). Growth and high-resolution paleoenvironmental signals of rhodoliths (coralline red algae): A new biogenic archive. *Journal of Geophysical Research* **105,** 22,107-22,116.

Harris, P., J., Tsuji, Y., Marshall, J., F., Davies, P., J., Honda, N., and Matsuda, H. (1996). Sand and rhodolith-gravel entrainment on the mid- to outer-shelf under a western

boundary current: Fraser Island continental shelf, eastern Australia. *Marine Geology* **129,** 313-330.

Hathorne, E. C., Alard, O., James, R. H., and Rogers, N. W. (2003). Determination of intratest variability of trace elements in foraminifera by laser ablation inductively coupled plasma-mass spectrometry. *Geochemistry, Geophysics, Geosystems* **4,** 8408.

Hetzinger, S., Halfar, J., Kronz, A., Steneck, R., Adey, W., H., Lebednik, P., A., and Schöne, B., R. (2009). High-resolution Mg/Ca ratios in a coralline red alga as a proxy for Bering Sea temperature variations from 1902 to 1967. *Palaios* **24,** 406-412.

Hetzinger, S., Halfar, J., Zack, T., Gamboa, G., Jacob, D. E., Kunz, B. E., Kronz, A., Adey, W., Lebednik, P. A., and Steneck, R. S. (2011a). High-resolution analysis of trace elements in crustose coralline algae from the North Atlantic and North Pacific by laser ablation ICP-MS. *Palaeogeography, Palaeoclimatology, Palaeoecology* **302**(1-2), 81-94.

Hetzinger, S., Halfar, J., Mecking, J. V., Keenlyside, N. S., Kronz, A., Steneck, R. S., Adey, W. H., and Lebednik, P. A. (2011b). Marine proxy evidence linking decadal North Pacific and Atlantic climate. *Climate Dynamics*, 1-9.

Kamenos, N., A., Cusack, M., Huthwelker, T., Lagarde, P., and Scheibling, R., E. (2009). Mg-lattice associations in red coralline algae. *Geochimica et Cosmochimica Acta* **73,** 1901-1907.

Kamenos, N., A., Cusack, M., and Moore, P., G. (2008). Coralline algae are global palaeothermometers with bi-weekly resolution. *Geochimica et Cosmochimica Acta* **72,** 771-779.

Kamenos, N. A., and Law, A. (2010). Temperature controls on coralline algal skeletal growth. *Journal of Phycology* **46,** 331-335.

Longerich, H. P., Jackson, S. E., and G¸nther, D. (1996). Laser ablation inductively coupled plasma mass spectrometric transient signal data acquisition and analyte concentration calculation. *Journal of Analytical Atomic Spectrometry* **11,** 899-904.

Love, K. M., and Woronow, A. (1991). Chemical changes induced in aragonite using treatments for the destruction of organic material. *Chemical geology* **93,** 291-301.

Martin, P. A., and Lea, D. W. (2002). A simple evaluation of cleaning procedures on fossil benthic foraminiferal Mg/Ca. *Geochemistry, Geophysics, Geosystems* **3,** 8401.

Milliman, J. D., Gastner, M., and Müller, J. (1971). Utilization of magnesium in coralline algae. *Geological Society of America Bulletin* **82,** 573-580.

Moberly Jr, R. (1968). Composition of Magnesian Calcites of Algae and Pelecypods by Electron Microprobe analysis. *Sedimentology* **11,** 61-82.

Nash, M. C., Troitzsch, U., Opdyke, B. N., Trafford, J. M., Russell, B. D., and Kline, D. I. (2011). First discovery of dolomite and magnesite in living coralline algae and its geobiological implications. *Biogeosciences* **8,** 3331-3340.

Nelson, W. A. (2009). Calcified macroalgae - critical to coastal ecosystems and vulnerable to change: a review. *Marine and Freshwater Research* **60,** 787-801.

Paillard, D., Labeyrie, L., and Yiou, P. (1996). Macintosh program performs time-series analysis. *Eos Transactions AGU* **77,** 379.

Schöne, B. R., Zhang, Z., Radermacher, P., Thébault, J., Jacob, D. E., Nunn, E. V., and Maurer, A. F. (2011). Sr/Ca and Mg/Ca ratios of ontogenetically old, long-lived bivalve shells (*Arctica islandica*) and their function as paleotemperature proxies. *Palaeogeography, Palaeoclimatology, Palaeoecology* **302,** 52-64.

Sinclair, D. J., Kinsley, L. P. J., and McCulloch, M. T. (1998). High resolution analysis of trace elements in corals by laser ablation ICP-MS. *Geochimica et Cosmochimica Acta* **62,** 1889-1901.

Steneck, R. S. (1986). The ecology of coralline algal crusts: convergent patterns and adaptative strategies. *Annual Review of Ecology and Systematics* **17,** 273-303.

Stoll, H. M., Encinar, J. R., Garcia Alonso, J. I., Rosenthal, Y., Probert, I., and Klaas, C. (2001). A first look at paleotemperature prospects from Mg in coccolith carbonate: Cleaning techniques and culture measurements. *Geochemistry, Geophysics, Geosystems* **200,** 2GC000144.